Nonlinear respiratory airway resistance and breathing effort estimation for respiratory disease monitoring and care.

Theodore Lerios

A thesis presented for the degree of

Doctor of Philosophy

in

Mechanical Engineering

at the

University of Canterbury

Christchurch, New Zealand

April 4, 2023

Acknowledgements

I would like to thank my primary supervisor, Geoffrey Chase, for inspiring me and challenging me to extend myself in my work and my life. Thank you for bringing concepts to life with your theatrical, passionate explanations. Thank you for your patience, your ever mysterious vision of my future which remains unrevealed, and allowing me to progress at my own pace, and for putting up with me over complicating most things. I will always remember your mentorship, and persistent support of my ambition and goals.

To my co-supervisor Jennifer Knopp, thank you for all of the effort mentoring me. Thank you for allowing me to be creative and think about my research in my own way, and encouraging me to be liberal in my approach to most things. Also, thank you for your personal support throughout my undergraduate and postgraduate studies.

To my co-supervisor Lui Holder-Pearson, thank you to you and your family for your friendship and constant support and motivation. Your drive for life and the caring of others has inspired me and taught me the value of the community around me.

A special thank you to my children, Brooklyn, Dylan and Luca who have inspired me to live up to my potential daily, and who have loved me unconditionally throughout my studies, regardless of the sacrifice they have had to make.

Finally, I wish to dedicate this dissertation to my wife Jessie Lerios for being my greatest cheerleader in everything I do, and for your unwavering and never ending support, enabling me to pursue a career I am so passionate about. I could not have accomplished any of this without you. Thank you so much for the sacrifice you have made for me.

Contents

1 CHAPTER 1: BACKGROUND **21**

1.1 Introduction 21

1.2 Pulmonary Anatomy and Physiology 25

1.2.1 Anatomy 26

1.2.2 Physiology 30

1.3 Pulmonary pathophysiology 32

1.3.1 Respiratory failure 32

1.3.2 Lung disease classifications 33

1.3.3 Ventilation-perfusion mismatch 34

1.3.4 COPD 35

1.4 Pulmonary Function Measurement 38

1.4.1 Lung Capacity Definitions 38

1.4.2 Measuring pressure and flow 40

1.4.3 Static vs. Dynamic measurements 42

1.4.4 Spirometry 43

1.4.5 Limitations of Spirometry in Restrictive disease 45

1.4.6 Occlusion technique 45

1.4.7 Weighted spirometer technique 47

1.4.8 Forced oscillation technique 47

1.4.9 Plethysmography 48

1.4.10 Gas dilution 49
1.5 Summary 51
1.6 Preface 51

2 CHAPTER 2: MODEL 53

2.1 Introduction 53
2.2 Review of Lung Modelling Approaches 53
2.2.1 Complex Finite Element Models 54
2.2.2 Elastic-Resistive Models 55
2.2.3 Lung Modelling Approach Summary 65
2.3 Model Development 65
2.3.1 Full model derivation 65
2.3.2 Adaptation for Plethysmography 67
2.4 Non-linear Resistance Model 68
2.5 Inspiratory Demand and Work of Breathing 69
2.6 Summary 71

3 CHAPTER 3: CLINICAL DATA 73

3.1 Introduction 73
3.2 Literature data 74
3.3 Italy data 74
3.4 MV Data 76
3.5 Summary 80

4 CHAPTER 4: PROOF OF CONCEPT 81

4.1 Introduction 81
4.2 Methods 81
4.2.1 Linear single-compartment model 82
4.2.2 Non-linear single-compartment model 84

4.2.3 Analyses 86
4.3 Results 87
4.3.1 Model Goodness of Fit 87
4.4 Discussion 91
4.5 Summary 95

5 CHAPTER 5: NONLINEAR DYNAMIC EXPIRATORY RESISTANCE 97
5.1 Introduction 97
5.2 Methods 97
5.2.1 Clinical Data 97
5.2.2 Model 98
5.2.2.1 Linear single compartment model 98
5.2.2.2 Nonlinear lumped model 100
5.2.3 Analyses 102
5.3 Results 103
5.4 Discussion 107
5.5 Summary 112

6 CHAPTER 6: WORK OF BREATHING AND ELASTANCE 115
6.1 Introduction 115
6.2 Methods 115
6.2.1 Model 115
6.2.2 Model Identification 118
6.2.3 Patient Data 119
6.2.4 Analyses 119
6.3 Results 120
6.4 Discussion 125
6.5 Summary 132

7 CHAPTER 7: ESTIMATING PATIENT EXPIRATORY EFFORT 133

7.1 Introduction 133

7.2 Methods 133

7.2.1 Clinical Data 133

7.2.2 Flow-Volume loops 134

7.2.3 Model 135

7.2.4 Analyses 136

7.3 Results 137

7.4 Discussion 141

7.5 Summary 147

8 CHAPTER 8: IDENTIFYING NONLINEAR RESISTANCE IN MECHANICAL VENTILATION 149

8.1 Introduction 149

8.2 Methods 150

8.2.1 Clinical Data 150

8.2.2 Model 151

8.2.2.1 Linear Model 151

8.2.2.2 Rohrer's resistance model 153

8.2.2.3 Nonlinear resistance model 153

8.2.3 Analyses 155

8.3 Results 155

8.4 Discussion 161

8.5 Summary 163

9 CHAPTER 9: WORK OF BREATHING IN MECHANICAL VENTILATION 165

9.1 Introduction 165

9.2 Methods 166
9.2.1 Clinical Data 166
9.2.2 Model Development 167
9.2.3 Analyses 169
9.2.4 Patient Effort Analysis 1 170
9.2.5 Patient Effort Analysis 2 171
9.2.6 Patient Effort Analysis 3 171
9.3 Results 172
9.4 Discussion 175
9.5 Summary 182

10 CHAPTER 10: CONCLUSIONS 185

11 CHAPTER 11: FUTURE WORK 189

11.1 Plethysmographic clinical trials 189
11.2 Mechanical ventilator clinical trials 190
11.3 Further model development 190

Appendices 257

A ADDITIONAL PATIENT DATA 259
A.1 Nonlinear expiratory resistance 259

List of Figures

1.1 The pleura surrounds the lungs, encased by the rib cage and intercostal muscles. Liquid inside the pleural cavity helps reduce friction caused by breathing [66]. 27

1.2 Schematic diagram of airway branching. LLL, Left lower lobe bronchus; LM, left main-stem bronchus; LUL, left upper lobe bronchus; RLL, right lower lobe bronchus; RM, right main-stem bronchus; RML, right middle lobe bronchus; RUL right upper lobe bronchus; Tr trachea [65]. 28

1.3 The branching structure of the airways, dividing 23 times from the trachea down to the alveolar sacs [69]. 29

1.4 The intercostal muscles and the diaphragm movement cause changes in lung volume during respiration [78]. 31

1.5 Static lung volumes and capacities based on a volume–time spirogram of an inspiratory vital capacity (IVC). IRV: inspiratory reserve volume; VT: tidal volume (TV); ERV: expiratory reserve volume; RV: residual volume; IC: inspiratory capacity; FRC: functional residual capacity; TLC: total lung capacity [150]. 38

1.6 An example of a forced expiration test in spirometry [185]. 44

1.7 FVC cannot be used alone, to diagnose restrictive disease. Both restrictive and obstructive disease can reduce FVC [198]. 46

1.8 Plethysmography results showing gas trapping of a COPD patient, compared to healthier young and elderly patients [219]. 49

2.1 Displacement vectors modelled with FEA at different locations in the lung. The two red vectors represent the mean orientation of the displacement vectors at a high level of the lungs (upper view) and at a low level of the lung near the diaphragm (lower view) [255]. 56

2.2 Airway resistance at each lung generation for a variety of patients [25]. . 59

2.3 The Bates viscoelastic model [2] with two degrees of freedom. 62

2.4 Single compartment model of spontaneous breathing. 67

3.1 Pressure-flow (PQ) loops from the Radovanovic et al. (2018) study depicting a loop for a Young, Elderly and COPD patient. 75

4.1 Single compartment model of spontaneous breathing. 83

4.2 Plethysmographic alveolar pressure (P_{alv}) data with linear and non-linear model fits for Patients 1 (Healthy) and 7 (COPD). A perfect linear model produces a straight line in a PQ plot. The PQ plot is arranged per [219, 302, 303] with expiration on the RHS of the plot. Expiratory flow is here defined negative as is consistent with the single compartment model sign convention. 88

4.3 Expiratory resistance ($R_2\Phi$) with time and flow for each patient. Linear inspiratory resistance ($R_{1,insp}$) is shown for comparison. Note: the scale for the resistance of Patient 7 is much larger than the other patients. . . 89

4.4 An example (Patient 7) of individual splines multiplied by individual identified coefficients to illustrate how the splines create the overall shape of the total expiratory resistance. 90

4.5 Pressure-Flow (PQ) loops depicting data (solid) and non-linear model (dashed) Patients 1 and 7 (a), Patient 2 (b), Patient 3 (c), Patient 4 (d), Patient 5 (e), and Patient 6 (f). The PQ loops are arranged per [219, 302, 303] with expiratory flow, negative per the sign convention of the single compartment model. 91

5.1 Modified single compartment model of spontaneous breathing. 99

5.2 shape metrics for expiratory resistance $R_{2,exp}(t)$ $[cmH_2O/L/s]$ as a function of airway flow Q $[L/s]$ 103

5.3 PQ loops for alveolar pressure (P_{alv}) with the linear and identified non-linear model results overlaid. 104

5.4 A cumulative distribution function (CDF) of inspiratory resistance (left), and mean $R_{exp}(t)$ (right) for all 4 cohorts. 105

5.5 A CDF (left) of the work of resistance $\int R_2 \Phi Q \, dV$ alongside the work of resistance (right) as a function of inspiratory resistance ($R_{1,insp}$). 106

5.6 Alveolar pressure (P_{alv}) $[cmH_2O]$, flow (Q) $[L/s]$, airway resistance (R) $[cmH_2O/L/s]$ and work of resistance (WOR $= \int R_2 \Phi Q \, dV$) $[cmH_2O]$ for the 4 patient cohorts of Young, Old, Non-Flow Limited (NFL), and Flow Limited (FL) subjects. 107

5.7 (left) Mean $R_2\Phi$ as a function of expiratory resistance ($R_{1,exp}$), The ratio of mean $R_2\Phi$ to $R_{1,exp}$ as a function of $R_{1,exp}$ (right). 108

5.8 A CDF of the area of the flow relative to resistance (left), compared with the flow-resistance area as a function of the inspiratory resistance $R_{1,insp}$ (right). 109

5.9 A CDF of the slope of the flow relative to resistance for each respective cohort compared with the same slope as a function of the expiratory resistance ($R_{2,exp}$). 110

5.10 Resistance (R) as a function of air flow (Q) for each patient in the Young cohort. 111

5.11 Resistance (R) as a function of air flow (Q) for each patient in the Elderly cohort. 112

5.12 Resistance (R) as a function of air flow (Q) for each patient in the NFL cohort. 113

5.13 Resistance (R) as a function of air flow (Q) for each patient in the FL cohort. 114

6.1 Single-compartment model (spontaneous). 117

6.2 A typical model fit for a Young patient compared to an FL patient. . . 121

6.3 Patient effort (P_{eff}) is shown increasing for a typical subject from each respective cohort, with flow (Q) and tidal volume (V) data for comparison. 122

6.4 Work of breathing for patient effort is shown to increase with inspiratory resistance. 123

6.5 Elastance (E) increases with an increase in inspiratory resistance and shows some linearity with $R^2 = 0.73$. 124

6.6 Elastic work of breathing shown to increase with resistive work of breathing. 124

6.7 Alveolar pressure (P_{alv}) is shown (Black) compared with patient effort (P_{eff}) (Red) for the Young cohort. 128

6.8 Alveolar pressure (P_{alv}) is shown compared with patient effort (P_{eff}) for the Elderly cohort. 129

6.9 Alveolar pressure (P_{alv}) is shown compared with patient effort (P_{eff}) for the NFL cohort. 130

6.10 Alveolar pressure (P_{alv}) is shown compared with patient effort (P_{eff}) for the FL cohort. 131

7.1 An example of flow-volume loops and how they differ with obstructive and restrictive disease [415]. 134

7.2 A flow-volume loop indicating how passive and active breathing affects the shape of the loop [416]. 135

7.3 Measured expiratory flow as a function of volume for a Young (a), Elderly (b), NFL (c), and FL (d) patient, displaying largely passive expiration compared with a Young (e), Elderly (f), NFL (g), and FL(h) patient displaying more active expiration. 138

7.4 Volume-Flow ($V - Q$) loops for all patients in the Young cohort. 139

7.5 Volume-Flow ($V - Q$) loops for all patients in the Elderly cohort. 140

7.6 Volume-Flow ($V - Q$) loops for all patients in the NFL cohort. 142

7.7 Volume-Flow ($V - Q$) loops for all patients in the FL cohort. 143

7.8 Q_P RMSE results depicted as a box plot, illustrating a lower RMSE values between measured Q and the modelled Q_P for the Young cohort, and relatively larger error moving through the cohorts toward the FL patients where active expiration is more prevalent. 144

7.9 Q_P correlation coefficient (r) results depicted as a box plot, illustrating a stronger correlation between measured Q and the estimated Q_P for the Young cohort, and relatively less correlation moving through the cohorts toward the FL patients as expected. 144

8.1 Model-fits to a typical breath for Patient 1. Resulting airway pressure (left) and resistance shapes with time (right) are shown for expiration, from peak-expiratory flow to end-expiratory flow. The b-spline model on the right additionally shows constituent b-splines as thin lines. 157

8.2 Different resistance model outcomes for a typical expiratory breath for each of the 6 patients. 158

8.3 Nonlinear resistance model outcomes as a function of airflow (Q) for a typical expiratory breath, corresponding to Figure 8.2, for each of the 6 patients. 159

8.4 Continuous distribution functions for patient-specific (n=20 breaths) parameters for each of the linear (R), Rohrer (R_1 and R_2) models, and the mean nonlinear resistance ($mean(R_exp = \sum(R_3\Phi))$). 160

8.5 Comparison of mean $R_{exp}\Phi$, and the mean resistance value obtained from the Rohrer model (R_{Rohrer}) for each breath across the 6 patients. 161

9.1 Typical breaths from each patient, depicting airway pressure (P_{aw}), esophageal pressure (P_{es}), and estimated patient effort (P_{eff}) from each respective analysis (1-3). 173

9.2 All breaths, depicting airway pressure (P_{aw}), esophageal pressure (P_{es}), and estimated patient effort (P_{eff}) from each respective patient, for Analysis 1. Patient 1-6 run top-bottom. 176

9.3 All breaths, depicting airway pressure (P_{aw}), esophageal pressure (P_{es}), and estimated patient effort (P_{eff}) from each respective patient, with analysis 2 patient effort. 177

9.4 All breaths, depicting airway pressure (P_{aw}), esophageal pressure (P_{es}), and estimated patient effort (P_{eff}) from each respective patient, with analysis 3 patient effort. 178

9.5 Correlation of minimum measured ($minP_{es}$) and modelled patient breathing effort ($minP_{eff,1-3}$) for all patients from each respective analysis. . 179

A.1 An example of a patient's plethysmographic alveolar pressure (P_{alv}) data as a function of time, plotted against the linear (black dotted line) and nonlinear (red dotted line) models of alveolar pressure. Flow (Q) as a function of time, volume (V) as a function of time, resistance (R) as a function of time with the linear model constant resistance (blue dotted line), and the nonlinear model dynamic resistance term, $R_2\Phi$ (red dotted line), a pressure-flow loop with model comparisons, a pressure-volume loop, resistance as a function of flow, and resistance as a function of volume. 259

List of Tables

3.1 Demographic data is median [Inter-quartile range] where relevant. FRC = functional residual capacity; VT = tidal volume; VC = vital capacity TLC = Total lung capacity; FVC = forced vital capacity; ITGV = intra-thoracic gas volume. 76

3.2 Young cohort demographic information from the Italy Data. 77

3.3 Elderly cohort demographic information from the Italy Data. 77

3.4 NFL cohort demographic information from the Italy Data. 78

3.5 FL cohort demographic information from the Italy Data. 79

4.1 Identified values for model parameters of inspiratory resistance ($R_{1,insp}$), expiratory resistance ($R_{1,exp}$), mean $R_2\Phi$, root mean squared error for the linear model ($RMSE_{lin}$) and root mean square error for the non-linear model $RMSE_{nlin}$. 87

5.1 Patient information collected during the study [219]. 98

5.2 Median [IQR] of model parameters and model-fit for linear and nonlinear models, where Y = Young, O = Old. 105

6.1 Patient information for each respective cohort. BMI = body mass index, FRC = functional residual capacity, VT = tidal volume 119

6.2 Median [IQR] of model parameters and WOB results for all patients in all four cohorts. 120

7.1 Median [IQR] of model parameters and WOB results for all patients in all four cohorts. 141

8.1 First quartile (Q1), median (MED), and third quartile (Q3) results for lung elastance, and predicted airway resistance for each respective nonlinear estimation, with constant resistance values for the linear estimation for each respective patient numbered 1 - 6. 156

8.2 As a measure of goodness of fit, median RMSE percentage for each patient, and each model for comparison. 157

9.1 Median RMSE [%] and correlation coefficients (r) for all breaths for each patient and each respective analysis. 174

A.1 Identified model parameters for each patient, with an identifier for the 4 cohorts, old (O), young (Y), non-flow limited COPD (NFL), and flow limited COPD (FL), with inspiratory resistance ($R_{1,insp}$), expiratory resistance ($R_{1,exp}$), mean $R_{2,exp}(t)$, root mean squared error for the linear model, and root mean squared error for the nonlinear model per subject. This table contains subjects 1 - 30 260

A.2 Table 1 continued for subjects 31-60. 261

A.3 Table 1 continued for subjects 61-100. 262

CHAPTER 1: BACKGROUND

1.1 Introduction

As with most other physical systems, respiration can be thought of as a mechanical process with feedback control. Contraction and relaxation of thoracic and respiratory muscles enables breathing to occur, approximately 30 000 times per day, or one billion times over a lifetime of 90 years [1]. For most, this process is involuntary. Muscle contraction moves the chest wall boundary, changing the pressure gradient and causing air displacement in the lungs via the airway openings at the mouth and nose, ultimately enabling gas exchange and the necessary uptake of oxygen and removal of waste CO_2 from the bloodstream. However, though always important, the act of breathing is not always easy. Breathing can be tiring and arduous for the majority of those with respiratory illness or failure [2].

Various conditions cause respiratory insufficiency or failure, most involving a change in the mechanical properties of the respiratory system. Conditions primarily contributing to the global burden of respiratory disease are asthma, chronic obstructive pulmonary disease (COPD), acute respiratory infections, tuberculosis, and lung cancer [3]. Hundreds of millions of people suffer globally and four million people die prematurely from respiratory diseases each year. [3–7]

In particular, COPD is a chronic, or ongoing, inflammatory lung disease which obstructs airflow, particularly during exhalation. Emphysema and Bronchitis are two common types of COPD, both involving inflammation or tissue damage of the small airways and/or alveoli. Ischaemic COPD imposes a substantial burden on individuals with symptoms including breathlessness, coughing, sputum production, wheezing, and chest tightness [8]. COPD is also associated with a significant socio-economic burden of approximately 0.3 - 0.6% in many countries [9, 10], which is predicted to increase over the coming decades [11–15].

COPD ranked as the sixth most common cause of death worldwide in 1990 [14]. It is predicted to be the fourth most common cause of death by the World Health Organisation (WHO) by 2030, only slightly behind ischaemic heart disease, cardiovascular disease, and HIV/AIDS. The significance of symptoms in COPD is recognised by the current Global initiative for chronic Obstructive Lung Disease (GOLD) document, which made recommendations promoting the evaluation of symptom burden and exacerbation history separately from airflow limitation. COPD is described by the GOLD as: *"A preventable and treatable disease, characterised by airflow limitation that is not fully reversible."* [16]. Another further quote concludes: *"COPD is a major and increasing global health epidemic that has received insufficient attention from the health-care profession, governments, and the pharmaceutical industry. Urgent action is now required to recognise the disease, predicted to soon become one of the major causes of death and disability, and to develop more effective prevention and treatment strategies"* [14].

COPD is characterised by a restriction in airflow, which is typically progressive and caused by an abnormal inflammation of the lungs in response to harmful particles or gases [17]. This steady decline in lung function is caused by both emphysema, which destroys lung tissue, and the narrowing of small airways due to chronic inflammation,

fibrosis, and loss of elasticity. The destruction of lung parenchyma has a negative impact on the compliance of the lung, thus reducing a patient's ability to expel air with the assistance of a healthy elastic lung [18]. The narrowing and inflammation of the airways increases the resistance to airflow through the pathways leading to the alveoli in the lungs. Thus, COPD leads to a progressive airflow limitation, air trapping, and progressive shortness of breath on exertion [19].

Current clinical methods for detection, diagnosis, and monitoring of COPD include spirometry, a simple, yet important tool described as 'lacking' in its ability to provide a full assessment [20]. Spirometry provides information relating to inhalation or exhalation volumes or flow rates, such as forced expiratory volume in $1s$ (FEV_1) or peak expiratory flow (PEF). Spirometry results are often highly dependent on whether the test was performed correctly by the patient, as it requires full patient co-operation. Some patients have limited ability to perform the test properly, causing the quality of results to vary [21]. A further limiting factor in improving the quality of spirometry results is it only provides a very intermittent measurement of lung function. All these factors impact the quality and timeliness of diagnosis and monitoring of several respiratory diseases.

For example, asthma is a disease with a high frequency of significant misdiagnosis [22–24]. One reason is lung mechanics in asthmatic patients can often appear normal between exacerbative events. Poor quality spirometry results further complicate diagnosis independent of other pulmonary function testing methods. As a consequence, clinicians often recommend patients monitor peak expiratory flow at home as an alternative [25]. This measure has its own limitations as flows are being measured based on different measuring principles, and meters measure with a scale nonlinearly related to flow. Using nonlinear scales would improve measurement, but would require greater

skill to measure correctly [26].

Looking specifically at standard practice for diagnosis and patient health evaluation, problems with spirometry lie mostly to almost exclusively in implementation, including its cost and availability [27]. Spirometry provides information about the condition of the lung by providing clinicians with results in the form of flow-volume diagrams, also known as Q-V loops. These results are indicative of breathing manoeuvres the patients undergo through testing. Although the results themselves provide an informative idea of lung health to clinicians, the quality of this data is often lacking without verification through further testing [28]. Despite best efforts to use spirometry to measure lung mechanics and use as a single method of testing for lung health, its value is limited to clinicians without further invasive testing methods, clinical effort and cost to the healthcare system [29].

Other pulmonary measurement techniques include occlusion methods [30], which block airflow during tidal breathing to estimate alveolar pressure, the weighted spirometer technique [31], and complex expensive methods, such as plethysmography [32]. Plethysmography in particular has a high clinical equipment requirement, and thus cost, with the patient seated in a sealed chamber of known volume with specialist sensors to detect pressure changes and airflow during breathing. Overall, no broad-based technique provides the required patient-specific diagnostic and monitoring required for adequate pulmonary health patient care. All aforementioned techniques have inherent flaws [29] and place burdens on the patient, clinician, and healthcare system. The result is increasing cost to governments and healthcare providers as the global population ages and lives longer [33–37].

With the rise of the availability, and decline in cost, of computing power, creating mathematical models to better understand and predict pulmonary mechanics has become increasingly popular over the past several decades [38–45]. Models vary in complexity depending on their purpose, where some detailed models are too complicated for use. [46–51]. Other models have inaccurate or insufficient representation of lung anatomy and physiology [2, 40, 52, 53], or are restricted to use only on fully sedated patients undergoing mechanical ventilation where pressure or flow is fully controlled as an input [54, 55]. Effective models must be physiologically relevant and clinically identifiable, capturing underlying dynamics and mechanics useful to clinicians for diagnosis and monitoring from accessible clinical data [56–61].

Overall, respiratory diseases are a significant problem in today's healthcare context, and pulmonary function can be difficult or burdensome to measure, limiting diagnosis and monitoring. This chapter provides an overview of the basic anatomy and physiology of breathing, as well as lung disease classifications and COPD in particular. It covers existing pulmonary measurement techniques, and the potentially useful area of physiological modelling. While impossible to write a comprehensive text on this subject, this review focuses on detail relevant and pertinent to the research project at hand.

1.2 Pulmonary Anatomy and Physiology

Cells in the human body require oxygen to function. Several minutes into a loss of oxygen, brain cells begin to die [62–64]. Effective gaseous exchange is enabled by multiple other systems in the human body [65]. The central nervous system interacts with the lungs to provide the rhythmic drive to breathe, controlling the diaphragm and muscular structure of the respiratory system. The chest wall acts as a bellows, providing differential pressure, driving air movement. The circulatory system provides blood flow through

the lung tissue for the uptake of oxygen and expulsion of carbon dioxide. Significant deviation from these inter-dependant processes results in gas exchange failure and other abnormalities which could have serious negative clinical implications. This research will focuses predominantly on the mechanics of the pulmonary anatomy and physiology.

1.2.1 Anatomy

The lungs are the primary organs of the respiratory system. Each lung is enclosed by a membrane called the pleura, which is comprised of two layers. These layers are called the visceral and pleural layers. The space between these layers is filled with pleural fluid and is referred to as the pleural cavity [66]. A section of the pleural layers is shown in Figure 1.1. This fluid acts as a lubricant, reducing friction and enabling the pleural and visceral layers to easily glide over one other without causing injury. The fluid also has adhesive capability, preventing the lung surface from separating from the thoracic wall. These effects of the pleural fluid allow the respiration process to transmit pressure generated by the diaphragm and intercostal muscles to allow the lungs to expand, while minimising trauma caused by friction.

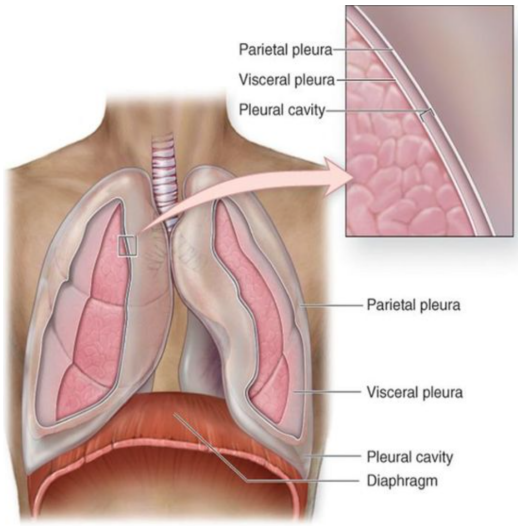

Figure 1.1: The pleura surrounds the lungs, encased by the rib cage and intercostal muscles. Liquid inside the pleural cavity helps reduce friction caused by breathing [66].

En route to the alveoli, gas flows through the oropharynx or nasopharynx, larynx, trachea, and finally a progressively arborizing system of bronchi and bronchioles of diminishing diameter. Figure 1.2 provides a comprehensive explanation for the naming convention for this part of the pulmonary system, with each generation of branching yielding approximately twice the number of airways as the previous generation [66]. The trachea divides into the left and right primary bronchi, which further divide into segmental bronchi. The bronchi continue to divide, down to the terminal bronchioles, the last airways without alveoli.

These first 16 of the total 23 generations do not take part in gas exchange, and make up the anatomical dead space with a volume of roughly 150ml [67]. These airways are important for air warming, humidification, and filtration, as well as playing roles in speech [68]. The terminal bronchioles divide into respiratory bronchioles (Figure 1.3), which have occasional alveoli appearing from their walls. The final four generations of the lungs are the alveolar ducts which are completely lined with alveoli, and the alveolar

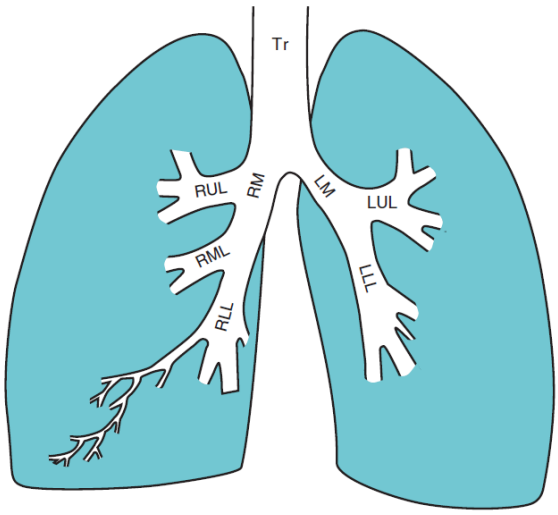

Figure 1.2: Schematic diagram of airway branching. LLL, Left lower lobe bronchus; LM, left main-stem bronchus; LUL, left upper lobe bronchus; RLL, right lower lobe bronchus; RM, right main-stem bronchus; RML, right middle lobe bronchus; RUL right upper lobe bronchus; Tr trachea [65].

sac at the end.

During airway branching, airways change structurally in several ways including the cellular makeup of the mucous membrane, and cartilage shape and distribution. Significantly, towards the distal bronchioles, the cartilage disappears, with a concomitant increase in smooth muscle. Because there is no longer any cartilage, these airways are more prone to narrowing, and muscle spasms, such as during asthma, can close off the airways completely.

Gas exchange occurs using the large surface area provided by the alveoli. It is estimated the adult human lung has on the order of 300 million alveoli, with a total surface area approximately the size of a tennis court [70]. The extremely high surface to volume ratio of the alveoli creates a highly efficient mechanism for O_2 and CO_2 exchange with the blood. Once oxygenated, red blood cells transport oxygen around the body, where

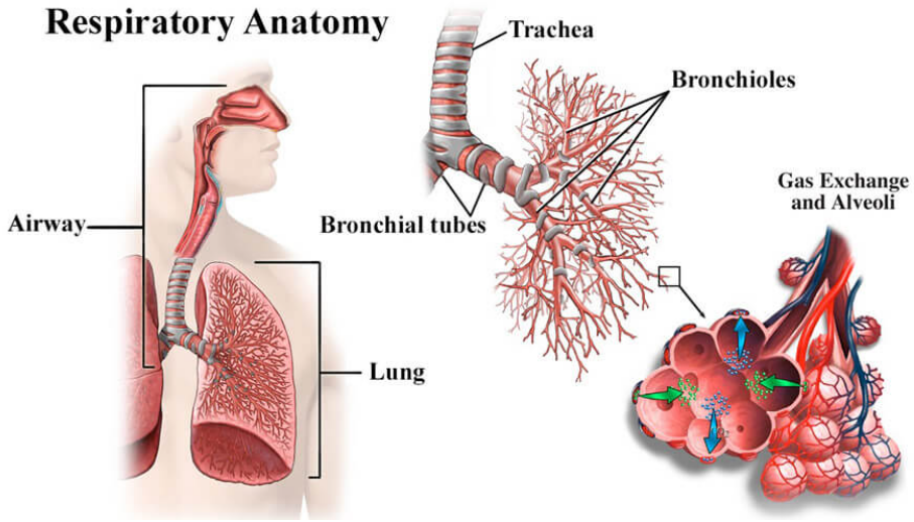

Figure 1.3: The branching structure of the airways, dividing 23 times from the trachea down to the alveolar sacs [69].

it is utilised by cells during production. The same red blood cells, once depleted of oxygen, collect carbon dioxide waste products for removal via the lungs. Oxygenated blood is pumped from the heart's left ventricle into the aorta, which branches into all other blood vessels in the body. De-oxygenated blood returns to the heart's right atrium via the vena cava, and is then pumped through the pulmonary artery to the lungs for re-oxygenation and the removal of carbon dioxide. It takes blood approximately one minute to complete a full circuit [71].

Much like a system of bubbles, the alveolar structure is inherently unstable. Large forces develop in the alveoli due to the surface tension of lining fluid. Smaller alveoli will tend to empty into larger ones. Laplace's law describes how the pressure, P, within a bubble is related to the radius, r, and surface tension, T, of the bubble:

$$P = \frac{2T}{r} \tag{1.1}$$

Laplace's law shows how as the alveoli begin to empty, pressure within the alveoli begins to increase. This increase in pressure, in turn, increases the rate of emptying and can result in alveolar instability and collapse. Cells in the lining of the alveoli secrete surfactant to break this cycle. Surfactant, an oily mixture of phospholipids and apoproteins, reduces surface tension, and is more effective in smaller alveoli. This reduction of surface tension caused by the surfactant more than offsets the reduction in radius, which improves stability [72–74].

1.2.2 Physiology

The primary function of the respiratory system is gas exchange. However, the lungs perform other vital functions including the breakdown of microthrombi (small blood clots). These clots are carried to the lungs by the veins, where toxins are filtered out of the blood [50]. Cells in the body require oxygen to create energy through the Krebs cycle. The waste product from this cycle is carbon dioxide. The mechanism of gas exchange at the blood-alveolar interface is diffusion, which occurs at the wall of the alveoli, assisted by a diffusive partial pressure difference in these gases [75–77].

The lungs need to draw air in from the atmosphere for this to take place. To enable this flow of air, a difference in pressure must exist between the inside of the lung and the atmosphere. Respiration occurs by the diaphragm and respiratory muscles in the chest wall contracting and relaxing as shown in Figure 1.4, changing the volume of the lungs. The relationship between pressure and volume in a gas (assuming constant temperature) is described by Boyle's law:

$$P_1 V_1 = P_2 V_2 \tag{1.2}$$

The relationship between pressure and volume can thus be described as inversely pro-

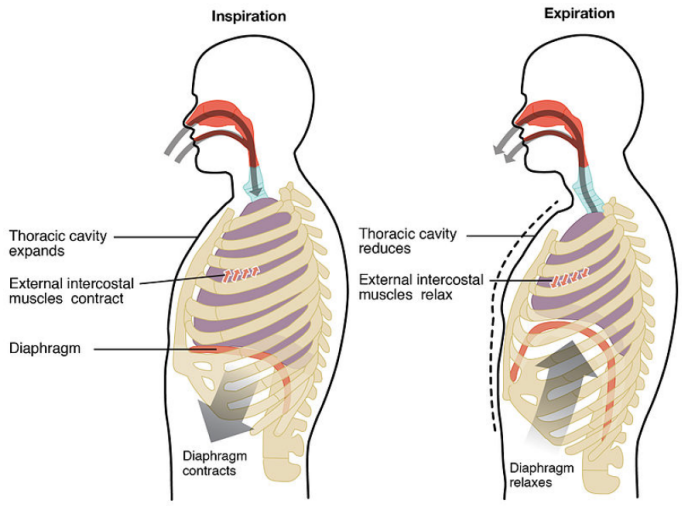

Figure 1.4: The intercostal muscles and the diaphragm movement cause changes in lung volume during respiration [78].

portional. An increase in volume will lead in a decrease in pressure and a decrease in volume will lead to a pressure increase. When the respiratory muscles and the diaphragm contract during inspiration to expand the chest cavity, a pressure lower than atmospheric pressure is created inside the lungs resulting in air being drawn into the lungs and all of the airways between the mouth opening and the alveoli. All of these movements facilitated by respiratory muscles are involuntary and controlled by the brain [77,79,80].

These movements of the chest and abdomen are opposed by elastic forces in the lung, ribs, and thorax. The pressure generated in the pleural cavity is called intrapleural pressure and is generated by opposing elastic recoils of the lung and chest wall [81]. In most cases, pleural pressure is negative, preventing the lung from collapsing easily. However, pleural pressure can be positive compared to atmosphere, when the intrapleural cavity is forcefully compressed by large expiration events, like coughing. Inspiration results in diaphragmatic contraction, increasing pleural cavity volume, and concomitantly decreasing the intrapleural pressure. The pressure drop generated results in lung expansion

and drives airflow. During expiration the thoracic wall recoils and the volume of the pleural cavity decreases proportionally. This decrease in volume returns the pressure to its equilibrium value and allows lung volume to decrease. Usually, expiration is largely passive, driven by elastic recoil. However, critically with respect to modelling and understanding, some respiratory diseases require additional muscle activation to achieve sufficient expiration.

1.3 Pulmonary pathophysiology

Pathophysiology is pathology and physiology, brought together and defined as the study of the disordered physiological processes, which cause, result from, or are otherwise associated with disease or injury. This section focuses on lung pathophysiology, and the pathophysiology of COPD in particular.

1.3.1 Respiratory failure

Respiratory failure occurs when the lungs are unable to carry out their primary responsibilities of oxygenating the blood and expelling carbon dioxide. The two primary designations of respiratory failure are Type I and Type II. Low oxygen concentrations and normal or low carbon dioxide levels are the hallmarks of Type I respiratory failure, while low oxygen levels and high carbon dioxide levels typify Type II respiratory failure. Type I respiratory failure is linked to illnesses damaging lung tissue, such as pneumonia, acute respiratory distress syndrome (ARDS), and pulmonary oedema [82–85]. Acute diffuse, inflammatory lung injury of the kind resulting in ARDS causes an increase in lung weight, a loss of aerated tissue, and increased pulmonary vascular permeability [86]. Hypoxaemia and bilateral tenderness are two of ARDS's clinical symptoms [82–85, 87].

Asthma and chronic obstructive pulmonary disease (COPD) are linked to Type II respiratory failure. Other, more sporadic causes, include respiratory muscle weakness, abnormalities of the chest wall, and extreme obesity. The entire lung is affected by these rare disorders, limiting lung expansion capacity. These causes, in turn, result in the blood retaining carbon dioxide, known as hypercapnia and hypoxaemia. According to Roussos et al. [88], hypercapnic respiratory failure is typically brought on by problems with the central nervous system, impairment of neuromuscular transmission, mechanical problems with the rib-cage, and exhaustion of the breathing muscles. It is yet unclear what pathophysiological processes lead to persistent carbon dioxide retention [89–93].

1.3.2 Lung disease classifications

Respiratory diseases are classified into two classes: obstructive and restrictive [37]. Obstructive lung disease is characterised by airway obstructions, such as collapse, blockages, or flow impedance. A large number of obstructive diseases are the result of narrowing of smaller bronchi and larger bronchioles. This narrowing frequently occurs due to the contraction of the smooth muscle itself [94–98]. Increased resistance to flow in these narrowed openings makes it strenuous to exhale fully. Examples of obstructive lung diseases include asthma, chronic obstructive pulmonary disease (COPD), and cystic fibrosis. Popular treatments for obstructive lung diseases include inhalers and steroids, which relax the smooth muscle to reduce or reverse airway narrowing [99].

Restrictive diseases reduce inspiration capacity, increasing oxygen levels inside the lung. Research suggests this reduction occurs due to an increase in lung elastance (stiffness), respiration muscle weakness, or, more rarely, increased external pressure constricting lung expansion. Examples of restrictive disease include fibrotic diseases of the lung, neuromuscular disorders, and obesity. Restrictive disease treatments are

seldom able to reverse disease effects, and instead aim to improve the patient's quality of life [100, 101]. Frequently used treatments include antibiotics, immunosuppressants, steroid or nonsteroidal pharmaceuticals, oxygen therapy, or non-invasive mechanical ventilation to assist or replace the work of breathing [102].

As obstructive and restrictive diseases tend to primarily affect expiration and inspiration respectively, one suggestion for diagnosing (lung function tests) and treating (clinical treatment) respiratory illness is separate approaches for inspiration and expiration respectively. Lung volume is predominantly affected by restrictive diseases, where reduced airflow has a negative outcome effect on expiration. Both inspiratory and expiratory problems lead to a reduction in blood oxygen levels causing cells in the body to malfunction. From an engineering perspective, the mechanics of the two breathing phases are different. Inhalation is actively driven by muscular ability to create negative pressure in the lungs. Expiration is normally a function of lung/muscle relaxation, and when forced is a function of chest wall stiffness and muscular contraction to create lung pressure and drive out air [25].

1.3.3 Ventilation-perfusion mismatch

The amount of air and blood entering the alveoli via the capillaries are known as perfusion and ventilation, respectively. According to the ventilation-perfusion (V/Q) ratio, the amount of blood and air entering the alveoli each minute is determined by the respiratory system [67]. Advanced disease is characterised by impaired gas exchange resulting in arterial hypoxaemia with or without hypercapnia. The primary cause for aberrant gas exchange is an irregular distribution of ventilation:perfusion ratios, which is brought on by the structural abnormalities seen in COPD [103]. The severity of emphysema is well correlated with the degree of impairment of carbon monoxide diffusing capacity per

litre of lung volume.

Pulmonary shunt refers to the situation where there is normal blood flow to the lungs, but impaired gas exchange due to inadequate ventilation of the alveoli. This poor ventilation of the alveoli results in a low ventilation-perfusion (V/Q) ratio, indicating the amount of air being inhaled is not proportional to the amount of blood perfused through the lungs. A common cause of pulmonary shunt is the accumulation of fluid in the alveoli, which obstructs their ability to participate in gas exchange. To mitigate the impact of pulmonary shunt, the body responds to low oxygen levels (hypoxia) by constricting the pulmonary blood vessels, directing blood flow towards well-ventilated regions of the lungs. This reflexive mechanism is believed to be a key regulator of ventilation-perfusion matching [104–107]. In cases where perfusion is reduced while ventilation remains normal, such as in pulmonary embolism (a blockage of an artery in the lungs), the dead space within the lungs increases. Dead space refers to the portion of the lungs where gas exchange does not occur, including structures like the trachea.

1.3.4 COPD

Chronic obstructive pulmonary disease (COPD) is a prominent cause of mortality and morbidity worldwide, and its main underlying conditions are emphysema and chronic bronchitis. It is a chronic and slowly progressive lung disease, characterised by obstruction to airflow which does not improve over several months [108]. The main cause of COPD is inhalation of irritants, such as cigarette smoke [109]. Other observed causes of COPD have included exposure to pollutants in the air, chronic asthma, genetic predisposition and impaired lung growth [3].

COPD is characterised by persistent respiratory symptoms, such as shortness of breath, cough, and sputum production, and results in a significant burden on healthcare systems and quality of life. COPD is widely regarded as a preventable and treatable disease, because of the link between COPD and smoking. Early detection and diagnosis, are thus crucial. Guidelines in New Zealand state COPD diagnosis requires spirometry [110–114]. However, in the medical research community, there is debate as to the benefits of using spirometry to guide COPD care [115–119]. This debate is mainly focused on the fact spirometry based estimates of COPD prevalence can vary by a factor of two, depending on which definition of mild COPD is used [108, 109, 120].

In general, COPD is thus a significant public health problem affecting millions of people worldwide. According to the World Health Organisation (WHO), COPD is the third leading cause death globally, with an estimated 251 million people affected in 2020 [14]. In the European Union alone, it is estimated around 25 million people have COPD [121–123]. The total number of hospital bed days related to COPD are predicted to rise by more than two fold by 2030 according to some model projections [13]. Cause for concern was emphasised in the Respiratory Disease in the World report, which suggests implementation of strategies to significantly improve respiratory health, reducing economic costs and enhancing health equality [3]. However, even a 20% modelled reduction in COPD over the next 15 years, still resulted in substantial clinical and economic burden [3].

COPD imposes a substantial burden on individuals with the disease, which can include a range of symptoms (breathlessness, cough, sputum production, wheezing, chest tightness) of varying severities. This burden can be analysed in terms of quality of life, health status, daily activities, physical activity, sleep, co-morbid anxiety, and depression, as well as risk of exacerbations and disease prognosis [8]. COPD also places a

physical, emotional and social well-being burden on individuals with the disease [3,124]. Emotionally, COPD can cause depression and anxiety, and social isolation can occur due to the disease's impact on a person's ability to participate in activities with friends and family [125].

Despite growing recognition as an important international health problem, COPD has suffered neglect from clinicians, researchers and the pharmaceutical industry [14]. This neglect is largely due to the misconception of COPD as solely a self-inflicted disease due to the strong reduction in the risk of COPD associated with a reduction or elimination of the daily habit of tobacco smoking [126–128]. Existing therapies for COPD are inadequate and none have been shown to slow the relentless progression of the disease [14]. COPD will undoubtedly place an increasing burden on health resources and this burden is likely to be particularly severe in developing countries [14].

This risk and burden is only increased in the current pandemic climate facing the world. Very recent studies are investigating the correlation between COPD and COVID-19 [129–132]. One such study in South Korea with n = 4610 subjects uses a multivariate analysis to show COPD is not a risk factor for respiratory failure. However, it also shows it is a significant independent risk factor for all-cause mortality. Amongst COVID-19 patients, relatively greater proportions of patients with COPD received mechanical ventilation and intensive critical care [133–135]. Therefore, COPD is an independent risk factor for all-cause mortality in COVID-19 patients [136].

Similar collaborative COVID-19 studies have been conducted in the USA, Canada, Europe, China and Singapore. These meta-analysis studies show heterogeneity, investigating co-morbidities [137–140] was moderate for both COPD, and ongoing smoking history [141] in terms of the severity of COPD. COPD and ongoing smoking history are

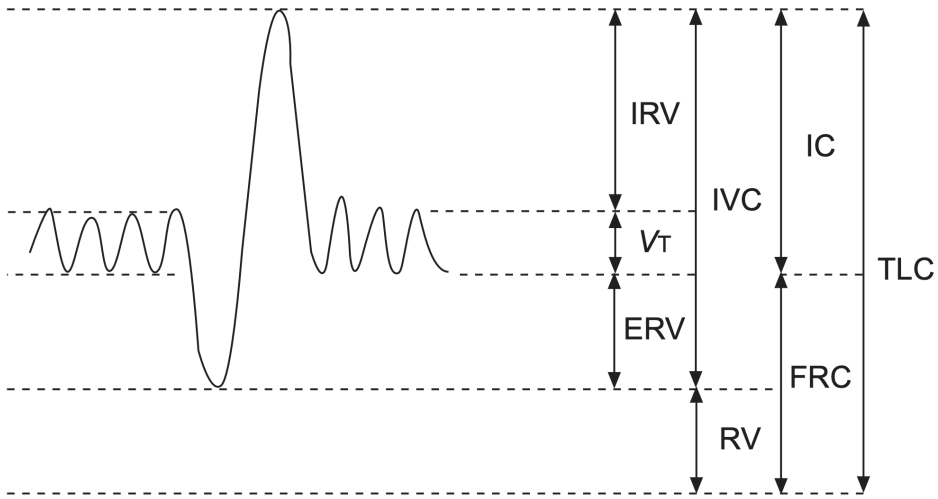

Figure 1.5: Static lung volumes and capacities based on a volume–time spirogram of an inspiratory vital capacity (IVC). IRV: inspiratory reserve volume; VT: tidal volume (TV); ERV: expiratory reserve volume; RV: residual volume; IC: inspiratory capacity; FRC: functional residual capacity; TLC: total lung capacity [150].

overall associated with worse progression and outcomes of COVID-19 [142–145]. The impact of the pandemic has also been felt by COPD patients due to a reduction in face-to-face clinic visits. Healthcare systems have been slow to adapt to these conditions [146].

1.4 Pulmonary Function Measurement

1.4.1 Lung Capacity Definitions

A healthy adult at rest has an average respiratory rate (RR) of 12 breaths per minute with 500mL tidal volume (V_T) [147–149]. A range of different measures are used to describe lung function and breathing, which are summarised in Figure 1.5.

Common measures of lung or breathing volumes/capacity include:

- *Minute ventilation*: The total volume inhaled and exhaled each minute. $MinuteVolume = RRxV_T$

- *Functional residual capacity (FRC)*: The amount of air remaining in the lungs post expiration during spontaneous, quiet breathing.

- *Inspiratory Capacity (IC) and Inspiratory Reserve Volume*: IC is the maximum volume of air which can be inhaled. The difference between the IC and V_T is known as the inspiratory reserve volume.

- *Expiratory Reserve (ER) and Residual Volume (RV)*: ER is the maximum volume of air which can be forcefully expired. RV is any remaining air volume after the ER volume has been forcefully expired. $ER + RV = FRC$

- *Vital Capacity (VC)*: The sum of the IC and ER, this represents the maximum theoretical volume which could be inspired in a single breath. $VC = ER + IC$

- *Total Lung Capacity (TLC)*: The sum of the IC and FRC, this represents the theoretical maximum possible volume capacity of lung. $TLC = FRC + IC$

- *Forced Capacities*: Forced capacities, such as forced VC (FVC) and forced expiration volume (FEV) are measures carried out under forceful breathing conditions.

FRC in particular is commonly used clinically to distinguish between various types of respiratory disease [151–154]. Direct measurements of FRC requires more specialist and invasive equipment than required for tidal volume measurements because it is impossible to expire the entire volume of the lungs. Thus, a spirometer is insufficient, and accurate measurement of FRC requires the use of full body plethysmography or a helium gas dilution test [155–159].

FRC is typically decreased by lung disease [160–162]. Lung fibrosis, a restrictive disease where the lungs have abnormally high elastic recoil, will cause a decrease in FRC. The reduction is due to the highly elastic lungs balancing with the opposing recoil of the chest wall at a lower lung volume. However, restrictive diseases caused by weakness of respiratory muscles do not affect FRC because the elastic forces are normal. This difference helps distinguish restrictive disease caused by lung fibrosis and muscle weakness. In emphysema, lung tissue involved in gas exchange is destroyed. This destruction reduces the lung's elastic recoil, increasing FRC. FRC can also be increased in obstructive diseases with high airway resistance like COPD and severe asthma. These diseases slow the rate of expiration, and the patient must breathe in before breathing out fully causing air trapping and leading to a rise in FRC and rising trapped CO_2.

1.4.2 Measuring pressure and flow

The breathing circuit including the lungs, airways, and any further resistance to airflow outside of the body due to, for example, spirometry devices, CPAP machines, or mechanical ventilators. Sensors can be introduced at various points in the breathing circuit to measure air pressure and flow, which can then be used to assess system properties [41, 59, 163–166]. These properties include:

- *Pressure*: Pressure sensors are typically piezoresistive transducers, which measure

deformation and potential difference via a electro-mechanical interface. Larger pressures cause greater deformations, which result in greater potential differences and higher sensor pressure readings. Some pressure sensors measure pressure difference between two locations, while others only measure from a single location. Sensors capable of measuring from two locations can be uni-directional, or bi-directional. A pressure drop across a component can be translated into a flow rate if the resistance of the same component is known. Spirometry uses pressure sensors measuring the pressure drop in the breathing circuit, and measured pressures are typically external. Using pressure as an input, and predicting resistance over time, enables flow rate and volume simulations in models [54,59,163,164,166–168].

- *Intrathoracic Pressure*: Intrathoracic pressure measurements are used to determine lung and chest wall mechanics, as well as work of breathing. Transpulmonary pressure, the difference between intrapulmonary pressure and pressure at the airway opening, is necessary for lung inflation. Obtaining direct pressure measurements inside the pleural cavity are highly risky as they require invasive procedures to open/puncture the chest wall, often changing respiratory system mechanics in the process, and introducing opportunities for infection and posing the risk of pneumothorax (lung collapse due to air in the pleural space). Oesophageal pressures are commonly used as a surrogate of pleural pressure, as it directly reflects pressure pleural cavity [169]. As pleural pressure varies within the pleural cavity, an oesophageal balloon sensor is typically placed in the lower third of the oesophagus to measure average pleural pressure [170], allowing the driving pressure of respiration to be estimated [25]. However, this measurement is highly invasive and not routinely used clinically.

- *Flow*: Airflow is commonly measured by hot-wire anemometers, orifice plate flow meters, and linear resistance pneumotachometers, or ultrasound flow meters [171].

Orifice plates and pneumotachometers applications are simple and easy to use, and operate via a known correlation between a measured pressure drop and known internal resistance. This approach is widely used in quantitative research and error is reduced to the error caused by the sensor itself, without compounding user error, such as might be the cause in ultrasound.

- *Volume*: Volume is calculated, by integrating flow rate with respect to time. Typically, the volume is measured relative to a reference volume, $V = 0$ at the start of inspiration, ignoring the volume of air already in the lungs and respiratory dead space. To directly measure the amount of air in the lung post expiration, invasive techniques are required, such as body plethysmography, nitrogen washout, helium dilution, and single-breath carbon monoxide (CO) uptake [172–175]. These techniques increase the risk of injury to the patient and offer relatively immaterial gain in terms of increasing the quality of data. As volume is calculated, researchers recognise error in volume data is inevitably caused by error in the flow data [172–175], and corrected by calibration.

1.4.3 Static vs. Dynamic measurements

When measuring lung mechanics, a static or dynamic approach can be chosen [176–180]. Static lung mechanics can be measured at a plateau or full occlusion during the respiratory cycle. In contrast, dynamic mechanics directly consider the effect of dynamic airflow and tissue velocity on tissue-mechanics. Lung mechanics have been shown to change during a breathing cycle as the lung tissue expands and contracts with inspired volume [40,41,54,181]. Tissue visco-elasticity is a further contributing factor to dynamic changes in lung properties [182–184].

1.4.4 Spirometry

Spirometry is a simple pulmonary test and an important tool in monitoring lung condition. It can be used to directly detect obstructive lung diseases, and rule out restrictive lung diseases. During spirometry, a subject breathes into a spirometer, a machine recording airflow, volume, and pressure at the mouth. The subject breathes into a mouthpiece, and typically wears a nose clip to prevent airflow from the nose, as in Figure 1.6.

Different breathing manoeuvres are used to assess whether a subject has reduced air flow or lung capacity, which would indicate possible respiratory disease. The simplest breathing manoeuvre in spirometry tests measures forced vital capacity (FVC). For this manoeuvre, the subject breathes a full lung of air, then exhales as forcefully as possible. Some of the major parameters measured by spirometry include the following:

- *Vital Capacity (**VC**)*: Maximal volume of air expired following maximum inspiration.
- *Forced Vital Capacity (**FVC**)*: Total volume of air forcibly exhaled after maximum inspiration.
- *Forced Expiratory Volume in 1 second (**FEV1**)*: Maximal volume of air forcibly expired the first second after maximal inspiration.
- *Functional Residual Capacity (**FRC**)*: Volume of air remaining in the lungs after forced expiration.
- *Residual Volume (**RV**)*: Volume of air remaining in the lungs after normal expiration.
- *Peak Expiratory Flow (**PEF**)*: Maximum flow rate in a forced expiration. Measured with a peak flow meter.

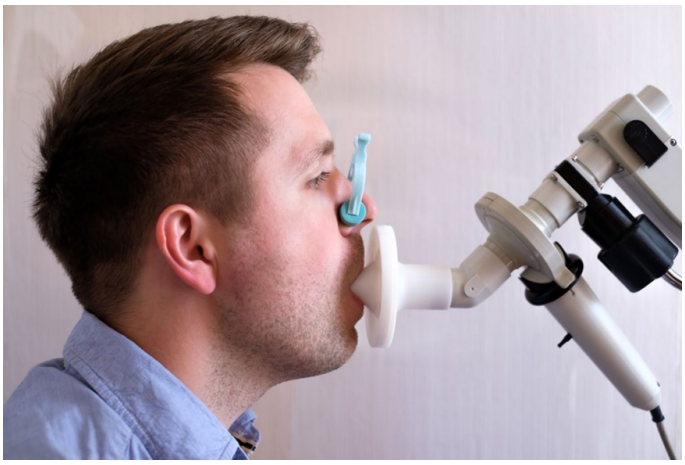

Figure 1.6: An example of a forced expiration test in spirometry [185].

- *Total Lung Capacity (**TLC**)*: Total volume of the lungs after maximal inspiration. The sum of RV and VC.

The results of spirometry are highly dependent on the patient's ability to cooperate or participate in the test [21]. Misdiagnosis can occur if the required manoeuvres are performed poorly or are unable to be repeated. For this reason, the elderly and children may not be able to participate effectively [29].

Spirometry results are compared against reference values for respiratory disease diagnosis [186]. A widely accepted standard for diagnosing COPD is the Global Initiative for Chronic Obstructive Lung Disease (GOLD) classification [187]. GOLD uses fixed cut-off values for FEV1/FVC to diagnose the severity of COPD by placing patients into one of four categories, from mild to very severe COPD. Additionally, GOLD specifies a recommended treatment plan for each level of COPD [188].

The ratio of FEV1/FVC is used to detect obstructive diseases. A rule of thumb is a FEV1/FVC ratio below 0.7 indicates an obstructive condition [189]. The use of fixed cut-offs causes misclassification of spirometric results, with a tendency to over diagnose

airway obstruction in the elderly and under diagnose in children [29,186,190,191]. This misclassification has led to debate around the efficacy of current spirometric standards to predict asthma, COPD, and other obstructive conditions [108,120,192,193].

Intermittent measurement of lung function is another limiting factor in diagnosis of some respiratory diseases. Asthma is a disease with reports of significant misdiagnosis [22–24]. Lung mechanics can appear normal in asthmatics between exacerbation events, further complicating diagnosis with spirometry [194]. As a consequence, physicians often recommend patients monitor peak expiratory flow at home as an alternative to spirometry [195].

1.4.5 Limitations of Spirometry in Restrictive disease

Spirometry is used to screen for restrictive disease, but cannot be used to diagnose restrictive disease. The notable characteristic of restrictive disease is a reduction in lung volume. Because spirometry is unable to directly measure RV or TLC, a decrease in FVC is used to detect possible restrictive lung patters. A decreased FVC can be caused by a decreased lung volume due to restrictive disease, but it may also be due to air trapping caused by airflow obstruction or an early termination of expiration (Figure 1.7). Due to this ambiguity, spirometry is reported to have a high sensitivity, but low specificity for detecting restrictive lung disease (low false negative and high false positive results) [196]. Therefore, spirometry is used as a screening tool to rule out restrictive disease. To diagnose restrictive diseases, direct measurements of TLC is needed [197].

1.4.6 Occlusion technique

Spirometry can identify the presence of airway obstruction using maximal flow efforts. However, the manoeuvres of forced expiration and inspiration can be difficult for small

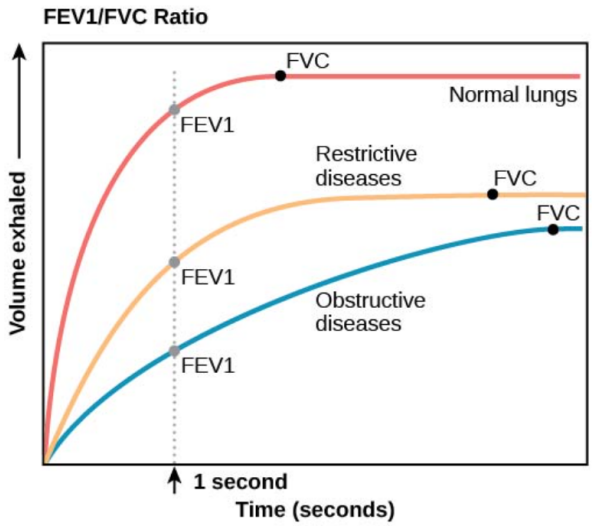

Figure 1.7: FVC cannot be used alone, to diagnose restrictive disease. Both restrictive and obstructive disease can reduce FVC [198].

children, or other patients with limited levels of cooperation [199–203]. Another way of identifying airway obstruction is to measure airway resistance. An obstructed airway will have a larger than normal resistance. A method of measuring airway resistance is the interrupter technique [30, 204]. This method blocks airflow during tidal breathing, which will cause a pressure drop equal to the airway resistance to flow. The interrupter resistance (R_{int}) is calculated by dividing the pressure difference by the pre-occlusion flow.

The flow and pre-occlusion pressure at the mouth are easily measured during the interrupter technique, but the alveolar pressure must be derived from the varying mouth pressure during the brief (approximately 100 ms) interruption of breathing. Immediately after occlusion, there is a rapid change in pressure followed by pressure oscillations and, finally, a slow pressure rise. R_{int} can then be derived from back extrapolation of the slowly rising pressure. This method relies on assuming lung and mouth pressures equalise quickly after occlusion. The results is R_{int} tends to underestimate resistance

for cases of severe airflow limitation [205].

1.4.7 Weighted spirometer technique

Weighted spirometry is a very uncommon test, which measures lung elastance [206–209]. During this test, the subject breathes into a closed system spirometer. During tidal breathing, weights are added to the spirometer bell to increase pressure in the spirometer by a small amount. The increased end expiratory pressure will hold a small volume of air in the lungs after expiration. The volume of air held in the lungs will depend on the amount of elastic recoil in the lungs: $\Delta\ V = \frac{\Delta\ P}{E}$. The elastance is obtained from this method is "quasi-static" because the subject still breathes spontaneously during the measurements. An assumption of this method is the chest wall muscles are completely and equally relaxed at the end of each breath [31, 210]. A similar approach to weighted spirometry has been shown to measure elastance and transpulmonary pressure during mechanical ventilation. This method measured the volume retention caused by PEEP changes [211].

1.4.8 Forced oscillation technique

The forced oscillation technique (FOT) measures respiratory system resistance and reactance [212]. This method superimposes high frequency oscillations on inspired air. Measurements are taken across a range of frequencies to assess the resistance at different branch levels of the airways [213, 214]. The resistance measured by FOT has contributions from both the lung and chest wall. The main benefit of this technique is complex manoeuvres are not required, although it does interrupt breathing and require more extensive equipment not typical of home care. Hence, it is possible to monitor lung mechanics in patients who are uncooperative or unable to participate in standard

spirometry, such as young children [215], but the method is intensive.

1.4.9 Plethysmography

Modern plethysmography started with DuBois et al in 1956 [32]. Whole body plethysmograph uses a sealed, glass walled box with a volume of 700-1000L. The subject sits inside the box during measurements. To account for slow pressure changes, such as the temperature in the box increasing during measurement, a controlled leak in the seal is used to stabilise the box's internal pressure. Two pressure sensors are used in plethysmography. One measures the pressure in the box relative to atmospheric pressure, the other measures pressure at the subject's mouth. A shutter mechanism placed after the mouth pressure sensor is able to completely block air flow during what is known as a shutter manoeuvre [216].

Plethysmography relies on measuring changes in box pressure in conjunction with changes in mouth pressure and flow rate. The underlying principle in plethysmography is Boyle's law in (Equation 1.2), which states relative changes in the volume inside a closed compartment are equal in magnitude and opposite in sign to the relative pressure changes within the same compartment. This assumption allows plethysmography to provide information on lung residual volume (RV), total lung capacity (TLC), airway resistance, and intra-thoracic gas volume (ITGV) during tidal breathing [32, 217].

During inspiration, the lung volume increases. However, airflow into the lung is not instantaneous because a pressure gradient between the lung and surroundings is required to create air flow. Thus, airway resistance causes airflow to lag behind lung volume. If the airways had no resistance, airflow would be infinite and pressure equalisation would be instantaneous. On the other hand, if the airways were occluded, such as during the

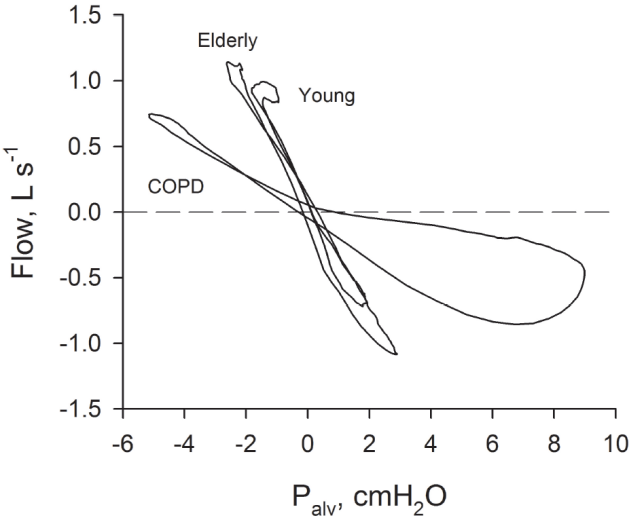

Figure 1.8: Plethysmography results showing gas trapping of a COPD patient, compared to healthier young and elderly patients [219].

shutter manoeuvre, pressure inside the lung would decrease due to inspiratory effort, but there would be no airflow. The small lag observed between airflow and lung volume during tidal breathing is called the "shift volume". During inspiration, the shift volume establishes the pressure drop required in the lung to drive inspiratory airflow. However, a disadvantage of using airway resistance to monitor the effect of intervention, is its low sensitivity. It requires relatively large changes (35 - 65%) to detect a significant response [218].

Figure 1.8 is a pressure flow diagram indicating the results from plethysmography for three separate patients. The change in slope of the result for the COPD patient indicates a change in elastance and the lobe shape is indicative of gas trapping [219].

1.4.10 Gas dilution

Respiratory diseases reduce the efficiency of gas transfer in the pulmonary capillaries. A reduction in gas exchange can be due to either a decrease in surface area of lung tissue or reduced airflow, or a combination of both. Gas diffusion testing uses a tracer gas to

measure the level of gas exchange in the lungs [28, 29]. A notable feature of COPD is air trapping, where a large amount of air is retained in the lungs after exhalation. This trapping leads to hyperinflation and CO_2 build-up in the lungs. Spirometry detects air trapping by measuring decreased FVC and FEV1. However, air trapping can only be confirmed by further tests, most typically invasive CT scans [220].

As full lung deflation cannot be achieved by forced expiration alone, indirect methods must be used to determine residual volume and end-expiration lung volume (FRC). Gas dilution is one method of measuring FRC, and involves diluting a known concentration and volume of inert gas with the air in the lungs [221–224]. However, this measurement is entirely dependent on the marker gas and lung gas mixing together completely. Diseases which create poor gas flow in the lungs, such as COPD, asthma, bronchitis, emphysema, pulmonary fibrosis, cystic fibrosis, lung cancer, pneumonia or pulmonary embolism will generally have inaccurate FRC estimates using this method, with the true FRC generally being underestimated [225–227].

Two gas-based techniques are used to measure FRC. The closed circuit re-breathing of an inert gas such as helium, or the wash in/out of an inert marker gas, which is normally present in the lung, such as nitrogen. Both of these techniques have been used for decades and have known limitations [228–230], namely complexity and difficulty of operation, expense, unreliable measurement of FRC in some patients, and the tests are time consuming and can be uncomfortable for the subjects [231–234].

1.5 Summary

Respiratory diseases are a significant problem in today's healthcare context, and are often preventable or can be mitigated through early intervention. To date, pulmonary function can be difficult or burdensome to measure significantly, limiting early diagnosis and monitoring.

The aim of this research is to develop model-based methods to assist in the diagnosis and monitoring of respiratory conditions, with a focus on COPD in particular. In the long run, this research aims to contribute to the development of a low-cost, portable or non-invasive approach to obtaining crucial lung health metrics. This thesis will explore model-based approaches to describing lung function, and apply them to outpatient respiratory care.

1.6 Preface

The remaining thesis chapters cover this topic as follows:

- Chapter 2 presents an overview of the current lung modelling approaches, as a method to quantify disease state in respiratory illness. It also derived the main models used in this research with relevant added terms.
- Chapter 3 will contain the clinical data used for all analyses in this thesis.
- Chapter 4 presents a proof of concept model identifying a nonlinear expiratory resistance in COPD patients using plethysmographic alveolar pressure.
- Chapter 5 explores the quantification of the nonlinear expiratory resistance in COPD patients.

- Chapter 6 examines the patient effort as elastive and resistive work of breathing in COPD patients.
- Chapter 7 analyses nonlinear expiratory effort using mechanical ventilation (MV) data.
- Chapter 8 investigates the presence of nonlinear resistance in expiration for patients undergoing MV, through a novel, model-based approach.
- Chapter 9 explores identifying patient effort with model-based estimation in patients undergoing MV.
- Chapter 10 summarises the conclusions drawn from this thesis.
- Chapter 11 explores and examines potential avenues for future work.

CHAPTER 2: MODEL

2.1 Introduction

The energy or work done by the pulmonary system to alter pressure inside the lungs depends on lung ability to stretch (elastance) and the resistance to airflow through the airways (resistance) [40, 235]. Healthier lungs have lower elastance and resistance compared with lungs of patients with respiratory disease. Disease can increase either both or one of these lung mechanics [68]. Increasing either elastance or resistance increases the energy required to maintain the same volume and flow of air.

This chapter explores different modelling approaches, and presents the basic model used in the rest of this thesis. Common to most of the modelling approaches is the quantification of lung mechanics via elastance and resistance parameters. These parameters, and their deviation from normal values in dysfunction, are important in the model-based diagnosis and monitoring of respiratory disease and its progression in response to care.

2.2 Review of Lung Modelling Approaches

Previous research shows the respiratory system can be modelled in various ways, from simple linear single compartment models to much more complex airway branching models [38, 40, 41, 54, 59, 164, 167, 181, 236–238]. One extreme end includes detailed finite

element analysis (FEA) of lung structure and function, including gas flow and exchange [46, 47, 61, 239–243]. Model complexity depends on model purpose, where clinically useful models are generally much simpler, and more easily tailored to individual patient characteristics, as they must rely on clinically available data [59, 236].

2.2.1 Complex Finite Element Models

Complex finite element pulmonary mechanics models, referred to as FEA (Finite Element Analysis) models are powerful computational tools which can be used to simulate the behaviour of the lungs in various conditions and provide insight into the effects of disease and drugs on the pulmonary system [244, 245]. These models are based on a numerical technique used to approximate and solve complex problems of spatial and time-varying mechanics in engineering and science [246]. The models can be used to study fluid-structure interaction between the airway walls, air flow, and tissue properties, as well as the effects of disease on the lung mechanics [247].

The models are highly complex and require advanced programming and numerical techniques to be used effectively [246]. The complexity of the models also means it can take a long time to simulate the different conditions and to get accurate results [245], limiting real time clinical utility. However, the results obtained can be extremely useful in understanding the behaviour of the lung mechanics and in designing treatments for various diseases in a general, non-patient-specific sense [247]. These models can also be used to predict the effects of different drugs on the lung mechanics, as well as to study the effects of age on the pulmonary system [244].

Many of these more complex pulmonary FEA models have been developed [240–242, 248–250], and typically use a high level of detail, produced from computed tomography

scans, or other similar medical imaging, as inputs. FEA models such as these, have also been used to simulate progression of disease [251]. However, these models fail to provide personalised results, as they are unidentifiable with the available data due to their large number of parameters [252–254].

An example of a FEA model used to simulate lung displacement changes is shown in Figure 2.1. Such a model shows the potential for detailed understanding of anatomical structures and their behaviour. However, personalisation of such models requires dense high-quality data for identifiability, and such models often rely on the applicability of underlying assumptions and boundary conditions.

2.2.2 Elastic-Resistive Models

Single Compartment Model The first single compartment model was developed in the 1950's [256]. While a very simple model, it describes the respiratory system as a resistive component representing all the airways, combined with an elastic component representing the lungs. It is fully identifiable, and thus readily personalised [40,41,54,181,236].

Lung elastance is a measure of how lung stiffness, where a highly elastic lung will require more force to deform to a certain volume. In mechanical engineering terms, this can be likened to a spring constant. Clinically, compliance, the inverse of elastance, is often used to describe lung stiffness. Mathematically, elastance is defined as the change in pressure in the lung per unit of volume:

$$Elastance = \frac{\Delta Lung\, pressure}{\Delta Volume} \tag{2.1}$$

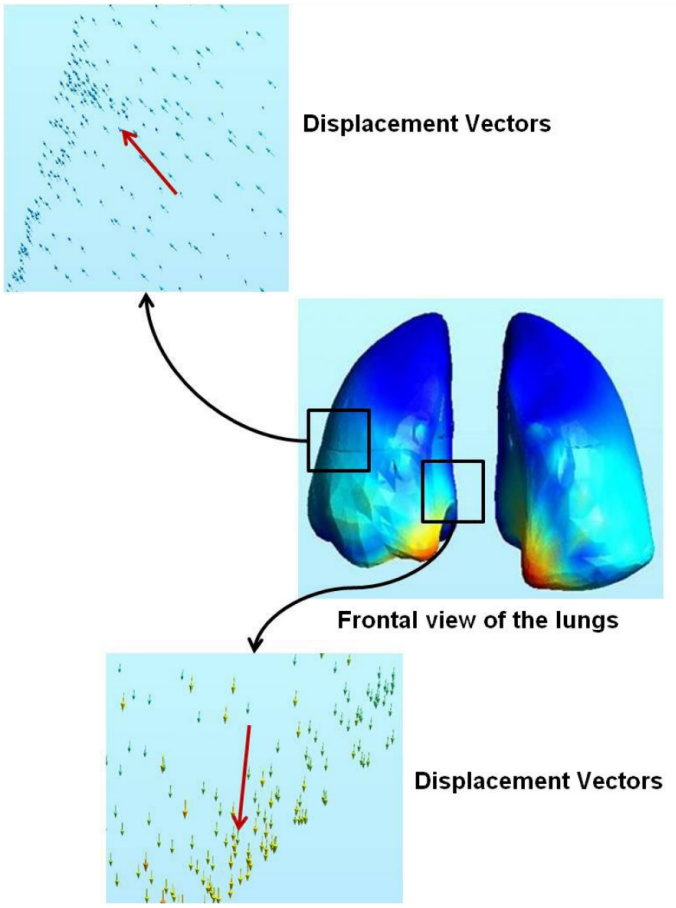

Figure 2.1: Displacement vectors modelled with FEA at different locations in the lung. The two red vectors represent the mean orientation of the displacement vectors at a high level of the lungs (upper view) and at a low level of the lung near the diaphragm (lower view) [255].

A lung with high elastance will have increased stiffness. In diseases such as fibrosis, high lung elastance is often observed [257–260], resulting in higher work of breathing compared to healthier patients, particularly during inspiration. In contrast, a lung with low elasticity is pliable and, if elastance is too low, it can fail to return to its resting position. One example is emphysema [261–264], a disease characterised by alveolar damage, where extra energy is required to expire air from the lungs. The low lung elastance is caused by collapsed alveoli, which will not be re-opened without a large amount of pressure [51].

Respiratory elastance is generally defined as the summation of lung and chest wall contributions, which are generally linear with volume during quiet tidal breathing [40, 41, 54, 181]:

$$E_{rs}(t) = E_{chest} + E_{lung} \tag{2.2}$$

Resistance causes a pressure drop across the airways, with typical units of pressure drop per unit flow rate:

$$Resistance = \frac{\Delta Pressure}{Flowrate} \tag{2.3}$$

For a sedated patient on mechanical ventilation with no patient-derived work of breathing, the Equations 2.1 and 2.3 combine to form the widely used and clinically accepted linear single compartment lung model defined [2, 25, 265–269]:

$$P_{aw}(t) = R_{rs}Q(t) + E_{rs}V(t) + P_0 \tag{2.4}$$

where P_{aw} is the inspiratory airway pressure, t is time, E_{rs} is the respiratory system elastance, R_{rs} is the combined resistance of the conducting airway and endotracheal tube, V is volume, Q is flow, and P_0 is the offset or positive end expiratory pressure, PEEP [2].

This model describes airway pressure as the sum of two pressures in the respiratory system. $R_{rs}Q(t)$ defines the pressure dissipated due to airflow through the airways and the endotracheal tube, and $E_{rs}V(t)$ defines the alveolar pressure created by the lung's elastic recoil. This model assumes air flow measured at the airway opening is equal to airflow at all points in the respiratory system. For any breathing cycle, time varying or

constant values for inspiratory E_{rs} and R_{rs} can be identified using a linear least squares fit to measured P_{aw}, V and Q during inspiration [40].

This model has been shown to effectively estimate lung mechanics for fully sedated, mechanically ventilated (MV) patients, but it does not produce reasonable parameter estimates for MV patients with lower sedation levels who are actively participating in breathing [40, 164, 166, 270–272]. Determining passive lung mechanics during spontaneous breathing requires additional equipment or invasive manoeuvres [273, 274]. Measuring oesophageal pressure is one method to determine mechanics during spontaneous breathing [275].

Anatomically Varying Resistance Model

While airways are often described as having an overall airway resistance, resistance values can be calculated for each of the 23 stages of airway branching. One airway resistance model describes each generation as having a different resistance depending on the airway length and diameter [276, 277]. Figure 2.2 describes airway resistances for a healthy patient and patients in intensive care as an example of how much resistance can vary when disease is introduced.

Time-varying elastance model

Lung mechanics vary with time, even within a breath [40, 41, 54, 181, 278]. Previous research in the intensive care context has extended the standard single compartment model in Equation 2.4 to include a time-varying respiratory elastance [40,54]. The model has been used in several studies and shown to capture and provide an understanding of lung mechanics in both sedated and spontaneously breathing (SB) mechanically ventilated patients [40, 41, 279, 280].

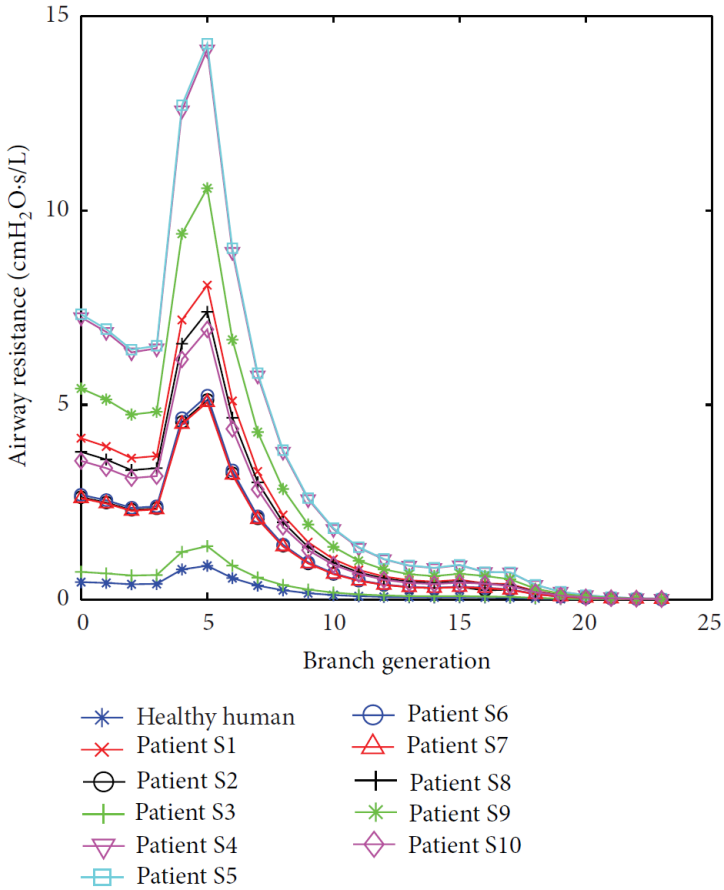

Figure 2.2: Airway resistance at each lung generation for a variety of patients [25].

The driving pressure is a function of the intrapleural pressure, P_{pl}. Clinically, it can only be measured with the use of oesophageal pressure, which is difficult and clinically burdensome. P_{pl} is divided between two pressure components in the time-varying elastance model. P_{chest} is the patient-specific pressure in the chest wall, dependent on patient position and weight and P_{demand} is the variable pressure changes dependent on patient breathing effort.

$$P_{pl}(t) = P_{chest}(t) + P_{demand}(t) = E_{drs}(t)V(t) \tag{2.5}$$

These pressure components are both generally proportional to the air volume en-

tering the lung, so each pressure can be represented as a combination of an elastic component and air volume.

$$E_{drs}(t) = E_{chest} + E_{demand} + E_{lung} \tag{2.6}$$

To maintain structural identifiability of Equation 2.5, the elastance terms are combined into one time-varying elastance, E_{drs}. In any breathing cycle, E_{drs} captures the combined effect of the driving elastance and lung elastance. It is assessed as the change in pressure for a given tidal volume of flow [40, 41, 54, 181].

$$P_{aw}(t) = R_{rs}Q(t) + E_{drs}(t)V(t) + P_0 \tag{2.7}$$

When a patient is fully sedated and with no patient effort ($E_{demand} = 0$), dynamic elastance represents lung and tissue dynamics over the breath, capturing visco-elastic and alveolar recruitment/de-recruitment or distension effects [236]. Lung elastance falls if new alveoli are recruited faster than pressure can build up in the lung. If pressure is increased and elastance increases, indicating the increase in pressure was unable to recruit a significant number of new alveoli, and instead the additional pressure is beginning to stretch already recruited alveoli and lung airways [281].

Iso-volumetric Elastance

Treating elastance as iso-volumetric assumes elastance is equal across isovolumes for inspiration and expiration. This assumption enables a quasi-static analysis of lung elastance from dynamic P-V loops, and is sometimes used in analysis of mechanical ventilation data [282–287]:

$$P_{aw}(t) = R_{rs}Q(t) + P_{DNS} \tag{2.8}$$

Assuming the dynostatic curve is the same during inspiration and expiration at iso-volumes, yields:

$$P_{aw,insp}(V) - R_{rs}Q(V) = P_{aw,exp}(V) - R_{rs}Q(V) \tag{2.9}$$

Equation 2.9 can be re-arranged for R. Iso-volumetric analysis is limited to sedated and non-spontaneously breathing mechanically ventilated patients, as in this context, $P_{DNS} = P_{alv}$. Spontaneous breathing requires the addition of an additional term:

$$P_{aw}(t) = R_{rs}Q(t) + P_{DNS} + P_{demand} \tag{2.10}$$

SLICE method

A method developed by Guttmann et al. (1995), incorporating the non-linearity found in the physiology of the lung in operation. Nonlinear, volume dependent lung mechanics present a challenge when attempting to fit clinical data to a model. The SLICE method applies a piece-wise approximation of lung mechanics by splitting the tidal volume into singular 'slices' with a single resistance and single compliance value per 'slice'. A combination of each individual 'slice' forms a quasi-dynamic compliance and resistance model. Further linearisation of the problem results in the Rohrer equation implementation for the calculation of tracheal pressure as opposed to airway pressure. Equation 2.13 is thus modified:

$$P_{aw,slice}(t) = \frac{V_{slice}(t)}{C_k} + Q_{slice}(t)R_k + P_k \tag{2.11}$$

where $P_{aw,slice}$, Q_{slice}, and V_{slice} are the pressure, airway flow and volume for a singular slice respectively.

Visco-elastic modelling

The Bates visco-elastic model [2] demonstrated in Figure 2.3 provides a comprehensive representation of the complex mechanical coupling between all of the elements in the airway tree, composed of a single conduit and three elements: resistance (R_{aw}), R_t, E_1, and E_2. The E_1 spring represents the static elastic behaviour of the lung, while the series combination of R_t and E_2 accounts for its visco-elastic behaviour.

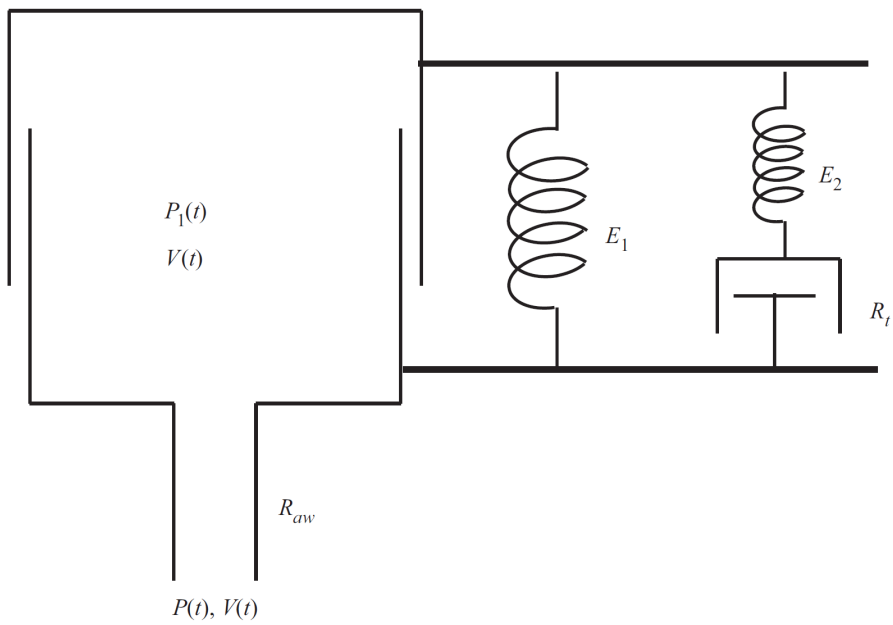

Figure 2.3: The Bates viscoelastic model [2] with two degrees of freedom.

The resulting equation of motion for the visco-elastic model is:

$$R_t\dot{P}(t) + E_2P(t) = R_{aw}R_t\ddot{V}(t) + (E_1R_t + E_2R_{aw} + E_2R_t)V(t) + E_1E_2V(t) \quad (2.12)$$

Visco-elastic models such as the Bates model [2] shown in Equation 2.12 have limitations [288–293] such as:

- The model assumes the lung tissue is homogeneous, isotropic and linear, which

may not be the case for all individuals.

- The model does not take into account the effects of airway closure and airway resistance, which can affect lung mechanics.
- The model is limited in its ability to account for the effects of different types of lung diseases and the changes in lung mechanics resulting from them.
- The model does not take into account the effects of patient-specific factors such as age and body size.
- The model does not account for the effects of inspiratory muscle strength, which can affect lung mechanics.
- The model does not consider the dynamic interaction between the lung parenchyma and the other components of the respiratory system.

The Inspiratory Demand Modelling Problem

The inspiratory demand modelling problem is a challenging problem in respiratory physiology, which seeks to identify the underlying mechanisms controlling a patient's breathing. The challenge lies in identifying the relationship between the various physiological parameters, such as the respiratory rate and tidal volume, and the underlying control mechanisms. Various models have been proposed to address this problem, but their accuracy and reliability are limited due to the difficulty in modelling spontaneous breathing patterns and disruptions to model identifiability [294–296].

The inspiratory demand modelling problem is a complex problem as it involves identifying the underlying physiological mechanisms that control a patient's breathing. The complexity arises from the fact that the respiratory parameters, such as the respiratory rate and tidal volume, are affected by a variety of physiological factors, including neural, chemical and mechanical processes. Various models have been proposed to address this

problem, such as the neural feedback model [294] and the mechano-chemical model [295]. These models attempt to identify the relationship between the various physiological parameters and the underlying control mechanisms.

However, the accuracy and reliability of these models is limited due to the difficulty in modelling spontaneous breathing patterns. Spontaneous breathing patterns are complex, unpredictable and can vary significantly between individuals. This makes it difficult to accurately model the dynamics of the respiratory system and to predict the response to external stimuli. As a result, the accuracy and reliability of existing models is limited.

In addition to the difficulty in modelling spontaneous breathing patterns, disruptions to model identifiability can further complicate the inspiratory demand modelling problem. Such disruptions can arise from changes in the patient's physiology, such as changes in lung mechanics or neuromuscular disease [296]. These changes can alter the underlying control mechanisms and make it difficult to accurately identify the relationship between the physiological parameters and the underlying control mechanisms. Further research is needed to improve the accuracy and reliability of existing models and to develop new models that can better account for the complexity of the respiratory system.

Models with time varying E have previously captured spontaneous breathing mechanics, but are unable to differentiate elastic and demand components [297–300]. All models relying on MV data with significant WOB carried out by a ventilator, include assumptions quantifying passive breathing.

2.2.3 Lung Modelling Approach Summary

To summarise, FEA models are powerful modelling tools providing an insight into the behaviour of respiratory disease affected lungs. However, these models are unsuitable for providing identifiable patient-specific metrics useful in clinical application to personalise care. Single compartment models must be modified for use with spirometry, allowing patient-specific metrics to be identified from tidal breathing without the use of difficult to perform breathing manoeuvres. Further chapters describe a novel method using plethysmographic data as a step toward achieving this outcome.

2.3 Model Development

2.3.1 Full model derivation

The methodology of this thesis builds upon the ubiquitous linear, single-compartment model [2, 25, 265–269], defined:

$$P_{aw}(t) = EV(t) + RQ(t) + P_0 \tag{2.13}$$

where $P_{aw}(t)$ $[cmH_2O]$ is pressure at the airway opening, $Q(t)$ $[L/s]$ is airflow defined positive for inspiration, R $[cmH_2O/L/s]$ is airflow resistance, $V(t)$ $[L]$ is tidal volume, E $[cmH_2O/L]$ is lung elastance, P_0 is the end-expiratory pressure and t $[s]$ is time. This single compartment model assumes no change in pleural pressure relative to alveolar pressure, causing inspiratory drive, and thus is only applicable for non-spontaneous breathing.

A modified single compartment model is presented in Figure 2.4, as a lumped alveolar volume with tissue elastance (stiffness) E $[cmH_2O/L]$ and an airway resistance

R $[cmH_2O/L/s]$. A surrogate term incorporating breathing effort is included via the transpulmonary pressure, which is the difference between alveolar pressure, P_{alv}, and pleural pressure, P_{pl}. The transpulmonary pressure difference across the lung wall is assumed to follow Hook's law [2]:

$$P_{alv}(t) - P_{pl}(t) = EV(t) \tag{2.14}$$

Where P_{pl} is modelled as a pressure deviating from a starting value of atmospheric pressure and is represented as a signal generator in the electrical circuit analogy in Figure 2.4. The pressure drop across the airways is defined as a function of flow rate:

$$P_{aw}(t) - P_{alv}(t) = RQ(t) \tag{2.15}$$

Thus, the single compartment model of 2.13 is shown to become:

$$P_{aw}(t) = EV(t) + RQ(t) + P_0 + P_{pl} \tag{2.16}$$

in the presence of breathing effort.

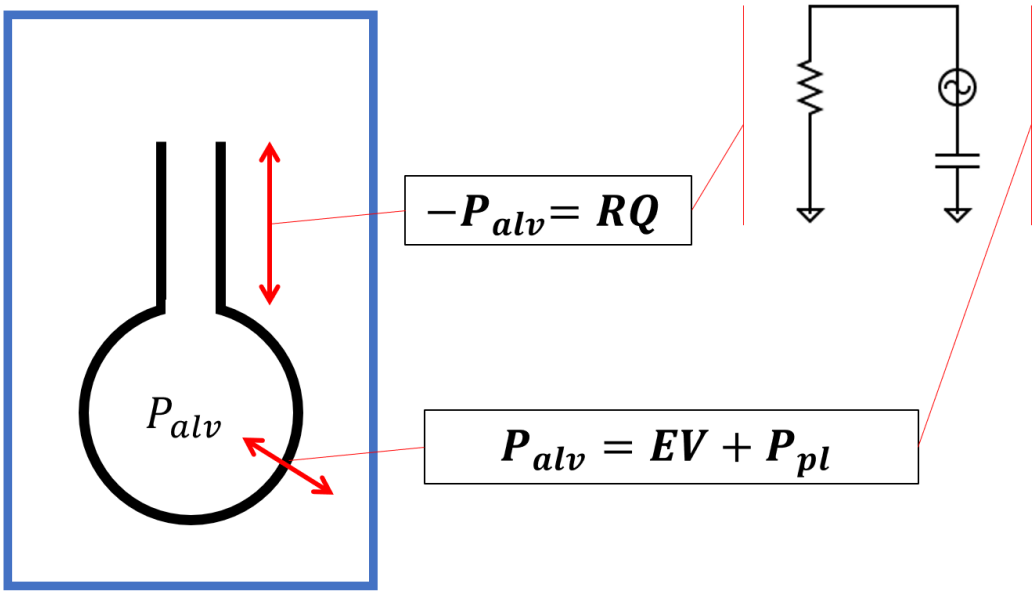

Figure 2.4: Single compartment model of spontaneous breathing.

2.3.2 Adaptation for Plethysmography

During clinical plethysmography, alveolar pressure (P_alv) and airway flow are measured [216, 219, 301–303]. In addition, there is no externally applied end expiratory pressure (P_0), and P_{alv} is calculated relative to the atmospheric pressure [219, 302], which also represents the pressure at the airway opening. Thus, Equation 2.16 becomes:

$$P_{aw}(t) = EV(t) + RQ(t) + P_{pl} \tag{2.17}$$

Measurement of alveolar pressure decouples E and R, enabling separate identification of both of these terms from the alveolar pressure data. Thus, Equations 2.14 and 2.15 reducing to yield:

$$-P_{alv}(t) = RQ(t) \tag{2.18}$$

$$P_{alv}(t) = EV(t) + P_{pl} \tag{2.19}$$

For $-P_{alv}$ $[cmH_2O]$ defined relative to $P_{atm} \cong 0$. Thus, plethysmographic measurements of alveolar pressure are commonly combined with a model-based approach to evaluate airway resistance. This linear model formulation holds resistance constant over the inspiratory and expiratory periods, and thus may not fully capture airway dynamics in COPD patients, where expiratory resistance can be volume dependent and nonlinear [216, 219, 302–304].

2.4 Non-linear Resistance Model

It is hypothesised a non-linear resistance is required to capture the non-linear airway behaviour during expiration in flow limited patients. The non-linear resistive model incorporates the constant linear term ($R_{1,insp}$) identified during inspiration (Q_{insp}) alongside an additional dynamic resistive term ($R_{exp} = \sum R_2\Phi(t)$), during expiration. Thus, Equation 2.15 becomes:

$$-P_{alv}(t) = R_{1,insp}Q_{insp}(t) + \left[\sum_{i=1}^{M} R_{2,exp,i}\Phi_{i,d=2}(t)\right]Q_{exp}(t) \tag{2.20}$$

where R_{exp} is modelled using M 2nd order ($d = 2$) b-spline functions to fit the unknown shape function, capturing any non-linear, time-varying dynamics during expiration. The second order b-splines are defined over time [164, 167, 270], with T equally spaced time points:

$$\Phi_{i,0}(t) = \begin{cases} 1 & T_i \leq t \leq T_{i+1} \\ 0 & otherwise \end{cases}$$

$$\Phi_{i,d}(t) = \frac{t - T_i}{T_{i+d} - T_i}\Phi_{i,d-1}(t) + \frac{T_{i+d+1} - t}{T_{i+d+1} - T_{i+1}}\Phi_{i+1,d-1}(t) \; for \; d \geq 1 \tag{2.21}$$

Where $R_{2,exp,i}$ are constant coefficients of these splines identified using the linear least squares method from measured data. The number of 2nd order ($d = 2$) splines with knot width (k_w) of 0.01s and a maximal spline timespan for expiration are defined:

$$M(n) = ceil\left(\frac{T_{max}(n)}{k_w}\right) + d \tag{2.22}$$

2.5 Inspiratory Demand and Work of Breathing

Current Plethysmographic methods do not directly capture breathing effort as the demand required to overcome both elastic and resistive components. This section presents a simple method for modelling this effort from Plethysmographic data. If the pleural pressure is used as a surrogate for inspiratory effort, Equation 2.19 can be rewritten:

$$P_{alv}(t) = EV(t) + P_{eff} \tag{2.23}$$

where P_{eff} is the pressure dynamic in the pleural cavity representing breathing effort, and E (cmH_2O/L) is tissue elastance. The P_{eff} term is modelled using the b-spline basis functions defined previously in Equations 2.21 and 2.22. Inspiratory breathing effort (P_{eff}) and E trade off parametrically in Equation 2.23. Thus, E is identified from expiration data under the assumption of passive expiration. Expiration is generally passive, driven by the elastic recoil of the lung, diaphragm, and chest wall. How-

ever, in COPD patients, particularly those with FL at end-expiration, there can be end-expiratory forced breathing effort to assist in tidal volume clearance and to avoid gas trapping. During inspiration, the relaxation time constant for muscles involved in breathing effort causes negative P_{eff} generated during inspiration to decay.

Thus, E is estimated from the middle portion of expiration, defined as 5 points either side of peak expiratory flow (T_{Qpeak}).

$$EV(T_{Qpeak} - 5 : T_{Qpeak} + 5) = P_{alv}(T_{Qpeak} - 5 : T_{Qpeak} + 5) \tag{2.24}$$

Work of breathing (WOB) is calculated as the integral of pressure volume:

$$WOB = \int_{insp} -P_{eff}\, dV \tag{2.25}$$

For ease of interpretation and presentation, in Equation 6.10, the WOB is now defined as positive (for a negative P_{eff} pressure signal). WOB breathing to overcome the elastic and resistive dynamics respectively are defined:

$$WOB_E = \int_{insp} RQ\, dV \tag{2.26}$$

$$WOB_R = \int_{insp} EV\, dV \tag{2.27}$$

2.6 Summary

This chapter presented an overview of the current lung modelling approaches, as a method to quantify disease state in respiratory illness. It also derived the main models used in this research with relevant added terms. The following chapter presents the data to which this model is applied and further developed.

CHAPTER 3: CLINICAL DATA

3.1 Introduction

This chapter presents the clinical data used in this thesis. Three data sets are used, referred to as the 'Literature data', 'Italy data', and 'MV data' sets, respectively. These three data sets span outpatient (Literature/Italy) and critical care mechanical ventilation (MV), enabling model-based methods to provide insight into each of these different clinical scenarios. The Literature data set was used to propose a novel proof of concept, the Italy data set was used to optimise the parameters of the proposed model and the MV data set was used to further evaluate nonlinear model-based methods.

More specifically, the Literature data set consists of observations from published studies. The Italy data set consists of observations from a prospective, observational, multicentric study conducted in Italy. The MV data set consists of observations from an observational study conducted in a critical care setting in Greece.

The first data-set was obtained using software which creates data points from graphically presented results called Engauge Digitizer (Open Source) [305](2022). The second, more comprehensive data-set was obtained from the Pecchiari et al. (2016) research group in Milan, Italy and is referred to as 'Italy data'. The MV data set was obtained from the Dimitrios et al. (2023) research group in Greece.

3.2 Literature data

The 'Literature data' was acquired from Radovanovic et al. (2018). Publication of full pressure-flow loops are unusual in the literature, and this data represents the clinical consensus on 'typical' healthy and COPD subjects. Pressure and flow (PQ) data, were obtained for a young healthy adult, and an adult with severe COPD [219] using Engauge Digitizer (Open Source) [305]. Further clinical details can be found in [219]. Radovanovic et al. (2018) present alveolar pressure (P_{alv}) and flow at the airway opening (Q), per standard plethysmographic analysis. P_{alv} is derived from changes in barometric pressure inside the plethysmography box using Boyle's law [216]. Use of Boyle's law implicitly treats the lungs as a single volume with a uniform pressure, P_{alv}, representing the average alveolar pressure across the entire lung.

As a proof of concept, these two patient states were interpolated to generate a fuller range of possible patient conditions between the healthy (here referred to as Patient 1) and COPD (Patient 7) patient disease states. Five intermediate patients (Patients 2-6) were generated by evenly spaced weighted averages of Patients 1 and 7. This data set provides a controlled environment method for testing a model on 'virtual patients' spanning two clinical extremes. In particular, it may provide insight to early onset COPD, and thus is used for development of a proof of concept model. Such a model would test utility on a range of possible disease states to assess resolution of identified model parameters as model-based markers of disease state.

3.3 Italy data

Plethysmographic data from 100 subjects, including 40 healthy subjects and 60 COPD patients, were collected in a previous study [301, 302] focused on COPD and pulmonary function testing. Full study methodology and details can be found in [301, 302], describ-

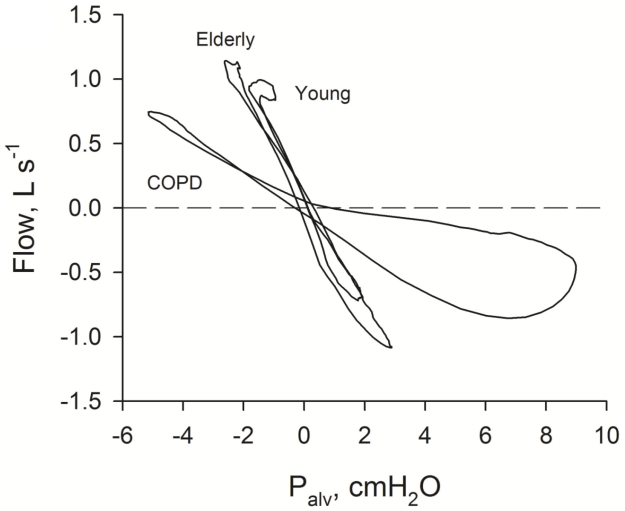

Figure 3.1: Pressure-flow (PQ) loops from the Radovanovic et al. (2018) study depicting a loop for a Young, Elderly and COPD patient.

ing 4 cohorts: 20 Young (20-32 years) and 20 Elderly (64-85 years) healthy subjects, and 60 COPD patients (age > 50 years), 25 with no expiratory flow limitation (NFL) and 35 patients with expiratory flow limitation (FL). Flow limitation was assessed by the NEP method [304, 306], where a -5 cmH_2O pressure was applied at the mouth during quiet breathing, and flow-volume (QV) loops of control and applied NEP breaths were compared. Patient demographics can be found in Table 6.1. Both healthy cohorts were confirmed to have no flow limitation via NEP.

Plethysmographic data from the Pecchiari et al. (2016) study were collected using a constant volume Plethysmograph (MasterScreen Body Plethysmograph, Erich Jaeger CmbH,Würzburg, Germany) and includes alveolar pressure ($P_{alv}(t)$) and flow at the airway opening ($Q(t)$). Intrathoracic gas volume (ITGV) was measured near end-expiration during quiet breathing [302]. P_{alv} is derived from changes in barometric pressure inside the plethysmography box using Boyle's Law [216] and shift volume. Data from COPD patients includes plethymographic measurements from before bronchodilator ad-

Table 3.1: Demographic data is median [Inter-quartile range] where relevant. FRC = functional residual capacity; VT = tidal volume; VC = vital capacity TLC = Total lung capacity; FVC = forced vital capacity; ITGV = intra-thoracic gas volume.

	Young	Elderly	NFL	FL
# Subjects	20	20	25	35
M/F	13/7	17/3	15/10	22/13
AGE (years)	22 [21-24]	71 [69-72]	71 [67-74]	72 [69-78]
BMI	23 [20-25]	26 [24-28]	27 [24-29]	25 [23-27]
FRC (L)	3.3 [2.6-3.9]	3.5 [3.2-4.3]	4.0 [3.3-4.5]	5.0 [4.2-5.9]
VT (L)	0.8 [0.3-1.3]	0.7 [0.3-1.1]	0.9 [0.4-1.5]	0.7 [0.3-1.1]
VC (L)	5.4 [4.1-5.9]	4.1 [3.5-4.8]	2.4 [3.0-3.7]	1.8 [2.3-3.1]
TLC (L)	7.3 [5.8-8.2]	6.7 [6.0-8.0]	6.4 [5.7-8.0]	7.3 [5.8-8.1]
FVC (L)	5.3 [5.0-5.9]	3.8 [3.4-4.5]	2.4 [1.9-3.1]	1.7[1.4-2.2]
ITGV (L)	3.5 [2.7-4.1]	3.5 [3.0-4.1]	4.0 [3.3-4.6]	5.0[4.2-6.0]

ministration. Long- and short- acting bronchodilators were withdrawn 24 and 8 hours before the study, respectively [302]. Demographic information for each patient in each respective cohort in the Pecchiari et al. (2016) study is shown in Tables 3.2 - 3.5.

3.4 MV Data

Airway pressure and flow data was collected for 6 patients undergoing mechanical ventilation (MV) in the University Hospital of Heraklion Intensive Care unit, Greece. Patients were spontaneously breathing. Flow (V) at the airway opening was measured with a heated pneumotachograph (Hans-Rudolf 3700, Kansas, USA) and a differential pressure transducer (Micro-Switch 140PC, Honeywell, Ontario, Canada), placed between the endotracheal tube and the Y-piece of the ventilator. Flow (Q) was electronically integrated to provide volume (V). Airway pressure (P_{aw}; Micro-Switch 140PC, Honeywell, Ontario, Canada) was measured from a side port between the pneumotachograph and the endotracheal tube. Esophageal pressure (P_{es}) and gastric pressure (P_{ga}) were measured (Micro-Switch 140PC, Honeywell, Ontario, Canada) with thin, latex balloon-tipped catheter systems connected by polyethylene catheters to separate differential

Table 3.2: Young cohort demographic information from the Italy Data.

No.	**Sex**	**Age**	**BMI**	**FEV1**	**IC**	**VC**	**FVC**	**TLC**	**RV**
		y		**L**	**L**	**L**	**L**	**L**	**L**
1	M	20	16	5.0	3.7	5.58	5.5	8.8	3.2
2	M	20	21	5.3	3.7	5.75	5.9	8.6	2.8
3	F	20	21	3.8	2.5	4.07	4.1	5.3	1.3
4	M	22	23	4.4	4.0	5.79	5.8	7.7	1.9
5	M	23	30	5.0	4.3	6.40	5.9	7.5	1.1
6	M	25	35	3.9	4.4	5.25	5.1	6.6	1.3
7	M	20	20	4.4	4.1	5.92	5.9	7.6	1.7
8	M	23	27	6.0	5.0	6.96	6.9	9.3	2.3
9	F	21	23	3.6	3.0	3.86	3.9	5.1	1.2
10	F	24	24	3.0	2.9	3.63	3.5	4.9	1.2
11	F	27	20	3.5	2.7	5.02	4.0	6.3	1.3
12	F	21	22	3.6	2.8	3.96	4.0	5.1	1.2
13	M	24	25	4.9	4.0	5.53	5.4	7.1	1.5
14	F	31	19	3.4	3.9	4.45	4.6	6.6	2.1
15	M	24	24	5.5	5.5	7.34	7.0	9.7	2.3
16	M	21	19	4.2	3.1	4.07	4.6	6.2	2.2
17	M	22	25	5.0	4.2	5.85	5.8	7.8	1.9
18	M	22	20	4.6	3.0	5.00	4.8	7.5	2.5
19	M	22	30	5.9	5.0	7.30	7.2	9.5	2.2
20	F	32	26	2.6	2.3	1.87	3.0	3.7	1.9

Table 3.3: Elderly cohort demographic information from the Italy Data.

No	**Sex**	**Age**	**BMI**	**FEV1**	**IC**	**VC**	**FVC**	**TLC**	**RV**
		y		**L**	**L**	**L**	**L**	**L**	**L**
1	M	67	23	3.5	3.5	4.36	4.0	6.5	2.1
2	F	71	22	1.9	2.2	2.93	2.9	5.3	2.4
3	M	69	27	3.4	3.4	4.87	4.6	8.0	3.1
4	F	68	23	3.0	2.9	3.97	3.7	6.3	2.3
5	M	69	29	2.8	2.8	3.57	3.3	5.4	1.9
6	M	67	24	3.4	3.6	5.07	4.4	8.0	3.0
7	M	64	25	3.1	2.8	4.11	3.8	6.3	2.2
8	M	66	30	3.4	3.2	5.52	5.0	8.2	2.7
9	M	70	23	3.1	2.7	4.53	4.2	9.7	5.2
10	M	69	23	2.9	3.3	4.36	3.9	7.3	3.0
11	M	71	26	2.9	3.4	3.48	3.6	5.9	2.4
12	M	71	28	2.8	3.2	3.69	3.6	6.7	3.1
13	M	76	28	2.8	3.7	4.14	3.9	7.1	3.0
14	F	72	25	1.9	2.1	2.41	2.4	5.4	2.9
15	M	73	28	3.4	2.8	4.90	4.8	8.6	3.7
16	M	73	24	3.0	2.7	3.40	3.5	5.9	2.5
17	M	72	27	3.7	3.6	4.89	4.7	8.2	3.3
18	M	75	27	2.8	3.3	3.42	3.3	6.1	2.7
19	M	72	27	3.7	4.1	4.84	4.5	6.7	1.8
20	M	85	24	2.2	3.1	3.86	3.0	6.6	2.7

Table 3.4: NFL cohort demographic information from the Italy Data.

No	Sex	Age	BMI	FEV1	IC	VC	FVC	TLC	RV
		y		L	L	L	L	L	L
1	M	67	21	2.5	3.35	4.9	4.5	7.7	2.8
2	M	77	27	2.1	2.98	3.9	3.1	6.3	2.4
3	M	81	29	1.8	1.92	3.2	3.1	6.4	3.2
4	F	61	24	1.1	2.00	2.2	2.1	6.1	3.9
5	M	61	23	2.2	2.50	4.6	4.0	7.7	3.1
6	M	60	28	1.6	2.54	3.4	3.1	6.0	2.5
7	M	69	25	1.6	3.33	5.5	4.3	8.3	2.9
8	M	73	28	1.2	2.53	3.8	2.9	7.3	3.5
9	F	74	30	1.2	1.92	2.4	2.1	5.9	3.4
10	F	71	23	0.8	1.35	1.9	1.6	5.7	3.8
11	M	73	30	1.0	2.39	3.4	2.3	8.7	5.3
12	M	62	30	1.9	2.87	3.4	2.7	5.9	2.5
13	F	74	32	1.1	1.52	2.0	1.5	4.8	2.8
14	F	71	28	1.1	1.75	2.8	2.0	5.4	2.6
15	F	79	23	1.3	1.87	2.2	1.7	5.4	3.2
16	M	65	26	0.7	2.38	3.2	1.4	8.4	5.2
17	F	69	28	1.7	1.92	2.5	2.4	4.2	1.7
18	F	67	19	1.2	1.62	1.8	1.6	4.6	2.8
19	M	71	31	1.3	3.43	3.7	1.9	8.6	5.0
20	F	72	26	1.0	1.43	1.7	1.4	4.5	2.8
21	F	68	24	0.9	1.67	2.8	2.4	5.4	2.7
22	M	83	29	1.4	1.75	2.5	1.9	5.9	3.4
23	M	74	29	2.3	2.94	3.7	3.3	7.4	3.7
24	M	78	27	1.0	1.93	2.9	2.5	5.9	3.1
25	M	80	26	2.1	2.44	3.0	3.3	5.7	2.7

pressure transducers. The proper position of the balloons was verified using standard tests. Transdiaphragmatic pressure (P_{di}) was derived by subtraction of P_{es} from P_{ga}. Each signal was sampled at 150 Hz (Windaq Instruments, Ohio, USA) and stored on a computer disk for later analysis. Esophageal pressure is commonly used as a surrogate for pleural pressure changes [307–309], thus providing additional insight into spontaneous breathing dynamics.

Table 3.5: FL cohort demographic information from the Italy Data.

No	**Sex**	**Age y**	**BMI**	**FEV1 L**	**IC L**	**VC L**	**FVC L**	**TLC L**	**RV L**
1	M	65	22	0.6	1.88	2.4	1.6	7.6	5.2
2	F	79	23	0.7	1.14	1.2	1.2	3.7	2.5
3	F	77	19	0.7	1.30	1.7	1.8	6.8	5.1
4	M	72	34	1.0	3.55	4.4	3.1	8.3	4.0
5	F	71	14	0.6	1.27	1.9	1.8	6.0	4.1
6	M	83	25	1.0	2.30	4.5	2.9	7.4	2.9
7	M	87	21	0.6	1.67	2.5	1.7	5.8	3.4
8	F	52	23	0.5	1.20	1.1	1.1	6.2	5.1
9	M	69	24	1.0	2.44	3.4	2.4	7.8	4.4
10	M	75	28	0.5	1.29	1.8	1.5	7.3	5.5
11	F	75	25	1.2	1.38	1.6	1.9	4.9	3.3
12	M	82	28	1.2	2.12	2.7	2.3	5.8	3.1
13	M	69	28	0.7	1.91	3.0	1.7	7.7	4.7
14	M	71	25	0.6	1.61	2.4	1.7	7.3	4.9
15	F	82	24	0.6	0.83	1.1	1.0	4.8	3.7
16	F	77	25	0.8	1.36	1.9	1.8	5.6	3.7
17	M	78	22	1.0	1.46	2.0	1.7	6.4	4.5
18	M	68	25	0.5	1.37	2.1	1.5	8.6	6.5
19	F	69	24	0.5	1.13	1.9	1.3	7.0	5.1
20	F	62	19	0.6	1.23	1.5	1.2	5.6	4.1
21	F	84	26	0.6	1.17	1.2	1.0	3.9	2.8
22	M	72	33	1.4	2.81	3.2	2.1	7.5	4.3
23	M	69	27	0.7	1.50	2.3	1.8	8.2	6.0
24	F	74	19	0.9	1.70	2.0	1.7	5.8	3.8
25	M	66	19	0.5	1.60	2.5	1.3	8.7	6.2
26	F	63	26	0.6	1.37	2.1	1.4	8.7	6.6
27	M	71	29	1.5	3.24	3.8	2.7	7.5	3.7
28	F	82	26	0.8	1.32	1.6	1.5	4.8	3.2
29	M	72	26	0.8	1.57	2.6	2.1	8.1	5.5
30	M	75	32	0.9	2.33	2.8	2.1	6.6	3.8
31	M	67	22	0.7	2.51	3.1	2.2	11.0	7.9
32	M	66	27	1.7	3.14	4.8	4.3	8.6	3.9
33	M	69	29	0.6	1.27	2.1	1.4	7.3	5.2
34	M	70	25	1.0	2.37	4.1	2.7	9.8	5.8
35	M	79	23	0.8	1.65	3.2	2.2	6.5	3.3

3.5 Summary

This chapter presents the clinical data utilised in the rest of this thesis for model development and analysis. Different data cohorts provide insight into different aspects of COPD and respiratory failure, thus furthering model development and application in different ways.

CHAPTER 4: PROOF OF CONCEPT

4.1 Introduction

Airway resistance, and compliance, are pulmonary mechanics properties used to diagnose respiratory disease. Clinically motivated prior studies treat resistance in COPD or other lung dysfunction as purely linear, even when graphical PQ loop analyses show expiration is strongly non-linear [216, 219, 241, 302, 303]. This study is a first quantification of the non-linear resistance in COPD, and an analyses of its potential as a model-based marker of disease severity. It utilises a literature data set from Radovanovic et al. (2018) [219], presented in Chapter 3.2 of this thesis, of virtual patients spanning the healthy to severe COPD range, to test the concept of a nonlinear resistance on a full range of possible COPD severity.

4.2 Methods

A linear single-compartment model is utilised as a method of comparison for a later nonlinear single-compartment model. The linear model was chosen due to its simplicity in comparison to the nonlinear model and its high level of clinical validation provides an initial base for comparison.

Details of the linear model are followed by a more comprehensive method and derivation of the nonlinear model with justification for its application. The goal is to evaluate if

the nonlinear model is capable of producing a more robust and reliable analysis of the data. If so, it would provide a more reliable comparison for the linear model and a better foundation for creating model-based diagnosis.

4.2.1 Linear single-compartment model

The relatively ubiquitous [2, 25, 265–269] linear, single-compartment model in non-spontaneous breathing is defined:

$$P_{aw}(t) = EV(t) + RQ(t) + P_0 \tag{4.1}$$

where $P_{aw}(t)$ $[cmH_2O]$ is pressure at the airway opening, $Q(t)$ $[L/s]$ is airflow defined positive for inspiration, R $[cmH_2O/L/s]$ is airflow resistance, $V(t)$ $[L]$ is tidal volume, E $[cmH_2O/L]$ is lung elastance, P_0 is the end-expiratory pressure and t $[s]$ is time. This single compartment model assumes no change in pleural pressure relative to alveolar pressure, causing inspiratory drive, and thus is used in instances of non-spontaneous breathing only.

A modified single compartment model is presented in Figure 4.1, as a lumped alveolar volume with tissue elastance (stiffness), E $[cmH_2O/L]$, and an airway resistance, R $[cmH_2O/L/s]$. A surrogate term incorporating breathing effort is included via the transpulmonary pressure, which is the difference between alveolar pressure, P_{alv}, and pleural pressure, P_{pl}. The transpulmonary pressure difference across the lung wall is assumed to follow Hook's law [2], yielding:

$$P_{alv}(t) - P_{pl}(t) = EV(t) \tag{4.2}$$

Where P_{pl} is modelled as a pressure deviating from a starting value of atmospheric

pressure and is represented as a signal generator in the electrical circuit analogy in Figure 4.1. The pressure drop across the airways is defined as a function of flow rate using Ohm's Law:

$$P_{aw}(t) - P_{alv}(t) = RQ(t) \tag{4.3}$$

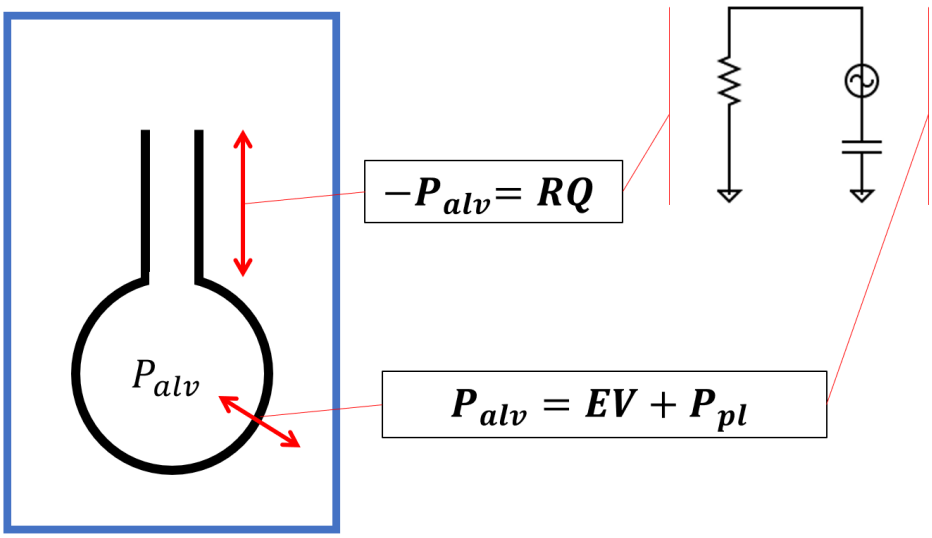

Figure 4.1: Single compartment model of spontaneous breathing.

In plethysmography, there is no externally applied end expiratory pressure (P_0), and P_{alv} is calculated relative to the atmospheric pressure [219, 302], which also represents the pressure at the airway opening.

Thus, Equation 4.3 reduces to:

$$-P_{alv}(t) = RQ(t) \tag{4.4}$$

where $-P_{alv}$ $[cmH_2O]$ is defined relative to $P_{atm} \cong 0$. Thus, plethysmographic mea-

surements of alveolar pressure are commonly combined with a model-based approach to evaluate airway resistance [310–313].

The linear, single compartment model in Equation 4.1 treats resistance as a constant R. A linear least squares parameter identification approach thus yields a linear regression problem defined [2, 40, 41, 54, 181]:

$$\underbrace{\begin{bmatrix} Q(t_0) \\ \vdots \\ Q(t_N) \end{bmatrix}}_{\mathbf{A}} \underbrace{\begin{bmatrix} R \end{bmatrix}}_{\mathbf{x}} = \underbrace{\begin{bmatrix} -P_{alv}(t_0) \\ \vdots \\ -P_{alv}(t_N) \end{bmatrix}}_{\mathbf{b}} \tag{4.5}$$

where t_0 is the first time point of a single breath and t_N is the last time point of a single breath.

Airway resistance is known to differ between inspiration and expiration [314,315]. Thus, airway resistance is identified separately for inspiration and expiration, yielding $R_{1,insp}$ and $R_{1,exp}$. This linear model formulation still holds resistance constant over the inspiratory and expiratory periods, and thus may not fully capture airway dynamics in COPD patients, where expiratory resistance can be volume dependent and nonlinear [216, 219, 302–304].

4.2.2 Non-linear single-compartment model

It is hypothesised a non-linear resistance is required to capture the non-linear airway behaviour during expiration in flow limited patients. The non-linear resistive model incorporates the constant linear term ($R_{1,insp}$) identified during inspiration (Q_{insp}) alongside an additional dynamic resistive term ($R_{exp} = \sum R_2\Phi(t)$), during expiration. Thus, Equation 4.3 becomes:

$$-P_{alv}(t) = R_{1,insp}Q_{insp}(t) + \left[\sum_{i=1}^{M} R_{2,exp,i}\Phi_{i,d=2}(t)\right]Q_{exp}(t) \tag{4.6}$$

where R_{exp} is modelled using M 2nd order ($d = 2$) b-spline functions to fit the unknown shape function, capturing any non-linear, time-varying dynamics during expiration.

The second order b-splines are defined over time [164, 166, 167], with T equally spaced time points:

$$\Phi_{i,0}(t) = \begin{cases} 1 & T_i \leq t \leq T_{i+1} \\ 0 & otherwise \end{cases}$$

$$\Phi_{i,d}(t) = \frac{t - T_i}{T_{i+d} - T_i}\Phi_{i,d-1}(t) + \frac{T_{i+d+1} - t}{T_{i+d+1} - T_{i+1}}\Phi_{i+1,d-1}(t) \; for \; d \geq 1 \tag{4.7}$$

Where $R_{2,exp,i}$ are constant coefficients of these splines identified using the linear least squares method from measured data.

The number of 2nd order ($d = 2$) splines with knot width (k_w) of 0.01s and a maximal spline time span for expiration are defined:

$$M(n) = ceil\left(\frac{T_{max}(n)}{k_w}\right) + d \tag{4.8}$$

Linear least squares is used to fit $R_{1,insp}$ and $R_{2,exp,i}$:

$$\underbrace{\begin{bmatrix} Q_{insp} & \emptyset & & \\ \emptyset & \Phi, Q_{exp} & \dots & \Phi_m Q_{exp} \end{bmatrix}}_{\mathbf{A}} \underbrace{\begin{bmatrix} R_{1,insp} \\ R_{2,exp,1} \\ \vdots \\ R_{2,exp,M} \end{bmatrix}}_{\mathbf{x}} = \underbrace{\begin{bmatrix} -P_{alv} \end{bmatrix}}_{\mathbf{b}} \tag{4.9}$$

Matlab command lsqlin (The Mathworks, Inc., Natick, Massachusetts, United States.) is used to constrain all identified parameters as positive, which is physiologically realistic and mitigates identifiability issues [238, 316–318].

4.2.3 Analyses

The linear and non-linear modelling approaches in Equations 4.4 and 4.6 are fit to alveolar pressure and airway flow data from the Literature data set presented in Chapter 3.2 (Patients 1-7). Both modelling approaches assume airway resistance is linear over inspiration ($R_{1,insp}$), but treat expiration differently with linear ($R_{1,exp}$) and non-linear ($R_2\Phi(t)$) resistance terms, respectively.

Root mean squared error (RMSE) is compared for both models to assess model fit to different degrees of COPD. Inspiratory and expiratory resistance are compared, and expected to be strongly linearly related with $R_{1,exp} > R_{1,insp}$ [319]. PQ loops are presented, as they are used clinically to evaluate COPD.

Where inspiratory and expiratory resistance is purely linear, the PQ loop reduces to a straight line. As non-linearity in R increases, one or both halves of the PQ loop balloons out. The shape of $R_{2,exp}$ with time and flow is assessed to examine the time and potential flow dependence of resistance during expiration, where previous clinical work suggests a flow or volume dependent resistance causing change in PQ loop shape [303, 304, 319].

4.3 Results

4.3.1 Model Goodness of Fit

Plethysmographic alveolar pressure is shown in Figure 4.2 with linear and non-linear resistive model fits for Patients 1 (Healthy) and 7 (COPD). Identified parameters and RMS errors for the resistive models are given in Table 4.1. Inspiratory resistance ($R_{1,insp}$), expiratory resistance ($R_{1,exp}$) and the mean non-linear $\sum R_2\Phi$ all increase with the progression from healthy toward COPD as expected. The linear model fits the data for the inspiratory part of the breath well, as shown in Figure 4.2, indicating inspiratory resistance is largely linear. A linear expiratory resistance term has relatively low RMS error for the healthy patient, as expected. However, the RMS error (Table 4.1) increases with increasing COPD when a linear expiratory model is used, reflecting the non-linear dynamics in expiration [219, 301, 302, 320–323].

Table 4.1: Identified values for model parameters of inspiratory resistance ($R_{1,insp}$), expiratory resistance ($R_{1,exp}$), mean $R_2\Phi$, root mean squared error for the linear model ($RMSE_{lin}$) and root mean square error for the non-linear model $RMSE_{nlin}$.

Patient		Linear		Non-linear	
	$R_{1,insp}$ $[cmH_2O/L/s]$	$R_{1,exp}$ $[cmH_2O/L/s]$	$RMSE_{lin}$ $[cmH_2O]$	Mean $R_2\Phi$ $[cmH_2O/L/s]$	$RMSE_{nlin}$ $[cmH_2O]$
1	2.1	2.4	0.4	2.5	0.2
2	2.8	4.1	0.5	4.7	0.2
3	3.2	5.1	0.7	5.6	0.2
4	4.2	7.1	1.1	7.9	0.2
5	5.2	8.8	1.6	11.2	0.2
6	5.8	9.4	1.9	13.7	0.2
7	7.3	10.0	2.7	24.4	0.2

Healthy Patient 1 data fits the linear model with a low RMSE value of 0.4 cmH_2O, as shown in Table 4.1. The mean non-linear resistance $R_2\Phi$ is identified as 2.5 $cmH_2O/L/s$, close to the linear value. The non-linear resistance model terms produce a model fit

with an RMS error 0.2 cmH_2O value for the severe COPD patient (Patient 7), with the mean $R_2\Phi = 24.4\ cmH_2O/L/s$ capturing the amplified dynamic behaviour of this severe COPD patient. Table 4.1 shows good resolution between patients and COPD severity for $R_{1,insp}$, $R_{1,exp}$ and mean $R_2\Phi$, with increasing $R_2\Phi$ as disease state worsens.

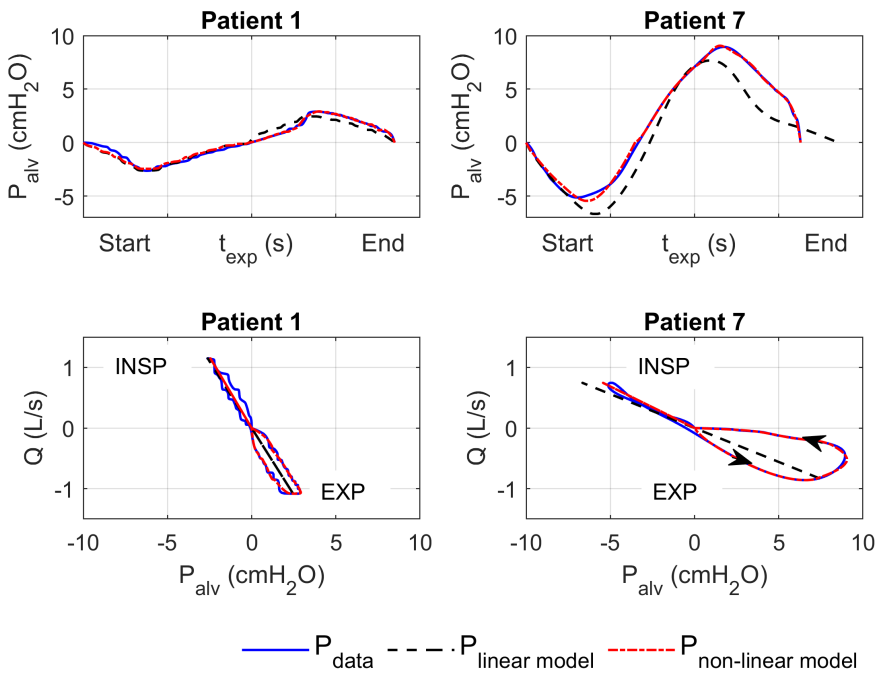

Figure 4.2: Plethysmographic alveolar pressure (P_{alv}) data with linear and non-linear model fits for Patients 1 (Healthy) and 7 (COPD). A perfect linear model produces a straight line in a PQ plot. The PQ plot is arranged per [219, 302, 303] with expiration on the RHS of the plot. Expiratory flow is here defined negative as is consistent with the single compartment model sign convention.

Constant resistance over time is compared with the time-varying dynamic resistance (left), and resistance as a function of flow is depicted as a comparison (right). As the tidal volume of the lungs depletes in the second half of expiration, the resistance in flow limited COPD patients increases almost exponentially. Resistance shown as a function of flow, in expiration, illustrates how resistance changes relative to flow. Figure 4.3 depicts the differences between the constant resistance ($R_{1\ insp}$) and the non-linear $R_2\ \Phi$.

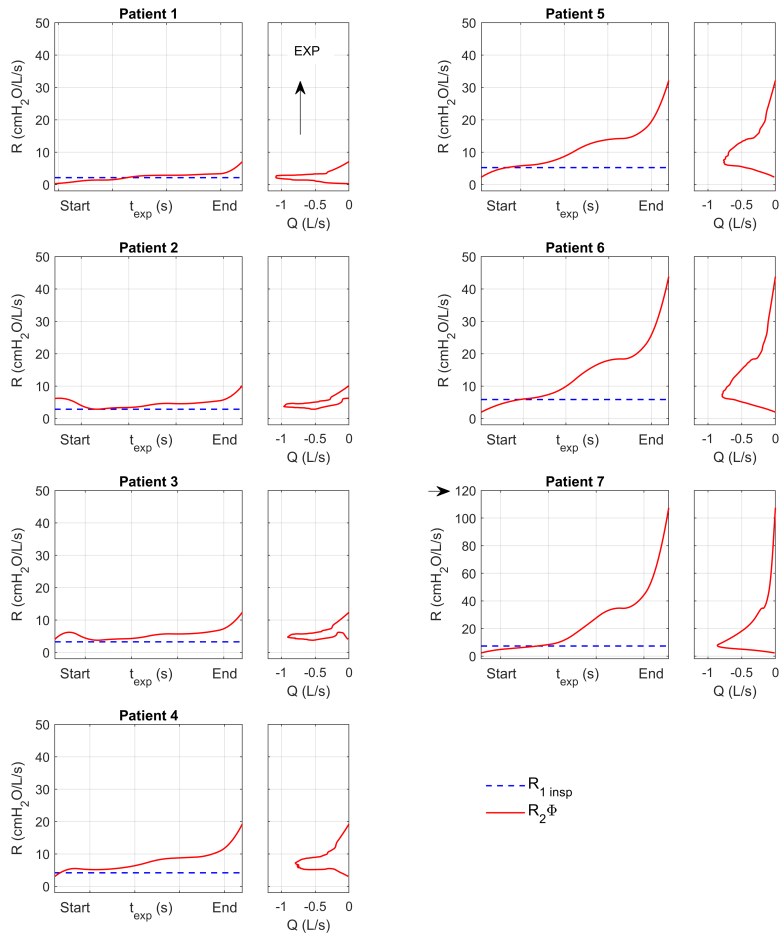

Figure 4.3: Expiratory resistance ($R_2\Phi$) with time and flow for each patient. Linear inspiratory resistance ($R_{1,insp}$) is shown for comparison. Note: the scale for the resistance of Patient 7 is much larger than the other patients.

The triangular shape increases in size from Patient 1 to Patient 7, and varies in shape. This non-linear increase in resistance increases in magnitude from Patient 1 through to Patient 7 as the severity of COPD increases, matching physiological expectations [216, 324]. Figure 4.3 also shows the change in non-linear resistance (R_2 Φ) with a change in flow for expiration.

An example of what the b-spline functions look like individually and collectively is shown in Figure 4.4. Increasing the number of b-splines could increase accuracy at the expense

of computational cost. Theoretically, using an infinite number of b-spline functions, model fit to the data would be perfect. However, the number of spline functions used is intended to capture overall dynamics, without over fitting. Future work could analyse the optimal number of splines required.

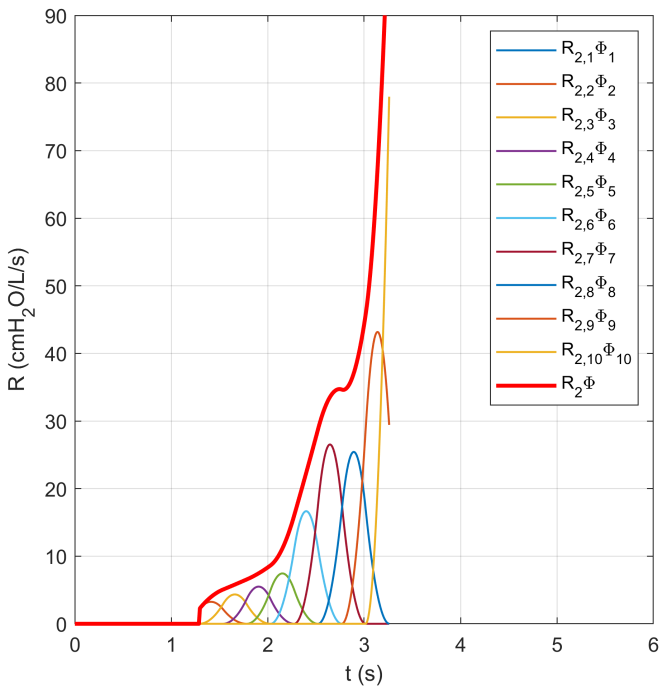

Figure 4.4: An example (Patient 7) of individual splines multiplied by individual identified coefficients to illustrate how the splines create the overall shape of the total expiratory resistance.

Pressure-Flow loops are shown in Figure 4.5 for Patient 1 and 7 plotted on the same axes (a) for comparison, with the other Patients (b-f) illustrated to show the progression from a healthy patient toward a COPD patient. The "ballooning" of the expiratory PQ loop is clearly visible for increasing COPD and contrasts with the linearity of the inspiratory portion of the loop.

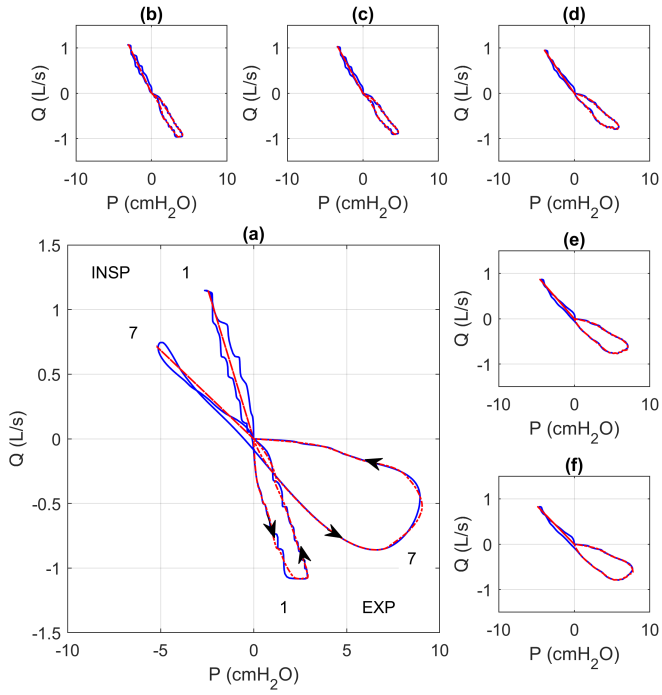

Figure 4.5: Pressure-Flow (PQ) loops depicting data (solid) and non-linear model (dashed) Patients 1 and 7 (a), Patient 2 (b), Patient 3 (c), Patient 4 (d), Patient 5 (e), and Patient 6 (f). The PQ loops are arranged per [219, 302, 303] with expiratory flow, negative per the sign convention of the single compartment model.

4.4 Discussion

This chapter presents alveolar pressure derived resistance for a range of patient disease states from healthy to advanced COPD. Figures 4.2 and 4.5 show good model fit, with largely linear resistance in inspiration and a clear non-linearity in resistance over expiration as disease state progresses toward advanced COPD. Identified constant inspiratory resistance $R_{1,insp}$ ranges from 2.1 $cmH_2O/L/s$ (Healthy) to 10.0 $cmH_2O/L/s$ (COPD) and time and flow varying, mean non-linear resistance $R_{2,exp}$ ranges from 2.5 $cmH_2O/L/s$ (Healthy) to 24.4 $cmH_2O/L/s$ (COPD). Overall, non-linear model-based resistance improves expiratory model fit, and captures potentially clinically relevant features for COPD diagnosis and monitoring.

The change in non-linear expiratory resistance over time and flow are depicted in Figure 4.3, showing small changes in resistance for healthier patients, compared to the larger changes in non-linear resistance in COPD patients, particularly toward the end of expiration. Thus, expiratory resistance is essentially constant in healthy subjects, and increasing non-linearity reflects physiological, or anatomical changes with increasing COPD disease severity. Increasing resistance with severity of COPD is consistent with literature [325–327], as is the result showing model-based expiratory resistance, $R_{1,exp}$, is greater than inspiratory resistance, $R_{1,insp}$ [216].

Resistance increases mostly during flow deceleration as shown in Figure 4.3. Previous studies show expiratory resistance causes a temporary imbalance in inhaled and exhaled volume, triggering dynamic hyperinflation and is indicative of COPD [314]. Such patients, typically with severe COPD, will begin to breathe at a higher respiratory rate [328]. Expiratory flow limitation (EFL) is observed in COPD, and results in no increase in flow, despite a rise in pressure [329, 330], which would be observed in a modelling approach as increasing nonlinear resistance. The mechanisms of EFL are not agreed upon in literature, but are believed to be related to airway obstruction [304] and/or small airway collapse [331]. Thus, EFL is more prominent in COPD patients in the supine position due to gravitational forces and increases with age and obesity [331]. EFL is associated with an increase in resistance and a concomitant decrease in tidal volume [219, 332]. The nonlinear, increasing, expiratory resistance observed here follows trajectories aligned with EFL and airway restriction/obstruction, and thus may be useful in non-invasive monitoring and diagnosis of COPD and its associated physiology.

Nonlinear expiratory resistance reflects an increased pressure gradient to achieve flow, indicative of airway narrowing and/or airway collapse during expiration. Typical linear

models miss characteristics of the expiratory behaviour, as seen in Figure 4.2. Using this nonlinear model, the mean nonlinear resistance captures significantly more of the dynamics of expiration, as can be seen in the significant difference in identified resistance in Table 4.1. Therefore, quantification of such a metric could be used with higher specificity to monitor disease state or progression and may have potential for enabling more targeted treatment by clinicians.

To date, no previous work directly models a non-linear COPD airway resistance from clinical data. Clinically, most derive an average resistance from $R = P/Q$, equivalent to the linear resistance $R_{1,exp}$ in this study. One previous study used geometric quantification of PQ loop "ballooning" [333], but this analysis is empirical, rather than physiological, and cannot directly reflect anatomical effects or changes. Many other studies [243, 334–336] have complex simulation models, with multiple resistance and elastance terms, which are unidentifiable from typical clinical data and non-invasive measurements, and thus not useful with plethysmography data without several population-based parametric assumptions or additional invasive pressure measurements.

This study uses only alveolar pressure and airflow plethysmography data, which restricts model complexity. Studies in the ICU with mechanically ventilated patients have examined the nonlinear resistive dynamics [337]. Approaches include viscoelastic [332, 338, 339] and flow and/or volume dependency of resistance [340–343]. No real consensus exists for flow or volume or flow and volume dependence [340], where reliance on model fit may collapse or alias different dynamics into model terms [337].

In particular it has been noted, volume and flow dependence may trade off [337]. Overall mechanically ventilated (MV) results in COPD patients match these presented here, with a negative dependence on flow and/or volume, capturing end-expiratory flow limi-

tation [340]. Full comparison is complicated by the difference between positive pressure MV, and levels of sedation, compared to the full negative pressure spontaneous breathing here where spontaneous breathing in particular may change dynamics [323].

Plethysmography measures shift volume and corresponding decreases in pressure, applying Boyle's law to enable the derivation of alveolar pressure P_{alv} [216, 219]. This derivation assumes no temperature dependence and some small pressure-volume effects are negated. Plethysmography derived alveolar pressure P_{alv} is essentially a lumped compartment pressure, which represents the average alveolar pressure, making this data perfect for single compartment model-based analyses. Assumptions made in the derivation of the plethysmographic, P_{alv}, are usually directly mitigated during data collection as part of standard plethysmographic methodology [216]. This plethysmographic data is useful for providing the alveolar pressure insights necessary for effective evaluation of airway resistance. Hence, this study adds to the clinical literature by considering the well known, observed non-linear characteristics of expiratory airway resistance.

In inspiration-expiration, and expiration-inspiration transitions there is a flow reversal. Expiratory flow experiences a different geometry and physical obstacles compared with inspiratory flow. For example, at airway bifurcations during inspiration, the flow splits around a wedge-shaped obstacle to create two separate flows into separate airways. During expiration the flow streams must merge from these two airways, and the resistance of splitting and merging flows is unequal. In addition, airways experience different forces during inspiration and expiration.

During forced expiration, typical of COPD patients with flow limitation, airway collapse and airway narrowing may result from muscle contraction to compress the abdomen/chest, which may change the diameter and/or geometry of an airway. In con-

trast, during inspiration the muscle activity acts to expand the volume of the chest cavity, and thus is going to act differently on the airways and affect the diameter and geometry differently. Thus, there are good physiological reasons why resistance may experience a discontinuous step or jump between inspiration and expiration.

The original data used for this study is comprised of only measured data from two patients. However, these two patients are indicative of the extremes of respiratory health in terms of COPD. Intermediate derived patients show possible disease progression in terms of nonlinear changes in PQ loop shape. The model is able to reflect all theoretical intermediate states, and the use of B-splines means it will describe any resistance shape. Thus, this study is an effective proof of concept to demonstrate the physiological relevance and capability of the model and methods. The results presented justify a larger study utilising clinical data from a much larger range of respiratory disease states.

Future work should include analysis of comprehensive patient data, and identifying similar model parameters from airway pressure (P_{aw}), without alveolar pressure (P_{alv}). Identifying clinically relevant metrics from measured airway pressures and flows could enable home or general practice clinic-based monitoring and thus could decrease time to diagnosis, making respiratory health monitoring more accessible to patients and clinicians. More accessible respiratory monitoring is desirable to decrease patient and clinical burden, and for improvement in health literacy and disease management, particularly as healthcare demand and costs rise beyond our ability to meet or afford them [344].

4.5 Summary

A novel method for quantitative analysis of plethysmographic PQ loops is presented with an identifiable nonlinear model capturing changes in COPD disease state. The model captures static and dynamic changes in resistance as model-based markers for COPD

diagnosis and monitoring. Finally, the nonlinear model presented delivers physiologically expected and relevant parameter values with possible future clinical use. Further validation with a wider range of clinical data is justified by the results presented here.

CHAPTER 5: NONLINEAR DYNAMIC EXPIRATORY RESISTANCE

5.1 Introduction

A range of clinical analyses have attempted to quantify disease state using the shape of the pressure-flow loop [219, 301–304, 345]. The analyses in this chapter attempts to combine these approaches to capture the nonlinear expiratory dynamics typical of COPD. In particular this study explores the nonlinearity of expiratory resistance in healthy young subjects (Young), healthy older patients (Old), non-flow-limited COPD patients (NFL) and flow-limited COPD patients (FL). The overall goal is to use novel, identifiable models to create a non-additionally-invasive model-based metric of COPD severity.

5.2 Methods

5.2.1 Clinical Data

Radovanovic et al. [219, 301, 346] present alveolar pressure (P_{alv}) and flow at the airway opening (Q), per standard plethysmographic analysis. P_{alv} is derived from changes in barometric pressure inside the plethysmography box using Boyle's law [216]. Four cohorts underwent standard plethysmography as part of the original observational mul-

Table 5.1: Patient information collected during the study [219].

	Young	Elderly	NFL	FL
Patients	20	20	25	35
AGE	22 [20-32]	71 [64-85]	71 [60-83]	72 [52-87]
M/F	13/7	17/3	15/10	22/13
BMI	23 [20-25]	26 [24-28]	27 [24-29]	25 [23-27]
FRC	3.2 [2.4-3.4]	3.5 [3.1-3.8]	3.2 [2.5-3.6]	3.1 [2.6-3.4]
VT	0.8 [0.3-1.2]	0.7 [0.3-1.1]	0.9 [0.4-1.5]	0.6 [0.3-1.1]

ticenter study focused on COPD and pulmonary function testing [346]. Cohorts were defined: Young (between the ages of 20-32 years) and Old (64-85 years) with no underlying COPD; and two cohorts with NEP confirmed flow limitation (FL) or no flow limitation (NFL). Cohort demographics can be found in Table 6.1.

5.2.2 Model

5.2.2.1 Linear single compartment model

The ubiquitous linear, single-compartment model [2, 25, 265, 266, 276] is defined:

$$P(t) = EV(t) + RQ(t) + P_0 \tag{5.1}$$

Where $P(t)$ $[cmH_2O]$ is airway pressure, $Q(t)$ $[L/s]$ is airflow, R $[cmH_2O/L/s]$ is airway resistance, E $[cmH_2O/L]$ is lung elastance, $V(t)$ $[L]$ is tidal volume, P_0 is end-expiratory pressure, and t $[s]$ is time. This model formulation assumes no spontaneous breathing [40, 54, 164, 166, 347]. The model formulation in Equation 5.1 can be modified to include a breathing effort term via the transpulmonary pressure, defined as the difference between alveolar pressure, P_{alv}, and pleural pressure, P_{pl}. The transpulmonary pressure difference across the lung wall is assumed to follow Hook's law:

$$P_{alv}(t) - P_{pl}(t) = EV(t) \tag{5.2}$$

Where P_{pl} is modelled as a pressure deviating relative to end-expiratory volume. The pressure drop across the airways is typically defined as a function of flow rate:

$$P_{aw}(t) - P_{alv}(t) = RQ(t) \tag{5.3}$$

Where R is typically assumed constant with time. The modified model of Equations 5.2-5.3 is described pictorially in Figure 5.1.

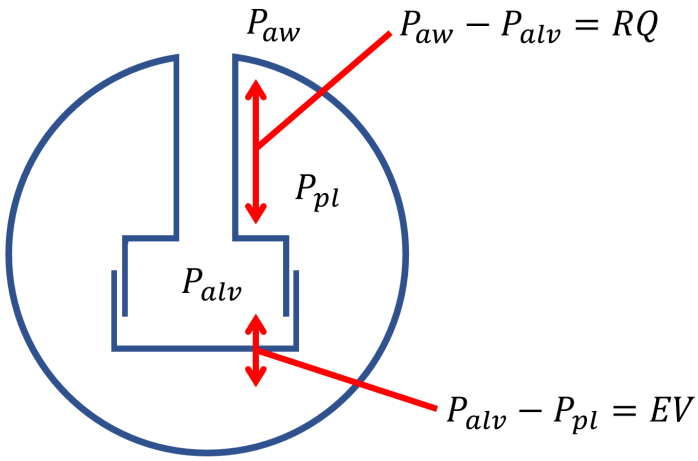

Figure 5.1: Modified single compartment model of spontaneous breathing.

In plethysmography, there is no externally applied end expiratory pressure (P_0), and P_{alv} is calculated relative to the atmospheric pressure [219, 301], which also represents the pressure at the airway opening. Thus, Equation 5.3 reduces to:

$$-P_{alv}(t) = RQ(t) \tag{5.4}$$

for $-P_{alv}$ $[cmH_2O]$ defined relative to $P_{atm} \cong 0$.

The use of Boyle's law implicitly treats the lungs as a single volume with a uniform pressure, P_{alv}, representing the average alveolar pressure across the entire lung, which matches the assumptions and formulation of the single compartment model in Equations 2-4.Thus, plethysmographic measurements of alveolar pressure are commonly combined with a model based approach to evaluate airway resistance.

The linear, single compartment model in Equation 5.1 treats resistance as a constant R. A linear least squares parameter identification approach thus yields [2, 40, 41, 54, 181]:

$$\underbrace{\begin{bmatrix} Q(t_0) \\ \vdots \\ Q(t_N) \end{bmatrix}}_{\mathbf{A}} \underbrace{\begin{bmatrix} R \end{bmatrix}}_{\mathbf{x}} = \underbrace{\begin{bmatrix} -P_{alv}(t_0) \\ \vdots \\ -P_{alv}(t_N) \end{bmatrix}}_{\mathbf{b}} \tag{5.5}$$

Airway resistance is known to differ between inspiration and expiration [314,315]. Thus, airway resistance is identified separately for inspiration and expiration, yielding $R_{1,insp}$ and $R_{1,exp}$. This linear model formulation still holds resistance constant over the inspiratory and expiratory periods, and thus may not fully capture airway dynamics in COPD patients, where expiratory resistance can be volume dependent and nonlinear [216, 219, 302–304].

5.2.2.2 Nonlinear lumped model

It is hypothesised a non-linear resistance is required to capture the non-linear airway behaviour during expiration in flow limited patients. The non-linear resistive model incorporates the constant linear term ($R_{1,insp}$) identified during inspiration (Q_{insp}) alongside an additional dynamic resistive term ($R_{2,exp}(t) = \sum R_2\Phi(t)$), during expiration.

Thus, Equation 5.3 becomes:

$$-P_{al}(t) = R_{1,insp}Q_{insp}(t) + \left[\sum_{i=1}^{M} R_{2,exp,i}\Phi_{i,d=2}(t)\right]Q_{exp}(t) \tag{5.6}$$

where R_{exp} is modelled using M 2nd order ($d = 2$) b-spline functions to fit the unknown and variable shape function, capturing any non-linear, time-varying dynamics during expiration. The second order b-spline functions [164, 166, 167, 237] are defined over time yielding:

$$\Phi_{i,0}(t) = \begin{cases} 1 & T_i \leq t \leq T_{i+1} \\ 0 & otherwise \end{cases}$$

$$\Phi_{i,d}(t) = \frac{t - T_i}{T_{i+d} - T_i}\Phi_{i,d-1}(t) + \frac{T_{i+d+1} - t}{T_{i+d+1} - T_{i+1}}\Phi_{i+1,d-1}(t) \; for \; d \geq 1 \tag{5.7}$$

Where $R_{2,exp,i}$ are constant coefficients of these splines identified using the linear least squares method from measured data. The number of 2nd order ($d = 2$) splines with knot width (k_w) of 0.01s and a maximal spline timespan for expiration are defined:

$$M(n) = ceil\left(\frac{T_{max}(n)}{k_w}\right) + d \tag{5.8}$$

Linear least squares is used to fit $R_{1,insp}$ and $R_{2,exp,i}$:

$$\underbrace{\begin{bmatrix} Q_{insp} & \emptyset & \dots & \emptyset \\ \emptyset & \Phi, Q_{exp} & \dots & \Phi_m Q_{exp} \end{bmatrix}}_{\mathbf{A}} \underbrace{\begin{bmatrix} R_{1,insp} \\ R_{2,exp,1} \\ \vdots \\ R_{2,exp,M} \end{bmatrix}}_{\mathbf{x}} = \underbrace{\begin{bmatrix} -P_{alv} \end{bmatrix}}_{\mathbf{b}} \tag{5.9}$$

Matlab command lsqlin (The Mathworks, Inc., Natick, Massachusetts, United States.)

is used to constrain all identified parameters as positive, which is physiologically realistic and mitigates identifiability issues [238].

5.2.3 Analyses

The linear (Equation 5.1) and nonlinear (Equation 5.6) models were fit to the plethysmographic pressure and flow data for expiration to yield $R_{1,exp}$ and $R_{2,exp}(t) = \sum(R_2\Phi)$ respectively. In both cases, inspiration is modelled with a linear R, yielding $R_{1,insp}$. Model fit is assessed via root mean squared error (RMSE) for all four cohorts. Model appropriateness is assessed separately, as improved model fit does not always result in improved clinical utility or physiological descriptiveness [59, 348–354].

Inspiratory and expiratory resistance are compared, and expected to be strongly linearly related with $R_{1,exp} > R_{1,insp}$ [314]. PQ loops are presented, as they are used clinically to evaluate COPD. Where inspiratory and expiratory resistance is purely linear, the PQ loop reduces to a straight line. As non-linearity in R increases, one or both halves of the PQ loop balloons out, displaying hysteretic behaviour. The shape of $R_{2,exp}(t))$ with time and flow is assessed to examine the time and potential flow dependence of airway resistance during expiration, where previous clinical work suggests a flow or volume dependent resistance causing this change in PQ loop shape [6, 24, 41].

The following metrics are used to assess differences in resistance shape and clinical impact:

- Mean non-linear expiratory resistance: $mean(R_{2,exp}(t)) = mean(\sum(R_2\Phi))$
- Work of resistance (WOR): $WOR = \int_{exp} P_{resistive} dV = \int(\sum R_2\Phi)QdV$
- Area under the Q-R curve (AUC_{RQ}): $AUC_{RQ} = \int_{exp} QdR$
- Rising slope on the Q-R curve ($m_{RQ} = dR/dQ$)

The latter two of these metrics are described pictorially in Figure 5.2 and used to assess measures proportional to nonlinear work due to this nonlinear added resistance. CDF (cumulative distribution function) plots are used to describe data distributions, capturing data values (x axis) and their percentile (y axis).

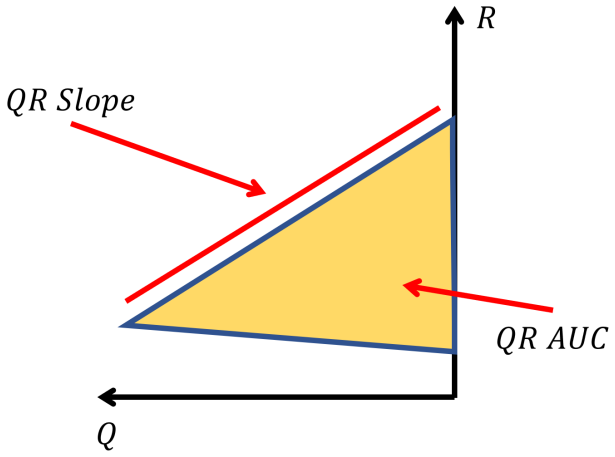

Figure 5.2: shape metrics for expiratory resistance $R_{2,exp}(t)$ $[cmH_2O/L/s]$ as a function of airway flow Q $[L/s]$

5.3 Results

Clinical data and modelling results are shown in Figures 5.3 and 5.6 for one "typical" patient for each of the 4 patient cohorts. The full set of model results can be found in Appendix A for each individual patient in Table A.1. Figure 5.3 shows resistance is largely linear over inspiration for all cohorts. Expiratory resistance is largely linear in non-COPD cohorts (Old and Young), but becomes increasingly nonlinear in NFL and FL COPD cohorts. Thus, RMSE in Table 5.2 is lower when using nonlinear $R_{2,exp}$ for COPD cohorts compared to a linear $R_{1,exp}$, as expected and matching clinical observations.

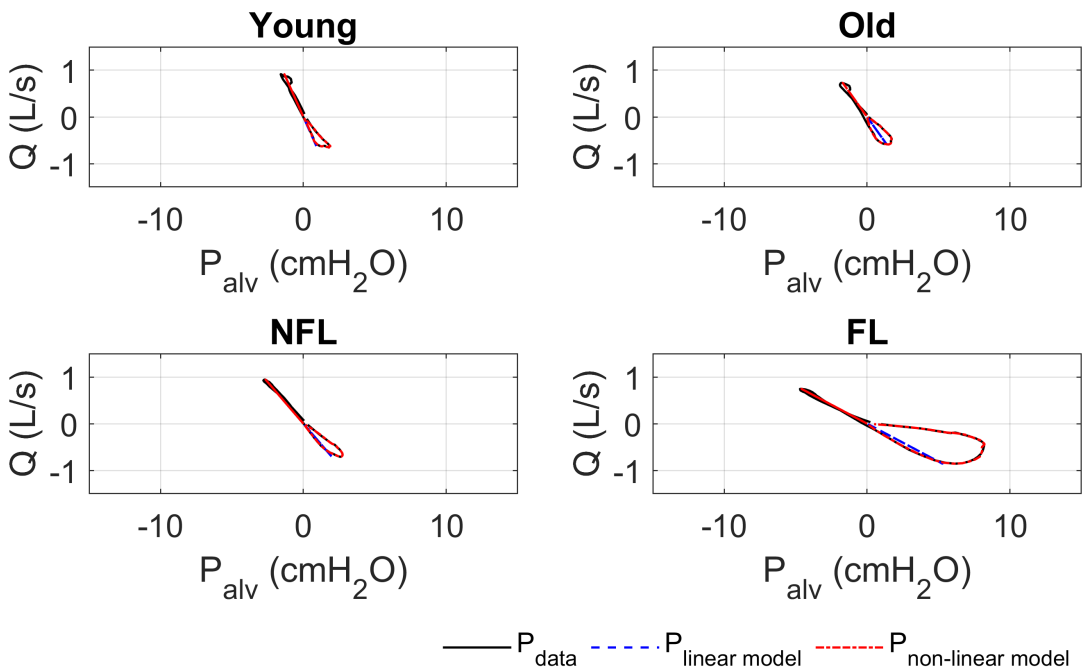

Figure 5.3: PQ loops for alveolar pressure (P_{alv}) with the linear and identified nonlinear model results overlaid.

Expiratory resistance in Table 5.2 is higher than inspiratory resistance, irrespective of whether the model is linear or non-linear, as expected. In Figure 5.6 resistance is slightly higher, but largely constant over inspiration and expiration for Young and Old cohorts.

In COPD cohorts, $R_{2,exp}$ increases nonlinearly over expiration, particularly in the FL cohorts (Figure 5.6). Plotting nonlinear $R_{2,exp}$ against flow shows the majority of non-linearity occurs during decelerating exhalatory flow, particularly towards the end of the breath. This outcome matches expected patterns for end-expiratory flow limitation. A full table presenting 'Italy Data' metrics is available in Appendix A as Table A.1

Figure 5.4 shows cohort overlap using the linear $R_{1,insp}$ (left) and nonlinear mean $R_{2,exp}$ (right). The Young and Old cohorts are near-identical in their resistance distributions.

COPD cohorts show comparatively greater inspiratory and expiratory resistance. In particular, FL patients have much higher expiratory resistance, with very little overlap with healthy Young and Old cohorts.

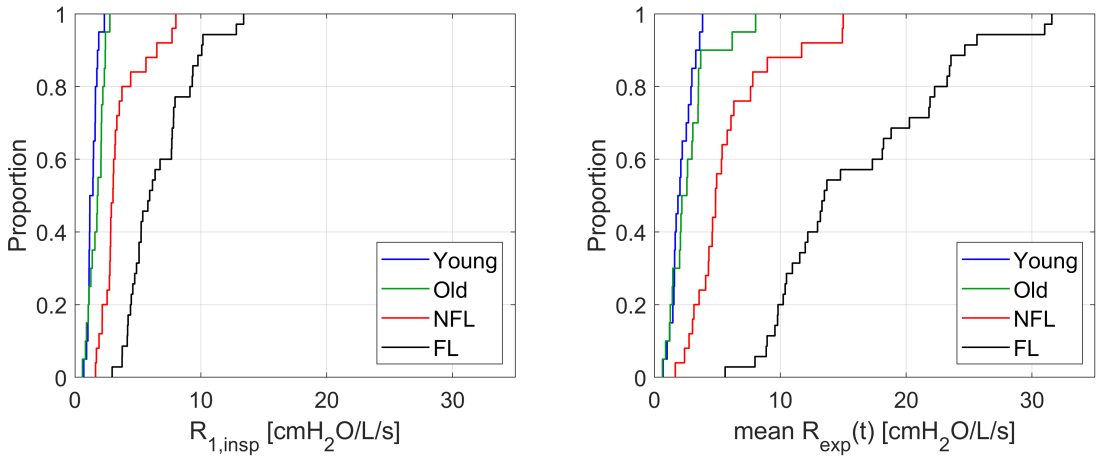

Figure 5.4: A cumulative distribution function (CDF) of inspiratory resistance (left), and mean $R_{exp}(t)$ (right) for all 4 cohorts.

Figure 5.5 demonstrates WOR is generally higher in the NFL and FL COPD cohorts. However, overlap in WOR between healthy Young and Old cohorts suggests lower tidal volumes with higher dynamic resistance ($R_{2,exp}$) results in similar WOR between cohorts for some subjects. The results presented in Figure 5.7 show strong linearity and inter-cohort consistency is shown between the Young and Old healthy subjects and even

Table 5.2: Median [IQR] of model parameters and model-fit for linear and nonlinear models, where Y = Young, O = Old.

		Linear		Nonlinear	
	$R_{1,insp}$ $[cmH_2O/L/s]$	$R_{1,exp}$ $[cmH_2O/L/s]$	RMSE $[cmH_2O]$	Mean $R_{2,exp}(t)$ $[cmH_2O/L/s]$	RMSE $[cmH_2O]$
Y	1.3 [1.1-1.6]	1.7 [1.5-2.8]	0.3 [0.2-0.3]	1.9 [1.6-2.8]	0.1 [0.1-0.1]
O	1.8 [1.2-2.2]	2.4 [1.5-2.9]	0.3 [0.3-0.4]	2.4 [1.4-3.5]	0.1 [0.1-0.1]
NFL	3.0 [2.7-3.6]	4.2 [3.7-6.6]	0.6 [0.4-1.0]	4.9 [3.9-6.6]	0.1 [0.1-0.2]
FL	5.9 [4.6-7.9]	5.9 [8.6-15.4]	1.7 [1.3-2.8]	13.5 [10.4-21.9]	0.3 [0.2-0.4]

the NFL subjects when comparing $R_{2,exp}$ and mean $R_{2,exp}$. However, the FL subjects show a divergence from linearity, indicating that nonlinear dynamics in expiration are most apparent in this cohort, matching Figure 5.6.

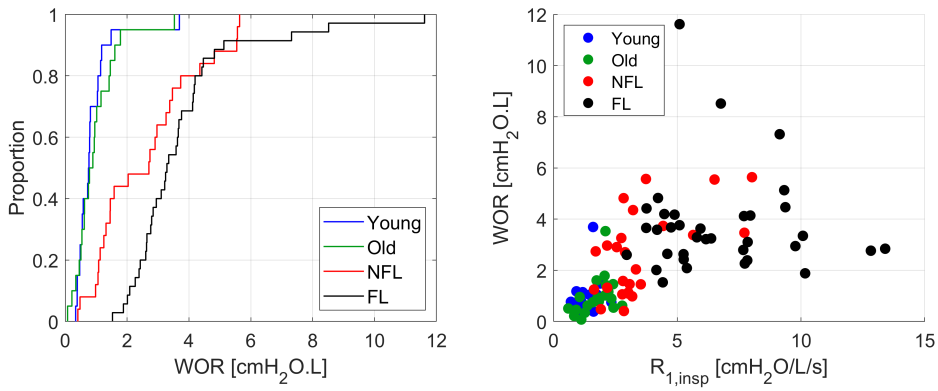

Figure 5.5: A CDF (left) of the work of resistance $\int R_2 \Phi Q \, dV$ alongside the work of resistance (right) as a function of inspiratory resistance ($R_{1,insp}$).

This outcome is reinforced in Figure 5.8 5.9, which show clear separation of FL COPD subjects from other cohorts when comparing the nonlinear $R_{2,exp}$ shape metrics AUC_{QR} and m_{QR}. Thus, overall, NFL patients show higher airway resistance than Young and Old cohorts, and FL patients are distinguishable by their significantly non-linear expiratory resistance.

Results depicted in Figures 5.10 to 5.13 demonstrate that the resistance of the Young and Elderly cohorts are lower than that of the NFL and FL COPD cohorts. Resistance as a function of flow presents itself in the form of a triangular shape, appearing flattened with the Young and Elderly cohorts, where less dynamic resistance is present. An example of a patient's alveolar pressure measurement along with air flow, volume, resistance as a function of volume and flow, P-Q and P-V loops are depicted in Appendix A in Figure A.1.

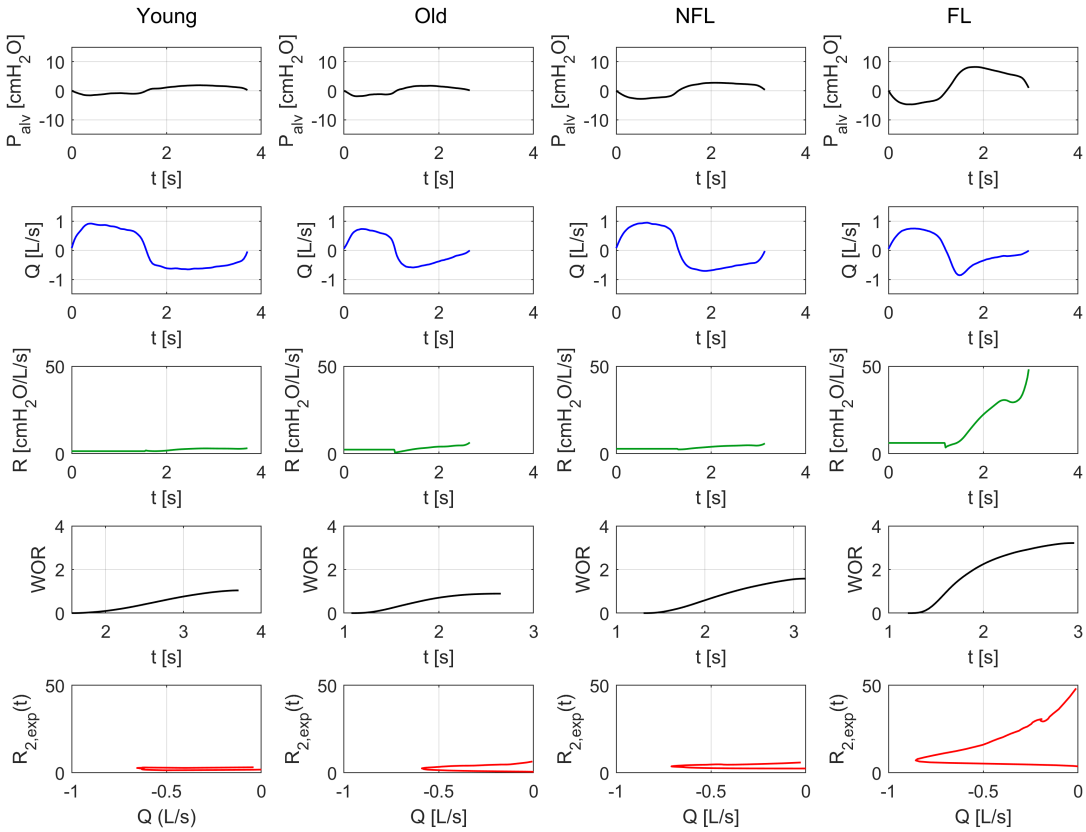

Figure 5.6: Alveolar pressure (P_{alv}) $[cmH_2O]$, flow (Q) $[L/s]$, airway resistance (R) $[cmH_2O/L/s]$ and work of resistance (WOR $= \int R_2 \Phi Q \, dV$) $[cmH_2O]$ for the 4 patient cohorts of Young, Old, Non-Flow Limited (NFL), and Flow Limited (FL) subjects.

5.4 Discussion

This study presents a method for examining nonlinear expiratory resistance in COPD patients. The linear model was a good fit over inspiration and expiration for healthy subjects, as shown in Figure 5.3 (RSME 0.3 cmH_2O in Table 6.2). However, the linear model resulted in a good fit only during inspiration for the two COPD cohorts. The nonlinear model captured nonlinear expiratory mechanics in the NFL and FL cohorts, resulting in a much better fit to clinical data (linear model RSME 0.6 and 1.7 cmH_2O vs nonlinear 0.1 and 0.3 cmH_2O for NFL and FL respectively). This nonlinearity likely reflects underlying physiological conditions and disease characteristics in these

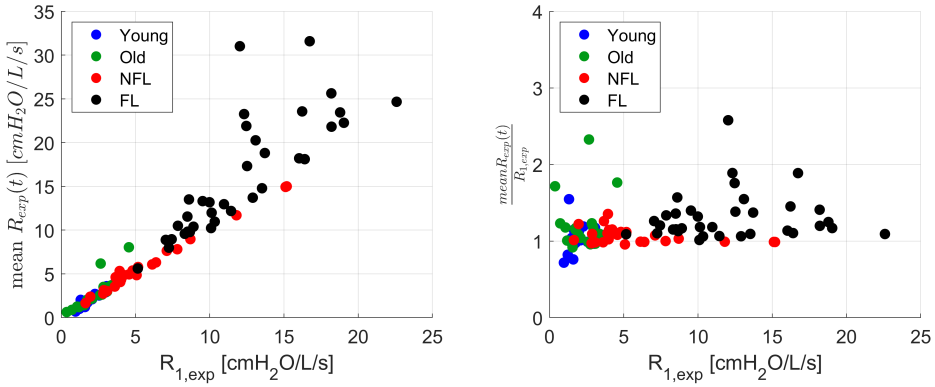

Figure 5.7: (left) Mean $R_2\Phi$ as a function of expiratory resistance ($R_{1,exp}$), The ratio of mean $R_2\Phi$ to $R_{1,exp}$ as a function of $R_{1,exp}$ (right).

subjects [355–360].

The Young and Old healthy cohort patients had virtually indistinguishable R for both inspiration and expiration. COPD patients with FL and without FL patients showed higher inspiratory and expiratory resistance by comparison,an expected result since resistance to airflow increases with an increase in COPD disease progression [325,361–366]. The FL patients were clearly distinguishable from healthy subjects in their nonlinear expiratory resistance $R_{2,exp}(t)$, shown in Figures 5.6 and 5.8, suggesting expiratory resistance is a significant dynamic in COPD patients with FL that is not currently described by existing linear methods.

Expiratory R has greatest nonlinearity during decelerating flow, as demonstrated in Figure 5.6. Resistance increases toward end-expiration suggesting flow limitation, as higher $R_{2,exp}(t)$ suggests a greater pressure gradient was required to achieve similar or lower flow as the breath progresses. This result is expected in subjects with expiratory flow limitation (EFL), where various mechanisms cause difficulty and active effort in end-expiratory tidal volume clearance [367–372].

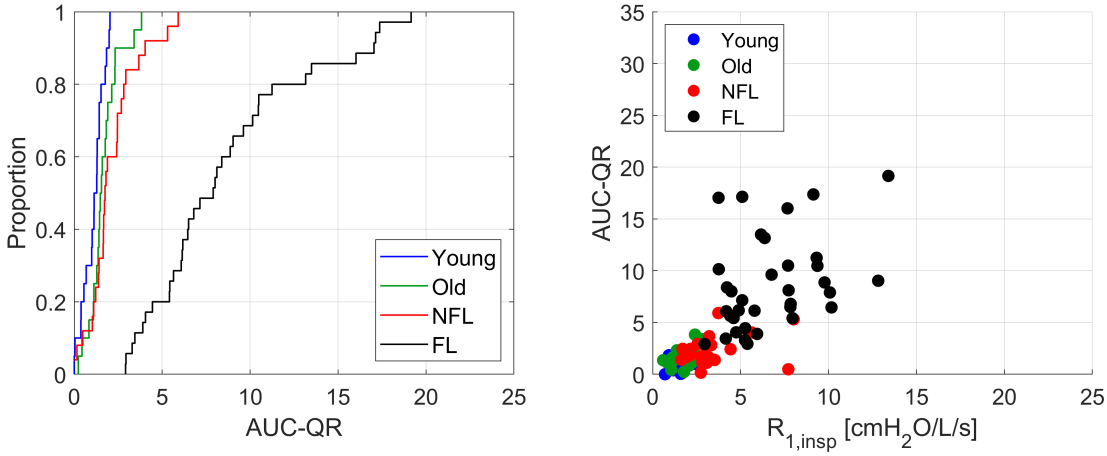

Figure 5.8: A CDF of the area of the flow relative to resistance (left), compared with the flow-resistance area as a function of the inspiratory resistance $R_{1,insp}$ (right).

Several mechanisms contribute toward the progression of EFL by reducing the expiratory flow reserve in the tidal volume range [332]. Increased airway resistance, age, obesity, augmented cholinergic bronchial tone, decreased lung elastance, airway- parenchyma uncoupling, and airways collapsibility are all mechanisms of EFL [332]. Mechanisms specific to COPD include chronic asthma, cystic fibrosis, constrictive bronchiolitis. Predominant reduction of maximal expiratory flow rates at lower lung volumes appears more crucial in promoting EFL [332]. In the presence of EFL, deformation of airways at choke points and downstream segments, coupled with local high air velocity, and possibly with small airways collapse, may cause peripheral airway and parenchymal injury [373].

Use of NEP in COPD patients requires an additional procedure, and clinical expertise for result interpretation. The model-based method presented here may assist in the determination of FL from standard plethysmographic data [306, 374]. In particular, the magnitude and shape of the nonlinear dynamic expiratory resistance $R_{2,exp}(t)$ can highlight end-expiratory FL. Figure 5.4 shows an increase in the constant inspiratory resistance $R_{1,insp}$ in COPD compared to healthy patients, irrespective of age. However,

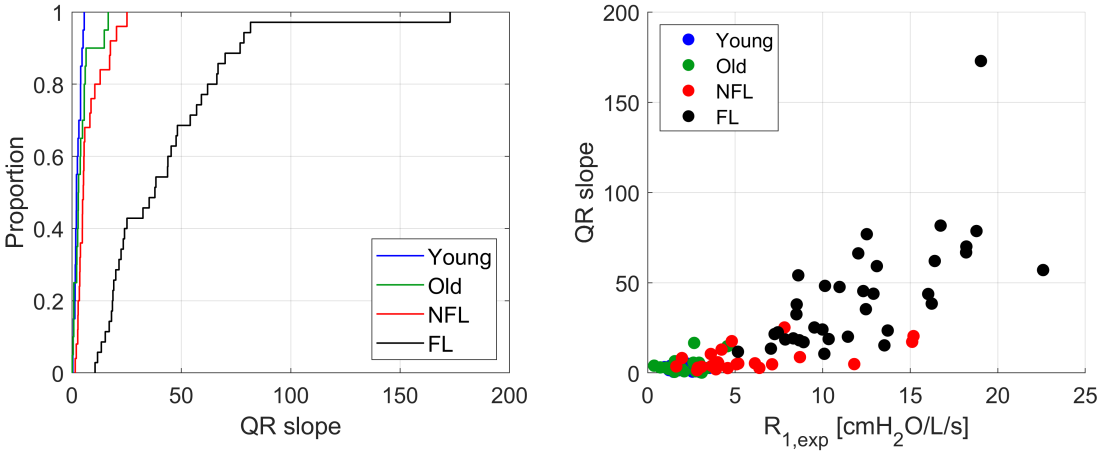

Figure 5.9: A CDF of the slope of the flow relative to resistance for each respective cohort compared with the same slope as a function of the expiratory resistance ($R_{2,exp}$).

the inter-cohort variability and overlap in airway resistance values makes elevated resistance alone imperfect for COPD and EFL determination. However, analysis of nonlinear $R_{2,exp}(t)$ here shows a separation between healthy and COPD cohorts. This indicates that this analysis may be useful in the diagnosis and monitoring of disease progression for FL COPD patients using plethysmography. This method of analysis may also remove the requirement for NEP to confirm flow limitation, or at the very least assist in confirmation where other methods may not be conclusive.

In particular, Figure 5.8 shows a clear separation of FL subjects from other cohorts, where Only 3/25 (12%) of NFL subjects overlap with FL subjects on the CDF. Further, given that NEP applies a set additional pressure gradient, it may miss EFL under different breathing or pressure gradient conditions. It may be possible that the NFL patients with high nonlinearity in expiratory resistance were in fact experiencing some degree of (mild) EFL that was not diagnosed via NEP.

A limitation of using plethysmographic data includes the assumptions made to calculate alveolar pressure from shift volume with the application of the ideal gas law

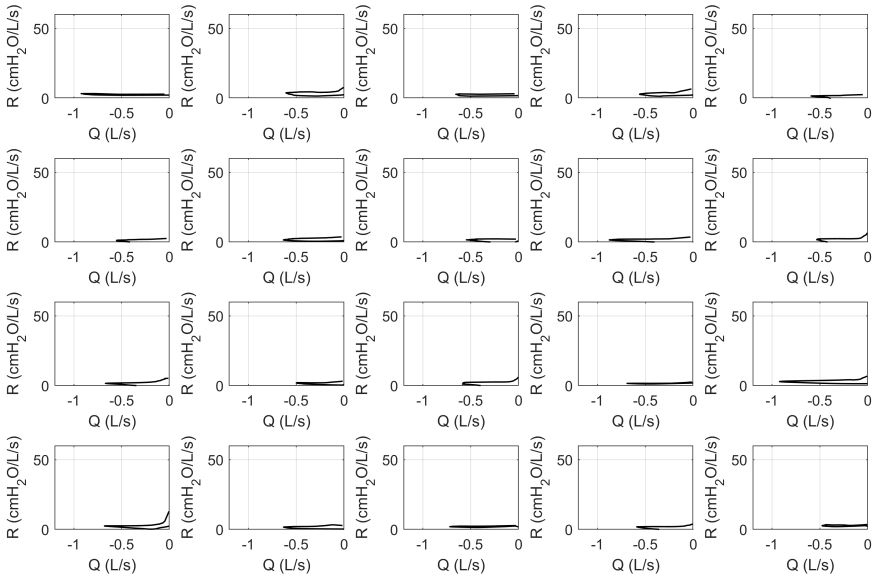

Figure 5.10: Resistance (R) as a function of air flow (Q) for each patient in the Young cohort.

[216, 375–377]. These limitations are mitigated by specific manoeuvres required of patients when undergoing plethysmography and relies on the manoeuvres being performed correctly [216,375,376]. A limitation of using a single compartment model for a complex respiratory system is that heterogeneity is not captured by the model [378–382]. The geometry of each side of the lung is significantly different, thus resulting in different flow velocities when a similar pressure is applied from the outside of the lung cavity. The material properties of each side of the lung could also vary, causing the fluid mechanics to be different on either side. Lung tissue damage caused by COPD is likely to also be heterogeneously spread throughout the lung cavities, and these differences are not captured with the use of the model in this study [383–388]. However, the study successfully separates the flow limited COPD patients from the other cohorts, and quantifies severity of disease state. Future studies will apply this method directly with a variety of COPD conditions with the goal of exploring its relationships with specific existing diagnoses, and ability to detect EFL without NEP. However, this study investigates a

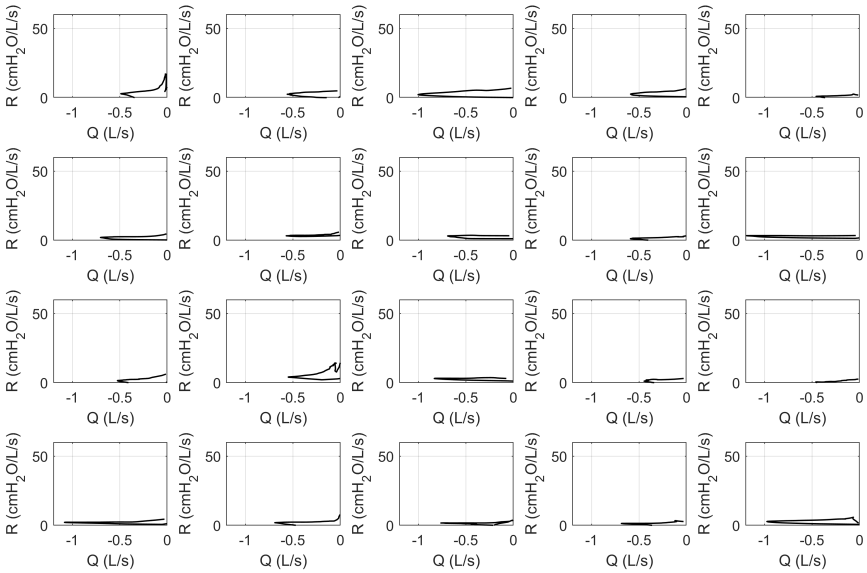

Figure 5.11: Resistance (R) as a function of air flow (Q) for each patient in the Elderly cohort.

large cohort of patients with varying lung mechanics and successfully identifies disease state.

5.5 Summary

Previous pressure and flow loop analyses have attempted to quantify disease state using the shape of the loop, and linear models. A novel nonlinear model captures underlying expiratory dynamics and mechanics indicative of COPD disease progression. Alveolar pressure and airflow data consisting of four cohorts (Young, Old, NFL, and FL) from the Radovanovic et al. [219, 301–303] studies were used to test various methods of quantifying disease state and separating healthier cohorts from those with COPD.

Linear resistance in expiration increases with each cohort from Young toward FL. Nonlinear expiratory resistance, and WOR increases significantly in FL COPD patients.

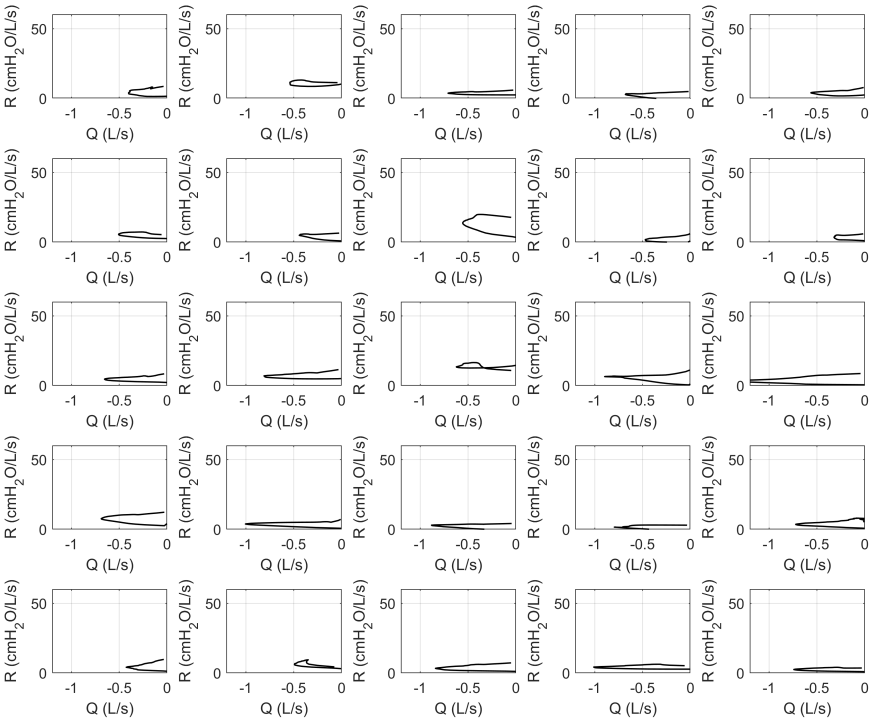

Figure 5.12: Resistance (R) as a function of air flow (Q) for each patient in the NFL cohort.

This resulting model-based method could be useful in detecting and confirming FL, where NEP is difficult or not available. The following chapter will investigate elastance (E) and the work of breathing (WOB) in inspiration.

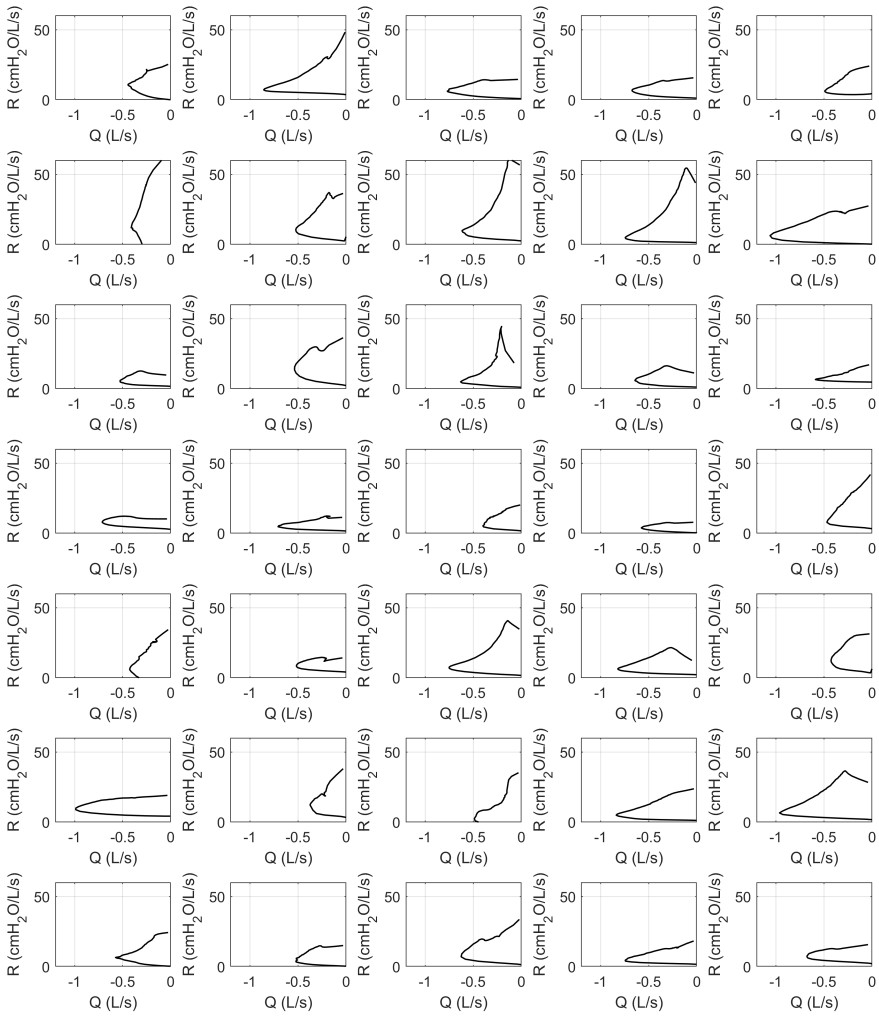

Figure 5.13: Resistance (R) as a function of air flow (Q) for each patient in the FL cohort.

CHAPTER 6: WORK OF BREATHING AND ELASTANCE

6.1 Introduction

This chapter fits the simple single compartment model to plethysmographic data in subjects who are healthy and those diagnosed with COPD. The goal is to identify model-based airway resistance, lung elastance, and overall work of breathing (WOB). The overall aim is to test and validate models of Chapter 4 - 5 in clinical plethysmographic data, as a first step towards a model-based low-clinical-burden tool for at-home and/or clinical COPD diagnosis and monitoring.

6.2 Methods

6.2.1 Model

The difference between pressure measured at the airway (P_{atm}) and alveoli (P_{alv}) give a measure of the resistive pressure across the airways alone [2]:

$$P_{atm}(t) - P_{alv}(t) = RQ(t) \tag{6.1}$$

where R $(cmH_2O/L/s)$ is airway resistance and Q (L/s) is flow. The equation of motion describing the elastic tissue dynamics is:

$$P_{alv}(t) - P_{pl} = EV(t) \tag{6.2}$$

where P_{pl} is the pressure in the pleural cavity. If the pleural pressure is used as a surrogate for inspiratory effort, Equation 6.2 can be rewritten:

$$P_{alv}(t) = EV(t) + P_{eff} \tag{6.3}$$

where P_{eff} is the pressure dynamic in the pleural cavity representing breathing effort, and E (cmH_2O/L) is tissue elastance. The modelled atmospheric pressure is thus defined:

$$P_{atm}(t) = RQ(t) + EV(t) + P_{eff} \tag{6.4}$$

where an electrical analogy is also shown in Figure 6.1. Equation 6.4 reflects the single-compartment model formed with an additional breathing effort term.

The P_{eff} term is modelled using b-spline basis functions [167, 238]:

$$P_{eff}(t) = \sum_{i=1}^{M=10} P_{c,i}\Phi_{i,d=2}(t) \tag{6.6}$$

with $M = 10$ second order $(d = 2)$ b-spline functions to fit the unknown shape function [39, 164, 270], with P_c the spline coefficients, capturing any nonlinear, time-varying dynamics during expiration for all patients. The second order splines are defined over

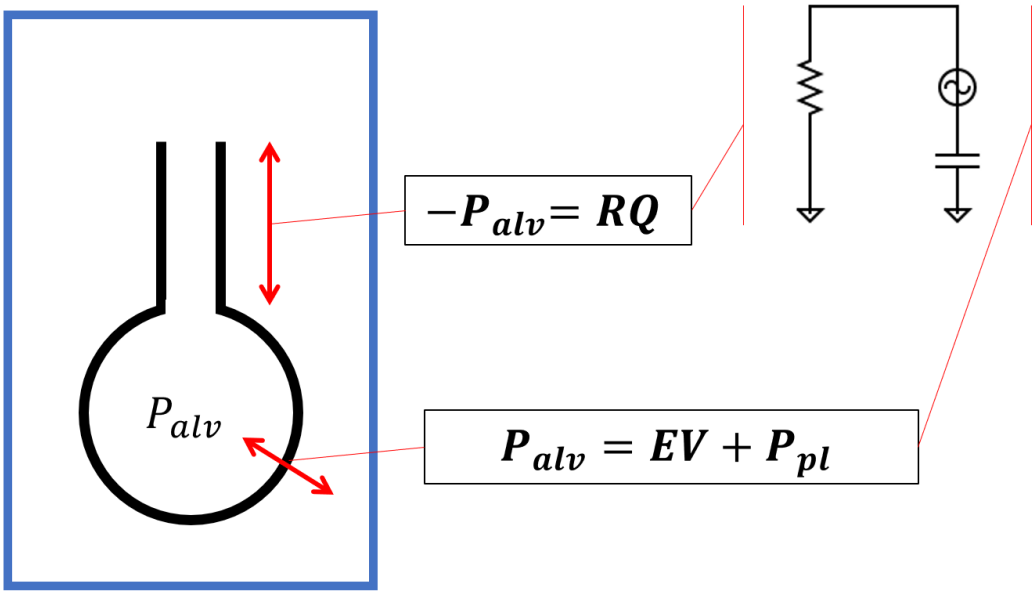

Figure 6.1: Single-compartment model (spontaneous).

$$\underbrace{\begin{bmatrix} V(T_{Qpeak}-5) & 0 & \dots & 0 \\ \vdots & \vdots & \vdots & \vdots \\ V(T_{Qpeak}-5) & 0 & \dots & 0 \\ V_{insp} & \Phi_1 & \dots & \Phi_M \end{bmatrix} \begin{bmatrix} E \\ P_{(c1)} \\ \vdots \\ P_{(cM)} \end{bmatrix}}_{\mathbf{Ax}} = \underbrace{\begin{bmatrix} -P_{alv(T_{Qpeak}-5)} \\ \vdots \\ -P_{alv(T_{Qpeak}+5)} \\ -P_{alv,insp} \end{bmatrix}}_{\mathbf{b}} \tag{6.5}$$

time, with T equally spaced time points:

$$\Phi_{i,0}(t) = \begin{cases} 1 & T_i \leq t \leq T_{i+1} \\ 0 & otherwise \end{cases}$$

$$\begin{aligned} &\Phi_{i,d}(t) = \tfrac{t-T_i}{T_{i+d}-T_i}\Phi_{i,d-1}(t) + \tfrac{T_{i+d+1}-t}{T_{i+d+1}-T_{i+1}}\Phi_{i+1,d-1}(t) \\ &for\ d \geq 1 \end{aligned} \tag{6.7}$$

where T_i the time points of the $M+1$ "knots" which define basis function spacing.

6.2.2 Model Identification

This analysis focuses on inspiratory lung mechanics and breathing effort. Measurement of alveolar pressure decouples E and R in Equations 6.2 and 6.3, enabling separate identification of both of these from the alveolar pressure data. Thus, inspiratory resistance is identified from inspiratory pressure-flow data:

$$-P_{alv} = R_{1,insp}Q(t) \tag{6.8}$$

Inspiratory breathing effort (P_{eff}) and E trade off parametrically in Equation 6.3. Thus, E is identified from expiration data under the assumption of passive expiration.

Expiration is generally passive, driven by the elastic recoil of the lung, diaphragm, and chest wall. However, in COPD patients there can be end-expiratory forced breathing effort to assist in tidal volume clearance and to avoid gas trapping, particularly those with FL at end-expiration. During inspiration, the relaxation time constant for muscles involved in breathing effort causes negative P_{eff} generated during inspiration to decay. Thus, E is estimated from the middle portion of expiration, defined as 5 points either side of peak expiratory flow (T_{Qpeak}), defined:

$$EV(T_{Qpeak} - 5 : T_{Qpeak} + 5) = P_{alv}(T_{Qpeak} - 5 : T_{Qpeak} + 5) \tag{6.9}$$

Work of breathing (WOB) is calculated as the integral of pressure over volume:

$$WOB = \int_{insp} -P_{eff}\, dV \tag{6.10}$$

For ease of interpretation and presentation, in Equation 6.10, the WOB is now defined as positive (for a negative P_{eff} pressure signal). WOB breathing to overcome the elastic

Table 6.1: Patient information for each respective cohort. BMI = body mass index, FRC = functional residual capacity, VT = tidal volume

	Young	Elderly	NFL	FL
Patients	20	20	25	35
AGE	22 [20-32]	71 [64-85]	71 [60-83]	72 [52-87]
M/F	13/7	17/3	15/10	22/13
BMI	23 [20-25]	26 [24-28]	27 [24-29]	25 [23-27]
FRC	3.2 [2.4-3.4]	3.5 [3.1-3.8]	3.2 [2.5-3.6]	3.1 [2.6-3.4]
VT	0.8 [0.3-1.2]	0.7 [0.3-1.1]	0.9 [0.4-1.5]	0.6 [0.3-1.1]

and resistive dynamics, respectively, are defined:

$$WOB_E = \int_{insp} RQ\, dV \tag{6.11}$$

$$WOB_R = \int_{insp} EV\, dV \tag{6.12}$$

6.2.3 Patient Data

Alveolar pressure and airflow measurements obtained during plethysmography [219,219, 302,303] were obtained from 40 subjects with COPD. They are separated into 4 cohorts of 10 patients each. Specifically: Young, Elderly, NFL, and FL. Patient demographics are summarised in Table 6.1. Pressure-flow data was recorded at a frequency of 66Hz. Data for a single breath is included.

6.2.4 Analyses

The resistance and elastance models were fit to the plethysmographic pressure and flow data to identify resistance ($R_{1,insp}$), elastance (E), work of breathing for breathing effort ($WOBP_{eff}$), resistance (WOB_R), and elastance (WOB_E). The linear resistance model

Table 6.2: Median [IQR] of model parameters and WOB results for all patients in all four cohorts.

	Young	Elderly	NFL	FL
$R_{1,insp}$	1.3 [1.1-1.6]	1.8 [1.2-2.2]	3.0 [2.7-3.6]	5.9 [4.6-9.0]
RMSE	0.3 [0.2-0.4]	0.3 [0.3-0.4]	0.6 [0.4-1.2]	1.8 [1.4-3.0]
E	3.6 [2.9-4.6]	4.5 [2.4-6.3]	8.0 [5.3-11.5]	18.9 [12.9-25.9]
$P_{eff,min}$	-3.6 [-4.5- -2.8]	-4.1 [-5.9- -2.6]	-8.4 [-12.9- -5.9]	-17.7 [-23.2- -14.0]
$WOB\ P_{eff}$	88.8 [61.5-108.2]	95.6.0 [69.6-145.0]	306.9 [156.9-382.9]	445.9 [356.7-584.9]
WOB_R	0.7 [0.5-0.9]	0.9 [0.6-1.4]	2.3 [1.2-3.3]	3.7 [2.9-5.4]
WOB_E	1.2 [1.0-1.6]	1.5 [0.9-2.4]	3.9 [2.0-5.3]	5.8 [4.1-7.3]

fit was assessed with a RMSE for all 4 cohorts. Results are presented in detail in Table 6.2.

6.3 Results

Linear inspiratory resistance, $R_{1,insp}$ (Equation 6.8) has a very good model fit over inspiration (RSME median [IQR] for all patients). RSME and resistance values for all patient cohorts can be found in Table 6.2, and $R_{1,insp}$ increased with age and COPD severity, as expected. Figure 6.2 shows this model fit for a typical FL patient, and indicates all key inspiratory resistance dynamics are captured by the linear term, even in FL patients.

Patient effort from the elastic model fit (Equation 6.4) is shown in Figure 6.3 for a single patient from each cohort. Negative P_{eff} shape and magnitude ranges match typical pleural/esophageal pressure measurements during spontaneous breathing in literature [42, 164, 165, 270].

Overall, E and the depth of the P_{eff} incursion increased with COPD, resulting in higher WOB, as seen in Figures 6.4 and 6.6. Figure 6.6 shows, as resistance increases, elastance also tends to increase concomitantly, resulting in higher WOB to overcome each of these dynamics (Figure 6.5). Interestingly, the elastic and resistive components of WOB were

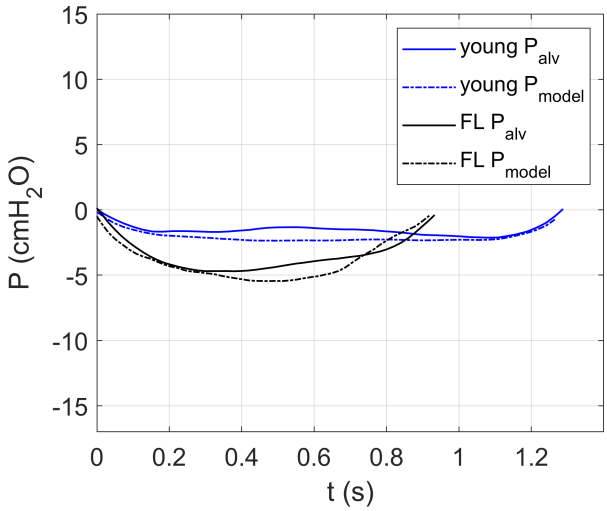

Figure 6.2: A typical model fit for a Young patient compared to an FL patient.

strongly correlated ($R^2 = 0.79$), suggesting both dynamics contribute to increased WOB in COPD.

Typical subjects from the Young and FL cohorts, depicted in Figure 6.3, were selected to illustrate the increasing patient effort (P_{eff}). Inspiratory air flow (Q) and tidal volume (V) for each respective typical subject is also shown in Figure 6.3 for comparison. Note the shorter breath (in time) of the FL subject compared to the Young subject and the lower total volume (VT). The P_{eff} is also notably larger for the FL subject compared to the NFL and other cohorts.

For a more detailed comparison, patient effort results for every patient in each respective cohort are presented later in this chapter as Figures 6.7 to 6.10. All patient data is presented over the same range of pressure (P) for easier reference.

WOB increases with inspiratory resistance (Figure 6.4), as expected. The scatter about the line of best fit (Figure 6.4) is likely a combination of differing elastic work of breathing

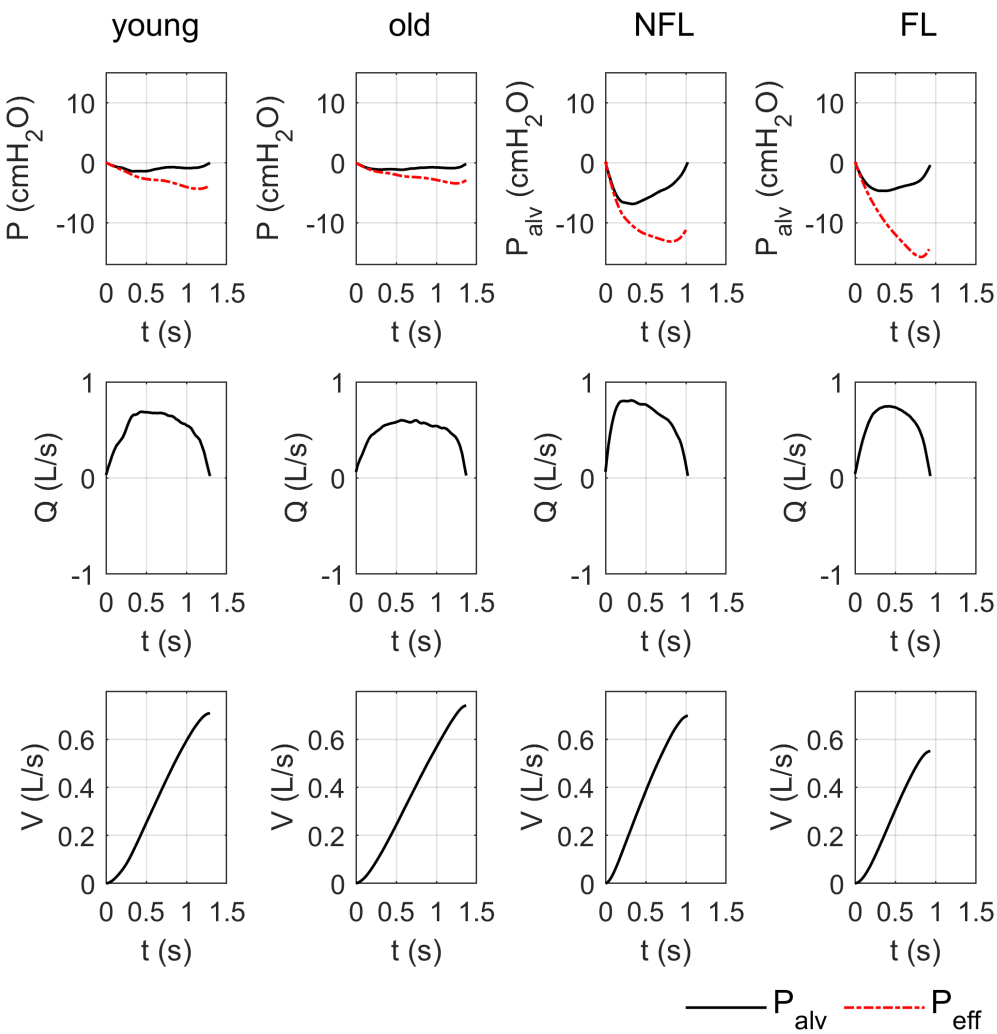

Figure 6.3: Patient effort (P_{eff}) is shown increasing for a typical subject from each respective cohort, with flow (Q) and tidal volume (V) data for comparison.

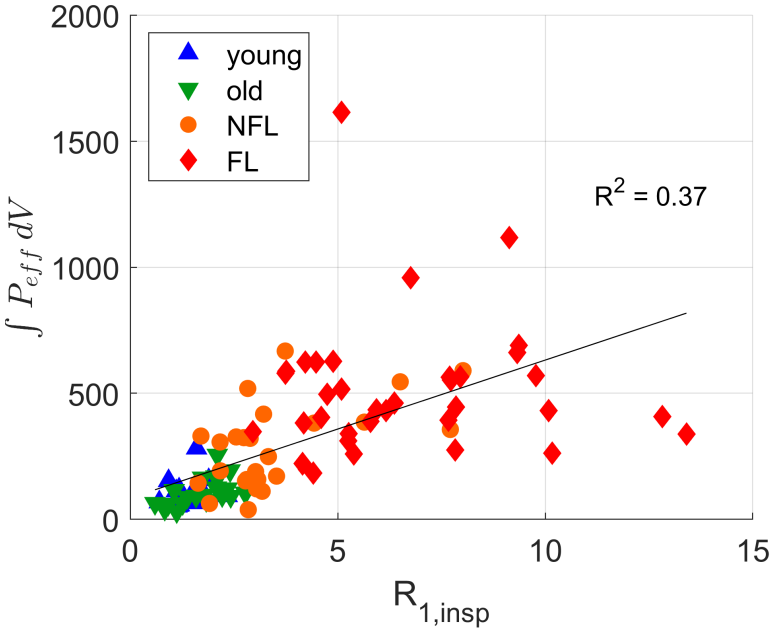

Figure 6.4: Work of breathing for patient effort is shown to increase with inspiratory resistance.

per patient, and different inspiratory volume demand resulting in different inspiratory effort. By and large, COPD patients had higher WOB per mL of tidal volume, as expected.

WOB increases slightly with age, though Young and Elderly cohorts overlap significantly. This could be due to a number of factors which are discussed late in this chapter. Figure 6.5 shows an increase in resistance is generally associated with an increase in elastance in the Young and Elderly cohorts. This correlation is also true for the COPD cohorts, though with the same linear slope. In the COPD cohorts, the resistance was higher per unit increase in elastance, which was associated with increased resistive WOB compared to elastic WOB shown in Figure 6.6. These results match expectations, where a primary indicator of COPD is increased airway resistance [219, 301–303, 389, 390].

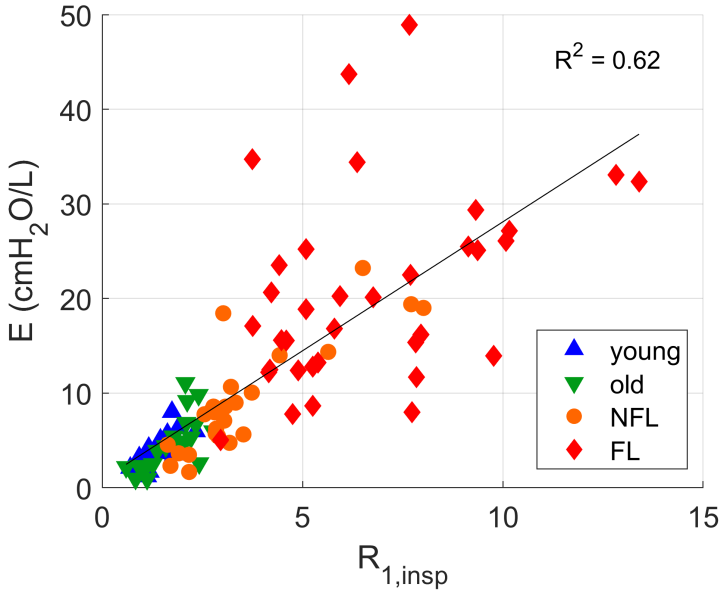

Figure 6.5: Elastance (E) increases with an increase in inspiratory resistance and shows some linearity with $R^2 = 0.73$.

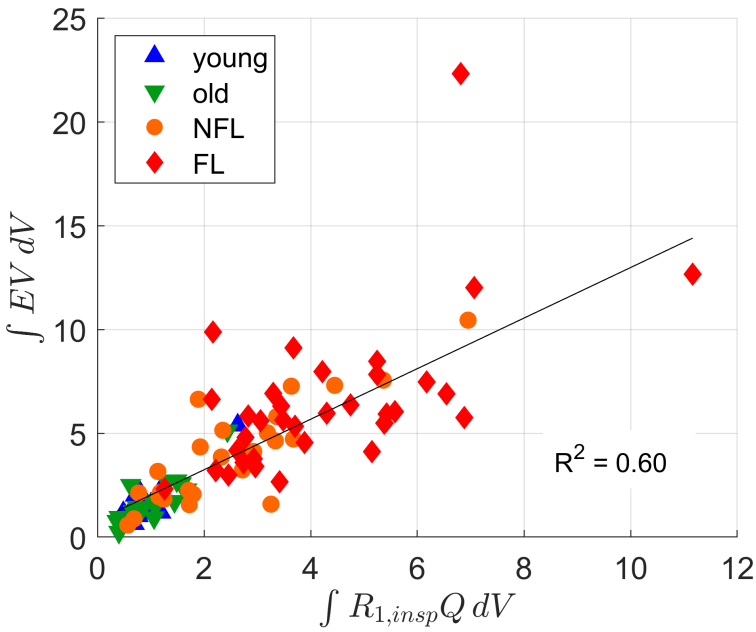

Figure 6.6: Elastic work of breathing shown to increase with resistive work of breathing.

6.4 Discussion

This study presents a simple model for estimating WOB from plethysmography data. Results showed increased WOB with age and COPD severity. Model-based effort shapes and magnitudes match existing literature [391–393]. Overall, this model captures WOB well in accordance with expected and previously observed clinical behaviours.

Plural pressure is modelled here as inspiratory effort. During inspiration, the diaphragm drops, creating a relative negative pressure in the pleural space compared to the lung alveoli, which in turn causes alveolar expansion. The relationship between pleural pressure dynamics and tidal volume inspired is a function of the lung elastance.

In this study, the modelled inspiratory effort comprises pressure deviations relative to end expiratory volume just prior to inspiration onset (V=0). These pressure swings are similar in magnitude (-2 to -10 cmH_2O typically) and shape to measured esophageal pressure changes in CPAP sleep literature [394–397], where esophageal pressure is a common surrogate for pleural pressure. These literature outcomes suggest the results presented here capture the key inspiratory effort dynamics.

All elastance values fell within the expected range [328, 398–401]. Elastance in healthy Young and Elderly subjects was < 6.3 cmH_2O (3.6 [2.9 – 4.6] and 4.5 [2.4 – 6.3] cmH_2O of Young and Elderly respectively), matching literature [328]. COPD can sometimes elevate elastance to 5 – 10 cmH_2O [328, 398–401], a result seen broadly in Figure 6.5 and Table 6.2. Emphysema related tissue damage can reduce elastic recoil [402–408], while inflammation may increase lung elastance [409]. In addition, higher measured elastance can be associated with increased rate of breathing, where shorter breaths tend to engage and (over)extend lung units with lower time constants. Thus, elastance can vary significantly between COPD patients, as seen in Figure 6.4, and the identified elastances in

this study are physiologically plausible.

Airway resistance is often increased in COPD patients [304, 319, 332, 374]. This increase in resistance is depicted in Figure 6.4 and Table 6.2, where FL COPD subjects, and some NFL COPD subjects, had resistances in the elevated $5 - 15\ cmH_2O.s/L$ range expected from literature [328]. Both inspiratory and expiratory resistance can be affected, where the causes of inspiratory resistance are generally related to airway narrowing and secretions/exudates related to inflammation [328].

Expiratory resistance can present additional dynamics, such as FL and airway collapse, where a expiratory resistance focused model-based analysis observed increasingly nonlinear expiratory resistance in COPD patients. This analysis has focused on inspiratory resistance, as part of an overall picture of inspiratory WOB. Calculation of WOB is complicated in expiration by FL [328], and future work will attempt to combine the results presented here with nonlinear expiratory models.

The single compartment model used here assumed linear homogeneous airway resistance and pulmonary elastance. A separate analysis has shown expiratory resistance is increasingly nonlinear in COPD patients (Chapter 5), particularly those with FL [163]. The linear airway resistance assumption is generally true even in COPD patients, where Figure 6.3 shows a typical case. In this case, as alveolar pressure is measured in this plethysmographic data, the elastic and resistive components of the single compartment model can be decoupled mathematically, allowing independent identification of both of these parameters, per Equations 6.1 and 6.2.

Identification of elastance and pleural pressure (inspiratory effort) requires a portion of the breath to be passive, with assumed pleural pressure at approximately zero, which is

generally true during normal expiration in healthy subjects. However, with increasing COPD severity resistance to flow and flow limitation can result in active expiration, particularly towards the end of the breath. Thus, using end-expiration to fit elastance under an assumption of passive expiration can cause high elastance values as it incorporates some positive pleural pressure generated by active expiration. At start-inspiration visco-elastic effects and the natural decay in pleural pressure as inspiratory muscle and tissue relaxation occurs going into expiration can also affect identification of an elastance value reflective of inspiratory dynamics. Hence, elastance was identified using data from the middle of expiration, as defined by peak flow. Future work should explore the effect of different expiratory dynamics on elastance identification.

This chapter explores model-based quantification of WOB in adults with and without COPD. WOB follows expected trends with disease state and associated resistance, but can also offer additional insight as it also includes the WOB to overcome the elastic components, as well as to meet volume demand. Normalisation of WOB by tidal volume, in combination with other model-based parameters, may offer further, improved insight into patient-specific condition and their unique medical and technical needs.

The data in this chapter includes plethysmography-derived alveolar pressure. Alveolar pressure is derived as part of plethysmography [216,219], but not directly measured. The plethysmographic method has been optimised to address potential inaccuracies [216,375]. The alveolar pressure here represents average alveolar pressure across both lung units, matching well with the single compartment lung formulation. As a result, the pleural pressures modelled here, representing inspiratory effort, are average pressures across the pleural spaces, and representative of overall breathing effort. The results of this chapter should thus be considered within the framework of the single compartment model.

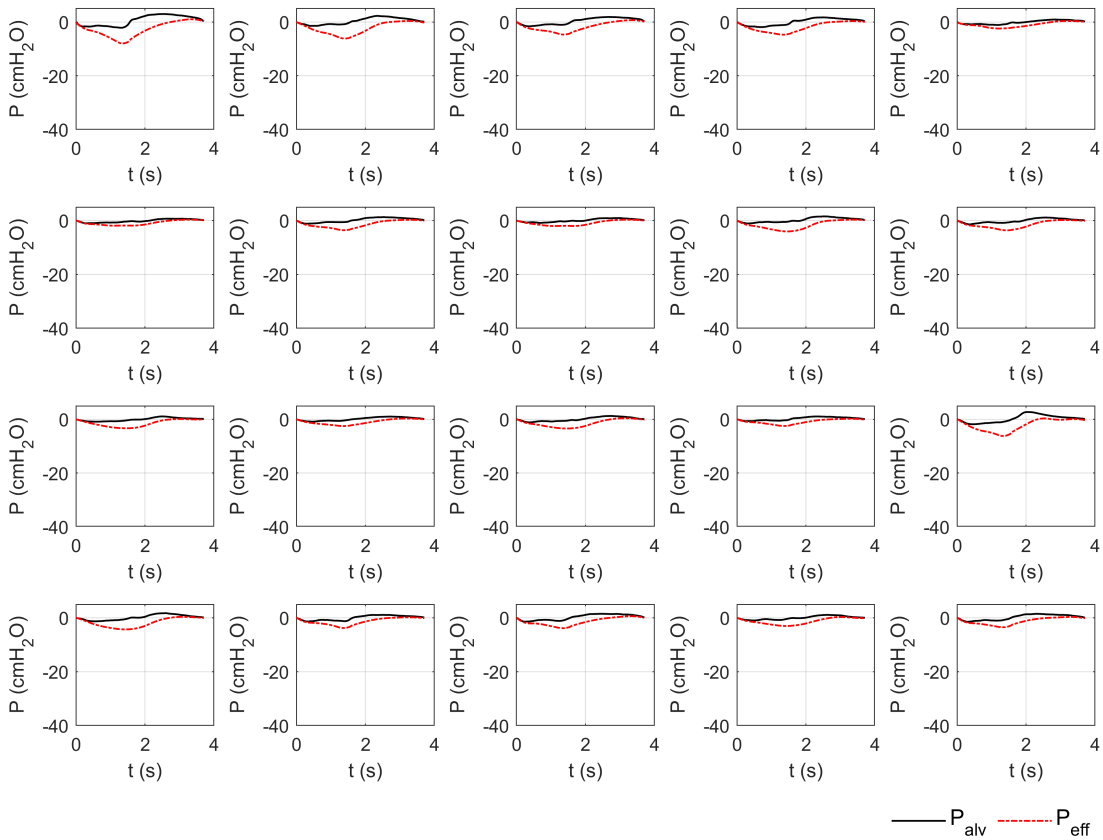

Figure 6.7: Alveolar pressure (P_{alv}) is shown (Black) compared with patient effort (P_{eff}) (Red) for the Young cohort.

This data set does not include measured pleural pressure as a final validation. Measurement of pleural pressure is extremely uncommon, as it is very invasive. Esophageal pressure is often used as a surrogate for pleural pressure, but measurements depend heavily on sensor placement, especially as typically pleural pressure differs across the pleural space. Measurement of esophageal pressures is not common, as it adds additional patient burden and clinical expense [410].

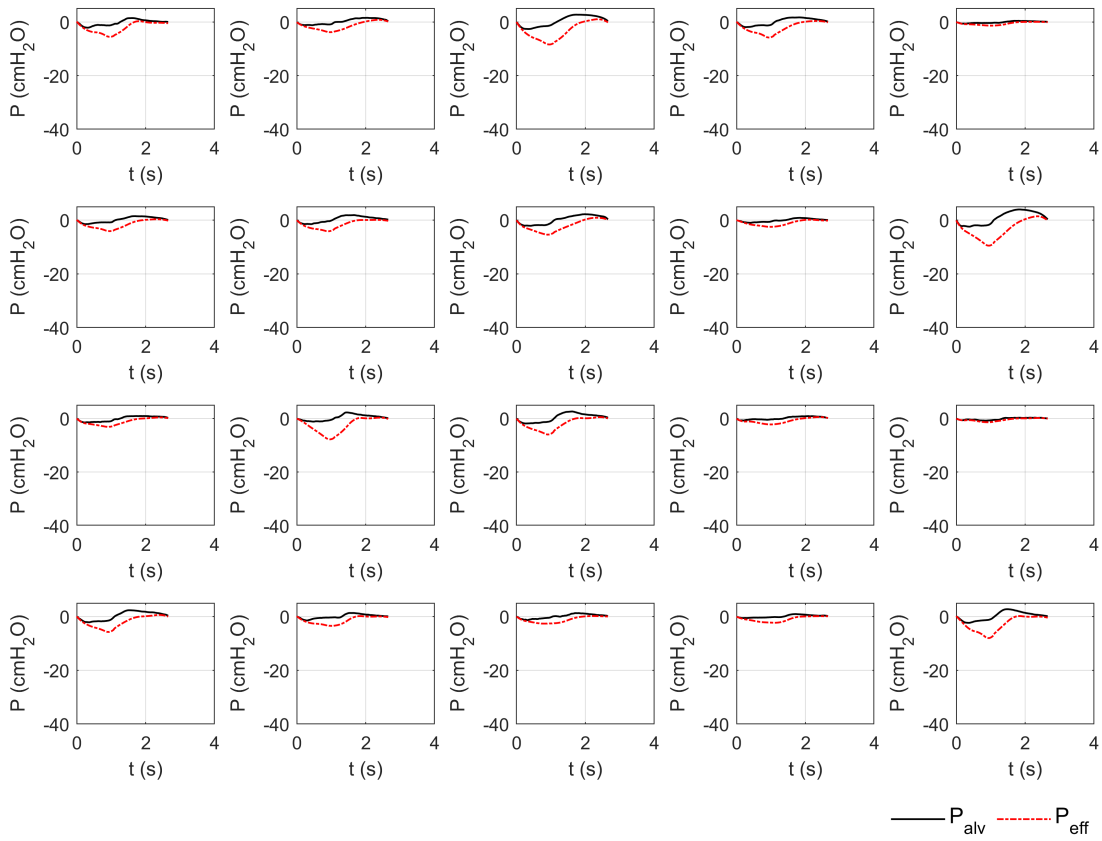

Figure 6.8: Alveolar pressure (P_{alv}) is shown compared with patient effort (P_{eff}) for the Elderly cohort.

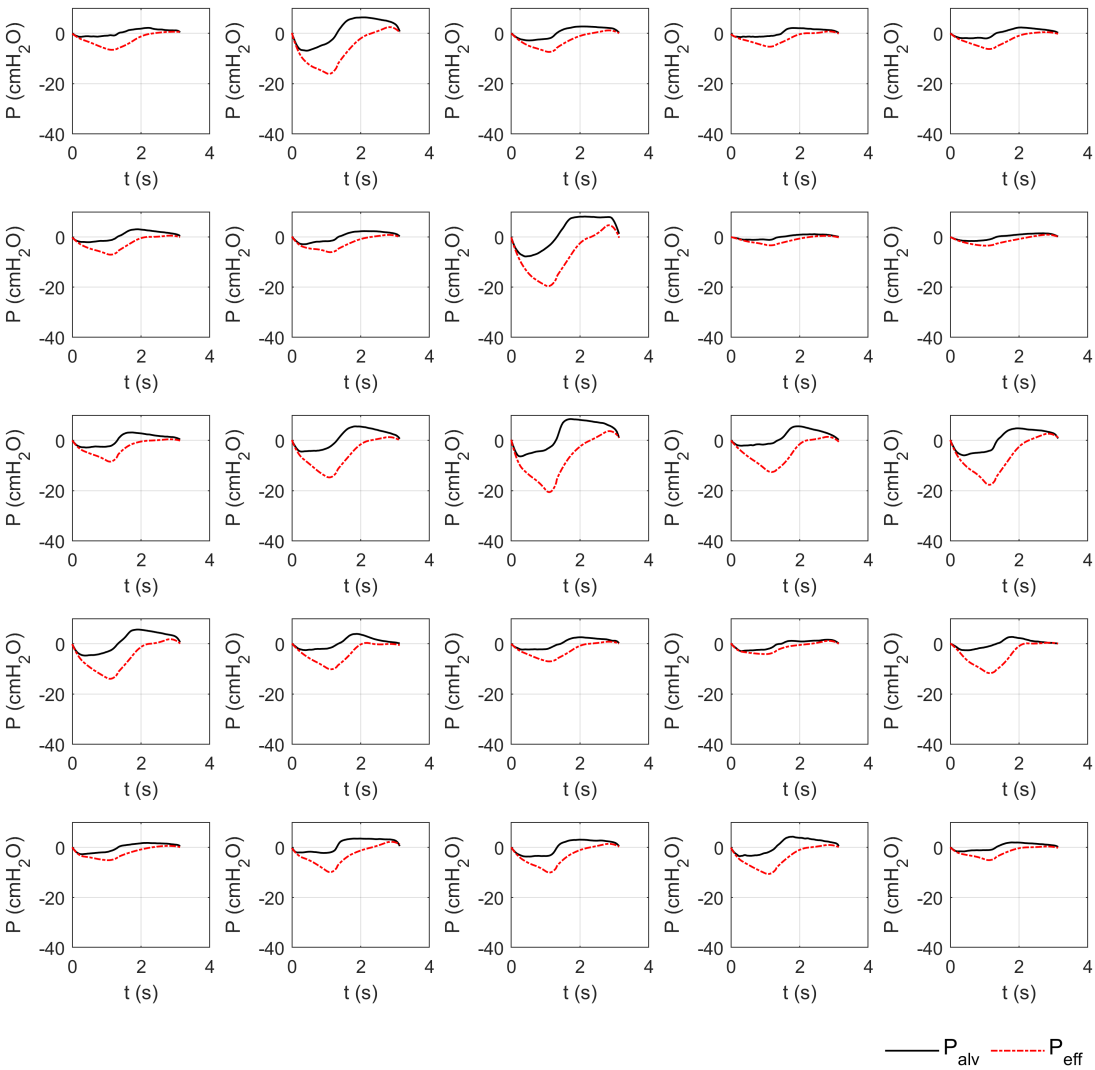

Figure 6.9: Alveolar pressure (P_{alv}) is shown compared with patient effort (P_{eff}) for the NFL cohort.

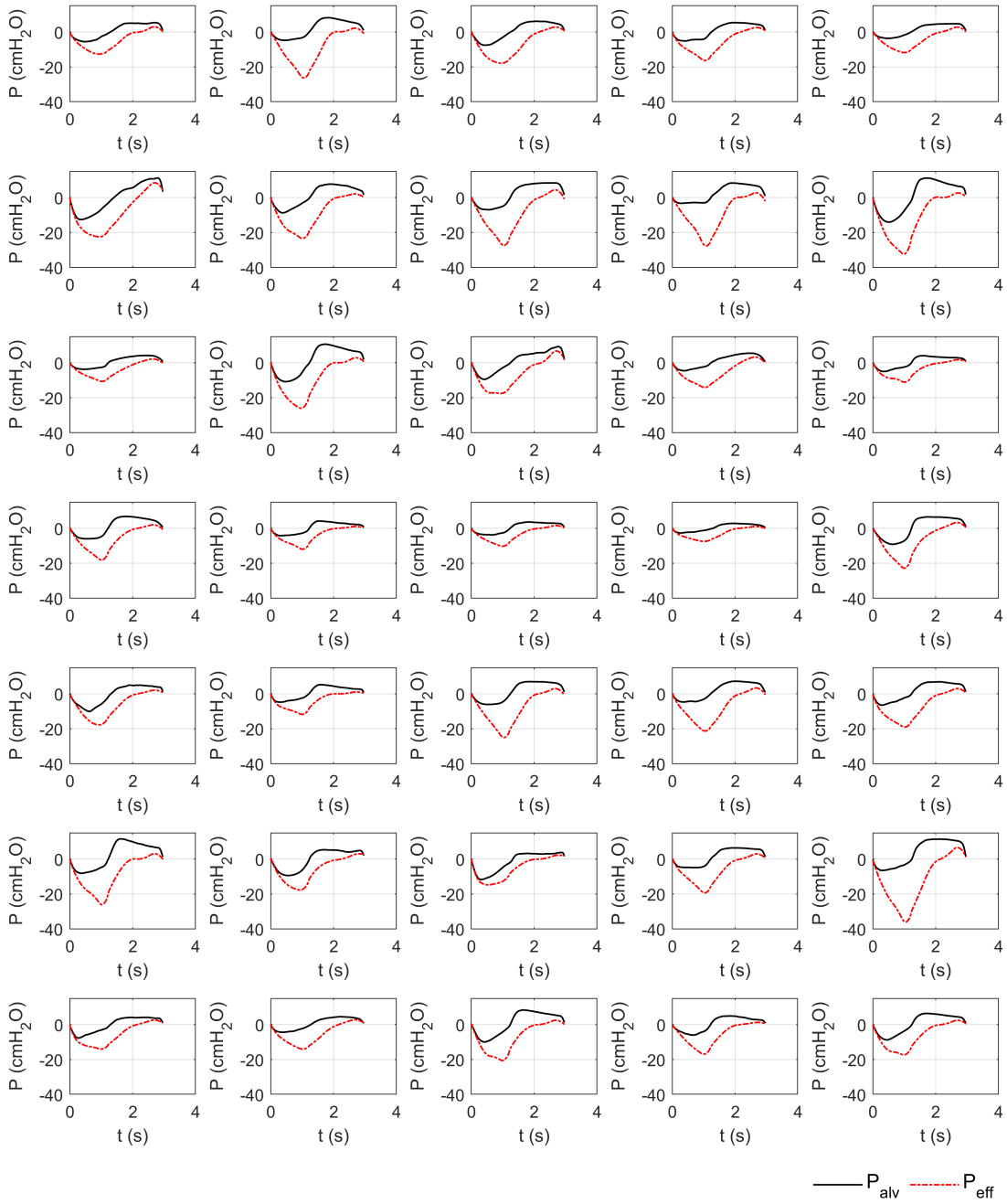

Figure 6.10: Alveolar pressure (P_{alv}) is shown compared with patient effort (P_{eff}) for the FL cohort.

6.5 Summary

This chapter utilises plethysmography data as a first step towards a less involved clinical diagnosis and monitoring tool. The aim is to apply a similar model to airway pressure and flow data to provide model-based estimations of lung condition. Future work will explore the generalisation of this model to such data, and the strengths and limitations of such an approach from a clinical perspective.

CHAPTER 7: ESTIMATING PATIENT EXPIRATORY EFFORT

7.1 Introduction

Chapter 5 focused on identifying nonlinear resistance in expiration for healthy and COPD patients using plethysmographic data. Chapter 6 quantified breathing effort in inspiration and expiration in the same data set. A key factor in the derivation of breathing effort was the assumption of passive expiration in the middle of expiration. The middle of expiration was chosen to avoid any nonlinear tissue relaxation effects across early expiration, and active breathing effort at end expiration in flow limited patients. This chapter explores the implications of active and passive breathing with a goal to provide insight into model assumptions around elastance, and its relationship with work of breathing and elastance.

7.2 Methods

7.2.1 Clinical Data

Plethysmographic alveolar pressure (P_{alv}), and air flow (Q) measurements form The Italy Data, collected by Pecchiari et al. (2016) is used for analysis. The data set consists of 100 patients separated into 4 cohorts: Young, Elderly, NFL and FL. A

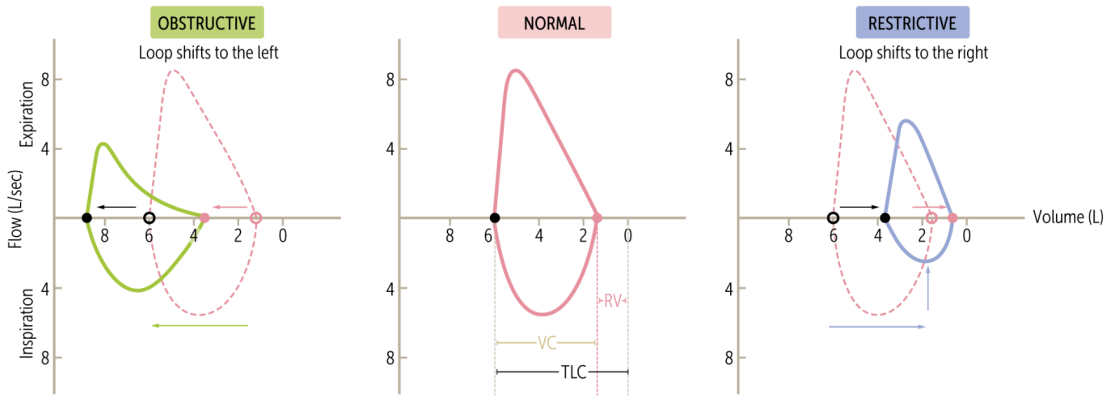

Figure 7.1: An example of flow-volume loops and how they differ with obstructive and restrictive disease [415].

detailed description of the data set is presented in Chapter 3.

7.2.2 Flow-Volume loops

Flow-volume loops are commonly used with forced expiration in spirometry to reveal characteristic patters suggestive of different types of pulmonary disease, and to examine response to therapy [411–414]. In addition to forced vital capacity (FVC), exhalation volume in the first second (FEV1), and peak expiatory flow (PEF), the curves can show different shapes depending on whether the underlying disease is obstructive or restrictive in nature, as shown in Figure 7.1.

QV loops typically plot expiratory flow along the positive y axis. They may include inspiration along the negative y axis. Volume is measured relative to peak volume, with decreasing volume along the positive direction of the x-axis, as shown in Figure 7.2.

This analysis proposes to take advantage of the QV loop shape characteristics of passive vs forced expiration to examine active effort in the clinical data set. In particular, passive expiration in a QV loop is characteristically more similar to a sinusoid, while increasing degrees of active or forced expiration causes a triangular, saturated peaking of flow early in expiratory volume clearance, as shown in Figure 7.1 or 7.2.

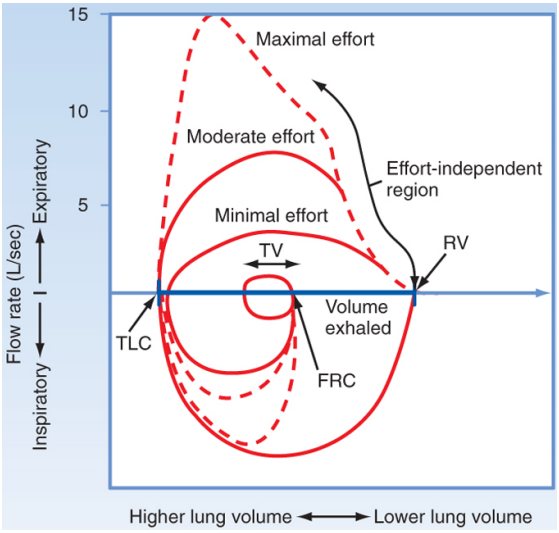

Figure 7.2: A flow-volume loop indicating how passive and active breathing affects the shape of the loop [416].

7.2.3 Model

The approximation of passive airflow Q_P $[L/s]$ using a sinusoidal waveform, as proposed in numerous studies [25, 417–420], can be explained by Hooke's Law and assumed minimal work of breathing effort, largely driven by the elastance in the lung. This estimation is characterised by its amplitude A $[L/s]$, time since expiration onset t $[s]$, and expiration time period t_{exp}:

$$Q_p = Asin\left(\pi \frac{t}{t_{exp}}\right) \tag{7.1}$$

Passive volume clearance, V_P, is thus derived from the integral of passive airflow:

$$V_p = \int_0^t Q_p(\tau)\, d\tau \tag{7.2}$$

where $t[s]$ is the time period of the integral. Total expiratory passive volume clearance, ($V_{P,exp}$, is thus:

$$V_{p,exp} = \int_0^{t_{exp}} Q_p(\tau)\, d\tau = -(t_{exp}/\pi) A cos\left(\pi \frac{t}{t_{exp}}\right)\Bigg|_0^{t_{exp}} \tag{7.3}$$

Rearranging Equation 7.3 for A, with expiatory tidal volume expressed V_{exp} yields:

$$A = \frac{V_{exp}\pi}{2t_{exp}} \tag{7.4}$$

Substituting Equation 7.4 into Equation 7.1 provides a model to approximate passive flow Q_P, and passive volume V_P for each patient in the data set:

$$Q_p = \frac{\pi V_{p,exp}}{2t_{exp}} sin\left(\pi \frac{t}{t_{exp}}\right) \tag{7.5}$$

The corresponding passive volume clearance is:

$$V_p = \frac{V_{p,exp}}{2}\left(1 - cos\left(\pi \frac{t}{t_{exp}}\right)\right) \tag{7.6}$$

Thus, knowing expiratory tidal volume and the period of expiration, the flow profile for an equivalent passive expiration can be estimated. The degree to which the passive approximation of Equation 7.5 overlaps the actual measured flow data can then be used to assess how active or passive expiration is.

7.2.4 Analyses

The sinusoidal passive expiration model of Equations 7.5 and 7.6 was generated from expiratory tidal volume, and the time period of expiration for each breath to yield an approximation for passive air flow (Q_P), and passive volume (V_P). Comparison of the passive approximation with the actual measured QV loops allows inference of active vs.

passive expiration.

Qualitative comparison simply compares the shapes of the passive approximation with the underlying data in plotted QV loops, where the presence of flow peaking before the middle of the breath, resulting in triangulation of hte QV-loop, is a easy visual indicator of active expiration. Quantitative approaches to this comparison include the use of root mean squared error (RMSE), and correlation coefficients (r), defined:

$$RMSE = \sqrt{\frac{1}{n}\Sigma_{i=1}^{n}\Big(Q - Q_P\Big)^2} \tag{7.7}$$

where n is the number of data points in the recorded/predicted waveform.

$$r = \frac{\sum_{i=1}^{n}(Q - \overline{Q})(Q_P - \overline{Q_P})}{\sqrt{\sum_{i=1}^{n}(Q - \overline{Q})^2(Q_P - \overline{Q})^2}} \tag{7.8}$$

where $\overline{Q}$ and $\overline{Q_P}$ are means of each respective vector.

Active breathing affects model-based estimation of work of breathing, and elastance, as undertaken in Chapter 6. Active breathing is expected to be more prevalent in the FL and NFL COPD cohorts, so the RSME and correlation coefficient outcomes are compared cohort to cohort, in addition to breath-breath examination of breathing effort at the individual subject level.

7.3 Results

Figure 7.3 shows examples of the most passive and significantly active expiration affected expiratory curves, based on QV loops shape comparisons between passive approximations and the measured data. The top row (a-d) demonstrates a typical patient with

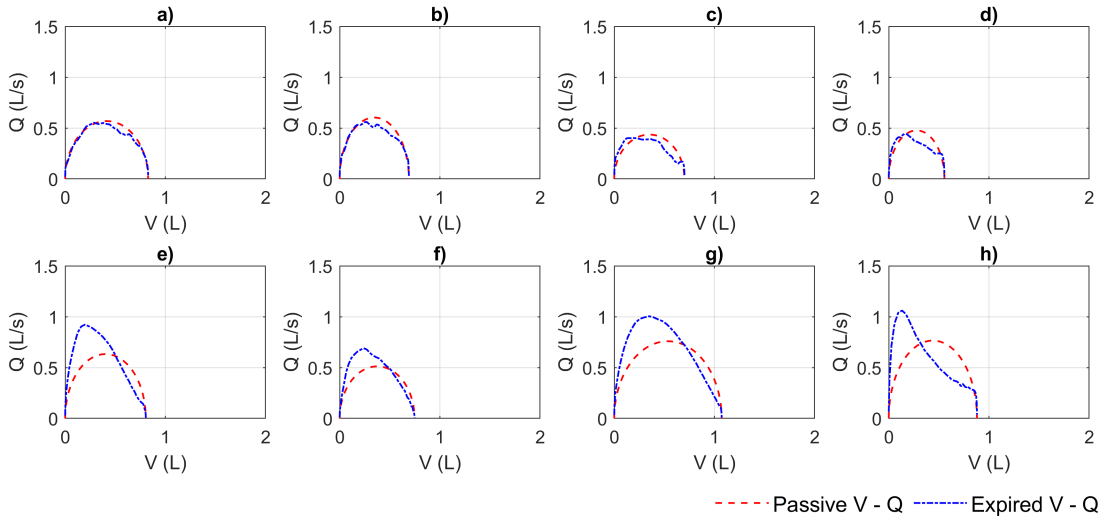

Figure 7.3: Measured expiratory flow as a function of volume for a Young (a), Elderly (b), NFL (c), and FL (d) patient, displaying largely passive expiration compared with a Young (e), Elderly (f), NFL (g), and FL(h) patient displaying more active expiration.

(more) passive expiratory flow for each cohort, showing, as expected, even the most passive breaths of the COPD cohorts show peak expiratory flow before the middle of the breath. The Young cohort has the highest peak expiratory flow, followed by Elderly, NFL, and finally FL. The bottom row (e-h) shows the active expiratory flow for each cohort, which is considerably different compared with the model-based estimation of passive expiratory flow, where the QV loop in the FL patient shows characteristics of obstructive lung disease. As noted, the more active expiration is, the greater the error.

The active expiratory flow was larger compared with active expiratory results from other cohorts, and slanted toward the beginning of expiration as expected in literature [421–426]. Furthermore, the active expiratory flow triangulation was found to be more frequent in patients in the FL cohort than any other cohorts, as demonstrated in Figures 7.4 to 7.7. These results demonstrate the importance of considering both passive and active expiratory flow differences when using model-based methods to estimate elastance and work of breathing, [427–432], as explored in Chapter 6.

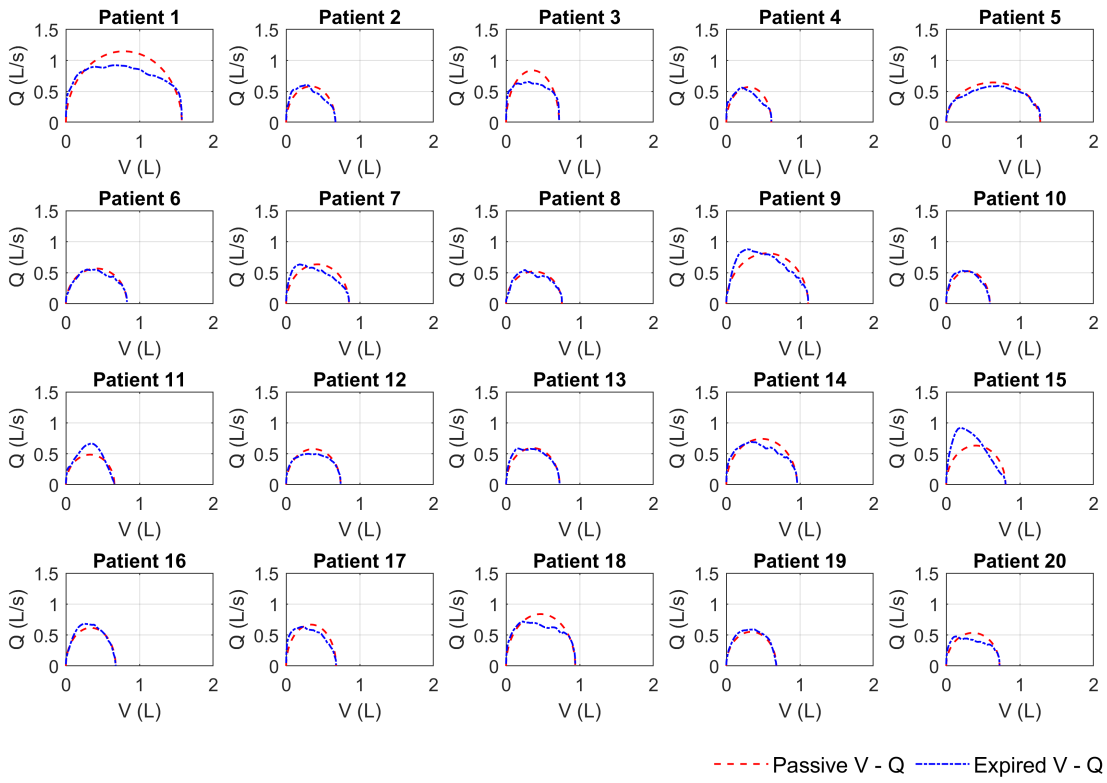

Figure 7.4: Volume-Flow ($V - Q$) loops for all patients in the Young cohort.

This behaviour is indicative of a larger difference between the estimated passive expiratory flow (Q_P) and measured air flow at the airway. This result is expected due to the obstructive disease causing patients to increase active exhalation. These results are presented per cohort in Table 7.1 with a corresponding RMSE (Figure 7.8) and correlation coefficient (Figure 7.9) box plot. Active breathing is more common in the COPD cohorts, as expected and supported by the literature [433–436].

Figures 7.4 to 7.7 illustrate measured flow-volume curves, compared with the sinusoidal approximation for passive expiration for each patient in each respective cohort. Table 7.1 presents quantitative metrics of for the difference between the measured plethysmographic V-Q data, and the approximated passive expiration V-Q curves. The results

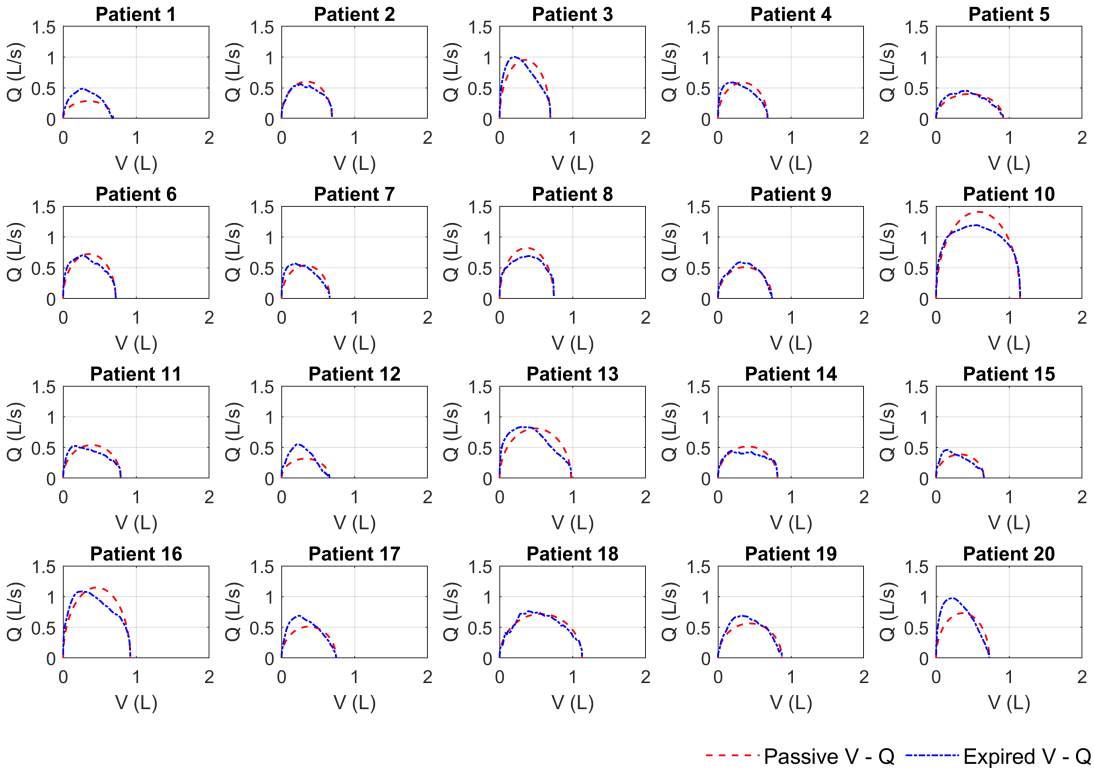

Figure 7.5: Volume-Flow ($V - Q$) loops for all patients in the Elderly cohort.

Table 7.1: Median [IQR] of model parameters and WOB results for all patients in all four cohorts.

	Young	Elderly	NFL	FL
Q_P RMSE	0.13 [0.07-0.15]	0.16 [0.11-0.18]	0.17 [0.12-0.23]	0.18 [0.15-0.25]
Q_P Correlation Coeff	0.86 [0.72-0.94]	0.76 [0.53-0.89]	0.69 [0.49-0.82]	0.27 [0.12-0.57]

demonstrate modelled Q_P to correlate strongly with the Young cohort, and relatively correlated with the Elderly cohort compared to the COPD cohorts.
In Figure 7.7, the FL patients have the highest number of expiratory V-Q wave-forms which are not highly correlated with the modelled sinusoidal passive breathing estimation. This result is as expected, as shown in Figure 7.2, where active expiration flow volume curves often depict a peak in flow at lower volumes due to obstructive disease. Note, the offset peak in flow in the FL patients occurs in many patients, regardless of the length of the breath in time or the magnitude of the air flow. The shape of the QV loop thus becomes more important for active expiration determination than the magnitude, lending more weight to qualitative methods of analysis, rather than quantitative methods.

7.4 Discussion

This chapter explored the prevalence of active expiration in the 'Italy' plethysmographic data set. All cohorts had instances of active expiration within their data sets. However, this behaviour was more prevalent in the COPD cohorts, and the FL cohort particularly, as would be expected.

Plethysmography commonly follows a pattern of quiet breathing, followed by a shutter manoeuvre, then a manoeuvre to examine forced vital capacity and other similar metrics of lung function [216]. The results of this chapter suggest the presence of active expiration during quiet breathing, which is counter to some typical clinical assumptions. In

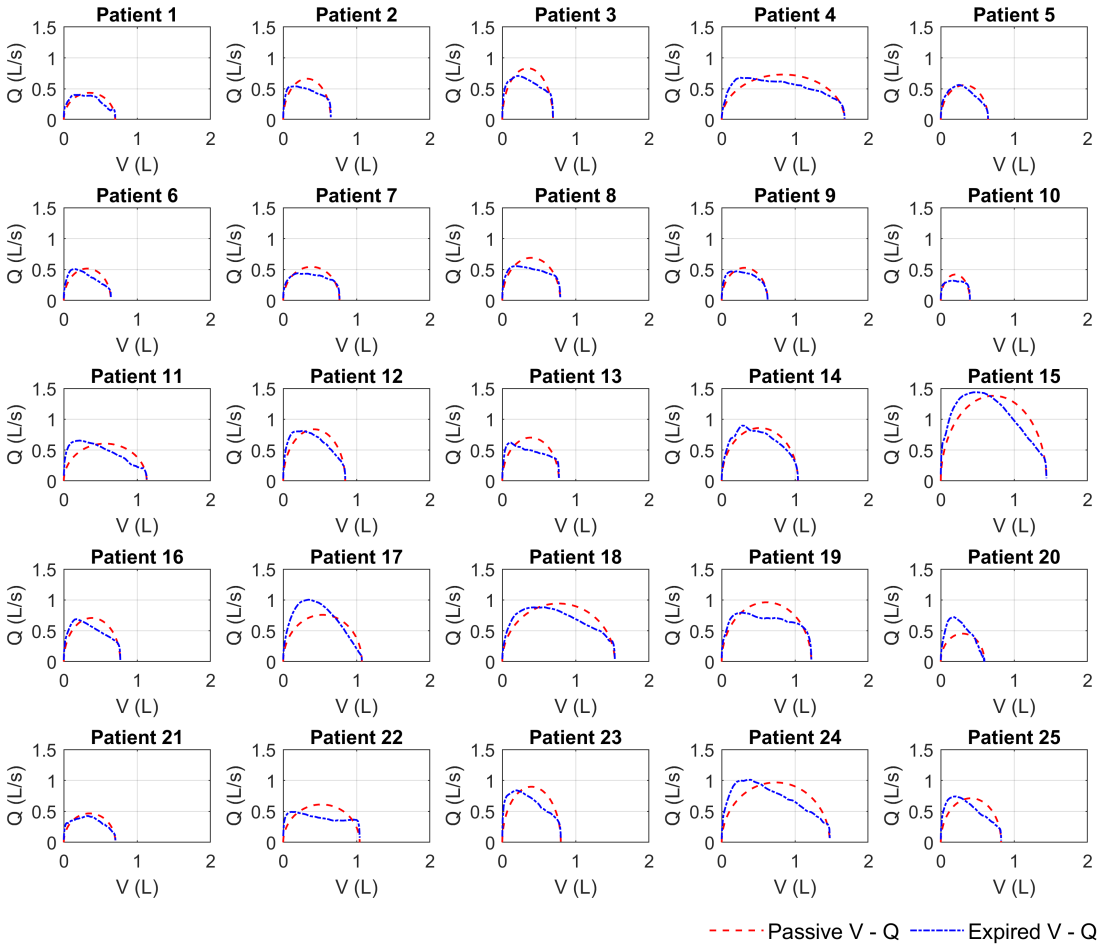

Figure 7.6: Volume-Flow ($V - Q$) loops for all patients in the NFL cohort.

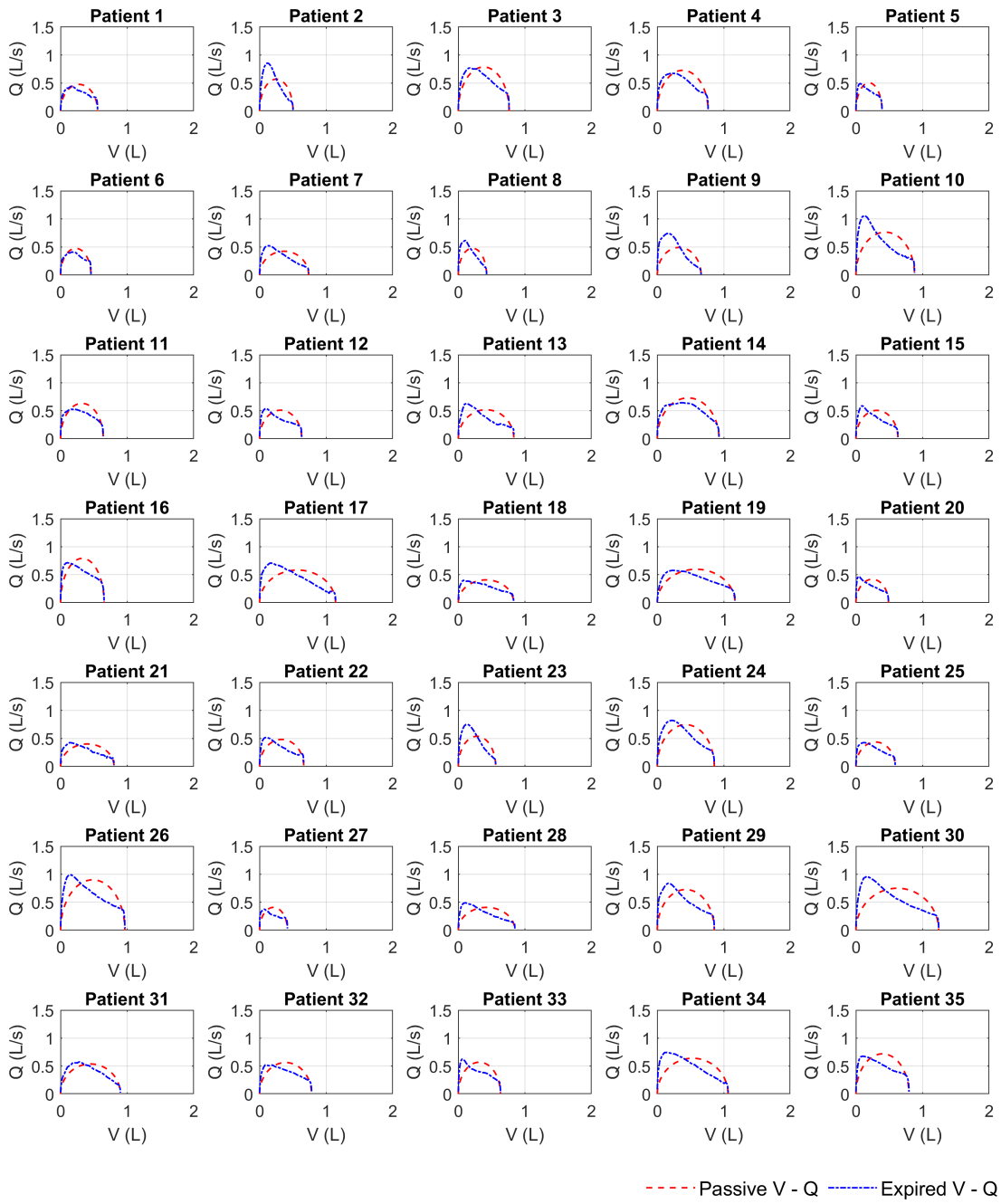

Figure 7.7: Volume-Flow ($V - Q$) loops for all patients in the FL cohort.

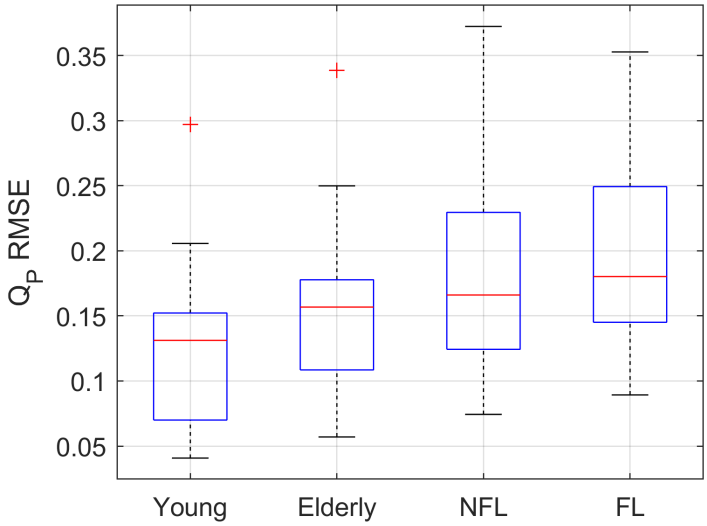

Figure 7.8: Q_P RMSE results depicted as a box plot, illustrating a lower RMSE values between measured Q and the modelled Q_P for the Young cohort, and relatively larger error moving through the cohorts toward the FL patients where active expiration is more prevalent.

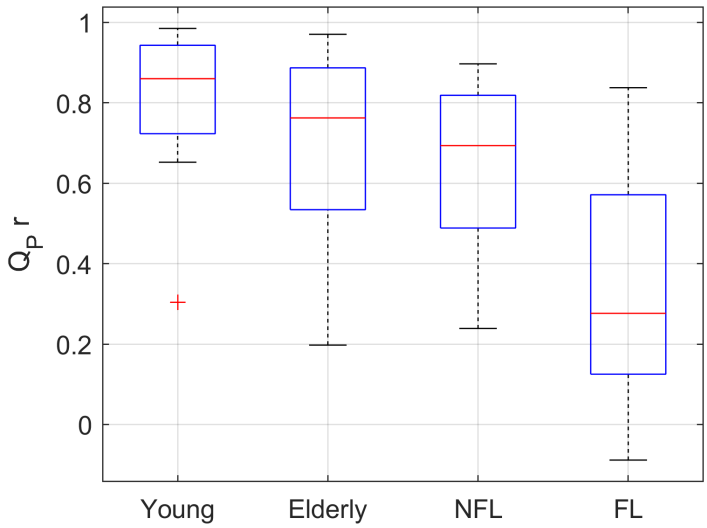

Figure 7.9: Q_P correlation coefficient (r) results depicted as a box plot, illustrating a stronger correlation between measured Q and the estimated Q_P for the Young cohort, and relatively less correlation moving through the cohorts toward the FL patients as expected.

the healthy young and elderly cohorts only 4-6 patients (≃25%) showed (qualitatively) active expiration in Figures 7.4 to 7.7, compared with most patients in the FL cohort. In the young cohort, the presence of active inspiration may be a function breathing consciousness, where consciousness of the breathing process and mechanics causes the subject to more actively control it. However, it could also reflect the persons' age and other underlying health conditions [437–442]. Chapter 5 showed some overlap between old and NFL cohorts with respect to airway resistance, where increasing airway resistance may result in active breathing effort during expiration [443–446].

By contrast, triangulation of expiratory flow was much more apparent in the COPD cohorts, occurring in at least 50 - 70% of the NFL cohort (Figure 7.6) and almost all of the FL cohort. This resulting lower occurrence of correlation of flow is not unexpected, as the presence of increased and nonlinear airway resistance (chapter 5) is well known to result in increased breathing effort (Chapter 6) to compensate. The findings of this chapter show the flow-volume curve becomes increasingly shallow toward the end of the breath, suggesting an increase in expiratory resistance and thus peak flow rate saturation [447–452].

This analysis also suggests the whole of expiration is active in these patients, with some patient's quiet breathing in the QV-loops in Figure 7.7 showing the curved decelerating flow typical of obstructive diseases during forced expiration ref some paper with a figure comparing the QV loops of restrictive vs obstructive disease. Thus, breathing effort during expiration is a significant consideration during modelling for many patients with COPD.

The analysis of Chapter 5 assumed the middle portion of expiration was passive in order to estimate lung elastance. This portion of the breath was chosen to avoid the relax-

ation tissue mechanics present during expiration onset, and any active expiration at end-expiration, due to the increasing resistance characteristic of FL COPD in Chapter 5. From a modelling perspective, elastance and breathing effort incur parametric trade-off. Thus, in the absence of passive expiration, and without some additional insight into the patient- and breath- specific mechanics of breathing effort, accurate estimation of lung elastance is not possible [25]. Active estimation, resulting in incorrect estimation of elastance [453–455], may lead to inaccurate assessments of their condition [456,457].A better understanding of the active and passive expiration patterns, or their direct management in test manoeuvres, could lead to more effective and efficient treatments [458].

In the context of this Chapter, the results in Chapter 6 may be less accurate with respect to elastance and work of breathing for the COPD cohorts. In particular, active breathing effort, resulting in increased transpulmonary driving pressure, may result in over-estimation of elastance. Thus, the results of Chapter 6 provide a measure of an upper estimate of breathing effort. Overall, the results for the NFL and FL COPD cohorts are within the physiologically sensible range for elastance [459–462], and any moderately lower underlying lung elastance will not significantly change the shape and trends in the results, instead shifting more of the resultant breathing effort positive during expiration.

The results of this chapter add insight and nuance to those presented in Chapters 5 and 6. In particular, they suggest the need for a breathing or shutter manoeuvre during Plethysmography to better estimate underlying lung elastance. When combined with the analysis of Chapter 6, improved lung elastance estimation provides significant insight into breathing effort across the whole breath.

In addition, the results of this chapter show active expiration during quiet breathing, the severity of which could also be used as a marker of disease severity. Overall, this

chapter provides insights to improve the accuracy of model-based methods of diagnosis and care, by providing insight into the impact of active expiration on elastance estimation.

7.5 Summary

This chapter shows active expiration in some patients from each cohort, suggesting it is a common occurrence during the quiet breathing portion of plethysmography. The results show active expiration is more prevalent in the FL cohort compared to the Young cohort, and could have important implications for model-based methods of diagnosis, monitoring and care, particularly when estimating elastance, resistance and work of breathing effort. Future research could further investigate the effects of active expiration on elastance estimation and other associated metrics, as well as exploring breathing manoeuvre or shutter methods for directly estimating elastance. In clinical contexts where they are more readily available, esophageal pressure measurements, applied to a model-based approximation, may add insight when identifying elastance, work of breathing and active expiration. In addition, further research could also focus on developing improved models of active and passive expiration, to improve the accuracy of diagnosis and care.

CHAPTER 8: IDENTIFYING NONLINEAR RESISTANCE IN MECHANICAL VENTILATION

8.1 Introduction

Chapters 4 through 7 focus on the identification of nonlinear resistance in expiration and the work of breathing in plethysmographic patient data for healthy patients, and for patients diagnosed with non-flow-limited (NFL) and flow-limited (FL) COPD. Chapter 8 explores the possibility of nonlinear resistance in expiration for patients undergoing mechanical ventilation.

Mechanical ventilation (MV) is a core life-support therapy for critically ill patients with respiratory failure [463, 464]. However, poorly applied MV can cause ventilator induced lung injury (VILI), and reduce patient comfort [465–467]. Mechanisms of VILI include excessive volume and/or pressure, and repeated opening and collapse of alveoli (atelectasis) [468, 469]. The management of mechanical ventilation is not standardised, with a variety of approaches [463,470]. In particular, there is a recent shift towards 'lung protective ventilation' [59,176,471], which must adapt to changing patient needs [236,472,473].

Model-based methods show promise for tailoring ventilator settings to patient-specific condition [40,60,176,236], with the intention to minimise lung stress and strain [54,474]. Model-based approaches commonly use patient-specific estimates of lung mechanics and/or gas exchange, to determine the optimal ventilator settings [54,475,476] or predict potential adverse effects [40, 60, 176, 236]. The goal is to provide sufficient oxygenation and ventilation, while avoiding lung injury and other complications.

Current model-based methods, clinically identifiable from in-hospital data, typically utilise the single compartment model described in Chapter 2. Within this model, airway resistance is described as either a constant, via Rohrer's equation [477, 478], or via visco-elastic terms [2, 293]. In visco-elastic models, a constant airway resistance is supplemented with tissue-resistance, which captures tissue mechanics, rather than classical airway resistance [2, 288, 293].

This chapter explores the potential of nonlinear expiratory resistance in MV patients. Around 20 - 30% of patients on MV have underlying COPD [479–481], which was shown in Chapters 4 and 5 to be associated with increasing nonlinearity in expiratory airway resistance specifically. Therefore, nonlinear resistance may be an informative or important dynamic when optimising MV for these patients.

8.2 Methods

8.2.1 Clinical Data

The MV Data of Chapter 3, was used in this analysis. In short, this data set comprised 6 patients on patient-triggered MV, and with some indications of patient-ventilator asynchrony, namely additional breathing efforts during inspiration or expiration. The data set comprised a minimum of 20 breaths per patient, and included airway pressure,

flow, and esophageal pressure measurements. In this analysis, the first 20 breaths per patient are used.

8.2.2 Model

8.2.2.1 Linear Model

This analysis is based on previous analysis from Chapter's 4 and 5. As MV data comprises airway pressure (P_{aw}) rather than alveolar pressure (P_{alv}), some modifications to the methodology must be made. The same single compartment model is used, repeated here:

$$P_{aw}(t) = EV(t) + RQ(t) + PEEP \tag{8.1}$$

Where $P_{aw}(t)$ $[cmH_2O]$ is airway pressure, $Q(t)$ $[L/s]$ is airflow, R $[cmH_2O/L/s]$ is airway resistance, E $[cmH_2O/L]$ is lung elastance, $V(t)$ $[L]$ is tidal volume, $PEEP$ is end-expiratory pressure, and t $[s]$ is time.

However, in contrast to Chapters 4 and 5, where alveolar pressure was known, typical MV data consists only of airway pressure and flow, and thus elastic dynamics must be accounted for when assessing airway resistance. Re-arranging Equation 8.1 for airway resistance yields:

$$R = \frac{P_{aw} - EV(t) - PEEP}{Q(t)} \tag{8.2}$$

In this analysis, only expiration is considered. Expiration is assumed passive, and no patient effort term is present in either Equation 8.1 or Equation 8.2. Including another term for patient effort in expiration could lead to non-identifiability issues [238]. As the MV data is patient-triggered, this assumption is not true of inspiration. Passive

expiration is a necessary starting assumption, given unknown time-varying effort and resistance functions directly trade-off within the model.

Elastance is estimated from end-inspiration, assuming complete ventilator unloading with no patient effort at end-inspiration:

$$E = \frac{P_{aw}(t_{insp,end}) - PEEP}{V(t_{insp,end})} \tag{8.3}$$

where $t_{insp,end}$ is defined as the last occurrence of non-negative flow (i.e. peak volume). E is calculated for each of the 20 breaths, and the median value used for all breaths when identifying non-linear resistance.

Where patient effort at end-inspiration is present, it is known to persist as a negative pressure into the start of expiration due to muscle relaxation time constants. In addition, the initial steep pressure drop during expiration in MV is also a function of ventilator mechanics. For this reason, expiratory resistance is calculated from peak expiratory flow (t_{Qpeak}), through to the end of expiratory flow (t_{end}), discarding the initial sharp pressure drop in expiration. It is identified using a least squares linear regression, defined:

$$\underbrace{\begin{bmatrix} Q(t_{Qpeak}) \\ \vdots \\ Q(t_{end}) \end{bmatrix}}_{\mathbf{A}} \underbrace{\begin{bmatrix} R \end{bmatrix}}_{\mathbf{x}} = \underbrace{\begin{bmatrix} P_{aw}(t_{Qpeak}) - EV(t_{Qpeak}) - PEEP \\ \vdots \\ P_{aw}(t_{end}) - EV(t_{Qpeak}) - PEEP \end{bmatrix}}_{\mathbf{b}} \tag{8.4}$$

Where this linear model formulation holds resistance constant and thus may not fully capture airway dynamics in COPD patients, where expiratory resistance can be volume dependent and nonlinear [216, 219, 302–304].

8.2.2.2 Rohrer's resistance model

Rohrer's nonlinear airway resistance equation is commonly used [236, 482–485] in MV modelling to describe a flow-dependant change in airway resistance. It is defined:

$$R_{roh}(t) = R_1 + R_2|Q(t)| \tag{8.5}$$

Substituting Rohrer's resistance term into Equation 8.1, and rearranging to solve the matrix equation gives:

$$\underbrace{\begin{bmatrix} Q(t_{Qpeak}), Q(t_{Qpeak})|Q(t_{Qpeak})| \\ \vdots \\ Q(t_{end}), Q(t_{end})|Q(t_{end})| \end{bmatrix}}_{\mathbf{A}} \underbrace{\begin{bmatrix} R_1 \\ R_2 \end{bmatrix}}_{\mathbf{x}} = \underbrace{\begin{bmatrix} P_{aw}(t_{Qpeak}) - EV(t_{Qpeak}) - PEEP \\ \vdots \\ P_{aw}(t_{end}) - EV(t_{Qpeak}) - PEEP \end{bmatrix}}_{\mathbf{b}} \tag{8.6}$$

Linear least squares can also be used to solve for R_1 and R_2, which are constrained positive. Rohrer's equation adds non-linear dynamics in airway resistance, but when it's parameters are constrained positive R decreases with decelerating flow, which is opposite to observations in COPD patients in Chapters 4-5.

8.2.2.3 Nonlinear resistance model

It is hypothesised a non-linear time-varying resistance is required to fully capture the non-linear airway behaviour during expiration in some MV patients. Thus, Equation 8.1 becomes:

$$P_{aw}(t) = EV(t) + \left[\sum_{i=1}^{M} R_{3,i}\Phi_{i,d=2}(t) \right] Q_{exp}(t) + PEEP \tag{8.7}$$

where $R_{exp} = \sum(R_3\Phi)$ is modelled using $M = 30$ 2nd order ($d = 2$) b-spline functions to fit the unknown and variable shape function, capturing any non-linear, time-varying dynamics during expiration. The second order b-spline functions [164, 166, 167, 237] are defined over time yielding:

$$\Phi_{i,0}(t) = \begin{cases} 1 & T_i \leq t \leq T_{i+1} \\ 0 & otherwise \end{cases}$$

$$\Phi_{i,d}(t) = \frac{t - T_i}{T_{i+d} - T_i}\Phi_{i,d-1}(t) + \frac{T_{i+d+1} - t}{T_{i+d+1} - T_{i+1}}\Phi_{i+1,d-1}(t) \; for \; d \geq 1 \tag{8.8}$$

Where $R_{3,i}$ are constant coefficients of these splines identified using linear least squares from measured data. The number of 2nd order ($d = 2$) splines with knot width (k_w) of 0.01s and a maximal spline time-span for expiration are defined:

$$M(n) = ceil\left(\frac{T_{max}(n)}{k_w}\right) + d \tag{8.9}$$

Linear least squares is used to fit $R_{3,i}$:

$$\underbrace{\begin{bmatrix} \Phi_1 Q_{exp} & \dots & \Phi_m Q_{exp} \end{bmatrix}}_{\mathbf{A}} \underbrace{\begin{bmatrix} R_{3,1} \\ \vdots \\ R_{3,M} \end{bmatrix}}_{\mathbf{x}} = \underbrace{\begin{bmatrix} P_{aw}(t) - EV(t) - PEEP \end{bmatrix}}_{\mathbf{b}} \tag{8.10}$$

Matlab command lsqlin (The Mathworks, Inc., Natick, Massachusetts, United States.) is used to constrain all identified parameters positive, $R_{3,i} > 0$, which is physiologically realistic and mitigates identifiability issues [238].

8.2.3 Analyses

Equations 8.4, 8.6 and 8.10 are identified using linear least squares and data from peak expiratory flow to no expiratory flow, yielding R_{lin}, R_1 and R_2, and $R_{exp}(t) = \sum(R_{3,i}\Phi)$ for the linear, Rohrer, and nonlinear spline models, respectively. CDF plots are used to show the breath-breath variability in these resistance terms across each patient. Chapters 4 and 5 showed increasing airway resistance with decreasing flow in COPD patients, a pattern expected to be repeated for some patients in the MV data. This pattern is opposite to the pattern described by the Rohrer equation, and thus may highlight its limitations in COPD patients on MV.

8.3 Results

Airway resistance models fit to the expiratory portion of the breath, beginning at peak expiration, are presented with estimated parameters shown in Table 8.1. Model fits in Table 8.2 were much lower for the Rohrer and nonlinear models, suggesting expiratory resistance has some nonlinear dynamics not well captured by a single linear constant. Figure 8.1 shows a typical expiratory breath (left) with measured airway pressure, P_{aw}, compared with the Rohrer model (Equation 8.6), and the nonlinear resistance model (Equation 8.7).

Figure 8.1 (right) also depicts the singular b-splines described in Equation 8.8. The sum of these spline terms which make up the nonlinear resistance term ($R_3\Phi$) found in Equation 8.7. Note, resistance estimated in the Rohrer, and nonlinear resistance model both decreases toward the end of expiration, as flow decreases, for this patient.

Figure 8.2 and Figure 8.3 depict airway resistance for a typical expiration from each

Table 8.1: First quartile (Q1), median (MED), and third quartile (Q3) results for lung elastance, and predicted airway resistance for each respective nonlinear estimation, with constant resistance values for the linear estimation for each respective patient numbered 1 - 6.

	E (Q1 MED Q3) $[cmH_2O/L]$			R_{lin} $[cmH_2O/L/s]$	R_1 (Q1 MED Q3) $[cmH_2O/L/s]$			R_2 (Q1 MED Q3) $[cmH_2O/L/s]$			$R_3\Phi$ (Q1 MED Q3) $[cmH_2O/L/s]$		
1	13.8	14.6	16.3	3.2	7.5	8.8	10.9	3.5	1.3	1.3	5.4	6.3	7.9
2	34.6	36.0	37.6	22.7	4.2	7.4	10.7	9.6	26.3	34.9	5.6	7.4	10.5
3	6.8	8.2	25.6	2.2	1.4	2.4	4.9	0.3	0.6	6.6	1.2	2.8	5.5
4	7.2	7.8	8.7	5.0	0.4	1.7	2.6	3.5	5.3	7.1	2.7	3.4	4.2
5	7.9	14.7	15.4	7.5	0.6	1.4	2.3	5.0	8.2	10.0	3.5	4.0	4.4
6	7.6	10.7	14.0	4.6	1.0	1.9	3.4	2.3	3.5	7.3	3.0	3.8	4.3

patient. The dynamic expiratory resistance sometimes increases toward the end of expiration, as seen previously in Chapters 4, and 5 in patients with flow limitation and obstructive disease. However, most breaths in the patients in the MV data in this chapter have a decrease in resistance toward the end of expiration, where flow is decreasing. This decrease in resistance toward the end of expiration is similar to the Rohrer resistance definition.

The CDFs in Figure 8.4 shows patient-specific average resistance values, with reasonably tight breath-breath distributions around these averages for linear and non-linear models. The less tight, more scattered distributions for Rohrer equation terms R_1 and R_2 suggest breath-breath parameter trade off within the Rohrer equation. Outlier breaths for each patient tend to occur when the breath recorded displays asynchronous behaviour. The values from all three models shown in the CDFs in Figure 8.4 are within a physiologically expected range [219, 301–303].

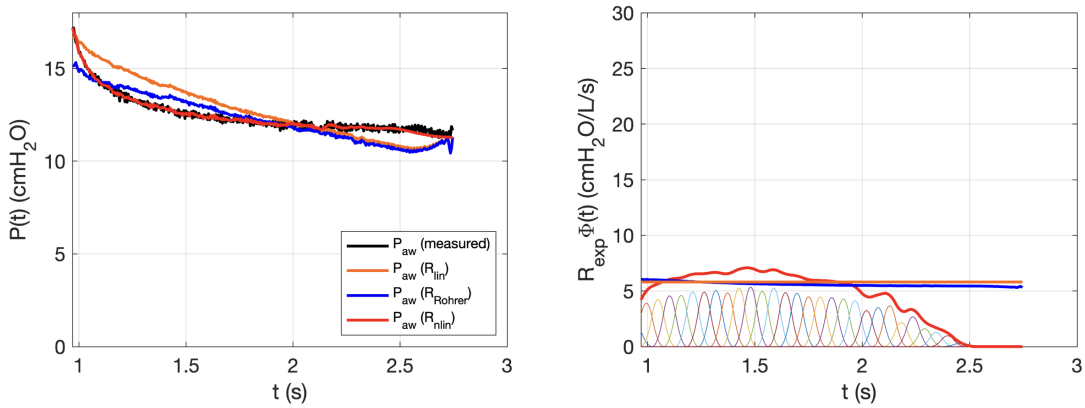

Figure 8.1: Model-fits to a typical breath for Patient 1. Resulting airway pressure (left) and resistance shapes with time (right) are shown for expiration, from peak-expiratory flow to end-expiratory flow. The b-spline model on the right additionally shows constituent b-splines as thin lines.

Table 8.2: As a measure of goodness of fit, median RMSE percentage for each patient, and each model for comparison.

	Median RMSE [%] (IQR)		
	Linear Model	Rohrer Model	Nonlinear Model
Patient 1	0.20 (0.17 - 0.22)	0.04 (0.04 - 0.05)	0.02 (0.01 - 0.02)
Patient 2	0.17 (0.14 - 0.20)	0.05 (0.04 - 0.06)	0.03 (0.03 - 0.05)
Patient 3	0.05 (0.03 - 0.16)	0.03 (0.02 - 0.05)	0.02 (0.01 - 0.04)
Patient 4	0.09 (0.08 - 0.11)	0.07 (0.06 - 0.09)	0.02 (0.02 - 0.03)
Patient 5	0.13 (0.11 - 0.14)	0.08 (0.07 - 0.09)	0.03 (0.02 - 0.04)
Patient 6	0.10 (0.07 - 0.13)	0.07 (0.04 - 0.09)	0.02 (0.01 - 0.04)

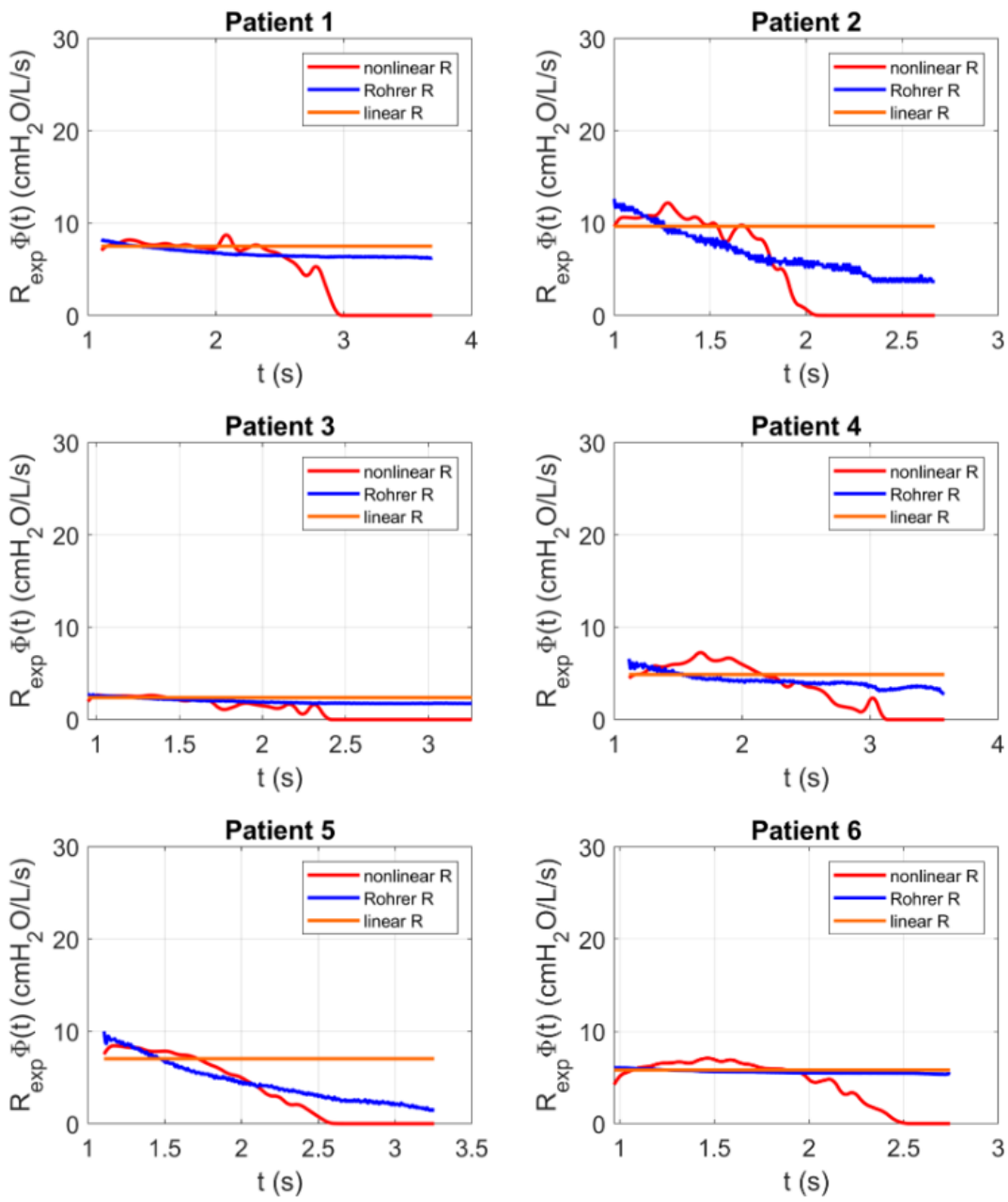

Figure 8.2: Different resistance model outcomes for a typical expiratory breath for each of the 6 patients.

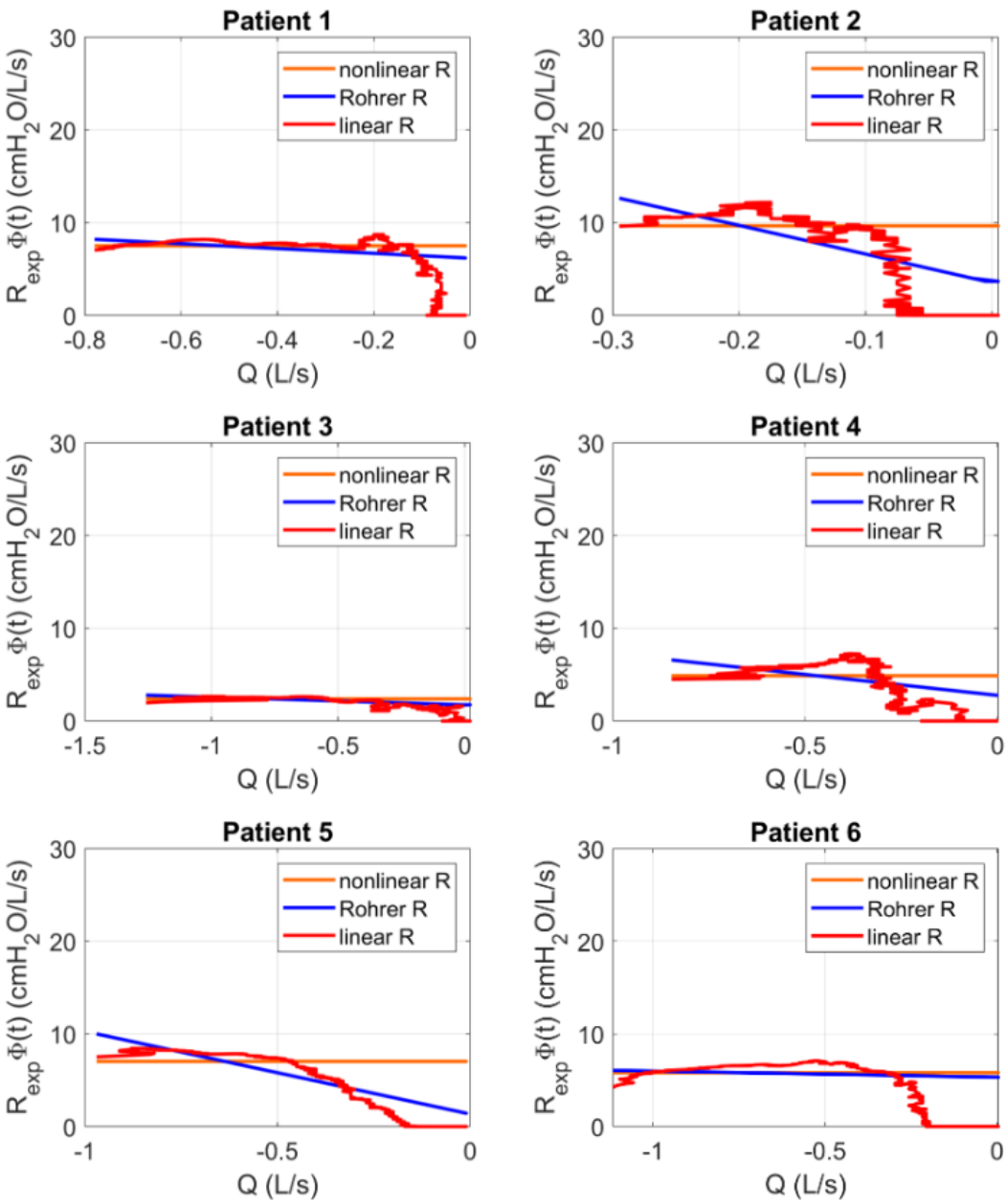

Figure 8.3: Nonlinear resistance model outcomes as a function of airflow (Q) for a typical expiratory breath, corresponding to Figure 8.2, for each of the 6 patients.

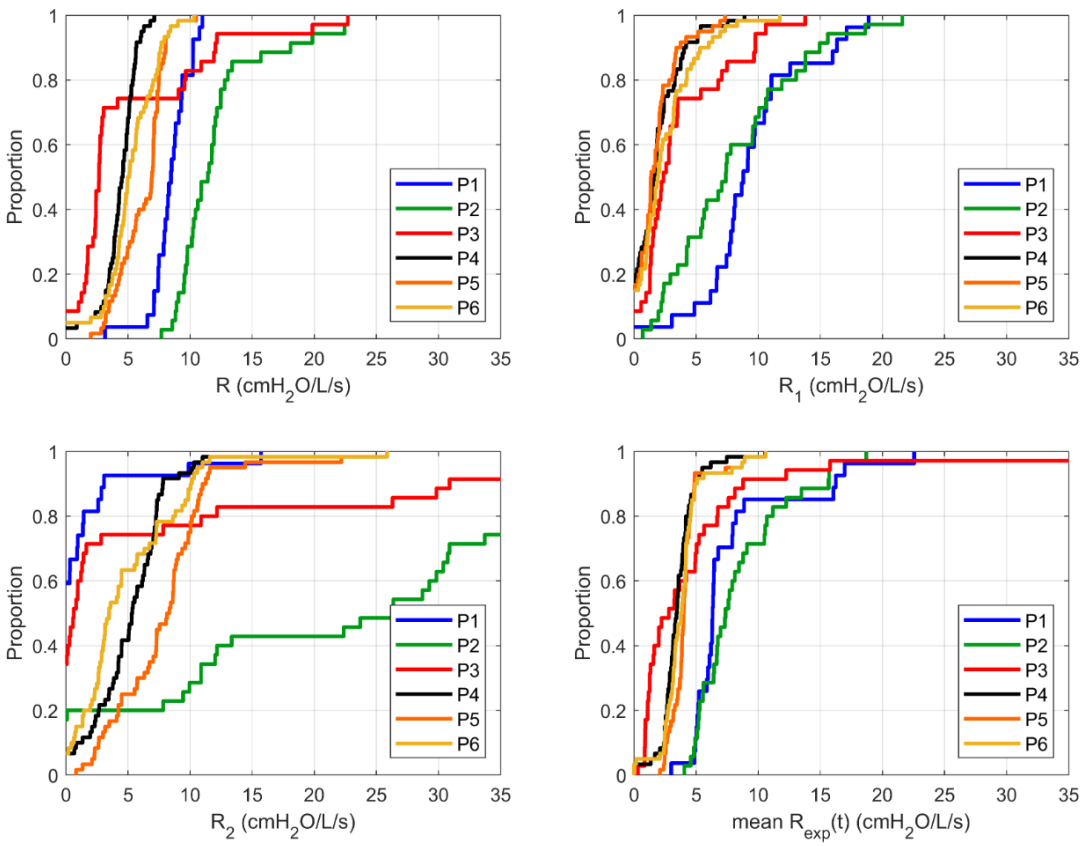

Figure 8.4: Continuous distribution functions for patient-specific (n=20 breaths) parameters for each of the linear (R), Rohrer (R_1 and R_2) models, and the mean nonlinear resistance ($mean(R_exp = \sum(R_3\Phi))$).

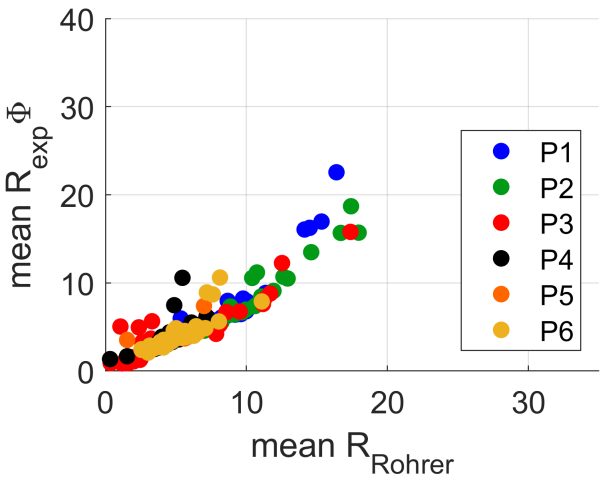

Figure 8.5: Comparison of mean $R_{exp}\Phi$, and the mean resistance value obtained from the Rohrer model (R_{Rohrer}) for each breath across the 6 patients.

8.4 Discussion

This analysis estimates expiratory elastance using several relatively simple methods. These methods include assuming expiration is mostly passive. Thus, the chapter focuses on the estimation of resistance in MV patients using linear and nonlinear models for comparison.

In Chapters 4 and 5, results show an increase in nonlinear expiratory resistance toward the end of a breath, where the MV data mostly shows (Figure 8.2) a decrease in resistance with a decrease in flow toward the end of a breath. The previous analysis results from Chapter 5 formed a distinct triangular shape, where results from the MV Data in Figure 8.3 show a less aggressive slope for most patients. Patients diagnosed with NFL and FL COPD may suffer from airway collapse, mitigated by PEEP when undergoing MV. Thus, for most patients on MV, typical COPD dynamics may not be apparent, given high enough PEEP. This outcome should not be unexpected given how common PEEP = 10-20 cmH_2O is in ICU MV care.

As shown in Table 8.2, the nonlinear model, employing b-splines, provided the best fit to the measured airway pressure, as anticipated. However, it is notable, while the model was a good fit, the sum of the splines and their respective coefficients may be capturing dynamics and mechanics unrelated to nonlinear, expiratory resistance. Nonetheless, the nonlinear model offers greater insight into the timing of such dynamics and mechanics, as well as the changes in resistance associated with a variation in air flow.

A limitation of the study undertaken in this chapter is the small number of patients (N=6). Further studies with larger cohorts could provide better observation in terms of identifying metrics useful in the diagnosis, monitoring and care of patients with respiratory illness. The patients in this MV data were originally selected as a cohort to examine known asynchronies in the data, and thus may have had 'better' airway resistance, with less collapse, due to a bias towards patients with strong breathing efforts. Equally, use of typical ICU PEEP levels have mitigated airway collapse, as intended, as part of overall typical ICU MV care.

In addition, lung elastance E is estimated based on an assumption of full unloading of the work of breathing (WOB) onto the ventilator by the end of the breath. The presence of end inspiratory effort may cause this estimate to under-estimate true elastance. However, estimating elastance offsets resistance relative to zero pressure, and hence changes magnitude, but not the shape of the modelled resistance.

In this study, the presence of inspiratory effort meant inspiratory resistance was not identified, as in the analysis of Chapter 5. Chapter 5 showed expiratory resistance was slightly higher in expiration than inspiration for patients without COPD. This result was expected to translate to MV and has been shown in other MV studies [165,236,486].

However, this outcome was not realised.

Finally, this study assumed largely passive expiration. Esophageal pressures, examined more closely in Chapter 9, show this assumption to be largely true in most patients, with the possible exception of Patient 5. Esophageal pressures in this data also show the typical decay at the start of expiration, justifying the use of peak-expiratory flow as a starting point for this analysis. Given the positive pressure ventilation strategy typical of MV, this passive expiratory dynamic is expected to be typical of most patients, even during patient triggered ventilation, in the absence of expiratory patient-ventilator asynchronies.

8.5 Summary

The analyses in this chapter presented a method of quantification and subsequent analysis of expiratory resistance in MV data. Nonlinear resistance was estimated using similar methods presented previously in data obtained by plethysmography in Chapters 4, and 5. A linear resistance model and the Rohrer model were compared to analyse resistance in expiration. Nonlinear models exhibited a better model fit, estimating the nonlinear expiratory behaviour more accurately. The next chapter attempts to quantify patient effort in patients undergoing MV.

CHAPTER 9: WORK OF BREATHING IN MECHANICAL VENTILATION

9.1 Introduction

Where Chapter 8 explored nonlinear expiratory resistance in mechanical ventilation (MV), this chapter focuses on patient-specific breathing effort in a similar manner to Chapter 6.

Increasing patient breathing effort is necessary for patient weaning from mechanical ventilation [487–489]. This effort is an integral part of patient-triggered modes, which require the patient to initiate breaths [490]. Depending on the level of support, the proportion of the work of breathing (WOB) provided by the ventilator versus the patient will change [491, 492].

In ventilator modes, such as NAVA (Neurally Adjusted Ventilatory Assist), increasing the level of ventilatory support decreases the patient contribution to the WOB [493–497], a phenomenon known as ventilator unloading. However, the optimum level of ventilator support is unknown [498]. Too much support can lead to muscle atrophy [499], but poor synchrony of the patient and ventilator can cause further VILI [500, 501]. Thus, patient synchrony and contributions to the WOB should be monitored carefully as an

important aspect of patient-specific optimised MV care [487–489, 502].

A common MV mode is pressure support (PS) ventilation, where the patient triggers ventilator support with their own breathing efforts. Synchronised intermittent mandatory ventilation (SIMV) [503] is similar, but support is provided intermittently, rather than every breath. Typically, when the patient is able to initiate breaths at a rate greater than the set rate, the support is decreased. This automatic decrease is done with the goal the patient automatically and gradually increases their respiratory effort, leading to successful weaning [504–507]. Directly monitoring patient contributions to WOB [164, 236, 270, 486, 508] may better inform clinical weaning protocols, and help identify patient-ventilator synchrony, as well as avoid VILI.

This Chapter aims to estimate patient contribution to breathing effort in MV patients. A model-based method is developed and evaluated against esophageal pressure measurements as validation.

9.2 Methods

9.2.1 Clinical Data

As in Chapter 8, the MV Data of Chapter 3, was used in this analysis. This data set comprises 6 patients on patient-triggered MV, with some indications of patient-ventilator asynchrony. In particular, additional breathing efforts are evident during inspiration or expiration. The data set comprised a minimum of 20 breaths per patient, and included airway pressure, flow, and esophageal pressure measurements. In this analysis, the first 20 breaths per patient are used.

Estimation of plural pressure, and thus breathing effort, is provided by esophageal pres-

sure. Esophageal pressure changes track plural pressure changes, with a baseline pressure offset [509–512]. Esophageal pressure measurements within the lower third of the esophagus [274] are used as a surrogate for pleural pressure [513, 514]. Thus, in this thesis pleural pressure is estimated from esophageal pressure via:

$$P_{eff,meas}(t) = P_{es}(t) - P_{es,baseline} \tag{9.1}$$

where the baseline is calculated as the mode of P_{es}.

9.2.2 Model Development

Similar to Chapter 6, the modified single compartment model is used:

$$P_{aw}(t) = EV(t) + RQ(t) + PEEP + P_{eff}(t) \tag{9.2}$$

The unconstrained model of Equation 9.2 is unidentifiable, due to the $P_{eff}(t)$ term. Thus, estimation of E (cmH_2O/L) and R ($cmH_2O/L/s$), or the assumption of passive breathing during at least part of the breath, is needed.

It should be noted other approaches use a slightly different model notation [515, 516]:

$$P_{aw}(t) = EV(t) + RQ(t) + PEEP + P_{musc}(t) \tag{9.3}$$

Where $P_{musc}(t)$ represents the effort required to overcome the chest wall dynamics in addition to the lung mechanics, typically modelled using defined shape functions and specific constraints [517–521]. Thus, in this sign convention, E is the sum of the lung (E_L) and chest wall (E_{CW}) elastances, rather than the lung elastance of Equation 9.2. The two modelling conventions of Equation 9.2 and Equation 9.3 are thus related [522]:

$$P_{eff}(t) = P_{musc}(t) + E_{CW}V \tag{9.4}$$

The approach of Equation 9.2 is used here as it is easily compared against esophageal pressure as a surrogate of pleural pressure, without additional measurement or estimation of E_{CW}.

Lung elastance, E, is estimated via three different approaches, outlined in the next section below. Given a pre-determined value of E, the value of R is identified from expiration under the assumption of largely passive expiration ($P_{eff} = 0$). Substituting E, $PEEP$, and the known pressure ($P_{aw}(t)$) and tidal volume ($V(t)$) into the model yields a least squares problem defined:

$$\underbrace{\begin{bmatrix} Q(t_{exp,1}) \\ \vdots \\ Q(t_{exp,N}) \end{bmatrix} \begin{bmatrix} R \end{bmatrix}}_{\mathbf{Ax}} = \underbrace{\begin{bmatrix} P_{aw}(t_{exp,1}) - PEEP - EV(t_{exp,1}) \\ \vdots \\ P_{aw}(t_{exp,N}) - PEEP - EV(t_{exp,N}) \end{bmatrix}}_{\mathbf{b}} \tag{9.5}$$

Linear least squares is used to estimate expiratory R from peak expiratory flow ($t_{exp,1}$) to the end of the breath ($t_{exp,N}$), which is then assumed reflective of resistance over the whole breath.

The period from expiration onset to peak expiratory flow is not used to identify R, as, during this period, tissue relaxation effects mean P_{eff} is not equal to zero, but decays from its end-inspiratory value. R is identified for each of the 20 breaths using a breath-specific E estimate, and then the median value across these 20 breaths (R_1, R_2, and R_3 for analyses 1-3, respectively) is used to model breath-breath breathing effort. This approach assumes airway resistance is not significantly different breath-breath, and variability in this value arises from clinical noise and variability in estimated E.

The breath-breath breathing effort ($P_{eff}(t)$), representing average pressure changes in the pleural cavity, is fit to the whole of each breath using b-spline basis functions [167, 238]:

$$P_{eff}(t) = \sum_{i=1}^{M=50} P_{c,i}\Phi_{i,d=2}(t) \tag{9.6}$$

with $M = 50$ second order ($d = 2$) b-spline functions to fit the unknown shape function [39, 164, 270], with P_c the spline constant coefficients, capturing any nonlinear, time-varying effort dynamics. The second order splines are defined over time, with T equally spaced time points, yielding:

$$\Phi_{i,0}(t) = \begin{cases} 1 & T_i \leq t \leq T_{i+1} \\ 0 & otherwise \end{cases}$$

$$\begin{aligned} &\Phi_{i,d}(t) = \tfrac{t-T_i}{T_{i+d}-T_i}\Phi_{i,d-1}(t) + \tfrac{T_{i+d+1}-t}{T_{i+d+1}-T_{i+1}}\Phi_{i+1,d-1}(t) \\ &for\ d \geq 1 \end{aligned} \tag{9.7}$$

where T_i is the time point of the $M + 1$ "knots" which define basis function spacing. Because of the assumption of (largely) passive expiration in Equation 9.5, it should be noted P_{eff} dynamics over most of expiration capture deviation from model assumptions of constant linear R and E.

9.2.3 Analyses

Patient effort is explored over three separate analyses estimating E via three different approaches. Each analysis compares patient effort ($P_{eff,1}$, $P_{eff,2}$,$P_{eff,3}$), with esophageal pressure (P_{es}), and airway pressure (P_{aw}) for each patient. Root mean squared error ($RMSE$) is used to assess model estimated breathing effort against the esophageal

derived breathing effort (Equation 9.1).

$$RMSE = \sqrt{\frac{1}{n}\Sigma_{i=1}^{n}\Big(P_{eff} - P_{es}\Big)^2} \tag{9.8}$$

where n is the number of data points in the recorded/predicted waveform.

Peak modelled effort (Equation 9.6) and measured esophageal pressure swing (Equation 9.1 are compared, as measures of peak patient effort. A linear correlation coefficient (r) is calculated:

$$r = \frac{\sum_{i=1}^{n}(P_{eff} - \overline{P_{eff}})(P_{es} - \overline{P_{es}})}{\sqrt{\sum_{i=1}^{n}(P_{eff} - \overline{P_{eff}})^2(P_{es} - \overline{P_{es}})^2}} \tag{9.9}$$

where $\overline{P_{eff}}$ and $\overline{P_{es}}$ are means of each respective pressure result. In addition, the 1:1 line of peak modelled effort vs measured esophageal pressure swing is compared to the linear correlation line. A correlation matching the 1:1 line and passing through the origin (0,0) implies good matching of modelled and measured efforts at the same scale and without offset bias. Correlations with slopes other than 1.0 may imply the esophageal sensor placement does not accurately reflect average pleural pressure swings.

9.2.4 Patient Effort Analysis 1

Assuming minimal patient breathing effort at the end of inspiration (complete ventilator unloading), lung elastance (E), from Equation 9.2 is replaced with E_1, and estimated:

$$E_1 = \frac{P_{aw}(t_{insp,end}) - PEEP}{V(t_{insp,end})} \tag{9.10}$$

where $t_{insp,end}$ is the time point in each respective breath at which inspiration ends, defined as the last occurrence of non-negative flow (i.e. peak volume). E_1 is calculated

for each of the 20 breaths, and the median value used alongside the corresponding median R_1 described above to model breathing effort ($P_{eff,1}$) across all 20 breaths using Equations 9.5 and 9.2.

9.2.5 Patient Effort Analysis 2

For the second analysis, lung elastance (E) from Equation 9.2, is replaced with E_2 defined:

$$E_2 = \frac{PIP - PEEP}{V(PIP)} \tag{9.11}$$

where PIP is the peak inspiratory pressure, and $V(PIP)$ volume at this maximum pressure. Where PIP occurred after end inspiration, implying asynchronous breathing effort against the ventilator, the pressure and volume at the end of inspiration was used. E_2 is calculated for each of the 20 breaths, and the median value used alongside the corresponding median R_2 described above to model breathing effort ($P_{eff,2}$) across all 20 breaths using Equations 9.5 and 9.2.

9.2.6 Patient Effort Analysis 3

For the third patient effort analysis, lung elastance (E) from Equation 9.2, is replaced with E_3 defined:

$$E_3 = \frac{P_{aw}(t_{V,max}) - PEEP - P_{es,meas}(t_{V,max})}{V(t_{V,max})} \tag{9.12}$$

This approach directly accounts for end-expiratory effort, and evaluates the efficacy of linear model dynamics in E and R when generating effort as the residual of single-compartment model dynamics. It is thus an exploration of linear model dynamcis given a known end-inspiratory effort. Again, E_3 is calculated for each of the 20 breaths, and

the median value used alongside the corresponding median R_3 described above to model breathing effort ($P_{eff,3}$) across all 20 breaths using Equations 9.5 and 9.2.

9.3 Results

Figure 9.1 shows a typical breath for each patient, with measured airway pressure (P_{aw}), and esophageal pressure (P_{es}) plotted against the three patient effort analyses ($P_{eff,1}$, $P_{eff,2}$, $P_{eff,3}$), derived as per Section 9.2.3. Figures 9.2 to 9.4 show modelled breathing efforts for all breaths and each analysis respectively. $P_{eff,1}$ from Analysis 1 follows esophageal pressure relatively well for Patient 3 (median RSME 1.0 cmH_2O (0.1 [%])), but significantly underestimates inspiratory patient effort dynamics in other Patients (median RSME 1.4 - 5.9 cmH_2O (0.1-0.5 [%])), resulting in low or positive $P_{eff,1}$ compared to the negative esophageal pressure changes measured. In particular, it appears to underestimate elastance, E, due to the presence of negative expiratory effort at end-inspiration. Low E and R have correspondingly lower inspiratory effort, as less negative pressure is required to overcome the elastic and restive dynamics.

The second approach, $P_{eff,2}$, represents reasonable estimate of inspiratory breathing effort for 4/6 patients (median RSME 0.9-4.6 (0.1-0.4 [%])). The method calculates a higher elastance value than Analysis 1, and the resulting $P_{eff,2}$, which must overcome this dynamic, is higher and much closer to the P_{es} pressure changes. However, it overestimates estimates elastance in patients with significant positive end-inspiratory esophageal pressure (Patient 5, median RSME 3.5 cmH_2O), and underestimates it in the case of major negative end-inspiratory effort (Patient 4, median RSME 4.6 cmH_2O) .

Similarly, in Analysis 3, $P_{eff,3}$ does not capture dynamics where there is positive end-inspiratory esophageal pressure (Patient 2 and Patient 5). Patient 5 in particular suggests non-linearity in lung mechanics around the shift from patient-effort to fully passive

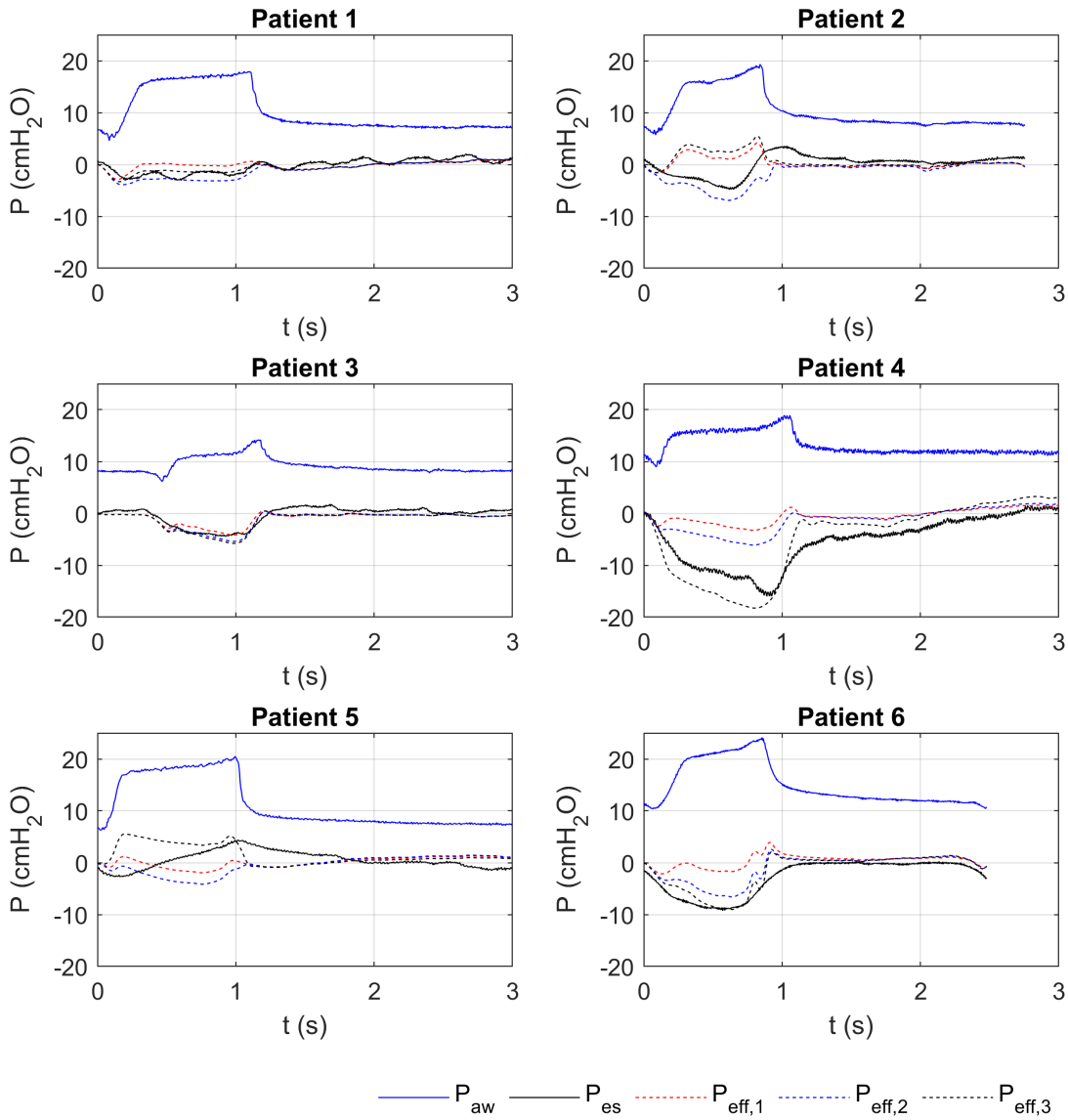

Figure 9.1: Typical breaths from each patient, depicting airway pressure (P_{aw}), esophageal pressure (P_{es}), and estimated patient effort (P_{eff}) from each respective analysis (1-3).

Table 9.1: Median RMSE [%] and correlation coefficients (r) for all breaths for each patient and each respective analysis.

	RMSE [%]			**r**		
	$P_{eff,1}$	$P_{eff,2}$	$P_{eff,3}$	$P_{eff,1}$	$P_{eff,2}$	$P_{eff,3}$
Patient 1	0.2	0.2	0.1	0.88	0.81	0.86
Patient 2	0.4	0.2	0.4	0.94	0.88	0.95
Patient 3	0.1	0.1	0.1	0.72	0.77	0.66
Patient 4	0.5	0.4	0.3	0.29	0.29	0.27
Patient 5	0.3	0.4	0.3	0.41	0.44	0.63
Patient 6	0.3	0.4	0.3	0.33	0.33	0.54

ventilation. The esophageal pressure measurements for Patient 5 in Figure 9.1 indicate the majority of inspiration is passively ventilated, where the esophageal pressure becomes positive shortly after ventilator support is initiated. This positive pressure likely reflects the additional elastance of the chest wall, where previously it's contribution was overcome by the net muscular forces working to create negative plural pressure.

The missed effort dynamics for Analysis 3 and Patient 2 suggest end-inspiratory effort against the ventilator, rather than transition to passive ventilation, when compared to Patient 5. In particular, when comparing $P_{eff,2}$ and $P_{eff,3}$, the former captures the majority of inspiratory effort dynamics, but significantly under estimates the rapid rise in esophageal pressure at the end of the breath. In contrast, $P_{eff,3}$ results in positive esophageal pressure for the majority of the breath, but without the linear relationship with volume seen in Patient 5. Thus, Patients 2 and 5 show different dynamics at play, potentially related to passive vs. asynchrony regarding exhalation onset.

Figure 9.2 - Figure 9.4 shows reasonable consistency breath-breath for model vs measured breathing effort peaks, or the gap between these peaks, indicating consistent breath-breath dynamics. It should be noted end-inspiratory and end-expiratory asynchronous behaviour can be clearly seen in some breaths across multiple patients, where

an additional patient breathing effort is made.

Figure 9.5 shows the correlation between peak modelled and measured pressure changes for each of the 6 patients across the 3 analyses ($P_{eff,1}$ - $P_{eff,3}$), with r values in Table 9.1. Where a particular analysis approach effectively models breathing effort, correlation coefficients are high, and generally overlap with the 1:1 line, indicating the analysis method works well for all breaths from the patient, and there is no significant change in breath-breath dynamics. Where correlation coefficients are poor, previously noted issues regarding elastance identification are at play, or points are tightly clustered with insufficient range to for an effective correlation.

Overall, for Patient 5 no analysis method was able to adequately capture patient breathing effort. A more comprehensive method of estimating elastance may provide better insight in terms of all data types.

9.4 Discussion

This analysis examined model-based estimation of patient inspiratory effort during MV, with comparison to measured esophageal pressure changes. It found no one specific model presented captured breathing effort for every patient, where different patient-ventilator interactions affected model efficacy.

In the first analysis (P_{eff_1}, Figure 9.2), patient effort was often underestimated (Patients 1,4,6), or resulted in a positive pressure to meet measured airway pressures (Patient 2). This analysis relied on an assumption of no end-inspiratory effort (complete ventilator unloading) to estimate elastance. However, most breaths had some small end-inspiratory negative pressure, as measured by esophageal pressure changes, thus resulting in under-

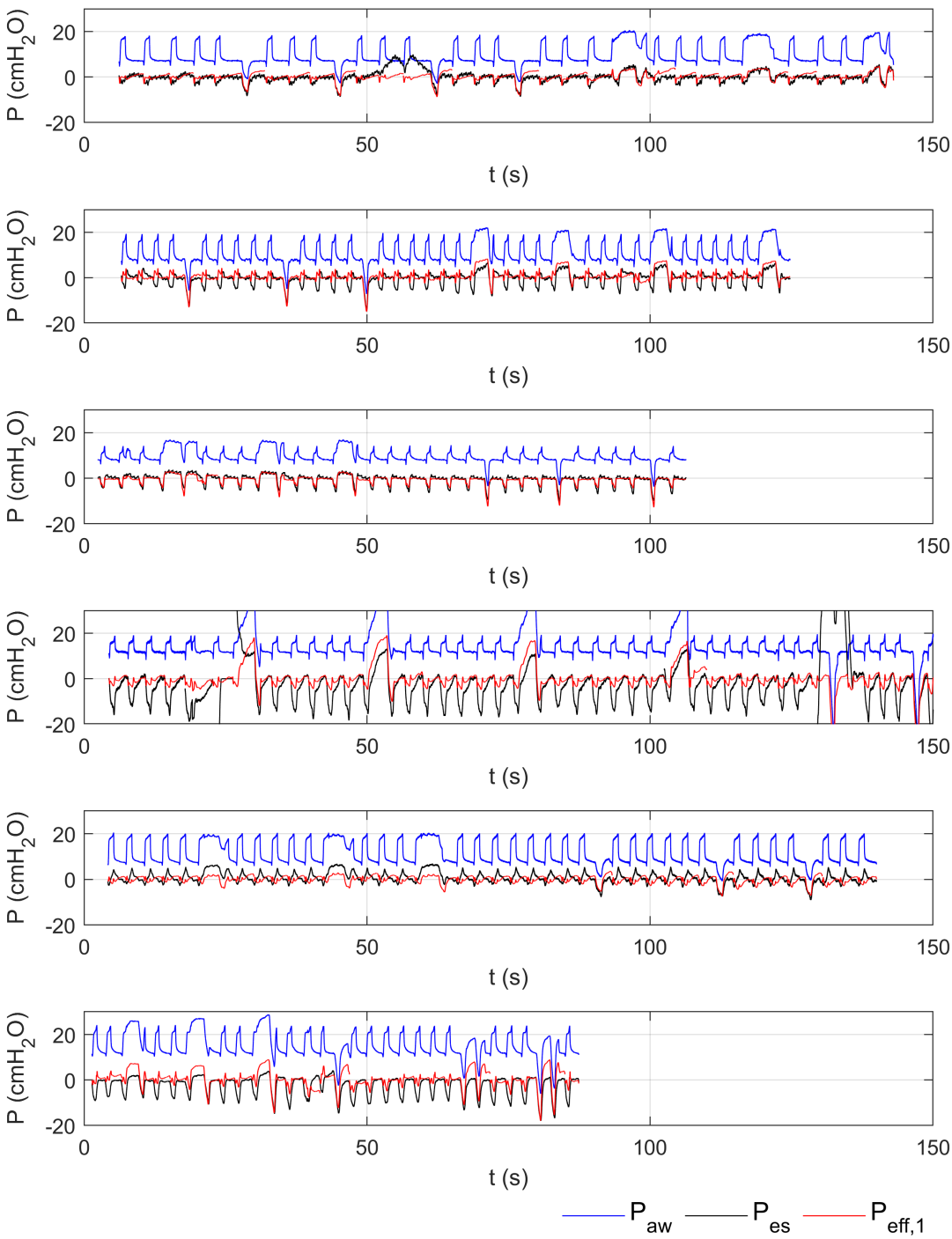

Figure 9.2: All breaths, depicting airway pressure (P_{aw}), esophageal pressure (P_{es}), and estimated patient effort (P_{eff}) from each respective patient, for Analysis 1. Patient 1-6 run top-bottom.

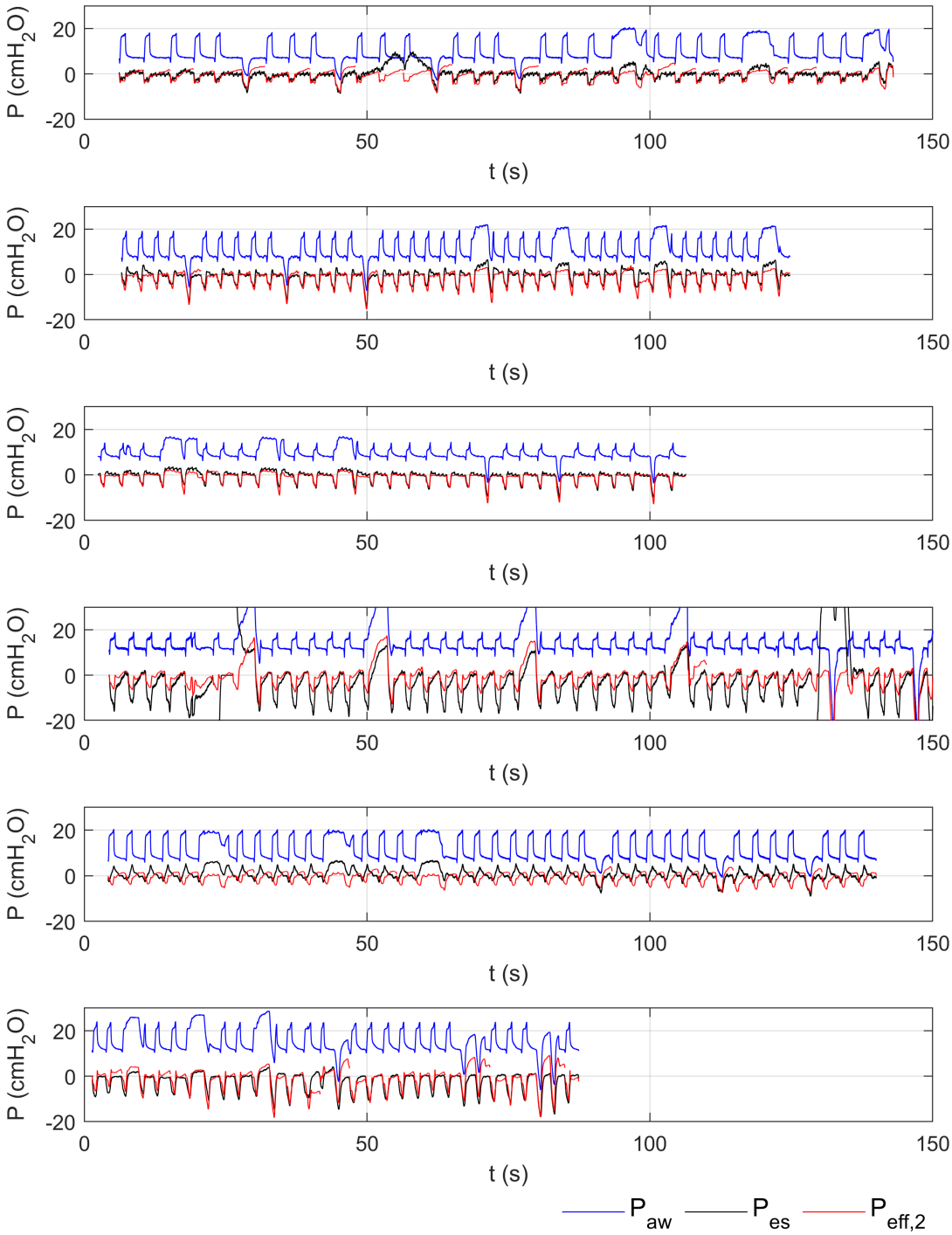

Figure 9.3: All breaths, depicting airway pressure (P_{aw}), esophageal pressure (P_{es}), and estimated patient effort (P_{eff}) from each respective patient, with analysis 2 patient effort.

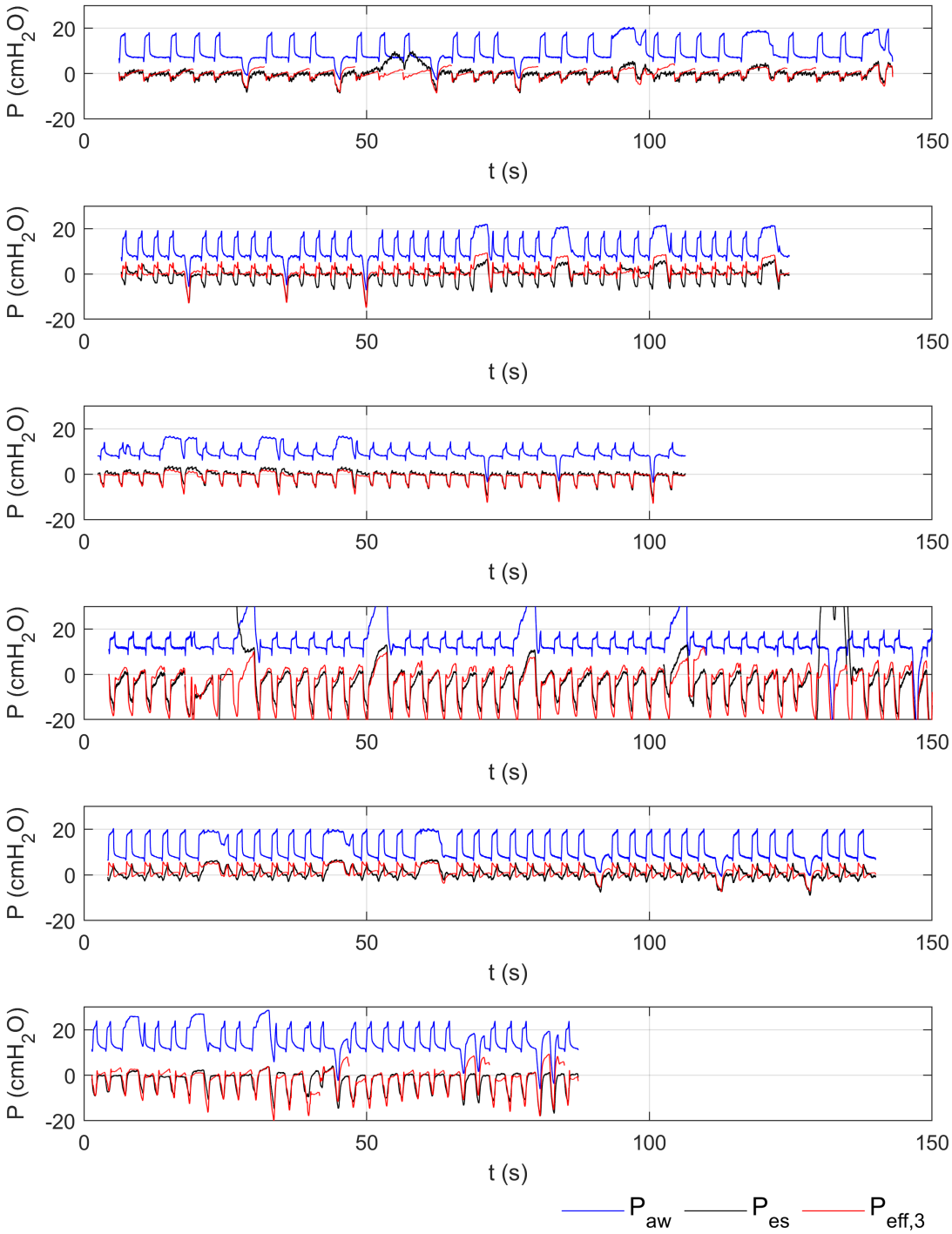

Figure 9.4: All breaths, depicting airway pressure (P_{aw}), esophageal pressure (P_{es}), and estimated patient effort (P_{eff}) from each respective patient, with analysis 3 patient effort.

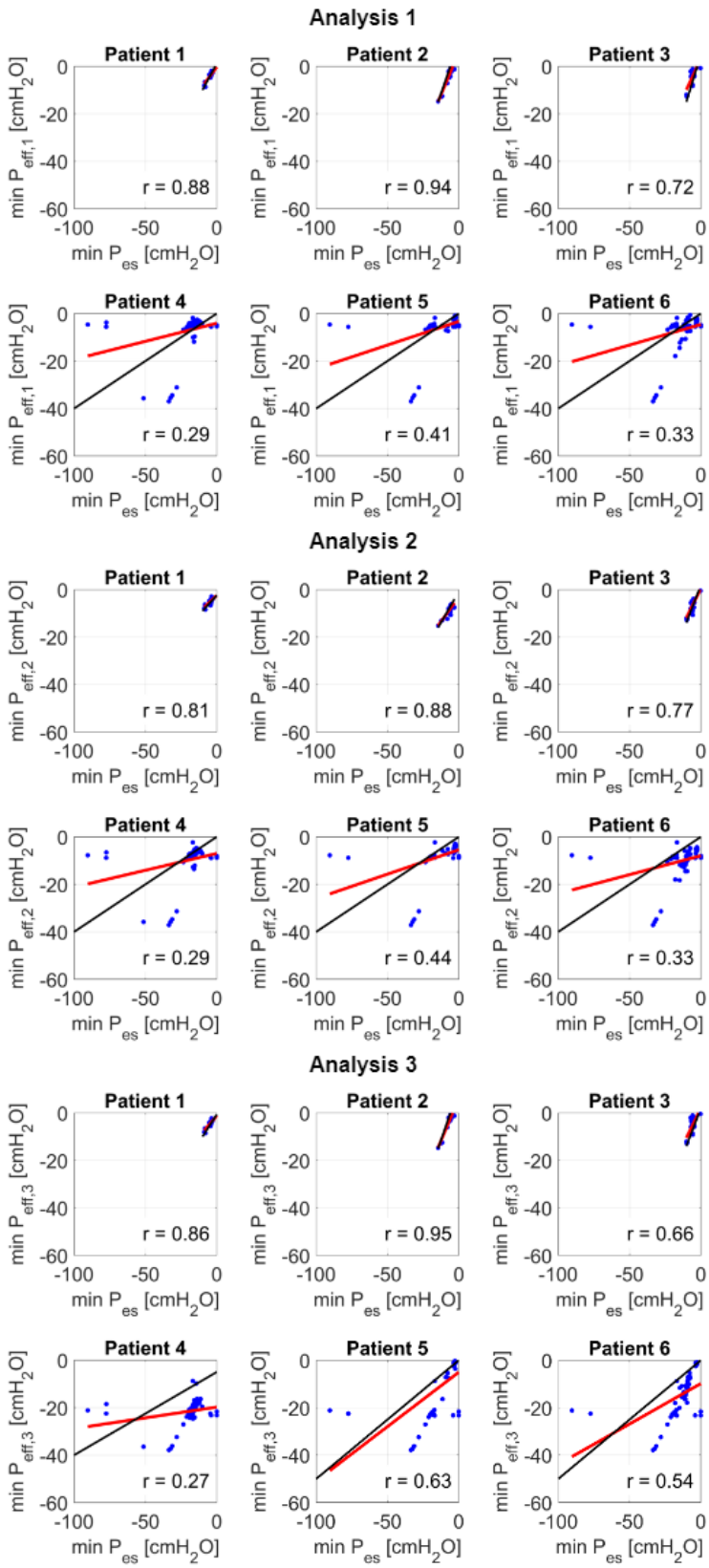

Figure 9.5: Correlation of minimum measured ($minP_{es}$) and modelled patient breathing effort ($minP_{eff,1-3}$) for all patients from each respective analysis.

estimation of elastance and failure to capture overall dynamic behaviour in inspiration and expiration.

Further work should explore the pervasiveness of end-inspiratory effort, as this cohort was collected from asynchronous patients who may have higher overall breathing effort. Overall, this analysis suggests an assumption of complete ventilator unloading is insufficient for reasonable estimation of elastance in spontaneously breathing MV patients.

No analysis captured the esophageal pressure changes very well. However, the second analysis showed the best match of the 3 analyses performed, to esophageal pressure changes, capturing effort shapes and magnitudes to within 1-2 $cmH2_O$ in 4/6 patients. This analysis relied on a peak-pressure derived estimation of elastance, suggesting at peak pressure ventilator unloading has typically occurred to the extent, the remaining breathing effort is roughly proportional to the pressure required to overcome airway resistance, and the vent has taken over most of the elastic work. Two notable exceptions were Patients 4 and 5, where significant end-expiratory effort, and passive ventilation over most of inspiration, were at play respectively.

The third analysis served as a comparison of model dynamics when the 'true' elastance is known, having accounted for end-inspiratory effort. Overall, it improved model outcomes for 4 patients (1,3,4,6), with no flaws in linear shape dynamics for E and R being observed in these patients. However, it failed to capture the shape of esophageal pressure changes in Patients 2 and 5, which may suggest the presence of nonlinear elastance dynamics. This could be due to patient effort against the ventilator or complete ventilator unloading during the breath.

Patient 5 was not well described by any analysis, possibly due to full ventilator unloading

early within the breath. The near-linear increase in positive esophageal pressure over inspiration for Patient 5 in Figure 9.1 matches an expected elastic trend with volume, and suggests the presence of an additional elastic term for the last 75% of inspiration. Equation 9.4 shows how during passive breathing a chest wall elastance will still modify pleural pressure, referred to in this chapter as patient effort, in the absence of any muscular effort. In this situation, modelling a P_{mus} term rather than pleural pressure has interpretive benefits, but requires knowledge of chest wall elastance to validate against esophageal pressure.

Patient 2 had similar modelled outcomes under Analysis 3, but very different underlying esophageal pressure changes. A comparison of the model outcomes for Analyses 2 and 3 for this patient suggests end-inspiratory asynchrony with regards to expiration onset was more likely the cause of the sudden end-inspiratory pressure rise, as opposed to a transition to passive breathing. This behaviour presents a different dynamic associated with end-inspiratory positive esophageal pressure changes, relative to baseline, compared to full ventilator unloading. Patient 2 was well modelled by Analysis 2, suggesting a good estimate of underlying lung elastance can help clarify breathing effort dynamics in this patient.

Overall, these results suggest an accurate measurement of underlying lung elastance will enable good modelling of breathing effort dynamics in most MV patients. Lung elastance determination typically requires additional clinical procedure(s), such as muscle relaxants to ensure entirely passive breathing mechanics, often combined with an end-inspiratory pause, a shutter/interrupter in the circuit, or some other breathing manoeuvre.

These additional requirements add clinical burden and expense, and are not always typ-

ically performed, or ever available, as part of normal care. Thus, future work should consider minimally additionally invasive/burdensome methods for elastance estimation.

Modelled efforts vs measured esophageal pressure changes within 1-2 cmH_2O have been deemed acceptable in this analysis, particularly if shape dynamics match, due to known uncertainty in the accuracy of esophageal pressure measurements. Esophageal balloons are often used as a surrogate for pleural pressure measurement, as pleural and esophageal pressures generally differ by an offset [523,524]. However, balloon placement affects measured outcome, as pleural pressure differs within the pleural cavity.

Esophageal balloons are typically placed within the mid third of the esophagus for an approximation of average pleural pressure [523, 524]. This average pleural pressure in theory matches the average pressure being modelled by this compartment model. Given the esophageal pressure is placement dependant, it is only ever an estimate of pleural pressure changes. Thus, some model error in inspiratory effort may in fact be expected, and it is clinically difficult to perfectly validate model-based methods against esophageal pressure measurements [524, 524]. Further, this type of measurement adds significant expense, clinical time cost, and clinical burden, and is thus very uncommon, especially in standard clinical care conditions [525].

Future studies may seek to improve these methodologies through validating the models with larger cohorts of patients undergoing MV. A more thorough data set would provide a larger range of variability between patients, and possibly better quality of data.

9.5 Summary

This chapter provides a non-invasive, model-based approach to estimating the patient effort, in MV data, often difficult to obtain without invasive and clinically expensive

methods. Three separate analyses were conducted to estimate patient effort, each with their respective trade-offs. While there is no "one-size-fits-all" solution to estimating patient effort in MV with the use of esophageal pressure, the second method suggested in this chapter provides the best overall solution. The following chapter will summarise the findings of the work presented in Chapters 1 - 9.

CHAPTER 10: CONCLUSIONS

This thesis presents a comprehensive study on the topic of nonlinear respiratory airway resistance and breathing effort estimation for respiratory disease monitoring and care. This section provides a concise overview of the main contributions of this study, insights gained, and discusses their potential impact on the field of respiratory disease monitoring and care using model-based, patient-specific methods.

Presently, spirometry is widely regarded as the foremost standard for diagnosing COPD, with a focus on identifying a reduction in lung function by measuring the FEV_1/vital capacity (VC) ratio and employing methods based on linear airway resistance. However, incorporating nonlinear resistance modelling may offer valuable insights into an individual patient's condition and the progression of the disease. Analysis of plethysmographic patient data with nonlinear modelling successfully identifies flow limited COPD patients with a nonlinear expiratory resistance in Chapter 5. Nonlinear modelling can provide novel insight into COPD patient-specific lung mechanics and potentially provide patient-specific, model-based metrics suitable for regular monitoring of COPD and lung status; and thus the ability to track disease state/progression.

Chapter 6 introduces a novel approach to estimate work of breathing (WOB) and elastance (E) from plethysmographic data, aimed at developing a diagnostic and monitoring tool for COPD patients. The proposed method employs nonlinear modelling. There are

novel further induced metrics using patient specific models which can be used to track disease and, using work of breathing, are directly related to patient specific feelings of disease management, as well as to critical or/and key clinical metrics such as WOB.

While expiration is typically regarded as a passive process, some degree of expiratory flow is generated through patient effort, referred to as expiratory effort. Like expiratory resistance, expiratory effort is nonlinear in nature and requires modelling using nonlinear methods. In Chapter 7, a successful approach is presented for identifying nonlinear expiratory effort in flow-limited COPD patients, utilising nonlinear modelling techniques. These findings, combined with methods for estimating nonlinear resistance, may offer a valuable alternative for identifying COPD patients without the need for spirometry. Expiration is not a passive process in disease states like COPD and FL COPD, which means modelling must be able to account for this issue, which is typical of all lung mechanics model assumptions, and thus typical of models developed for healthy subjects which in turn are not optimal for dysfunction.

Chapter 8 investigates the presence of nonlinear resistance in expiration for patients who have undergone mechanical ventilation (MV). A large subset of patients undergoing MV have underlying COPD. The aim of identifying this nonlinear expiratory resistance in MV patients is to improve optimisation of MV through model-based methods, reducing ventilator induced injury, and improving care. The expected result of translating methods from Chapter 5 to Chapter 8 was not realised without the quantification of inspiratory effort. There are potential areas where the key results translate to in hospital fully MV patients, but they require further modelling for some MV modes. However, the results can be generalised or have the potential to be generalised. This outcome contributes toward the aim of a single useful model in all or most all dysfunction scenarios.

Chapter 9 presents three attempts at quantifying non-invasive, model-based estimation of patient effort in the MV patient data using esophageal pressure measurements. Each of the three methods had their respective trade-offs. While none of the methods demonstrated an ideal solution across all patients in the data, the second analysis provided the best overall approach. The models and methods presented can be translated to MV patients and initial invasive validation efforts showed good, though not perfect correlation where errors are attributable to model errors or assumptions made to ensure models remain identifiable and thus clinically useful. These final results show the trade-off of modelling efforts for accuracy with maintaining identifiability to ensure clinical utility.

CHAPTER 11: FUTURE WORK

This thesis presents a comprehensive study on the topic of nonlinear respiratory airway resistance and breathing effort estimation for respiratory disease monitoring and care. While presented findings have shed light on many important aspects of this subject, there are still several areas requiring further exploration. This future work section, outlines three main areas which are particularly promising for future research. Pursuing these avenues of inquiry, will deepen understanding of nonlinear respiratory airway resistance and breathing effort estimation and contribute to the advancement of knowledge in this critical area of respiratory disease monitoring and care.

11.1 Plethysmographic clinical trials

To fully establish the validity of nonlinear expiratory resistance identification in respiratory disease monitoring, it is crucial to conduct clinical trials with diverse patient populations. In particular, these trials should involve patients who are healthy, patients with NFL COPD, and those with FL COPD undergoing plethysmography and spirometry.

Testing the accuracy of nonlinear expiratory resistance identification in these different groups, will enable a more comprehensive understanding of its potential as a clinical tool. Additionally, these trials will aid in the identification of any potential limitations or challenges associated with its use in various patient populations. Therefore, con-

ducting further clinical trials with these populations is critical for advancement, and understanding of nonlinear expiratory resistance identification and its potential for respiratory disease monitoring and care.

11.2 Mechanical ventilator clinical trials

To improve the validation of the methods outlined in Chapters 8 and 9 for mechanically ventilated (MV) patients, further research with a larger cohort is necessary. This research will help to identify the potential variability in these methods across different patient populations. Additionally, it is essential to develop a successful method of quantifying the work of breathing (WOB) in MV patients. To do this, it is necessary to explore the pervasiveness of end-inspiratory effort, which is a critical factor in determining the level of WOB in these patients. Understanding the factors contributing to end-inspiratory effort and quantifying the level of WOB accurately, increases development potential and provides more effective strategies for monitoring and managing MV patients. Therefore, further research in this area is essential for advancing our understanding of WOB in MV patients and improving the methods outlined in Chapters 8 and 9.

11.3 Further model development

To develop a successful model-based diagnostic and monitoring tool for respiratory disease, it is necessary to further develop the model to include all relevant terms in one model. This model should be applicable with tidal breathing measurements and exclude alveolar and esophageal pressure measurements, which are invasive and require specialised equipment. By including all relevant terms in one model, we can better understand the underlying mechanics of respiratory function and develop more accurate and precise diagnostic tools. Additionally, a non-invasive model utilising only tidal

breathing measurements would be more practical for clinical use and could lead to more widespread adoption of the tool. Therefore, further development of the model to include all terms in one model, applicable with tidal breathing measurements is crucial for the successful development of a model-based diagnostic and monitoring tool for respiratory disease.

Bibliography

[1] A. Aliverti and A. Pedotti, *Mechanics of breathing: new insights from new technologies.* Springer, 2014.

[2] J. H. Bates, *Lung mechanics: an inverse modeling approach.* Cambridge University Press, 2009.

[3] T. Ferkol and D. Schraufnagel, "The global burden of respiratory disease," *Annals of the American Thoracic Society*, vol. 11, no. 3, pp. 404–406, 2014.

[4] K. Fong and T. Welte, "Forum of international respiratory societies (firs)," *World Lung Day: what, why, and where to.*

[5] A. A. Cruz, *Global surveillance, prevention and control of chronic respiratory diseases: a comprehensive approach.* World Health Organization, 2007.

[6] S. S. Lim, T. Vos, A. D. Flaxman, G. Danaei, K. Shibuya, H. Adair-Rohani, M. A. AlMazroa, M. Amann, H. R. Anderson, K. G. Andrews, *et al.*, "A comparative risk assessment of burden of disease and injury attributable to 67 risk factors and risk factor clusters in 21 regions, 1990–2010: a systematic analysis for the global burden of disease study 2010," *The lancet*, vol. 380, no. 9859, pp. 2224–2260, 2012.

[7] W. UNICEF, W. UNICEF, *et al.*, "Pneumonia: the forgotten killer of children," *UNICEF/WHO*, vol. 140, 2006.

[8] M. Miravitlles and A. Ribera, "Understanding the impact of symptoms on the burden of copd," *Respiratory research*, vol. 18, no. 1, pp. 1–11, 2017.

[9] J. Hudock, J. J. Lyons, M. A. Puhan, and C. B. White, "The economic burden of copd in the united states," *Respiratory Medicine*, vol. 125, pp. 1–9, 2017.

[10] M. Cazzola, L. Calzetta, M. G. Matera, P. Maestrelli, P. Paggiaro, C. Mapp, K. F. Rabe, and T. Tonia, "The economic burden of chronic obstructive pulmonary disease in europe," *International Journal of Chronic Obstructive Pulmonary Disease*, vol. 14, pp. 2099–2113, 2019.

[11] A. D. Lopez, K. Shibuya, C. Rao, C. Mathers, A. Hansell, L. Held, V. Schmid, and S. Buist, "Chronic obstructive pulmonary disease: current burden and future projections," *European Respiratory Journal*, vol. 27, no. 2, pp. 397–412, 2006.

[12] T. L. Feenstra, M. L. van GENUGTEN, R. T. Hoogenveen, E. F. Wouters, and M. P. Rutten-van Molken, "The impact of aging and smoking on the future burden of chronic obstructive pulmonary disease: a model analysis in the netherlands," *American journal of respiratory and critical care medicine*, vol. 164, no. 4, pp. 590–596, 2001.

[13] A. Khakban, D. D. Sin, J. M. FitzGerald, B. M. McManus, R. Ng, Z. Hollander, and M. Sadatsafavi, "The projected epidemic of chronic obstructive pulmonary disease hospitalizations over the next 15 years. a population-based perspective," *American journal of respiratory and critical care medicine*, vol. 195, no. 3, pp. 287–291, 2017.

[14] P. J. Barnes, "Chronic obstructive pulmonary disease: a growing but neglected global epidemic," *PLoS medicine*, vol. 4, no. 5, p. e112, 2007.

[15] J. Bryce, R. E. Black, N. Walker, Z. A. Bhutta, J. E. Lawn, and R. W. Steketee, "Can the world afford to save the lives of 6 million children each year?," *The Lancet*, vol. 365, no. 9478, pp. 2193–2200, 2005.

[16] N. Siafakas, "Definition and differential diagnosis of chronic obstructive pulmonary disease," *European Respiratory Monograph*, vol. 38, p. 1, 2006.

[17] A. Agarwal, A. Raja, and B. Brown, "Chronic obstructive pulmonary disease," 2020.

[18] D. Papandrinopoulou, V. Tzouda, and G. Tsoukalas, "Lung compliance and chronic obstructive pulmonary disease," *Pulmonary medicine*, vol. 2012, 2012.

[19] J. C. Hogg and W. Timens, "The pathology of chronic obstructive pulmonary disease," *Annual Review of Pathology: Mechanisms of Disease*, vol. 4, pp. 435–459, 2009.

[20] P. Jones, S. Lareau, and D. A. Mahler, "Measuring the effects of copd on the patient," *Respiratory Medicine*, vol. 99, pp. S11–S18, 2005.

[21] M. R. Miller, J. Hankinson, V. Brusasco, F. Burgos, R. Casaburi, A. Coates, R. Crapo, P. Enright, C. Van Der Grinten, P. Gustafsson, *et al.*, "Standardisation of spirometry," *European respiratory journal*, vol. 26, no. 2, pp. 319–338, 2005.

[22] M. S. Magnoni, M. Caminati, G. Senna, F. Arpinelli, A. Rizzi, A. R. Dama, M. Schiappoli, G. Bettoncelli, and G. Caramori, "Asthma under/misdiagnosis in primary care setting: an observational community-based study in italy," *Clinical and Molecular Allergy*, vol. 13, no. 1, pp. 1–5, 2015.

[23] S. Pakhale, A. Sumner, D. Coyle, K. Vandemheen, and S. Aaron, "(correcting) misdiagnoses of asthma: a cost effectiveness analysis," *BMC pulmonary medicine*, vol. 11, no. 1, pp. 1–9, 2011.

[24] M. B. Stanbrook and A. Kaplan, "The error of not measuring asthma," 2008.

[25] S. Howe, "Measurement of lung mechanics during spontaneous tidal breathing in out-patient care.," 2020.

[26] P. Quanjer, M. Lebowitz, I. Gregg, M. Miller, O. Pedersen, *et al.*, "Peak expiratory flow: conclusions and recommendations of a working party of the european respiratory society," *European respiratory journal*, vol. 10, no. 24, p. 2s, 1997.

[27] C. Jenkins, "Spirometry performance in primary care: the problem, and possible solutions," *Primary care respiratory journal: journal of the General Practice Airways Group*, vol. 18, no. 3, p. 128, 2009.

[28] H. Ranu, M. Wilde, and B. Madden, "Pulmonary function tests," *The Ulster medical journal*, vol. 80, no. 2, p. 84, 2011.

[29] G. L. Ruppel and P. L. Enright, "Pulmonary function testing," *Respiratory care*, vol. 57, no. 1, pp. 165–175, 2012.

[30] P. Panagou, I. Kottakis, A. Tzouvelekis, S. Anevlavis, and D. Bouros, "Use of interrupter technique in assessment of bronchial responsiveness in normal subjects," *BMC pulmonary medicine*, vol. 4, no. 1, pp. 1–6, 2004.

[31] R. S. Tepper, R. D. Pagtakhan, and L. M. Taussig, "Noninvasive determination of total respiratory system compliance in infants by the weighted-spirometer method," *American Review of Respiratory Disease*, vol. 130, no. 3, pp. 461–466, 1984.

[32] A. B. DuBois, S. Y. Botelho, J. H. Comroe, *et al.*, "A new method for measuring airway resistance in man using a body plethysmograph: values in normal subjects and in patients with respiratory disease," *The Journal of clinical investigation*, vol. 35, no. 3, pp. 327–335, 1956.

[33] J. Behr and D. Furst, "Pulmonary function tests," *Rheumatology*, vol. 47, no. suppl_5, pp. v65–v67, 2008.

[34] M. R. Miller, R. Crapo, J. Hankinson, V. Brusasco, F. Burgos, R. Casaburi, A. Coates, P. Enright, C. M. van der Grinten, P. Gustafsson, *et al.*, "General considerations for lung function testing," *European Respiratory Journal*, vol. 26, no. 1, pp. 153–161, 2005.

[35] B. G. Cooper, "An update on contraindications for lung function testing," *Thorax*, vol. 66, no. 8, pp. 714–723, 2011.

[36] P. H. Quanjer, "Standardized lung function testing," 1983.

[37] R. Pellegrino, G. Viegi, V. Brusasco, R. Crapo, F. Burgos, R. Casaburi, A. Coates, C. Van Der Grinten, P. Gustafsson, J. Hankinson, *et al.*, "Interpretative strategies for lung function tests," *European respiratory journal*, vol. 26, no. 5, pp. 948–968, 2005.

[38] A. Ben-Tal, "Simplified models for gas exchange in the human lungs," *Journal of theoretical biology*, vol. 238, no. 2, pp. 474–495, 2006.

[39] Q. Sun, J. G. Chase, C. Zhou, M. H. Tawhai, J. L. Knopp, K. Möller, and G. M. Shaw, "Over-distension prediction via hysteresis loop analysis and patient-specific basis functions in a virtual patient model," *Computers in Biology and Medicine*, vol. 141, p. 105022, 2022.

[40] Y. S. Chiew, J. G. Chase, G. M. Shaw, A. Sundaresan, and T. Desaive, "Model-based peep optimisation in mechanical ventilation," *Biomedical engineering online*, vol. 10, no. 1, pp. 1–16, 2011.

[41] Y. S. Chiew, "Model-based mechanical ventilation for the critically ill," 2013.

[42] K. T. Kim, J. Knopp, and J. G. Chase, "Quantifying patient spontaneous breathing effort using model-based methods," *Biomedical Signal Processing and Control*, vol. 69, p. 102809, 2021.

[43] M. T. Hinds and R. E. Hyatt, "Pulmonary mechanics models: development, current status, and future directions," *Journal of applied physiology*, vol. 59, no. 3, pp. 717–722, 1985.

[44] D. Wang, W. Zhang, Y. Chen, and Q. Chen, "Review of computational models for pulmonary mechanics," *Computer methods and programs in biomedicine*, vol. 134, pp. 1–19, 2016.

[45] G. P. Dungan and J. H. Bates, "Computational models of pulmonary mechanics: history, current status, and challenges for the future," *Chest*, vol. 130, no. 2, pp. 541–551, 2006.

[46] M. H. Tawhai, P. Hunter, J. Tschirren, J. Reinhardt, G. McLennan, and E. A. Hoffman, "Ct-based geometry analysis and finite element models of the human and ovine bronchial tree," *Journal of applied physiology*, vol. 97, no. 6, pp. 2310–2321, 2004.

[47] M. H. Tawhai and J. H. Bates, "Multi-scale lung modeling," *Journal of Applied Physiology*, vol. 110, no. 5, pp. 1466–1472, 2011.

[48] P. I. Reddy, A. M. Al-Jumaily, and G. T. Bold, "Dynamic surface tension of natural surfactant extract under superimposed oscillations," *Journal of biomechanics*, vol. 44, no. 1, pp. 156–163, 2011.

[49] H. Kitaoka, G. F. Nieman, Y. Fujino, D. Carney, J. DiRocco, and I. Kawase, "A four-dimensional model of the alveolar structure," *The Journal of Physiological Sciences*, pp. 0706010006–0706010006, 2007.

[50] J. de Ryk, J. Thiesse, E. Namati, and G. McLennan, "Stress distribution in a three dimensional, geometric alveolar sac under normal and emphysematous conditions," *International journal of chronic obstructive pulmonary disease*, vol. 2, no. 1, p. 81, 2007.

[51] K. Schirrmann, M. Mertens, U. Kertzscher, W. M. Kuebler, and K. Affeld, "Theoretical modeling of the interaction between alveoli during inflation and deflation in normal and diseased lungs," *Journal of biomechanics*, vol. 43, no. 6, pp. 1202–1207, 2010.

[52] U. Lucangelo, F. Bernabè, and L. Blanch, "Lung mechanics at the bedside: make it simple," *Current opinion in critical care*, vol. 13, no. 1, pp. 64–72, 2007.

[53] E. J. Van Drunen, Y. S. Chiew, J. G. Chase, G. M. Shaw, B. Lambermont, N. Janssen, N. S. Damanhuri, and T. Desaive, "Expiratory model-based method to monitor ards disease state," *Biomedical engineering online*, vol. 12, no. 1, pp. 1–15, 2013.

[54] Y. S. Chiew, C. Pretty, P. D. Docherty, B. Lambermont, G. M. Shaw, T. Desaive, and J. G. Chase, "Time-varying respiratory system elastance: a physiological model for patients who are spontaneously breathing," *PloS one*, vol. 10, no. 1, p. e0114847, 2015.

[55] T. Yuta, "Minimal model of lung mechanics for optimising ventilator therapy in critical care," 2007.

[56] C. Gonzalez and L.-H. Ting, "Advances in computational modeling of human movement: Toward personalized and predictive modeling," *IEEE Reviews in Biomedical Engineering*, vol. 8, pp. 83–92, 2015.

[57] J. Gomes, A. Lobo, and J. Bessa, "Physiologically relevant biomechanical models of the human body: A review," *International Journal of Medical Robotics and Computer Assisted Surgery*, vol. 14, no. 5, p. e1942, 2018.

[58] M. A. Hochberg, J. He, and J. F. Talbott, "Computational modeling of human movement for clinical applications," *Annual Review of Biomedical Engineering*, vol. 13, no. 1, pp. 57–85, 2011.

[59] J. G. Chase, J.-C. Preiser, J. L. Dickson, A. Pironet, Y. S. Chiew, C. G. Pretty, G. M. Shaw, B. Benyo, K. Moeller, S. Safaei, *et al.*, "Next-generation, personalised, model-based critical care medicine: a state-of-the art review of in silico virtual patient models, methods, and cohorts, and how to validation them," *Biomedical engineering online*, vol. 17, no. 1, pp. 1–29, 2018.

[60] A. Sundaresan, J. Chase, G. Shaw, Y. Chiew, and T. Desaive, "Model-based optimal peep in mechanically ventilated ards patients in the intensive care unit," *BioMedical Engineering OnLine*, vol. 10, no. 1, p. 64, 2011.

[61] M. Tawhai, A. Clark, and J. Chase, "The lung physiome and virtual patient models: From morphometry to clinical translation," *Morphologie*, vol. 103, no. 343, pp. 131–138, 2019.

[62] C. Robertson and A. Bullock, "Hypoxia and brain injury," *Journal of Clinical Investigation*, vol. 118, no. 5, pp. 1646–1655, 2008.

[63] G. Lodygensky and P. Herson, "Hypoxic-ischemic brain injury," *Journal of Neuropathology and Experimental Neurology*, vol. 69, no. 4, pp. 373–385, 2010.

[64] R. Sutton, C. Robertson, and A. Bullock, "Hypoxia and brain injury," *Journal of Clinical Investigation*, vol. 118, no. 5, pp. 1646–1655, 2008.

[65] S. E. Weinberger, B. A. Cockrill, and J. Mandel, *Principles of Pulmonary Medicine E-Book*. Elsevier Health Sciences, 2017.

[66] K. T. Patton and G. A. Thibodeau, *Mosby's handbook of anatomy & physiology.* Elsevier Health Sciences, 2013.

[67] J. B. West, *Respiratory physiology: the essentials.* Lippincott Williams & Wilkins, 2012.

[68] J. Ward, "Physiology of breathing i," *Surgery (Oxford)*, vol. 23, no. 11, pp. 419–424, 2005.

[69] "Respiratory system."

[70] J. H. Bates, J. T. Edwards, and D. A. Jenkins, "Surface area of the alveolar region of the human lung," *The Journal of physiology*, vol. 590, no. 2, pp. 291–300, 2012.

[71] J. Rottman, "Cardiac psychiatry: cardiac cycle and blood flow," *Journal of Clinical Psychiatry*, vol. 62, no. 12, pp. 843–853, 2001.

[72] M. Matthay, "Surfactant and alveolar stability," *American Journal of Respiratory and Critical Care Medicine*, vol. 160, no. 1, pp. 3–12, 1999.

[73] R. Mason and K. Thurlbeck, "Surfactant, alveoli, and lung mechanics," *American Review of Respiratory Disease*, vol. 143, no. 4, pp. 823–829, 1991.

[74] R. Hyatt and C. Doherty, "Surfactant and alveolar stability," *Annual Review of Physiology*, vol. 51, pp. 717–735, 1989.

[75] D. Nadel and J. Babb, "Gas exchange in the lung," *Annual Review of Physiology*, vol. 64, pp. 259–287, 2002.

[76] J. West, "Gas exchange in the lung," *Journal of Applied Physiology*, vol. 95, no. 1, pp. 357–364, 2003.

[77] J. Babb and P. Macklem, "The mechanics of breathing," *American Review of Respiratory Disease*, vol. 130, no. 6, pp. 1329–1339, 1984.

[78] "The process of breathing."

[79] R. Sapienza, "Respiratory muscle function," *Journal of Applied Physiology*, vol. 77, no. 3, pp. 1324–1334, 1994.

[80] J. Dempsey and A. Ihsan, "Respiratory control," *Annual Review of Physiology*, vol. 77, pp. 569–590, 2015.

[81] S. J. Lai-Fook and J. R. Rodarte, "Pleural pressure distribution and its relationship to lung volume and interstitial pressure," *Journal of Applied Physiology*, vol. 70, no. 3, pp. 967–978, 1991.

[82] R. Garcia-Vidal, J. del Pozo, R. Moreno-Garcia, J. Huerta, and J. Esquinas, "Bilateral pleural effusion and tenderness: a rare complication of pneumococcal pneumonia," *European Respiratory Journal*, vol. 20, no. 4, pp. 907–910, 2002.

[83] D. Angus and A. Slutsky, "Acute respiratory distress syndrome," *New England Journal of Medicine*, vol. 342, no. 18, pp. 1334–1349, 2000.

[84] L. Gattinoni, G. Bellani, P. Caironi, D. Chiumello, S. Coppola, V. Ranieri, and A. Slutsky, "The berlin definition of ards: An official american thoracic society/european society of intensive care medicine/society of critical care medicine clinical practice guideline," *American Journal of Respiratory and Critical Care Medicine*, vol. 186, no. 6, pp. 724–727, 2012.

[85] C. Calfee and M. Matthay, "Acute respiratory distress syndrome," *American Journal of Respiratory and Critical Care Medicine*, vol. 193, no. 3, pp. 259–272, 2016.

[86] A. D. T. Force, V. Ranieri, G. Rubenfeld, B. Thompson, N. Ferguson, E. Caldwell, E. Fan, L. Camporota, and A. Slutsky, "Acute respiratory distress syndrome," *Jama*, vol. 307, no. 23, pp. 2526–2533, 2012.

[87] R. Beale and P. Hillman, "Hypoxaemia in critically ill patients," *British Medical Bulletin*, vol. 55, no. 1, pp. 49–57, 1999.

[88] C. Roussos and A. Koutsoukou, "Respiratory failure," *European Respiratory Journal*, vol. 22, no. 47 suppl, pp. 3s–14s, 2003.

[89] M. E. Nunnally and J. J. Marini, "Hypercapnic respiratory failure: pathogenesis, diagnosis, and management," *American Journal of Respiratory and Critical Care Medicine*, vol. 198, no. 2, pp. 129–140, 2018.

[90] A. J. C. Ward, "Hypercapnic respiratory failure in chronic obstructive pulmonary disease," *American Journal of Respiratory and Critical Care Medicine*, vol. 191, no. 2, pp. 119–127, 2015.

[91] M. E. Nunnally and J. J. Marini, "Hypercapnic respiratory failure in chronic obstructive pulmonary disease," *American Journal of Respiratory and Critical Care Medicine*, vol. 183, no. 9, pp. 1157–1165, 2011.

[92] J. J. Marini, "Hypercapnic respiratory failure," *Chest*, vol. 135, no. 4, pp. 1116–1125, 2009.

[93] D. J. Pierson, "Hypercapnic respiratory failure," *Critical Care Medicine*, vol. 35, no. 12, pp. S657–S664, 2007.

[94] M. J. Schultz and A. L. Ries, "Obstructive lung disease: A review of current understanding and management strategies," *American Family Physician*, vol. 96, no. 4, pp. 247–254, 2017.

[95] M. J. Holtzman, "Obstructive lung disease," *Chest*, vol. 148, no. 6, pp. 1633–1650, 2015.

[96] D. E. Wood, "Obstructive lung disease: mechanisms and management," *Mayo Clinic Proceedings*, vol. 87, no. 6, pp. 585–595, 2012.

[97] P. J. Barnes and D. A. Beuther, "Pathogenesis of obstructive lung disease," *American Journal of Respiratory and Critical Care Medicine*, vol. 182, no. 4, pp. 432–445, 2010.

[98] P. J. Barnes, "Obstructive lung disease," *The New England Journal of Medicine*, vol. 343, no. 5, pp. 269–280, 2000.

[99] B. Antus, "Pharmacotherapy of chronic obstructive pulmonary disease: a clinical review," *International Scholarly Research Notices*, vol. 2013, 2013.

[100] R. M. Amirian and C. E. Ferrans, "Managing restrictive diseases," *Journal of palliative medicine*, vol. 11, no. 4, pp. 699–702, 2008.

[101] R. C. Chang, "The role of palliative care in treating restrictive diseases," *The American journal of medicine*, vol. 125, no. 1, pp. 9–14, 2012.

[102] N. Ambrosino, N. Carpene, and M. Gherardi, "Chronic respiratory care for neuromuscular diseases in adults," *European respiratory journal*, vol. 34, no. 2, pp. 444–451, 2009.

[103] W. MacNee, "Pathology, pathogenesis, and pathophysiology," *Bmj*, vol. 332, no. 7551, pp. 1202–1204, 2006.

[104] H. Kazemi, A. R. Frank, and E. Bae, "The role of hypoxic pulmonary vasoconstriction in ventilation-perfusion matching," *Respiratory physiology & neurobiology*, vol. 208, pp. 1–9, 2015.

[105] T. D. Bradley, "The reflex control of the pulmonary circulation," in *Proceedings of the Royal Society of Medicine*, vol. 52, pp. 769–776, Sage UK: London, England, 1959.

[106] H. Robertson, M. Fisher, and J. Fisher, "The effect of hypoxia on pulmonary artery pressure in the dog," *The Journal of clinical investigation*, vol. 45, no. 3, pp. 453–460, 1966.

[107] M. Das, K. P. White, and G. E. Foster, "Ventilation-perfusion matching: physiology, measurement and clinical applications," *Respiratory physiology & neurobiology*, vol. 211, pp. 94–103, 2015.

[108] M. Arne, K. Lisspers, B. Stallberg, G. Boman, H. Hedenstrom, C. Janson, and M. Emtner, "How often is diagnosis of copd confirmed with spirometry?," *Respiratory medicine*, vol. 104, no. 4, pp. 550–556, 2010.

[109] I. A. Yang, J. L. Brown, J. George, S. Jenkins, C. F. McDonald, V. M. McDonald, K. Phillips, B. J. Smith, N. A. Zwar, and E. Dabscheck, "Copd-x australian and new zealand guidelines for the diagnosis and management of chronic obstructive pulmonary disease: 2017 update," *Medical Journal of Australia*, vol. 207, no. 10, pp. 436–442, 2017.

[110] N. R. G. Committee, *New Zealand Respiratory Guidelines: COPD*. NZ Respiratory Guidelines Committee, 2020.

[111] J. Crane, S. Flack, H. Murphy, R. Beasley, M. Sneyd, S. Sullivan, and et al., "Clinically important copd in new zealand: what are the characteristics?," *Respirology*, vol. 13, no. 3, pp. 356–365, 2008.

[112] M. Parsons, S. Flack, S. Sullivan, and J. Crane, "Early diagnosis and management of copd in new zealand: a primary care perspective," *Respirology*, vol. 21, no. 8, pp. 1402–1410, 2016.

[113] R. Beasley, H. Murphy, J. Crane, S. Sullivan, S. Flack, M. Sneyd, and et al., "Screening for chronic obstructive pulmonary disease (copd) in new zealand," *Respirology*, vol. 14, no. 3, pp. 365–373, 2009.

[114] Z. McKeough, M. Wallis, D. O'Donnell, and G. Devereux, "Gold guidelines for the diagnosis and management of copd in new zealand—2015 update," *New Zealand medical journal*, vol. 128, no. 1420, pp. 15–31, 2015.

[115] J. Enright and A. Burge, "The use of spirometry in the diagnosis of chronic obstructive pulmonary disease," *European Respiratory Journal*, vol. 19, no. 6, pp. 1165–1173, 2002.

[116] C. Fanta and J. Shin, "Spirometry in copd: use and limitations," *Journal of thoracic disease*, vol. 11, no. 4, pp. 1139–1149, 2019.

[117] P. Lareau and M. Criner, "Diagnosis of copd: moving beyond spirometry," *American Journal of Respiratory and Critical Care Medicine*, vol. 197, no. 4, pp. 439–447, 2018.

[118] A. Maclay and S. Jenkins, "Spirometry in the diagnosis and management of copd," *Thorax*, vol. 64, no. 6, pp. 503–508, 2009.

[119] J. Jones, "Diagnosing copd: what is the role of spirometry?," *British Medical Journal*, vol. 329, no. 7475, pp. 903–906, 2004.

[120] W. M. Vollmer, T. Gislason, P. Burney, P. L. Enright, A. Gulsvik, A. Kocabas, and A. S. Buist, "Comparison of spirometry criteria for the diagnosis of copd: results from the bold study," *European Respiratory Journal*, vol. 34, no. 3, pp. 588–597, 2009.

[121] T. Glaab, L. Mihalic, H. Schulz, P. Schulz, H. Watz, H. Magnussen, and H. Magnussen, "Prevalence of COPD in Europe: Systematic review and meta-analysis," *BMC Pulmonary Medicine*, vol. 23, no. 1, p. 23, 2011.

[122] J. L. Lopez-Campos, J. B. Soriano, V. Pinto-Plata, A. Agusti, J. Ancochea, J. M. Marin, and B. R. Celli, "Prevalence of COPD in Europe: A systematic review," *European Respiratory Journal*, vol. 94, pp. 1245–1258, Nov. 2014.

[123] M. Miravitlles, J. J. Soler-Cataluña, M. Calle, J. Molina, P. Almagro, R. Ochando, and M. Ferrer, "Epidemiology of COPD: Prevalence, incidence, mortality and risk factors," *European Respiratory Journal*, vol. 27, pp. 153–161, Feb. 2006.

[124] A. P. C. R. Group, "Global initiative for chronic obstructive lung disease strategy for the diagnosis, management and prevention of chronic obstructive pulmonary disease: An asia–pacific perspective," *Respirology*, vol. 10, no. 1, pp. 9–17, 2005.

[125] D. Doherty, D. Tashkin, E. Kerwin, B. Knorr, T. Shekar, and S. Banerjee, "International journal of chronic obstructive pulmonary disease," 2012.

[126] M. Decramer, R. Pauwels, S. A. Buist, P. Calverley, C. Jenkins, P. Jones, B. Yawn, V. Brusasco, D. O'Donnell, O. F. Pedersen, *et al.*, "Global strategy for the diagnosis, management, and prevention of chronic obstructive pulmonary disease," *American journal of respiratory and critical care medicine*, vol. 167, no. 2, pp. 347–365, 2003.

[127] A. Burden, S. Sullivan, S. Dharmage, J. Ayres, D. Johns, K. Burgess, M. Abramson, E. Walters, R. Wood-Baker, E. Belousova, *et al.*, "Global burden of copd: Systematic review and meta-analysis," *The European respiratory journal*, vol. 31, no. 2, pp. 393–408, 2008.

[128] D. D. Sin and D. M. Mannino, "Epidemiology and burden of chronic obstructive pulmonary disease," *The Lancet*, vol. 372, no. 9646, pp. 1815–1825, 2008.

[129] C. Shu, J. Li, Z. Zhang, J. Wu, C. Li, H. Li, W. Zhang, C. Chen, and W. Xu, "Chronic obstructive pulmonary disease and the risk of coronavirus disease 2019: a systematic review and meta-analysis," *International journal of infectious diseases*, vol. 94, pp. 255–263, 2020.

[130] M. Al-Mahmoud, F. Al-Husein, S. Al-Rahbi, A. Al-Shidhani, A. Al-Kandari, J. Al-Ajmi, A. Al-Kandari, A. Al-Hassani, S. Al-Taweel, M. Al-Hajri, *et al.*, "Chronic

obstructive pulmonary disease (copd) and coronavirus disease 2019 (covid-19): a systematic review and meta-analysis," *International journal of infectious diseases*, vol. 94, pp. 1–10, 2020.

[131] T. Barreto, V. Barbosa, J. Barbosa, T. Viana, J. Carvalho, J. Fernandes, M. Rodrigues, R. Nascimento, A. Lopes, J. de Oliveira, *et al.*, "Chronic obstructive pulmonary disease and covid-19: a systematic review," *International journal of COPD*, vol. 15, pp. 1485–1499, 2020.

[132] S. Choudhury, S. R. Mishra, A. Jain, S. Jain, A. Bhat, A. Sharma, P. Dutta, A. Sharma, R. Pandey, S. Saini, *et al.*, "Severe copd and covid-19: a narrative review," in *Annals of medicine and surgery*, vol. 63, pp. e1–e4, Elsevier, 2020.

[133] A. Siddiqui, S. Iqbal, A. Abbas, S. Akhtar, H. AlHassan, A. Qamar, U. Ahmad, and A. Anjum, "Impact of copd on outcome of hospitalized patients with coronavirus disease 2019 (covid-19) infection: a systematic review and meta-analysis," *International journal of infectious diseases*, vol. 95, pp. 363–370, 2020.

[134] D. S. Hui, E. I. Azhar, T. A. Madani, F. Ntoumi, R. Kock, O. Dar, G. Ippolito, and Z. A. Memish, "Clinical characteristics of coronavirus disease 2019 in china," *The new England journal of medicine*, vol. 382, no. 18, pp. 1708–1720, 2020.

[135] C. Huang, Y. Wang, X. Li, L. Ren, J. Zhao, B. Hu, L. Zhang, G. Fan, J. Xu, X. Gu, *et al.*, "Clinical features of patients infected with 2019 novel coronavirus in wuhan, china," *The lancet*, vol. 395, no. 10223, pp. 497–506, 2020.

[136] S. C. Lee, K. J. Son, C. H. Han, S. C. Park, and J. Y. Jung, "Impact of copd on covid-19 prognosis: A nationwide population-based study in south korea," *Scientific reports*, vol. 11, no. 1, pp. 1–8, 2021.

[137] P. G. Wijkstra and R. A. J. J. Laarse, "Copd patients and covid-19: a systematic review," *The European Respiratory Journal*, vol. 55, no. 6, p. 2000972, 2020.

[138] L. G. van der Meijden and P. H. A. Quaedackers, "Copd and covid-19: A review of the current literature," *COPD: Journal of Chronic Obstructive Pulmonary Disease*, vol. 17, no. 6, pp. 660–667, 2020.

[139] A. T. W. Yew and S. S. G. Lim, "Copd and covid-19: A review of the literature," *CHEST Journal*, vol. 158, no. 5, pp. 1638–1651, 2020.

[140] J. A. Wedzicha and P. J. Barnes, "Copd and covid-19: a systematic review of observational studies," *The European Respiratory Journal*, vol. 55, no. 6, p. 2000973, 2020.

[141] T. K. Lim and Y. H. Loke, "Copd and covid-19: A review of the literature," *Journal of Thoracic Disease*, vol. 12, no. 7, pp. 3201–3214, 2020.

[142] Q. Zhao, M. Meng, R. Kumar, Y. Wu, J. Huang, N. Lian, Y. Deng, and S. Lin, "The impact of copd and smoking history on the severity of covid-19: A systemic review and meta-analysis," *Journal of medical virology*, vol. 92, no. 10, pp. 1915–1921, 2020.

[143] G. Lippi and B. M. Henry, "Chronic obstructive pulmonary disease is associated with severe coronavirus disease 2019 (covid-19)," *Respiratory medicine*, vol. 167, p. 105941, 2020.

[144] D. M. Halpin, C. F. Vogelmeier, and A. A. Agusti, "Copd & covid-19," *Archivos de bronconeumologia*, vol. 57, no. 3, p. 162, 2021.

[145] R. Tal-Singer and J. D. Crapo, "Copd at the time of covid-19: a copd foundation perspective," *Chronic Obstructive Pulmonary Diseases: Journal of the COPD Foundation*, vol. 7, no. 2, p. 73, 2020.

[146] J. M. Leung, M. Niikura, C. W. T. Yang, and D. D. Sin, "Covid-19 and copd," *European Respiratory Journal*, vol. 56, no. 2, 2020.

[147] Y. Tang, J. Sowinski, and M. Grap, "Respiratory physiology: An introduction to normal respiratory function," *Elsevier Health Sciences*, 2014.

[148] R. Brown, "Respiratory physiology: Understanding the control of breathing," *Elsevier Health Sciences*, 2012.

[149] P. Barker and M. Levitzky, "Respiratory physiology: A clinical approach," *Elsevier Health Sciences*, 2016.

[150] J. Wanger, J. Clausen, A. Coates, O. Pedersen, V. Brusasco, F. Burgos, R. Casaburi, R. Crapo, P. Enright, C. Van Der Grinten, *et al.*, "Standardisation of the measurement of lung volumes," *European respiratory journal*, vol. 26, no. 3, pp. 511–522, 2005.

[151] D. D. Sin and S. F. Man, "The use of the flow rate coefficient in the diagnosis of respiratory diseases," *The Lancet*, vol. 358, no. 9285, pp. 919–923, 2001.

[152] P. Blanco, M. Lopez, and P. Dominguez, "Evaluation of the flow rate coefficient for clinical monitoring of respiratory diseases," *European Respiratory Journal*, vol. 30, no. 2, pp. 367–375, 2007.

[153] J. M. Bates, J. Milic-Emili, and D. M. Grodzinsky, "The use of flow rate coefficient in the assessment of respiratory mechanics," *Respiration Physiology*, vol. 14, no. 1, pp. 125–137, 1972.

[154] S. R. Thom and J. Milic-Emili, "Flow rate coefficient in respiratory research," *American Review of Respiratory Disease*, vol. 121, no. 3, pp. 617–633, 1980.

[155] J. Ostrowski, M. Wysocki, E. Stelmaszczyk, E. Górska, and J. Niczyporuk, "Functional residual capacity measured by body plethysmography, helium dilution and nitrogen washout in healthy adults," *Medical science monitor*, vol. 17, no. 11, pp. CR556–CR560, 2011.

[156] D. Saey, O. M. Vanderveken, R. De Becker, and A. De Troyer, "Comparison of helium dilution and body plethysmography measurements of functional residual capacity in healthy adults," *Respiratory physiology & neurobiology*, vol. 171, no. 2, pp. 131–136, 2010.

[157] P. Paggiaro, G. Valerio, E. Pigozzi, and M. Cazzola, "Comparison of a new body plethysmograph, the quark pft, with conventional spirometry and body plethysmography for the measurement of lung volumes," *Respiratory medicine*, vol. 107, no. 3, pp. 385–391, 2013.

[158] I. Wilcox, M. R. Miller, and H. Chrystyn, "Comparison of the quark pft, an automated body plethysmograph, and wet spirometry for the assessment of forced vital capacity in healthy adults," *Respiratory Medicine*, vol. 117, pp. 125–129, 2016.

[159] E. Westerdahl, K. Engström, L. Eriksson, and H. Hedenström, "Lung volume measurement: plethysmography, helium dilution and nitrogen washout compared with body plethysmography," *Clinical physiology and functional imaging*, vol. 27, no. 6, pp. 435–442, 2007.

[160] R. J. Pierce, B. J. Make, G. R. Washko, E. A. Hoffman, and D. A. Lynch, "Functional residual capacity in patients with chronic obstructive pulmonary disease," *American Journal of Respiratory and Critical Care Medicine*, vol. 162, no. 4, pp. 1430–1437, 2000.

[161] S. Nava, L. Corbino, C. Rampulla, G. Viegi, M. Pistolesi, G. Pedrielli, and L. Fabbri, "Functional residual capacity in chronic obstructive pulmonary disease," *European Respiratory Journal*, vol. 11, no. 6, pp. 1330–1337, 1998.

[162] V. H. Y. Mak, S. Y. Mak, K. Y. Leung, S. S. F. Lui, G. K. H. Leung, K. W. Tsui, and C. K. Wong, "Functional residual capacity in patients with chronic obstructive

pulmonary disease," *European Respiratory Journal*, vol. 7, no. 11, pp. 2001–2005, 1994.

[163] T. Lerios, J. L. Knopp, L. Holder-Pearson, E. F. Guy, and J. G. Chase, "An identifiable model of lung mechanics to diagnose and monitor copd," *Computers in Biology and Medicine*, p. 106430, 2022.

[164] E. F. S. Guy, J. G. Chase, J. L. Knopp, and G. M. Shaw, "Quantifying Ventilator Unloading in CPAP Ventilation," *Computers in Biology and Medicine*, vol. 142, p. 105225, 2022.

[165] K. T. Kim, J. Knopp, B. Dixon, and J. G. Chase, "Quantifying neonatal patient effort using non-invasive model-based methods," *Medical & Biological Engineering & Computing*, vol. 60, no. 3, pp. 739–751, 2022.

[166] J. L. Knopp, J. G. Chase, K. T. Kim, and G. M. Shaw, "Model-based estimation of negative inspiratory driving pressure in patients receiving invasive nava mechanical ventilation," *Computer Methods and Programs in Biomedicine*, vol. 208, p. 106300, 2021.

[167] R. Langdon, P. D. Docherty, Y.-S. Chiew, K. Moeller, and J. G. Chase, "Use of basis functions within a non-linear autoregressive model of pulmonary mechanics," *Biomedical Signal Processing and Control*, vol. 27, pp. 44–50, 2016.

[168] J. Kretschmer, C. Bibiano, B. Laufer, P. D. Docherty, Y. S. Chiew, D. Redmond, J. G. Chase, and K. Möller, "Differences in respiratory mechanics estimation with respect to manoeuvres and mathematical models," *Biomedical Physics & Engineering Express*, vol. 3, no. 1, p. 014002, 2017.

[169] M. McIlroy and E. Tomlinson, "The mechanics of breathing in newly born babies," *Thorax*, vol. 10, no. 1, p. 58, 1955.

[170] G. Hofmann, L. Haan, and J. Anderson, "Esophageal pressure measurements in patients with acute respiratory distress syndrome," *Critical care nurse*, vol. 36, no. 5, pp. 27–35, 2016.

[171] E. Schena, C. Massaroni, P. Saccomandi, and S. Cecchini, "Flow measurement in mechanical ventilation: A review," *Medical engineering & physics*, vol. 37, no. 3, pp. 257–264, 2015.

[172] R. A. Wise and R. N. Brody, "Single-breath carbon monoxide uptake in lung function testing," *American Family Physician*, vol. 81, no. 6, pp. 739–744, 2010.

[173] J. R. Rodarte, "Helium dilution for measurement of lung volumes," *American Journal of Respiratory and Critical Care Medicine*, vol. 153, no. 4, pp. 1376–1384, 1996.

[174] R. C. S. Chang, "Lung function testing: measurement of lung volumes," *The Lancet Respiratory Medicine*, vol. 2, no. 6, pp. 429–438, 2014.

[175] E. H. G. Heijdra, *Pulmonary Function Testing.* Springer, 2007.

[176] V. J. Major, Y. S. Chiew, G. M. Shaw, and J. G. Chase, "Biomedical engineer's guide to the clinical aspects of intensive care mechanical ventilation," *Biomedical engineering online*, vol. 17, no. 1, pp. 1–31, 2018.

[177] M. K. Johnson and S. H. Loring, "Static and dynamic lung mechanics: comparison between different pressure-volume curves," *Respiratory care*, vol. 58, no. 4, pp. 629–635, 2013.

[178] A. Kumar, B. Geetha, S. Chandy, J. Jacob, and S. Bhandari, "Static and dynamic lung compliance in mechanically ventilated patients with acute respiratory distress syndrome," *Indian journal of medical sciences*, vol. 61, no. 9, pp. 476–481, 2007.

[179] X. Gao, X. Xu, J. Wang, Y. Zhao, J. Zheng, X. Zeng, and Y. Li, "Dynamic lung mechanics: an overview of the methods and their clinical applications," *Chinese medical journal*, vol. 124, no. 2, pp. 135–140, 2011.

[180] V. Bordas and A. Thille, "Static and dynamic measurements of lung mechanics in humans," *Respiratory physiology & neurobiology*, vol. 164, no. 1-2, pp. 67–74, 2008.

[181] Y. S. Chiew, S. F. Poole, D. P. Redmond, E. J. Van Drunen, N. S. Damanhuri, C. Pretty, P. D. Docherty, B. Lambermont, G. M. Shaw, T. Desaive, *et al.*, "Time-varying respiratory elastance for spontaneously breathing patients," *IFAC Proceedings Volumes*, vol. 47, no. 3, pp. 5659–5664, 2014.

[182] J. Nederhof and P. Macklem, "Viscoelastic properties of lung parenchyma and their relation to dynamic changes in lung volume," *American review of respiratory disease*, vol. 116, no. 6, pp. 1157–1173, 1977.

[183] D. Leith and J. Mead, "Dynamics of lung parenchyma and its viscoelastic properties," *Journal of Applied Physiology*, vol. 31, no. 5, pp. 819–828, 1971.

[184] J. Hogg and P. Macklem, "The viscoelastic properties of lung tissue," *Journal of Applied Physiology*, vol. 35, no. 3, pp. 407–414, 1973.

[185] T. Allergy, "Do you need a spirometry lung function test?," December 2020.

[186] S. Stanojevic, A. Wade, and J. Stocks, "Reference values for lung function: past, present and future," *European Respiratory Journal*, vol. 36, no. 1, pp. 12–19, 2010.

[187] G. I. for Chronic Obstructive Lung Disease, "Global strategy for the diagnosis, management, and prevention of chronic obstructive pulmonary disease," *American journal of respiratory and critical care medicine*, vol. 177, no. 4, pp. 389–416, 2008.

[188] K. F. Rabe, S. Hurd, A. Anzueto, P. J. Barnes, S. A. Buist, P. Calverley, Y. Fukuchi, C. Jenkins, R. Rodriguez-Roisin, C. Van Weel, *et al.*, "Global strategy for the diagnosis, management, and prevention of chronic obstructive pulmonary disease: Gold executive summary," *American journal of respiratory and critical care medicine*, vol. 176, no. 6, pp. 532–555, 2007.

[189] F. A. M. Hoesein, P. Zanen, and J.-W. J. Lammers, "Lower limit of normal or fev1/fvc¡ 0.70 in diagnosing copd: an evidence-based review," *Respiratory medicine*, vol. 105, no. 6, pp. 907–915, 2011.

[190] T. Gólczewski, W. Lubiński, and A. Chciałowski, "A mathematical reason for fev1/fvc dependence on age," *Respiratory research*, vol. 13, no. 1, pp. 1–7, 2012.

[191] M. R. Miller, P. H. Quanjer, M. P. Swanney, G. Ruppel, and P. L. Enright, "Interpreting lung function data using 80% predicted and fixed thresholds misclassifies more than 20% of patients," *Chest*, vol. 139, no. 1, pp. 52–59, 2011.

[192] A. L. Coates, I. E. Tamari, and B. L. Graham, "Role of spirometry in primary care," *Canadian Family Physician*, vol. 60, no. 12, pp. 1069–1070, 2014.

[193] M. X. Owens, W. M. Anderson, and R. B. George, "Indications for spirometry in outpatients with respiratory disease," *Chest*, vol. 99, no. 3, pp. 730–734, 1991.

[194] E. D. Schifano, J. P. Hollenbach, and M. M. Cloutier, "Mismatch between asthma symptoms and spirometry: implications for managing asthma in children," *The Journal of pediatrics*, vol. 165, no. 5, pp. 997–1002, 2014.

[195] J. M. Ignacio-Garcia and P. Gonzalez-Santos, "Asthma self-management education program by home monitoring of peak expiratory flow.," *American journal of respiratory and critical care medicine*, vol. 151, no. 2, pp. 353–359, 1995.

[196] A. H. Mehrparvar, M. J. Z. Sakhvidi, M. Mostaghaci, M. H. Davari, S. H. Hashemi, and Z. Zare, "Spirometry values for detecting a restrictive pattern in occupational health settings," *Tanaffos*, vol. 13, no. 2, p. 27, 2014.

[197] J. D. Johnson and W. M. Theurer, "A stepwise approach to the interpretation of pulmonary function tests," *American family physician*, vol. 89, no. 5, pp. 359–366, 2014.

[198] iastate Pressbooks Pub, *Pulmonary Function.* iastate Pressbooks Pub, 2020.

[199] S. Eigen, "Spirometry in children: A review," *Journal of Pediatric Health Care*, vol. 22, no. 6, pp. 329–336, 2008.

[200] A. Jain and K. Patel, "Spirometry in children: A review of current recommendations," *Journal of Asthma*, vol. 50, no. 7, pp. 719–726, 2013.

[201] J. Miller and J. Hankinson, "Practical spirometry," *American Journal of Respiratory and Critical Care Medicine*, vol. 144, no. 4, pp. 1202–1208, 1991.

[202] J. Phelan and D. Ruppel, "Spirometry in children: A practical guide," *American Journal of Respiratory and Critical Care Medicine*, vol. 165, no. 6, pp. 827–833, 2002.

[203] E. Wohl, "Spirometry in children: A review," *Chest*, vol. 133, no. 6, pp. 1662–1672, 2008.

[204] E. Y.-T. Chan, "Use of the interrupter technique in assessment of lung function," *J Paediatr Respirol Crit Care*, vol. 3, no. 4, pp. 6–8, 2007.

[205] J. Kivastik, J. Talts, K. Jagomägi, and R. Raamat, "Interrupter technique for assessing respiratory resistance: a review.," *Proceedings of the Estonian Academy of Sciences*, vol. 63, no. 3, 2014.

[206] A. Al-Ramadhan, M. Johnson, R. Chaudhuri, R. Sapsford, and A. Wilson, "Weighted spirometry: A novel technique for measuring lung elastance in asthma," *Respiratory care*, vol. 59, no. 11, pp. 1732–1737, 2014.

[207] J. Dowman, G. J. Redding, L. Blaustein, J. D. Crapo, and B. J. Make, "Weighted spirometry: a comparison of three different methods for measuring lung elastance," *Respiratory physiology & neurobiology*, vol. 212, pp. 19–25, 2015.

[208] N. Hill, T. Rapley, R. Primhak, and M. Greenstone, "Assessment of respiratory mechanics by forced oscillation technique and comparison with conventional spirometry," *The European respiratory journal*, vol. 36, no. 2, pp. 383–391, 2010.

[209] M. M. Budev and S. C. Kalhan, "Weighted spirometry," *American Journal of Respiratory and Critical Care Medicine*, vol. 180, no. 5, pp. 476–480, 2009.

[210] R. Cherniack and E. Brown, "A simple method for measuring total respiratory compliance: normal values for males," *Journal of applied Physiology*, vol. 20, no. 1, pp. 87–91, 1965.

[211] O. Stenqvist, C. Grivans, B. Andersson, and S. Lundin, "Lung elastance and transpulmonary pressure can be determined without using oesophageal pressure measurements," *Acta anaesthesiologica scandinavica*, vol. 56, no. 6, pp. 738–747, 2012.

[212] D. Kaczka and R. L. Dellacá, "Oscillation mechanics of the respiratory system: applications to lung disease," *Critical Reviews™ in Biomedical Engineering*, vol. 39, no. 4, 2011.

[213] B. Brashier and S. Salvi, "Measuring lung function using sound waves: role of the forced oscillation technique and impulse oscillometry system," *Breathe*, vol. 11, no. 1, pp. 57–65, 2015.

[214] D. Navajas Navarro and R. Farré Ventura, "Forced oscillation assessment of respiratory mechanics in ventilated patients," *Critical Care, 2001, vol. 5, num. 1, p. 3-9*, 2001.

[215] C. Delacourt, H. Lorino, M. Herve-Guillot, P. Reinert, A. Harf, and B. Housset, "Use of the forced oscillation technique to assess airway obstruction and reversibility in children," *American journal of respiratory and critical care medicine*, vol. 161, no. 3, pp. 730–736, 2000.

[216] C. Criée, S. Sorichter, H. Smith, P. Kardos, R. Merget, D. Heise, D. Berdel, D. Köhler, H. Magnussen, W. Marek, *et al.*, "Body plethysmography–its principles and clinical use," *Respiratory medicine*, vol. 105, no. 7, pp. 959–971, 2011.

[217] J. Stocks, S. Godfrey, C. Beardsmore, E. Bar-Yishay, R. Castile, *et al.*, "Plethysmographic measurements of lung volume and airway resistance," *European Respiratory Journal*, vol. 17, no. 2, pp. 302–312, 2001.

[218] D. A. Kaminsky, "What does airway resistance tell us about lung function?," *Respiratory care*, vol. 57, no. 1, pp. 85–99, 2012.

[219] D. Radovanovic, M. Pecchiari, F. Pirracchio, C. Zilianti, E. D'Angelo, and P. Santus, "Plethysmographic loops: a window on the lung pathophysiology of copd patients," *Frontiers in physiology*, vol. 9, p. 484, 2018.

[220] E. Mavili, H. Büyükoğlan, N. B. Çomu, and M. Güleç, "Expiratory ct: Correlation with pulmonary function tests and value for discriminating lung diseases.," *European Journal of General Medicine*, vol. 7, no. 1, 2010.

[221] D. A. Kaminsky, D. Mehta, and R. Singh, "Comparison of four functional residual capacity measurement techniques in mechanically ventilated patients," *American journal of respiratory and critical care medicine*, vol. 180, no. 3, pp. 242–248, 2009.

[222] S. Garverick, P. Smith, and J. Hoidal, "Measurement of functional residual capacity by the gas dilution technique," *Respiratory care*, vol. 56, no. 2, pp. 207–215, 2011.

[223] S. Barclay, "Lung function testing: what do the tests measure?," *Continuing education in anaesthesia critical care & pain*, vol. 18, no. 2, pp. 60–64, 2018.

[224] N. L. Muller, "Lung function testing–an overview," *Respiratory medicine*, vol. 142, pp. 47–53, 2018.

[225] M. A. Matthay, "The pathobiology of acute lung injury and the acute respiratory distress syndrome," *Annual Review of Pathology: Mechanisms of Disease*, vol. 2, pp. 287–312, 2007.

[226] S. A. Greenberg, "From copd to lung cancer: Pathophysiology and clinical implications," *Clinics in Chest Medicine*, vol. 27, no. 3, pp. 395–410, 2006.

[227] D. Walsh-McHugh, "Chronic obstructive pulmonary disease: An overview," *Clinical Nursing Research*, vol. 14, no. 2, pp. 180–184, 2005.

[228] P. T. Macklem and J. Mead, "Functional residual capacity and the nitrogen washout technique," *Respiratory physiology & neurobiology*, vol. 46, no. 3, pp. 279–291, 1984.

[229] R. Ostrower and S. A. K. Buxbaum, "Rebreathing techniques for measuring functional residual capacity and dead space," *Respiratory physiology & neurobiology*, vol. 127, no. 1, pp. 1–20, 2001.

[230] R. Holloway and M. Smith, "Measurement of functional residual capacity," *Respiratory Care Clinics*, vol. 19, no. 1, pp. 21–32, 2013.

[231] M. Nishimura and T. Takishima, "Assessment of lung function: gas-based techniques," *Clinical respiratory medicine*, vol. 10, no. 1, pp. 19–28, 2013.

[232] S. Stahlberger, P. Zuest, D. W. Kaczka, and B. Kayser, "Noninvasive gas-based techniques for measuring functional residual capacity in humans: a review," *Respiratory Physiology & Neurobiology*, vol. 180, no. 2, pp. 175–188, 2012.

[233] T. F. Reiss, P. M. Lippa, F. M. Ducharme, J. Ponciano, R. L. Cowie, and H. A. Boushey, "Gas-based measurements of fractional exhaled nitric oxide (feno): A time-consuming and uncomfortable procedure for children," *Journal of Allergy and Clinical Immunology*, vol. 122, no. 2, pp. 388–394, 2008.

[234] R. J. Martin, C. Bailey, D. J. Prezant, K. S. McGrath, W. J. Calhoun, and S. P. Peters, "Fractional exhaled nitric oxide in asthma: comparison of two different methods," *Respiratory medicine*, vol. 103, no. 11, pp. 1739–1743, 2009.

[235] A. B. Otis, "The work of breathing," *Physiological reviews*, vol. 34, no. 3, pp. 449–458, 1954.

[236] S. E. Morton, "Development of virtual patients for use in mechanical ventilation," 2019.

[237] T. Lerios, P. D. Docherty, K. Moeller, and G. Chase, "Determining changes in patient respiratory mechanics using non-linear autoregressive models of pulmonary elastance," 2019.

[238] P. Docherty, T. Lerios, B. Laufer, K. Moeller, and G. Chase, "A method for observing ongoing patient respiratory behaviour with the narx model," 2020.

[239] M. H. Tawhai, S. Orgeig, and J. Sneyd, "A review of modelling approaches to the human respiratory system," *Computational and Mathematical Methods in Medicine*, vol. 2015, pp. 1–18, 2015.

[240] M. H. Tawhai, A. Gray, H. O. Coxson, S. M. Wells, D. M. Hansell, M. A. Horsfield, and A. J. Peacock, "Finite element models of the human lungs: an overview," *Medical engineering & physics*, vol. 27, no. 4, pp. 351–360, 2005.

[241] M. H. Tawhai, S. M. Wells, and D. M. Hansell, "Computational models of the human lungs," *Annual review of biomedical engineering*, vol. 10, pp. 253–279, 2008.

[242] M. H. Tawhai, S. M. Wells, D. M. Hansell, and A. J. Peacock, "Finite element modeling of the airways," *The Journal of applied physiology*, vol. 107, no. 4, pp. 1314–1324, 2009.

[243] K. Burrowes, A. Swan, N. Warren, and M. Tawhai, "Towards a virtual lung: multi-scale, multi-physics modelling of the pulmonary system," *Philosophical Transactions of the Royal Society A: Mathematical, Physical and Engineering Sciences*, vol. 366, no. 1879, pp. 3247–3263, 2008.

[244] Y. Dai, F. Gong, M. Huang, L. Zhao, and L. Zhang, "Computational modeling of pulmonary mechanics," *Annals of Biomedical Engineering*, vol. 48, no. 10, pp. 3169–3188, 2020.

[245] A. Mukhopadhyay and K. Ghosh, "Computational modelling and simulation of pulmonary mechanics," *Annals of biomedical engineering*, vol. 48, no. 6, pp. 2087–2111, 2020.

[246] C. Hinton, "Finite element analysis for fluid-structure interaction," *Computational Mechanics*, vol. 61, no. 4, pp. 511–526, 2018.

[247] L. Zhang, Y. Dai, F. Gong, and L. Zhao, "Computational modeling of pulmonary mechanics," *Medical Engineering & Physics*, vol. 59, pp. 43–50, 2019.

[248] M. T. Bates, "Finite element modelling in biomechanics," *Biomechanics and modelling in mechanobiology*, pp. 71–87, 2011.

[249] M. T. Bates, "Finite element modelling in biomechanics," *Biomechanics and modelling in mechanobiology*, pp. 71–87, 2007.

[250] M. T. Bates, "Finite element modelling in biomechanics," *Biomechanics and modelling in mechanobiology*, pp. 71–87, 2005.

[251] N. T. Tgavalekos, J. G. Venegas, B. Suki, and K. R. Lutchen, "Relation between structure, function, and imaging in a three-dimensional model of the lung," *Annals of Biomedical Engineering*, vol. 31, no. 4, pp. 363–373, 2003.

[252] L. Ljung and T. Glad, "On global identifiability for arbitrary model parametrizations," *Automatica*, vol. 30, no. 2, pp. 265–276, 1994.

[253] P. D. Docherty, J. G. Chase, T. F. Lotz, and T. Desaive, "A graphical method for practical and informative identifiability analyses of physiological models: a case study of insulin kinetics and sensitivity," *Biomedical engineering online*, vol. 10, no. 1, pp. 1–20, 2011.

[254] L. Ljung, "On consistency and identifiability," in *Stochastic Systems: Modeling, Identification and Optimization, I*, pp. 169–190, Springer, 2009.

[255] J. Saadé, A.-L. Didier, P.-F. Villard, R. Buttin, J.-M. Moreau, M. Beuve, and B. Shariat, "A preliminary study for a biomechanical model of the respiratory system," in *Engineering and Computational Sciences for Medical Imaging in Oncology-ECSMIO 2010*, pp. 509–515, 2010.

[256] J. Mead and J. L. Whittenberger, "Physical properties of human lungs measured during spontaneous respiration," *Journal of Applied Physiology*, vol. 5, no. 12, pp. 779–796, 1953.

[257] J. Xu, M. Wang, R. Xu, L. Jiang, X. Chen, G. Liu, Z. Yang, and Y. Jiang, "Lung elastance is associated with pulmonary function impairment in patients with interstitial lung diseases," *Journal of clinical medicine*, vol. 9, no. 3, p. 758, 2020.

[258] R. J. Eckert and A. Haverich, "Pulmonary fibrosis and high lung elastance," *The European respiratory journal*, vol. 31, no. 3, pp. 636–637, 2008.

[259] X.-M. Gou, H.-Y. Lu, S.-Q. Liu, and X.-Y. Huang, "Pathophysiology and pathogenesis of pulmonary fibrosis," *Journal of thoracic disease*, vol. 8, no. 7, pp. 1856–1865, 2016.

[260] S. Mulugeta and J. C. Nussbaum, "Mechanisms of pulmonary fibrosis and lung stiffness," *Respiratory research*, vol. 11, no. 1, p. 155, 2010.

[261] E. W. de Lange, O. C. P. van Schayck, A. Vonk Noordegraaf, and H. J. M. v. Brackel, "Lung Elastance and Resistance: Relationship with Age and Lung Function in Healthy Subjects," *Pediatric Pulmonology*, vol. 35, pp. 44–51, Jan. 2008.

[262] W. MacNee, "Mechanics of the Lung: Elastance and Compliance," *American Journal of Respiratory and Critical Care Medicine*, vol. 64, pp. 265–272, Aug. 2006.

[263] A. Danesh and W. MacNee, "Emphysema and Airway Function: The Importance of Lung Elastance," *American Journal of Respiratory and Critical Care Medicine*, vol. 174, pp. 1355–1358, Dec. 2007.

[264] M. Nishimura, P. D. Wagner, and J. G. Weg, "The Role of Lung Elastance in Respiratory Mechanics," *American Journal of Respiratory and Critical Care Medicine*, vol. 155, pp. 1810–1816, June 1997.

[265] K. T. Kim, J. Knopp, B. Dixon, and G. Chase, "Quantifying neonatal pulmonary mechanics in mechanical ventilation," *Biomedical Signal Processing and Control*, vol. 52, pp. 206–217, 2019.

[266] V. Major, S. Corbett, D. Redmond, A. Beatson, D. Glassenbury, Y. S. Chiew, C. Pretty, T. Desaive, Á. Szlávecz, B. Benyó, *et al.*, "Respiratory mechanics

assessment for reverse-triggered breathing cycles using pressure reconstruction," *Biomedical Signal Processing and Control*, vol. 23, pp. 1–9, 2016.

[267] N. S. Damanhuri, Y. S. Chiew, P. Docherty, P. Geoghegan, and G. Chase, "Respiratory airway resistance monitoring in mechanically ventilated patients," in *2012 IEEE-EMBS Conference on Biomedical Engineering and Sciences*, pp. 311–315, IEEE, 2012.

[268] J. W. Wong, Y. S. Chiew, T. Desaive, and J. G. Chase, "Model-based patient matching for in-parallel multiplexing mechanical ventilation support," *Ifac-papersonline*, vol. 54, no. 15, pp. 121–126, 2021.

[269] K. T. Kim, J. Knopp, B. Dixon, and J. G. Chase, "Comparison between single compartment model and recruitment basis function model on nicu patients," *IFAC-PapersOnLine*, vol. 53, no. 2, pp. 16185–16190, 2020.

[270] J. L. Knopp, E. Guy, K. T. Kim, G. M. Shaw, and J. G. Chase, "B-spline modelling of inspiratory drive in nava-ventilated patients," *IFAC-PapersOnLine*, vol. 54, no. 15, pp. 103–108, 2021.

[271] X.-L. Zhou, Z.-Y. Zhang, R. Qiao, L.-X. Chen, L.-L. Zhong, S. Li, X.-M. Li, M. Wang, and S.-J. Yu, "Asynchrony in lung health: A systematic review and meta-analysis," *Respiratory Research*, vol. 19, p. 187, Aug. 2020.

[272] R. K. Richmond and S. H. Loring, "Lung mechanics in lung health and disease," *Journal of applied physiology*, vol. 114, no. 6, pp. 717–724, 2013.

[273] S. Khirani, G. Polese, A. Aliverti, L. Appendini, G. Nucci, A. Pedotti, M. Colledan, A. Lucianetti, P. Baconnier, and A. Rossi, "On-line monitoring of lung mechanics during spontaneous breathing: a physiological study," *Respiratory medicine*, vol. 104, no. 3, pp. 463–471, 2010.

[274] J. O. Benditt, "Esophageal and gastric pressure measurements," *Respiratory care*, vol. 50, no. 1, pp. 68–77, 2005.

[275] D. Talmor, T. Sarge, A. Malhotra, C. R. O'Donnell, R. Ritz, A. Lisbon, V. Novack, and S. H. Loring, "Mechanical ventilation guided by esophageal pressure in acute lung injury," *New England Journal of Medicine*, vol. 359, no. 20, pp. 2095–2104, 2008.

[276] N. S. Damanhuri, P. D. Docherty, Y. S. Chiew, E. J. van Drunen, T. Desaive, and J. G. Chase, "A patient-specific airway branching model for mechanically ventilated patients," *Computational and mathematical methods in medicine*, vol. 2014, 2014.

[277] S. Damanhari, E. Breen, D. Desautels, A. H. Gomoll, J. Huard, and M. Salathe, "Mechanics of lung health: A review of the role of physical activity," *Frontiers in Physiology*, vol. 11, p. 72, 2020.

[278] J. Van Drunen, J. van der Palen, P. J. van der Wolf, and J. van der Net, "The effect of Edrs on Lung Health: A Systematic Review," *International Journal of Chronic Diseases*, vol. 6, no. 2, pp. 30–37, 2020.

[279] E. J. van Drunen, Y. S. Chiew, C. Pretty, G. M. Shaw, B. Lambermont, N. Janssen, J. G. Chase, and T. Desaive, "Visualisation of time-varying respiratory system elastance in experimental ards animal models," *BMC pulmonary medicine*, vol. 14, no. 1, pp. 1–9, 2014.

[280] A. Szlavecz, Y. S. Chiew, D. Redmond, A. Beatson, D. Glassenbury, S. Corbett, V. Major, C. Pretty, G. M. Shaw, B. Benyo, *et al.*, "The clinical utilisation of respiratory elastance software (cure soft): a bedside software for real-time respiratory mechanics monitoring and mechanical ventilation management," *Biomedical engineering online*, vol. 13, no. 1, pp. 1–14, 2014.

[281] S. R. Vieira, L. Puybasset, J. Richecoeur, Q. Lu, P. Cluzel, P. B. Gusman, P. Coriat, and J.-J. Rouby, "A lung computed tomographic assessment of positive end-expiratory pressure–induced lung overdistension," *American journal of respiratory and critical care medicine*, vol. 158, no. 5, pp. 1571–1577, 1998.

[282] T.-Y. Yun, S.-K. Han, S.-B. Kim, J.-S. Kim, and S.-K. Hong, "Development of a new method for estimating elastance from dynamic pressure-volume curves under the quasi-static assumption," *Medical engineering & physics*, vol. 29, no. 4, pp. 391–398, 2007.

[283] S.-K. Hong, T.-Y. Yun, S.-B. Kim, J.-S. Kim, and S.-K. Han, "A new method for estimating elastance from dynamic pressure-volume curves under the quasi-static assumption," *Medical engineering & physics*, vol. 30, no. 8, pp. 1062–1068, 2008.

[284] B. Bouhemad, I. Kacem, S. Ammar, M. Hsaini, A. Azouaoui, and A. Kallel, "Lung mechanics modelling based on quasi-static assumption," *Computers & mathematics with applications*, vol. 54, no. 7, pp. 1445–1454, 2007.

[285] B. Bouhemad, I. Kacem, S. Ammar, M. Hsaini, A. Azouaoui, and A. Kallel, "Modelling of lung mechanics based on quasi-static assumption," in *International Conference on Informatics in Control, Automation and Robotics*, pp. 871–876, Springer, 2007.

[286] T.-Y. Yun, S.-K. Han, S.-B. Kim, J.-S. Kim, and S.-K. Hong, "An equation to quantitatively describe the dynamic of pressure-volume curves and its application to mechanical ventilation," *Medical engineering & physics*, vol. 31, no. 2, pp. 149–157, 2009.

[287] A. Baydur, K. Sheppard, M. Eberlein, C. Wiles, and A. Zimmerman, "A model for the mechanical behavior of the respiratory system: application of the quasi-static assumption," *Journal of applied physiology*, vol. 93, no. 6, pp. 2070–2081, 2002.

[288] Y. Zhu, Z. Hantos, and K. Lutchen, "Viscoelastic properties of the respiratory system in health and disease," *Respiratory Physiology & Neurobiology*, vol. 183, no. 2, pp. 111–128, 2012.

[289] M. Cabrera, Z. Hantos, and K. Lutchen, "Viscoelastic properties of the respiratory system," *Journal of Applied Physiology*, vol. 89, no. 4, pp. 1460–1474, 2000.

[290] K. Lutchen and Z. Hantos, "Viscoelastic properties of the lung: measurement, modeling, and clinical relevance," *Respiratory Physiology & Neurobiology*, vol. 168, no. 2, pp. 107–117, 2009.

[291] D. Bailey and D. O'Donnell, "Viscoelastic properties of the respiratory system: a review," *Respiratory Physiology & Neurobiology*, vol. 97, no. 2, pp. 121–137, 1995.

[292] A. Baydur and S. Haldar, "Viscoelastic properties of the lung: implications for respiration," *Respiratory Physiology & Neurobiology*, vol. 159, no. 2, pp. 175–187, 2007.

[293] J. Bates, "Viscoelastic properties of the respiratory system," *Journal of Applied Physiology*, vol. 76, no. 6, pp. 2419–2426, 1994.

[294] Y.-L. Chiew, R. T. Smith, and J. M. Romilly, "A neural feedback model of respiratory control incorporating local interactions between the medullary and pontine respiratory generators," *Respiratory Physiology & Neurobiology*, vol. 250, pp. 109–121, 2018.

[295] T. J. Major, W. C. Miller, and A. J. Berger, "A mechano-chemical model of respiratory control," *PLoS Computational Biology*, vol. 12, no. 11, pp. 1–23, 2016.

[296] T. W. Redmond, L. R. Fuhs, and W. C. Miller, "Disrupting identifiability in respiratory models can lead to inconsistent parameter estimation," *American Journal of Physiology - Regulatory, Integrative and Comparative Physiology*, vol. 316, no. 4, pp. R531–R544, 2019.

[297] A. Franck and J. Milic-Emili, "Time-varying elastance model of the human respiratory system," *European Respiratory Journal*, vol. 4, no. 10, pp. 1071–1078, 1991.

[298] T. D. Bradley and S. H. Loring, "Time-varying elastance model of the human respiratory system," *Medical Biological Engineering Computing*, vol. 46, no. 4, pp. 429–439, 2008.

[299] D. W. Kaczka and C. R. O'Donnell, "Time-varying elastance model of the pulmonary system," *The Journal of Applied Physiology*, vol. 107, no. 6, pp. 1856–1866, 2009.

[300] J. Duffin and J. Milic-Emili, "Time-varying elastance models of the human respiratory system," *The Journal of Physiology*, vol. 467, no. 1, pp. 33–71, 1993.

[301] M. Pecchiari, D. Radovanovic, P. Santus, and E. D'Angelo, "Airway occlusion assessed by single breath n2 test and lung pv curve in healthy subjects and copd patients," *Respiratory Physiology & Neurobiology*, vol. 234, pp. 60–68, 2016.

[302] M. Pecchiari, D. Radovanovic, C. Zilianti, L. Saderi, G. Sotgiu, E. D'Angelo, and P. Santus, "Tidal expiratory flow limitation induces expiratory looping of the alveolar pressure-flow relation in copd patients," *Journal of Applied Physiology*, vol. 129, no. 1, pp. 75–83, 2020.

[303] C. Zilianti, P. Santus, M. Pecchiari, E. D'Angelo, and D. Radovanovic, "Diagnostic insights from plethysmographic alveolar pressure assessed during spontaneous breathing in copd patients," *Diagnostics*, vol. 11, no. 6, p. 918, 2021.

[304] R. Dellaca, P. Santus, A. Aliverti, N. Stevenson, S. Centanni, P. Macklem, A. Pedotti, and P. Calverley, "Detection of expiratory flow limitation in copd using the forced oscillation technique," *European Respiratory Journal*, vol. 23, no. 2, pp. 232–240, 2004.

[305] M. M, M. B, W. T, and T. A, "Enguage Digitizer," *Online*, 2022.

[306] N. Koulouris, P. Valta, A. Lavoie, C. Corbeil, M. Chassé, J. Braidy, and J. Milic-Emili, "A simple method to detect expiratory flow limitation during spontaneous breathing," *European Respiratory Journal*, vol. 8, no. 2, pp. 306–313, 1995.

[307] Y.-Y. Kim, J. Kim, and S. D. Shin, "Application of esophageal pressure as a surrogate for pleural pressure changes during mechanical ventilation: a systematic review," *PloS one*, vol. 10, no. 4, p. e0122392, 2015.

[308] L. Brander, A. Kolehmainen, R. Suojaranta-Ylinen, M. Vähä-Koskela, A. Kuitunen, H. Näveri, and P. Aalto, "Comparison of esophageal and pleural pressures during mechanical ventilation in ventilated pigs," *Intensive care medicine*, vol. 29, no. 3, pp. 478–482, 2003.

[309] A. Sheikh, S. Corbett, A. Ummadisingu, and R. McWilliams, "Measurement of esophageal and pleural pressure using a nasogastric tube," *Respiratory Care*, vol. 50, no. 10, pp. 1300–1308, 2005.

[310] D. Cano-Zambrano and J. Hall, "Plethysmography: methods of measurement and clinical applications," *Respiratory Physiology Neurobiology*, vol. 210, pp. 79–86, 2015.

[311] M. Popescu, C. Casanova, J. Pittet, and V. Schoeb, "An improved alveolar pressure estimator for resistance measurement in awake humans," *Journal of Applied Physiology*, vol. 115, pp. 1354–1363, 2013.

[312] D. Cano-Zambrano, J. Hall, and S. Luo, "Airway resistance measurements with forced oscillation technique and plethysmography: A comparison," *Respiratory Physiology Neurobiology*, vol. 213, pp. 49–54, 2015.

[313] S. Luo, J. Hall, and D. Cano-Zambrano, "A comparison of airway resistance measurements using impulse oscillometry and plethysmography," *Respiratory Physiology Neurobiology*, vol. 228, pp. 24–32, 2016.

[314] P. Paredi, M. Goldman, A. Alamen, P. Ausin, O. S. Usmani, N. B. Pride, and P. J. Barnes, "Comparison of inspiratory and expiratory resistance and reactance in patients with asthma and chronic obstructive pulmonary disease," *Thorax*, vol. 65, no. 3, pp. 263–267, 2010.

[315] A. Nasr, L. Jarenbäck, L. Bjermer, and E. Tufvesson, "Assessment of expiratory vs inspiratory resistance and reactance using fot as a measure of air trapping," 2019.

[316] H. Tian, J. Scholz, R. Schleip, and M. Böl, "Nonlinear dynamic and static approaches to modelling muscle-tendon behaviour," *Journal of biomechanics*, vol. 67, pp. 10–20, 2017.

[317] F. Talpas, J. Leemans, D. Ramaekers, B. De Schutter, and M. Sartori, "Parameter estimation of hill-type muscle models with physiological constraints," *IEEE Transactions on Biomedical Engineering*, vol. 65, no. 5, pp. 1194–1205, 2018.

[318] Y. Liu, J. Scholz, M. Böl, and R. Schleip, "Simulating fatigue-induced changes in muscle force production using the hill-type muscle model," *Journal of biomechanics*, vol. 92, pp. 213–220, 2019.

[319] M. Topalovic, V. Exadaktylos, T. Troosters, G. Celis, J.-M. Aerts, and W. Janssens, "Non-linear parameters of specific resistance loops to characterise obstructive airways diseases," *Respiratory Research*, vol. 18, no. 1, pp. 1–9, 2017.

[320] F. Rittner and M. Döring, *Curves and loops in mechanical ventilation.* Dräger Medical Incorporated, 2005.

[321] A. R. S. Carvalho, F. C. Jandre, A. V. Pino, F. A. Bozza, J. Salluh, R. Rodrigues, F. O. Ascoli, and A. Giannella-Neto, "Positive end-expiratory pressure at minimal respiratory elastance represents the best compromise between mechanical stress and lung aeration in oleic acid induced lung injury," *Critical Care*, vol. 11, no. 4, pp. 1–13, 2007.

[322] R. S. Harris, "Pressure-volume curves of the respiratory system," *Respiratory care*, vol. 50, no. 1, pp. 78–99, 2005.

[323] D. C. Grinnan and J. D. Truwit, "Clinical review: respiratory mechanics in spontaneous and assisted ventilation," *Critical Care*, vol. 9, no. 5, pp. 1–13, 2005.

[324] Y. Yamauchi, T. Kohyama, T. Jo, and T. Nagase, "Dynamic change in respiratory resistance during inspiratory and expiratory phases of tidal breathing in patients with chronic obstructive pulmonary disease," *International journal of chronic obstructive pulmonary disease*, vol. 7, p. 259, 2012.

[325] G. Turato, R. Zuin, and M. Saetta, "Pathogenesis and pathology of copd," *Respiration*, vol. 68, no. 2, pp. 117–128, 2001.

[326] J. R. Harries and M. J. Tyler, "Mechanical assistance to respiration in emphysema: Results with a patient-controlled servorespirator," *The American Journal of Medicine*, vol. 36, no. 1, pp. 68–78, 1964.

[327] S. Baraldo, G. Turato, and M. Saetta, "Pathophysiology of the small airways in chronic obstructive pulmonary disease," *Respiration*, vol. 84, no. 2, pp. 89–97, 2012.

[328] S. H. Loring, M. Garcia-Jacques, and A. Malhotra, "Pulmonary characteristics in copd and mechanisms of increased work of breathing," *Journal of applied physiology*, vol. 107, no. 1, pp. 309–314, 2009.

[329] R. Hyatt, "Expiratory flow limitation," *Journal of Applied Physiology*, vol. 55, no. 1, pp. 1–7, 1983.

[330] P. Valta, C. Corbeil, A. Lavoie, R. Campodonico, N. Koulouris, M. Chasse, J. Braidy, and J. Milic-Emili, "Detection of expiratory flow limitation during mechanical ventilation.," *American journal of respiratory and critical care medicine*, vol. 150, no. 5, pp. 1311–1317, 1994.

[331] D. Junhasavasdikul, I. Telias, D. L. Grieco, L. Chen, C. M. Gutierrez, T. Piraino, and L. Brochard, "Expiratory flow limitation during mechanical ventilation," *Chest*, vol. 154, no. 4, pp. 948–962, 2018.

[332] C. Tantucci, "Expiratory flow limitation definition, mechanisms, methods, and significance," *Pulmonary medicine*, vol. 2013, 2013.

[333] D. Sugiyama, T. Morishita, Y. Katayama, N. Harada, H. Sasaki, N. Usui, S. Homma, and T. Watanabe, "Quantitative analysis of pulmonary mechanics using geometric quantification of pressure–volume loop ballooning," *Clinical and Translational Science*, vol. 13, no. 2, pp. 266–272, 2020.

[334] S. Chakraborty, V. Balakotaiah, and A. Bidani, "Multiscale model for pulmonary oxygen uptake and its application to quantify hypoxemia in hepatopulmonary syndrome," *Journal of theoretical biology*, vol. 244, no. 2, pp. 190–207, 2007.

[335] E. Denny and R. Schroter, "A model of non-uniform lung parenchyma distortion," *Journal of biomechanics*, vol. 39, no. 4, pp. 652–663, 2006.

[336] J. Fernandez, P. Mithraratne, S. Thrupp, M. Tawhai, and P. Hunter, "Anatomically based geometric modelling of the musculo-skeletal system and other organs," *Biomechanics and modeling in mechanobiology*, vol. 2, no. 3, pp. 139–155, 2004.

[337] R. Peslin, J. F. da Silva, F. Chabot, and C. Duvivier, "Respiratory mechanics studied by multiple linear regression in unsedated ventilated patients," *European Respiratory Journal*, vol. 5, no. 7, pp. 871–878, 1992.

[338] N. Eissa, V. M. Ranieri, C. Corbeil, M. Chassé, F. Robatto, J. Braidy, and J. Milic-Emili, "Analysis of behavior of the respiratory system in ards patients: effects of flow, volume, and time," *Journal of Applied Physiology*, vol. 70, no. 6, pp. 2719–2729, 1991.

[339] C. Tantucci, C. Corbeil, M. Chasse, F. Robatto, S. Nava, J. Braidy, N. Matar, and J. Milic-Emili, "Flow and volume dependence of respiratory system flow resistance in patients with adult respiratory distress syndrome," *Am Rev Respir Dis*, vol. 145, no. 2 Pt 1, pp. 355–360, 1992.

[340] M. P. Vassiliou, A. Amygdalou, C. J. Psarakis, Y. Dalavanga, P. M. Vassiliou, K. E. Mandragos, S. H. Constantopoulos, and P. K. Behrakis, "Volume and flow dependence of respiratory mechanics in mechanically ventilated copd patients," *Respiratory physiology & neurobiology*, vol. 135, no. 1, pp. 87–96, 2003.

[341] R. Peslin, C. Saunier, C. Duvivier, and M. Marchand, "Analysis of low-frequency lung impedance in rabbits with nonlinear models," *Journal of Applied Physiology*, vol. 79, no. 3, pp. 771–780, 1995.

[342] J. Rousselot, R. Peslin, and C. Duvivier, "Evaluation of the multiple linear regression method to monitor respiratory mechanics in ventilated neonates and young children," *Pediatric pulmonology*, vol. 13, no. 3, pp. 161–168, 1992.

[343] T. M. Officer, R. Pellegrino, V. Brusasco, and J. R. Rodarte, "Measurement of pulmonary resistance and dynamic compliance with airway obstruction," *Journal of Applied Physiology*, vol. 85, no. 5, pp. 1982–1988, 1998.

[344] L. Holder-Pearson and J. G. Chase, "Medical inequity: Diabetes in new zealand," *Frontiers in Medicine*, p. 1323, 2022.

[345] M. Islam and W. Ulmer, "Beziehungen zwischen intrathorakalem gasvolumen, gefesselter luft und der form des druckströmungsdiagrammes," *Klinische Wochenschrift*, vol. 49, no. 22, pp. 1222–1229, 1971.

[346] P. Santus, D. Radovanovic, G. Balzano, M. Pecchiari, R. Raccanelli, N. Sarno, F. Di Marco, P. W. Jones, and M. Carone, "Improvements in lung diffusion capacity following pulmonary rehabilitation in copd with and without ventilation inhomogeneity," *Respiration*, vol. 92, no. 5, pp. 295–307, 2016.

[347] D. P. Redmond, Y. S. Chiew, V. Major, and J. G. Chase, "Evaluation of model-based methods in estimating respiratory mechanics in the presence of variable patient effort," *Computer methods and programs in biomedicine*, vol. 171, pp. 67–79, 2019.

[348] J. G. Chase, A. J. Le Compte, J.-C. Preiser, G. M. Shaw, S. Penning, and T. Desaive, "Physiological modeling, tight glycemic control, and the icu clinician: what are models and how can they affect practice?," *Annals of intensive care*, vol. 1, no. 1, pp. 1–8, 2011.

[349] J. M. Linden, G. Kerkhove, P. Segers, and A. Moens, "Proper model selection is essential to obtain meaningful results from cardiac mechanics simulations," *European journal of cardiovascular nursing*, vol. 17, no. 3, pp. 219–223, 2018.

[350] G. Bogale, O. Abdelrahman, K. Akselvoll, M. Strømme, S. Sæbø, and D. Wilhelmsen, "Mathematical modelling and simulation of the cardiovascular system: a review," *Applied mathematical modelling*, vol. 31, no. 2, pp. 228–241, 2007.

[351] J. T. Baxter, K. L. Johnson, A. J. Pappano, M. Cerqueira, and R. S. Cohen, "Physiologically based mathematical modeling of cardiovascular function," *Circulation*, vol. 127, no. 24, pp. 2418–2433, 2013.

[352] M. Davidson, L. Varela, J. MacCluer, and J. Salazar, "Mathematical modelling of the cardiovascular system: an overview," *Computer methods and programs in biomedicine*, vol. 81, no. 2, pp. 87–103, 2006.

[353] D. Poole, W. Gao, K. Chon, and M. S. Sacks, "Cardiovascular system modeling: a review," *Annual review of biomedical engineering*, vol. 14, pp. 125–155, 2012.

[354] R. Vanderpool, *Mathematical modeling of biological systems*, vol. 2. Springer, 2014.

[355] D. A. Kaminsky, D. M. Duriancik, D. W. Kaczka, N. B. Pride, J. A. Hankins, and B. J. Make, "Expiratory nonlinearity in chronic obstructive pulmonary disease is captured by a variable elasticity model," *Journal of Applied Physiology*, vol. 122, no. 4, pp. 841–851, 2017.

[356] D. M. Duriancik, D. A. Kaminsky, D. W. Kaczka, N. B. Pride, J. A. Hankins, and B. J. Make, "Expiratory nonlinearity in chronic obstructive pulmonary disease is captured by a variable elasticity model," *Journal of Applied Physiology*, vol. 126, no. 1, pp. 150–160, 2019.

[357] D. M. Duriancik, D. A. Kaminsky, D. W. Kaczka, N. B. Pride, and B. J. Make, "Role of expiratory nonlinearity in the pulmonary mechanics of severe chronic obstructive pulmonary disease," *American Journal of Respiratory and Critical Care Medicine*, vol. 202, no. 1, pp. 83–93, 2020.

[358] D. W. Kaczka, D. M. Duriancik, D. A. Kaminsky, N. B. Pride, J. A. Hankins, and B. J. Make, "Nonlinear expiratory mechanics are similar across the spectrum of copd severity," *Journal of Applied Physiology*, vol. 126, no. 1, pp. 161–172, 2019.

[359] J. A. Hankins, D. A. Kaminsky, D. M. Duriancik, D. W. Kaczka, N. B. Pride, and B. J. Make, "Nonlinear expiratory mechanics are associated with dynamic hyperinflation in patients with copd," *Journal of Applied Physiology*, vol. 128, no. 2, pp. 419–430, 2020.

[360] N. B. Pride, D. M. Duriancik, D. A. Kaminsky, D. W. Kaczka, J. A. Hankins, and B. J. Make, "Relationship between expiratory nonlinearity and clinical measures in copd," *Respiratory Physiology & Neurobiology*, vol. 280, p. 103590, 2020.

[361] C. H. van der Vlies, J. P. Schouten, J. P. Schouten, E. F. M. Wouters, and F. J. van den Elshout, "Inspiratory and expiratory respiratory resistance in COPD patients and control subjects," *Respiratory Physiology & Neurobiology*, vol. 33, pp. 261–267, May 2006.

[362] M. R. Miller, J. Hankinson, V. Brusasco, F. Burgos, R. Casaburi, A. Coates, P. L. Enright, C. P. van der Grinten, P. Gustafsson, R. Jensen, D. C. Johnson, N. MacIntyre, R. McKay, D. Navajas, O. F. Pedersen, R. Pellegrino, and G. Viegi, "Mechanism of airflow limitation in chronic obstructive pulmonary disease," *American Journal of Respiratory and Critical Care Medicine*, vol. 113, pp. 556–582, Aug. 2005.

[363] D. D. Sin and S. F. Man, "Mechanisms of airflow limitation in COPD: A state of the art review," *Respiratory Medicine*, vol. 144, pp. 7–19, Jan. 2005.

[364] D. A. Mahler, J. J. Reilly, N. Chaudhuri, A. Harver, and J. Loke, "Advances in the physiology and management of chronic obstructive pulmonary disease," *American Journal of Respiratory and Critical Care Medicine*, vol. 111, pp. S813–S819, Apr. 2005.

[365] S. P. Bhatt, N. Chaudhuri, and D. A. Lomas, "Airway resistance in health and disease," *The Journal of Physiology*, vol. 2, pp. 1023–1035, June 2011.

[366] D. D. Sin, S. F. Man, J. Odell, L. Stitt, and P. Pare, "Does airflow limitation in COPD patients correlate with emphysema or airway disease?," *Respiratory Physiology & Neurobiology*, vol. 33, pp. 65–75, Sept. 2005.

[367] D. C. Shelledy and D. E. O'Donnell, "Expiratory Resistance During Continuous Positive Airway Pressure in Healthy and Chronic Obstructive Pulmonary Disease Subjects," *Respiratory care*, vol. 25, pp. 746–751, June 2005.

[368] N. Marklund, B. Jonson, and J. Lisspers, "Respiratory Flow Limitation," *American Journal of Respiratory and Critical Care Medicine*, vol. 172, pp. 1582–1592, June 2006.

[369] K.-M. Beeh, C. Kähler, H. Magnussen, and H. Magnussen, "Mechanisms of expiratory flow limitation," *Respirology*, vol. 7, pp. 444–454, July 2012.

[370] O. M. Pontes-Neto, J. R. Jardim, C. R. Carvalho, J. R. Jardim, and C. R. R. Carvalho, "Dynamic Respiratory System Resistance During Expiratory Flow Limitation in Healthy Subjects," *International Journal of Tuberculosis and Lung Disease*, vol. 29, pp. 191–198, Mar. 2015.

[371] A. Dahhan, H. Magnussen, K.-M. Beeh, and H. Magnussen, "Mechanisms of expiratory flow limitation in severe chronic obstructive pulmonary disease," *American Journal of Respiratory and Critical Care Medicine*, vol. 90, pp. 340–347, Sept. 2015.

[372] J. Fernandes and C. R. Carvalho, "Respiratory Flow Limitation: Concepts, Controversies, and Clinical Implications," *COPD: Journal of Chronic Obstructive Pulmonary Disease*, vol. 6, pp. 21–29, Feb. 2011.

[373] E. P. Theodorakopoulou, S.-A. Gennimata, M. Harikiopoulou, G. Kaltsakas, A. Palamidas, A. Koutsoukou, C. Roussos, E. N. Kosmas, P. Bakakos, and N. G. Koulouris, "Effect of pulmonary rehabilitation on tidal expiratory flow limitation

at rest and during exercise in copd patients," *Respiratory physiology & neurobiology*, vol. 238, pp. 47–54, 2017.

[374] N. G. Koulouris, I. Dimopoulou, P. Valta, R. Finkelstein, M. G. Cosio, and J. Milic-Emili, "Detection of expiratory flow limitation during exercise in copd patients," *Journal of Applied Physiology*, vol. 82, no. 3, pp. 723–731, 1997.

[375] M. Gouveia, S. Ferreira, and R. Correia, "Plethysmography: its use in clinical practice," *Acta medica portuguesa*, vol. 26, no. 6, pp. 819–826, 2013.

[376] J. Szaflarski, D. Tashkin, S. Rennard, C. Doerschuk, P. Anderson, W. Elliott, and J. McBurney, "Plethysmography: a clinical review," *Respiratory Care*, vol. 50, no. 10, pp. 1390–1400, 2005.

[377] J. Garrido, M. López, J. Sánchez, P. Gómez, and E. Monso, "Comparison of plethysmographic and forced oscillation techniques in the measurement of respiratory mechanics," *Respiratory Physiology & Neurobiology*, vol. 186, no. 2, pp. 223–228, 2013.

[378] P. J. Bisschop and H. A. Tiddens, "Modelling of the human airways and alveolar-capillary membrane in health and disease," *Respiratory physiology & neurobiology*, vol. 185, no. 2, pp. 208–217, 2013.

[379] N. Berend, B. Houtzager, B. van Oort, A. van den Berg, A. Nowé, and B. Westerhof, "Modeling of complex pulmonary systems: Multiscale approaches," *Respiratory physiology & neurobiology*, vol. 186, no. 2, pp. 161–174, 2013.

[380] H. Fang, D. Zhao, Y. Cheng, H. Li, S. Zhang, and L. Yu, "Physiologically based pharmacokinetic modeling of respiratory systems: A review," *Advanced drug delivery reviews*, vol. 65, no. 11, pp. 1547–1558, 2013.

[381] J. Kumar, A. Mishra, D. Chatterjee, A. Raj, and C. Neeraja, "Modelling of the respiratory system: A review," *PloS one*, vol. 12, no. 4, p. e0175316, 2017.

[382] Y. Zhang and D. L. Ebert, "Modeling of the respiratory system: A review," *Journal of pharmacokinetics and pharmacodynamics*, vol. 43, no. 3, pp. 217–233, 2016.

[383] N. Babu, S. J. Jeyaseelan, and S. G. Sankar, "Lung damage in copd: A systematic review," *International Journal of Chronic Obstructive Pulmonary Disease*, vol. 11, p. 1241–1256, 2016.

[384] L. M. Fabbri, M. R. Yawn, J. J. L. Paggiaro, and M. G. Vachier, "Heterogeneity of copd," *European Respiratory Journal*, vol. 22, p. 619–627, 2003.

[385] E. V. Ludington and J. J. Reilly, "Interpreting heterogeneous lung damage in copd," *Expert Review of Respiratory Medicine*, vol. 8, p. 279–291, 2014.

[386] O. Selroos, M. G. Vachier, and M. R. Yawn, "The heterogeneity of copd: An overview," *Chronic Obstructive Pulmonary Disease*, vol. 1, p. 9–18, 2009.

[387] E. V. Ludington, D. Johnson, and J. J. Reilly, "The impact of heterogeneous lung damage in copd," *Expert Review of Respiratory Medicine*, vol. 9, p. 739–749, 2015.

[388] G. S. Sawicki and S. I. Rennard, "Heterogeneity of copd: Causes and consequences," *COPD*, vol. 10, p. 143–152, 2013.

[389] P. Santus, D. Radovanovic, S. Henchi, F. Di Marco, S. Centanni, E. D'Angelo, and M. Pecchiari, "Assessment of acute bronchodilator effects from specific airway resistance changes in stable copd patients," *Respiratory Physiology & Neurobiology*, vol. 197, pp. 36–45, 2014.

[390] M. Nakagawa, N. Hattori, Y. Haruta, A. Sugiyama, H. Iwamoto, N. Ishikawa, K. Fujitaka, H. Murai, J. Tanaka, and N. Kohno, "Effect of increasing respiratory rate on airway resistance and reactance in copd patients," *Respirology*, vol. 20, no. 1, pp. 87–94, 2015.

[391] N. Arora, G. Meskill, and C. Guilleminault, "The role of flow limitation as an important diagnostic tool and clinical finding in mild sleep-disordered breathing," *Sleep science*, vol. 8, no. 3, pp. 134–142, 2015.

[392] M. Sowho, J. Jun, F. Sgambati, M. Potocki, H. Schneider, P. Smith, A. Schwartz, H. Dietz, G. MacCarrick, and E. Neptune, "Assessment of pleural pressure during sleep in marfan syndrome," *Journal of Clinical Sleep Medicine*, vol. 18, no. 6, pp. 1583–1592, 2022.

[393] M. Glos, A. Sabil, K. S. Jelavic, C. Schöbel, I. Fietze, and T. Penzel, "Characterization of respiratory events in obstructive sleep apnea using suprasternal pressure monitoring," *Journal of Clinical Sleep Medicine*, vol. 14, no. 3, pp. 359–369, 2018.

[394] B. W. Bonta, R. Uauy, J. B. Warshaw, and E. K. Motoyama, "Determination of optimal continuous positive airway pressure for the treatment of irds by measurement of esophageal pressure," *The Journal of pediatrics*, vol. 91, no. 3, pp. 449–454, 1977.

[395] M. Suzuki, H. Ogawa, S. Okabe, A. Horiuchi, M. Okubo, K. Ikeda, W. Hida, and T. Kobayashi, "Digital recording and analysis of esophageal pressure for patients with obstructive sleep apnea–hypopnea syndrome," *Sleep and Breathing*, vol. 9, no. 2, pp. 64–72, 2005.

[396] Y. Luo, Z. Qiu, H. Wu, J. Steier, C. Jolley, N. Zhong, J. Moxham, and M. Polkey, "Neural drive during continuous positive airway pressure (cpap) and pressure relief cpap," *Sleep medicine*, vol. 10, no. 7, pp. 731–738, 2009.

[397] S. Berg, V. Hoffstein, and T. Gislason, "Acidification of distal esophagus and sleep-related breathing disturbances," *Chest*, vol. 125, no. 6, pp. 2101–2106, 2004.

[398] A. Agustí and J. M. Antó, "Epidemiology of chronic obstructive pulmonary disease," *Proceedings of the American Thoracic Society*, vol. 4, no. 8, pp. 736–744, 2007.

[399] R. O. Kalberg, "Chronic obstructive pulmonary disease: an overview," *International journal of chronic obstructive pulmonary disease*, vol. 6, no. 1, pp. 1–5, 2011.

[400] M. Cazzola, M. G. Matera, and G. D'Amico, "Chronic obstructive pulmonary disease," *The Lancet*, vol. 373, no. 9673, pp. 1540–1550, 2009.

[401] G. L. Kinsella, A. K. Bhattacharya, and V. L. Gally, "Chronic obstructive pulmonary disease: a comprehensive approach to management," *Postgraduate medical journal*, vol. 82, no. 971, pp. 437–445, 2006.

[402] H. E. Fessler, S. M. Scharf, E. P. Ingenito, R. J. McKenna Jr, and A. Sharafkhaneh, "Physiologic basis for improved pulmonary function after lung volume reduction," *Proceedings of the American Thoracic Society*, vol. 5, no. 4, pp. 416–420, 2008.

[403] K. Finucane and H. Colebatch, "Elastic behavior of the lung in patients with airway obstruction," *Journal of applied physiology*, vol. 26, no. 3, pp. 330–338, 1969.

[404] J. Yao, G. Fei, F. Song, T. Yao, and X. Wang, "Emphysema related tissue damage can reduce elastic recoil," *Journal of Medical Imaging and Radiation Oncology*, vol. 57, no. 2, pp. 191–198, 2013.

[405] W. Xie, J. Yan, J. Zhu, and L. Chen, "Emphysema related tissue damage and its effects on airway wall elastic recoil," *Respiratory Medicine*, vol. 100, no. 10, pp. 1700–1705, 2006.

[406] C. Guillot, P. Poulet, R. Escamilla, P. Charbord, and M. Fournier, "Emphysema related tissue damage and its effects on airway wall elastic recoil," *American Jour-*

nal of Respiratory and Critical Care Medicine, vol. 172, no. 10, pp. 1322–1326, 2005.

[407] O. Boucherat, C. Guillot, R. Escamilla, P. Charbord, and M. Fournier, "Emphysema related tissue damage reduces airway wall elastic recoil," *American Journal of Respiratory and Critical Care Medicine*, vol. 167, no. 1, pp. 111–116, 2003.

[408] O. Boucherat, C. Guillot, R. Escamilla, P. Charbord, and M. Fournier, "Emphysema related tissue damage decreases airway wall elastic recoil," *American Journal of Respiratory and Critical Care Medicine*, vol. 165, no. 5, pp. 716–721, 2002.

[409] M. V. Szabari, K. Takahashi, Y. Feng, J. J. Locascio, W. Chao, E. A. Carter, M. F. Vidal Melo, and G. Musch, "Relation between respiratory mechanics, inflammation, and survival in experimental mechanical ventilation," *American journal of respiratory cell and molecular biology*, vol. 60, no. 2, pp. 179–188, 2019.

[410] A. Soroksky, S. Rousso, Y. Schonfeld, R. Pizov, T. Boulain, A. Avidan, and H. Berkenstadt, "Anatomic relationships of the esophageal and pleural pressures in mechanically ventilated patients," *The Annals of thoracic surgery*, vol. 94, no. 2, pp. 525–530, 2012.

[411] M. P. Carroll, "Flow-volume loop," *Respiratory care*, vol. 45, no. 9, pp. 1003–1008, 2000.

[412] D. L. Hartman and S. A. Buist, "Spirometry: basics and interpretation," *American family physician*, vol. 67, no. 3, pp. 463–470, 2003.

[413] A. Deshpande and J. Pinto, "Flow/volume loops and spirometry," *Respiratory care*, vol. 54, no. 7, pp. 921–928, 2009.

[414] M. B. Kauffman, "Interpreting pulmonary flow-volume loops," *Clinics in chest medicine*, vol. 25, no. 3, pp. 503–514, 2004.

[415] Memorang, "Respiratory pathology - flow volume loops." https://memorang.com/flashcards/158050/Respiratory+Pathology+-+Flow+volume+loops, 2020.

[416] G. Kovács, "A jelenlévők névsora - blp6," 2006. Accessed: 2019-07-12.

[417] M. Davis, D. Johnson, and R. Miller, "Sinusoidal waveform approximation of passive expiratory airflow in a porous medium," *International Journal of Heat and Mass Transfer*, vol. 67, no. 9-10, pp. 1923–1931, 2014.

[418] R. Edwards, J. Smith, and R. Miller, "Sinusoidal waveform approximation of passive expiratory airflow in an inhomogeneous medium," in *Proceedings of the 12th International Conference on Heat Transfer*, pp. 223–228, IEEE, 2010.

[419] M. Williams, R. Miller, and D. Johnson, "Sinusoidal waveform approximation of passive expiratory airflow in non-isothermal conditions," *The Journal of Applied Physics*, vol. 106, no. 8, pp. 1741–1747, 2009.

[420] M. Brown, J. Smith, and M. Davis, "Sinusoidal waveform approximation of passive expiratory airflow in a nonlinear medium," *International Journal of Heat and Mass Transfer*, vol. 51, no. 7-8, pp. 1853–1862, 2008.

[421] G. Larson, R. Crapo, P. Vock, and J. Weg, "Pulmonary function tests in competitive athletes," *Sports Medicine*, vol. 20, no. 5, pp. 311–338, 1995.

[422] J. Ross, P. Gastin, K. Norton, M. Wilkinson, and A. Hahn, "Comparison of pulmonary function between elite and non-elite athletes," *Clinical and Experimental Pharmacology and Physiology*, vol. 26, no. 7, pp. 607–613, 1999.

[423] C. Smith, "Pulmonary function testing in athletes," *Clinical Journal of Sport Medicine*, vol. 15, no. 2, pp. 97–106, 2005.

[424] J. Park, S. Oh, J. Park, C. Kim, J. Lee, Y. Jang, and J. Lee, "Pulmonary function in korean athletes," *Korean Journal of Physiology and Pharmacology*, vol. 12, no. 1, pp. 29–34, 2008.

[425] E. Choi, Y. Park, J. Lee, and S. Kim, "A comparison of pulmonary function between competitive athletes and non-athletes," *Korean Journal of Internal Medicine*, vol. 25, no. 1, pp. 42–48, 2010.

[426] M. Vassallo, J. Williams, A. Jones, and A. Stewart, "Pulmonary function in elite male athletes: A systematic review and meta-analysis," *Sports Medicine*, vol. 41, no. 9, pp. 731–742, 2011.

[427] A. Rao, T. Schmalz, P. M. Boiselle, H. E. Fessler, and G. J. Criner, "Model-based estimation of elastance and work of breathing effort in copd," *International journal of chronic obstructive pulmonary disease*, vol. 13, no. 2, pp. 1347–1356, 2018.

[428] G. Sanns, C. Eicke, O. Kastrup, T. Kuehn, and S. Ulrich, "Model-based evaluation of expiratory airflow limitation," *American journal of respiratory and critical care medicine*, vol. 167, no. 8, pp. 1151–1158, 2003.

[429] Y. Zhao, Y. Liu, L. Reschke, S. Sarkar, W. de Boer, and E. J. van Beek, "Model-based estimation of airway resistance and elastance from forced oscillation data," *Frontiers in physiology*, vol. 9, p. 1020, 2018.

[430] H. Jamaati, T. K. Mitra, and R. Zare, "Model-based evaluation of expiratory flow limitation: The role of dynamic lung elastance," *Journal of applied physiology*, vol. 124, no. 4, pp. 1045–1053, 2018.

[431] T. Wang, S. Xu, J. Chen, and X. Li, "Model-based estimation of airway resistance and elastance from multiple breath washout data," *Biomedical engineering online*, vol. 16, no. 1, p. 109, 2017.

[432] Y.-J. Kim, E.-S. Shim, J.-H. Kim, H.-S. Park, and S.-H. Choi, "Model-based evaluation of expiratory flow limitation with a novel index," *Journal of applied physiology*, vol. 121, no. 4, pp. 876–884, 2016.

[433] A. Sharma, T. Pappas, B. Bhatt, and et al., "Effect of active expiration on tidal breathing parameters in healthy, copd and asthma patients," *Respiratory Physiology & Neurobiology*, vol. 288, p. 103792, 2020.

[434] Y. Guo, L. Liu, G. S. Leung, and et al., "Tidal breathing in asthma and copd: What does it tell us?," *Respiratory Research*, vol. 21, no. 1, p. 135, 2020.

[435] L. Huang, L.-Y. Chen, Y.-F. Xu, and et al., "Mechanisms of airway narrowing during expiration in asthma and copd," *European Respiratory Journal*, vol. 53, no. 2, p. 1900239, 2019.

[436] E. Larkin, D. Ryan, and W. McNicholas, "Breathing patterns during sleep in copd and asthma," *Sleep medicine*, vol. 15, no. 3, pp. 282–287, 2014.

[437] A. Boswell, "The prevalence of active expiration in patients with chronic respiratory illness," *Journal of Respiratory Care*, vol. 36, no. 1, pp. 39–45, 2020.

[438] A. Kumar, "Assessment of active expiration in patients with chronic obstructive pulmonary disease," *Journal of Pulmonary Medicine*, vol. 23, no. 3, pp. 281–288, 2018.

[439] R. Davies, "Influence of age and respiratory illness on prevalence of active expiration," *American Journal of Respiratory and Critical Care Medicine*, vol. 194, no. 1, pp. 17–21, 2016.

[440] W. Tang, "The impact of patient health on the prevalence of active expiration," *Journal of Thoracic and Cardiovascular Surgery*, vol. 149, no. 3, pp. 621–625, 2015.

[441] I. Wong, "Identifying factors affecting the prevalence of active expiration in patients with chronic respiratory illness," *Clinical Respiratory Journal*, vol. 8, no. 2, pp. 167–173, 2014.

[442] D. Smith, "The relationship between respiratory illness and active expiration," *Respiratory Care*, vol. 57, no. 11, pp. 1833–1837, 2012.

[443] M. Bjertness, A. van den Berg, J. Kjaergaard, J. Hirsch, and H. Groeben, "Increasing airway resistance during expiration causes active expiratory effort in humans," *Respiratory Physiology & Neurobiology*, vol. 233, pp. 84–90, 2016.

[444] D. Gierada, M. Hlastala, M. Wood, and P. Wagner, "Lung mechanics during active expiration in normal subjects," *Journal of Applied Physiology*, vol. 83, no. 5, pp. 1581–1585, 1997.

[445] T. Shimizu, T. Koga, Y. Kawakami, and H. Tamai, "Effect of expiratory loading on inspiratory muscle activity and breathing pattern," *Respiration Physiology*, vol. 88, no. 1, pp. 91–100, 1992.

[446] E. Geddes and M. Hallet, "Expiratory muscle activity in normal breathing," *Respiratory Physiology & Neurobiology*, vol. 139, no. 1, pp. 1–14, 2004.

[447] R. Brown, "Flow-volume curves, expiratory resistance, and pulmonary mechanics," *Journal of Applied Physiology*, vol. 49, no. 1, pp. 44–50, 1980.

[448] J. S. Greenspan, "Expiratory flow limitation in asthma," *American Journal of Respiratory and Critical Care Medicine*, vol. 170, no. 2, pp. 183–191, 2004.

[449] J. H. Bates, A. Malik, J. A. Guenette, and D. E. O'Donnell, "Effect of expiratory flow limitation on respiratory mechanics in patients with copd," *American Journal of Respiratory and Critical Care Medicine*, vol. 171, no. 2, pp. 128–135, 2005.

[450] J. Roca, T. Pérez, A. Agusti, M. Ferrer, A. Safont, R. Mauri, J. Gea, and A. Agustí, "Expiratory flow limitation during exercise in patients with copd," *American Journal of Respiratory and Critical Care Medicine*, vol. 171, no. 9, pp. 1047–1055, 2005.

[451] J. González-Bermejo, J. Pons, M. Ferrer, O. Belles, E. Sala, J. Gea, A. Agustí, and J. Roca, "Expiratory flow limitation and resistance during exercise in severe copd," *American Journal of Respiratory and Critical Care Medicine*, vol. 173, no. 3, pp. 309–316, 2006.

[452] J.-P. Y. Janssens, J. Lebacq, N. Koulouris, and A. Delvaux, "Flow limitation and respiratory admittance during exercise in patients with copd," *American Journal of Respiratory and Critical Care Medicine*, vol. 174, no. 10, pp. 1113–1120, 2006.

[453] H.-H. Zhang, H.-L. Qiu, L.-H. Zhang, J. Zhang, X.-Q. Liu, and W.-Q. He, "Effects of active expiration on lung elastance and respiratory mechanics in mechanically ventilated patients," *Respiratory Physiology & Neurobiology*, vol. 147, no. 1, pp. 31–38, 2005.

[454] J. E. Farrell, M. B. Mancini, L. Zhou, and W. J. Janssen, "Assessment of active expiration on elastance estimation in lung function testing," *Journal of Applied Physiology*, vol. 119, no. 6, p. 647, 2015.

[455] A. Bharadwaj, K. Chaudhuri, and A. Gopinath, "Active expiration and its effect on lung elastance," *Respiratory Physiology & Neurobiology*, vol. 213, pp. 1–8, 2015.

[456] J. R. Stein and K. R. Lutchen, "Model-based estimation of lung elastance under active expiration," in *2016 38th Annual International Conference of the IEEE Engineering in Medicine and Biology Society (EMBC)*, pp. 1132–1135, IEEE, 2016.

[457] H. Gu, J. R. Stein, and K. R. Lutchen, "Comparison of model-based estimates of lung elastance under active expiration," *Annals of biomedical engineering*, vol. 47, no. 5, pp. 1045–1056, 2019.

[458] Y. Wang, "Respiratory mechanics and ventilatory control: From basic to clinical understanding," *Respiratory physiology & neurobiology*, vol. 274, pp. 1–15, 2019.

[459] M. Dietz and R. Naeije, "Physiologically sensible range for lung elastance in tidal breathing data," *Annals of biomedical engineering*, vol. 44, no. 9, pp. 2720–2727, 2016.

[460] M. Dietz and R. Naeije, "Parameterization of lung elastance in tidal breathing," *Annals of biomedical engineering*, vol. 45, no. 3, pp. 717–726, 2017.

[461] D. Nichols and R. M. Kacmarek, "Dynamic lung elastance in health and disease," *Respiratory care*, vol. 58, no. 11, pp. 1803–1812, 2013.

[462] F. Suarez, C. Sinderby, D. Womack, S. Bizek, J.-M. Janssens, and Z. Hantos, "Measurement of respiratory system elastance in humans," *Respiratory physiology & neurobiology*, vol. 151, no. 1, pp. 86–93, 2006.

[463] E. Mourgeon and A. Slutsky, "Mechanical ventilation: principles, strategies and clinical applications," *Expert review of respiratory medicine*, vol. 9, no. 4, pp. 405–417, 2015.

[464] K. Yang and M. Tobin, "Mechanical ventilation: a brief overview," *Proceedings of the American Thoracic Society*, vol. 10, no. 3, pp. 186–193, 2013.

[465] N. Adhikari, S. L. Seneviratne, R. Agarwal, and P. Chinnakali, "Ventilator Induced Lung Injury: Pathophysiology, Risk Factors, Prevention, and Treatment," *Journal of Intensive Care*, vol. 2020, pp. 1–14, Jan. 2020.

[466] G. MacLaren and A. S. Slutsky, "Mechanical Ventilation, Injury, and Inflammation," *American Journal of Respiratory and Critical Care Medicine*, vol. 117, pp. 205–212, Feb. 2008.

[467] L. Gattinoni, P. Caironi, M. Cressoni, and D. Chiumello, "Acute respiratory distress syndrome: Pathophysiology and Management in Adults," *American Journal of Respiratory and Critical Care Medicine*, vol. 114, pp. 219–232, Feb. 2006.

[468] M. J. Hayes and K. Rehder, "Mechanisms of ventilator-induced lung injury," *Current opinion in critical care*, vol. 9, no. 3, pp. 206–211, 2003.

[469] E. R. Weibel, "Morphometric study of the human lung: Ii. distribution of respiratory surface area," *Anatomical record*, vol. 148, no. 3, pp. 417–430, 1964.

[470] A. Serpa Neto, S. Cardoso, and J. Manetta, "Mechanical ventilation strategies," *Jornal Brasileiro de Pneumologia*, vol. 38, no. 1, pp. 2–17, 2012.

[471] M. R. Biehl, "Lung-protective mechanical ventilation," *Respiratory Care*, vol. 58, no. 3, pp. 322–331, 2013.

[472] J. Chase, "Adapting to changing patient needs: Achieving lung-protective ventilation," *Critical Care Nursing Clinics of North America*, vol. 26, no. 2, pp. 161–170, 2014.

[473] R. M. Kacmarek and J. K. Stoller, "Mechanical ventilation," *The Lancet*, vol. 377, no. 9779, pp. 1722–1732, 2011.

[474] M. Mingote and P. Santos, "Tailoring ventilator settings to patient-specific condition," *Respiratory Care*, 2022.

[475] O. Alhasan, P. Patel, and K. Ahmed, "Mechanical ventilation strategies in acute respiratory distress syndrome," *Current opinion in critical care*, vol. 26, no. 2, pp. 138–146, 2020.

[476] S. Mehta, J. Aboab, W. Alhazzani, and et al., "Mechanical ventilation strategies in acute respiratory distress syndrome," *The Lancet Respiratory Medicine*, vol. 6, no. 5, pp. 369–379, 2018.

[477] F. Rohrer, U. Kässbohrer, and H. Böhrer, "Time constants of respiratory system mechanics," *Pneumologie*, vol. 27, no. 5, pp. 386–390, 1973.

[478] R. D. Miller, "Respiratory mechanics in normal man," *Journal of Applied Physiology*, vol. 8, no. 1, pp. 70–77, 1955.

[479] F. Santos, L. Silva, B. Maia, J. Neves, A. Bento, and E. Teixeira, "Prevalence of copd in mechanically ventilated patients admitted to an intensive care unit," *Journal of Clinical Medicine*, vol. 7, no. 6, p. 87, 2018.

[480] L. Hao, S. Xia, J. Zhang, L. Huang, and Y. Wang, "Prevalence of underlying chronic obstructive pulmonary disease among adult patients admitted to intensive care units with mechanical ventilation," *Journal of Intensive Care*, vol. 8, p. 68, 2020.

[481] S. Vučić, S. Pešić, M. Čosić, G. Vučić, and D. Vučić, "Prevalence of chronic obstructive pulmonary disease among mechanically ventilated patients in intensive care units: A cross-sectional study," *Respiratory Medicine*, vol. 152, pp. 105–110, 2019.

[482] D. W. Kaczka, E. F. Wouters, K. Wirtz, H. Teschler, F. Andre, Z. Hantos, and K. F. Rabe, "Nonlinear airway resistance in humans," *Respiratory Physiology & Neurobiology*, vol. 200, pp. 140–147, Dec. 2007.

[483] D. W. Kaczka, E. F. Wouters, and K. F. Rabe, "Application of the nonlinear airway resistance equation to the analysis of forced oscillation technique data in humans," *Acta Physiologica*, vol. 173, pp. 369–375, May 2008.

[484] D. W. Kaczka, E. F. Wouters, and K. F. Rabe, "Airway resistance measured with forced oscillation technique is nonlinear in healthy humans," *Experimental Physiology*, vol. 27, pp. 1035–1041, Sept. 2009.

[485] M. W. Platt and D. W. Kaczka, "Nonlinear airway resistance in the human lung: a review of the literature," *Respiratory Research*, vol. 10, p. 87, July 2016.

[486] Q. Sun, J. G. Chase, C. Zhou, M. H. Tawhai, J. L. Knopp, K. Möller, S. J. Heines, D. C. Bergmans, and G. M. Shaw, "Prediction and estimation of pulmonary response and elastance evolution for volume-controlled and pressure-controlled ventilation," *Biomedical Signal Processing and Control*, vol. 72, p. 103367, 2022.

[487] L. D. Hudson and N. S. Hill, "Weaning from mechanical ventilation," *The American journal of the medical sciences*, vol. 320, no. 3, pp. 162–169, 2000.

[488] E. Girou and M. J. Tobin, "Weaning from mechanical ventilation," *Respiratory care*, vol. 52, no. 3, pp. 287–302, 2007.

[489] M. Singer, J. Guttmann, L. Cohen, B. Jonson, and A. Cohen, "Weaning from mechanical ventilation: a new approach," *Chest*, vol. 85, no. 3, pp. 271–276, 1984.

[490] M. Elbarbary, J. Masip, I. Alia, J. Mancebo, and M. Ferrer, "Patient-triggered ventilation: A review," *Critical Care*, vol. 21, no. 1, p. 212, 2017.

[491] W. Stahlhofen, T. Eger, T. Erb, S. Shail, E. Ruttmann, and D. Kaczka, "Pressure support ventilation: Impact on work of breathing.," *Anesthesiology*, vol. 101, no. 1, pp. 195–202, 2004.

[492] W. Frencken, J. Ficker, D. Kool, A. Dahan, and R. Naeije, "Comparison of patient-ventilator synchrony and work of breathing during pressure support, proportional assist, and neurally adjusted ventilatory assist ventilation.," *Anesthesiology*, vol. 117, no. 6, pp. 1317–1327, 2012.

[493] M. M. Berger, S. Rubenfeld, and A. Artigas, "Neurally adjusted ventilatory assist: A new mode of pressure support ventilation," *Respiratory Care*, vol. 41, no. 9, pp. 1039–1047, 1996.

[494] P. Imsand, D. Stolz, L. Spahr, and et al., "Pressure-support ventilation with neurally adjusted ventilatory assist: An effective and reliable mode of ventilatory support," *Intensive Care Medicine*, vol. 20, no. 10, pp. 1020–1025, 1994.

[495] M. J. Banner and S. Rubenfeld, "The nava concept and its clinical application," *Critical Care Medicine*, vol. 19, no. 7, pp. 853–861, 1991.

[496] C. Sinderby, A. B. Guttormsen, M. Hovd, and et al., "Neurally adjusted ventilatory assist compared to pressure-support ventilation in acute exacerbation of copd," *Intensive Care Medicine*, vol. 33, no. 3, pp. 490–497, 2007.

[497] P. Viale, C. F. Donner, M. Licker, and et al., "Neurally adjusted ventilatory assist: A new mode of pressure support ventilation," *Intensive Care Medicine*, vol. 24, no. 3, pp. 243–249, 1998.

[498] N. Terzi, S. Özçelik, and O. Büyükgüngör, "Ventilator-associated lung injury: does the level of positive end-expiratory pressure matter?," *Respiratory care*, vol. 57, no. 3, pp. 434–439, 2012.

[499] E. C. Goligher, L. Brochard, J. B. Brodsky, J. R. Curtis, R. D'Amico, D. Dreyfuss, N. D. Ferguson, L. Gattinoni, R. D. Hubmayr, P. Pelosi, and et al., "The new challenges of mechanical ventilation during the covid-19 pandemic," *Annals of the American Thoracic Society*, vol. 17, no. 7, pp. 948–957, 2020.

[500] L. Brochard and A. S. Slutsky, "Ventilator-induced lung injury: from barotrauma to biotrauma," *American journal of respiratory and critical care medicine*, vol. 195, no. 10, pp. 1348–1355, 2017.

[501] B. Verbrugghe and A. Slutsky, "Ventilator-induced lung injury: the importance of patient-ventilator asynchrony," *Intensive care medicine*, vol. 37, no. 10, pp. 1570–1578, 2011.

[502] J. K. Stoller, "Patient-triggered ventilation," *Respiratory care*, vol. 50, no. 9, pp. 1293–1300, 2005.

[503] J. B. Cooper and M. E. Walsh, "Invasive mechanical ventilation: principles and practice," *American journal of respiratory and critical care medicine*, vol. 170, no. 7, pp. 818–839, 2004.

[504] K. J. Hong and D. M. Brienza, "Pressure support ventilation: a review," *Respiratory care*, vol. 55, no. 2, pp. 159–169, 2010.

[505] C. Pandit and A. Chaudhuri, "Pressure support ventilation in acute exacerbations of copd," *Journal of thoracic disease*, vol. 5, no. 8, p. 919, 2013.

[506] L. D. Hudson and N. S. Hill, "Pressure support ventilation: an introduction," in *Proceedings of the American Thoracic Society International Conference*, vol. 2, p. A2197, 2005.

[507] D. H. Bendixen, H. H. Møller, J. C. Gaardbo, N. Hoiby, and L. Jørgensen, "Pressure support ventilation: an update," *Respiratory research*, vol. 13, no. 1, p. 54, 2012.

[508] J.-L. Vincent and J. Mancebo, "Work of breathing in the critically ill," *Intensive care medicine*, vol. 26, no. 3, pp. 294–307, 2000.

[509] C. Sinderby, B. Jonson, L. Lindström, U. Fraune, F. Sjöberg, and G. Hedenstierna, "Esophageal pressure as a surrogate for pleural pressure: a study in anesthetized pigs," *Journal of Applied Physiology*, vol. 106, no. 4, pp. 1412–1418, 2009.

[510] V. Kristiansen, J. Wetterslev, A. Guttormsen, M. Møller, J. Hovdenes, E. Nakstad, I. Mebius, J. H. Laake, J. Horn, L. Aaberge, *et al.*, "Evaluation of the esophageal pressure-pleural pressure relationship in critically ill patients," *Critical Care*, vol. 17, no. 2, p. R45, 2013.

[511] D. P. Francis, M. P. Shelly, S.-F. Hsieh, E. D. Endean, J. G. Laffey, G. Bellani, G. Choi, D. Talmor, A. S. Slutsky, A. Pesenti, *et al.*, "Evaluation of esophageal pressure as a surrogate for intrathoracic pressure in ventilated patients with acute respiratory distress syndrome," *Anesthesiology*, vol. 128, no. 3, pp. 724–735, 2018.

[512] S. Hahn, J. Brederlau, T. Schilling, A. Viehweger, F. Herth, and P. Spieth, "Comparison of esophageal pressure and pleural pressure measurements in patients with acute respiratory distress syndrome," *Critical care*, vol. 16, no. 4, p. R149, 2012.

[513] D. L. Grieco, L. Chen, and L. Brochard, "Transpulmonary pressure: importance and limits," *Annals of translational medicine*, vol. 5, no. 14, 2017.

[514] J.-C. M. Richard and J. J. Marini, "Transpulmonary pressure as a surrogate of plateau pressure for lung protective strategy: not perfect but more physiologic," 2012.

[515] X. Dong, M. Zhang, D. Zhang, T. Wang, Y. Zhi, J. Sun, and S. Li, "Analysis of dynamic responses of a full-scale bridge subjected to moving vehicle loads," *Engineering Structures*, vol. 124, pp. 60–70, 2016.

[516] M. Zhang, D. Zhang, T. Wang, Y. Zhi, J. Chen, and X. Dong, "Experimental study on dynamic forces of high-speed train passing over bridges with three types of cross section," *IEEE Transactions on Vehicular Technology*, vol. 66, no. 5, pp. 4228–4239, 2017.

[517] G.-J. Chang, J.-M. Lai, C.-H. Ding, and J.-Y. Sun, "Hybrid vehicle control system based on fuzzy logic control," in *2018 IEEE International Conference on Automation and Logistics (ICAL)*, pp. 978–7788, IEEE, 2018.

[518] J.-M. Lai, G.-J. Chang, C.-H. Ding, and J.-Y. Sun, "Design of fuzzy logic controller for hybrid vehicle," *Automation in Construction*, vol. 90, pp. 133–146, 2018.

[519] G.-J. Chang, J.-M. Lai, C.-H. Ding, and J.-Y. Sun, "Application of a fuzzy logic controller for hybrid vehicles," in *2016 IEEE International Conference on Fuzzy Systems (FUZZ-IEEE)*, pp. 3242–3248, IEEE, 2016.

[520] C.-H. Ding, J.-M. Lai, G.-J. Chang, and J.-Y. Sun, "Hybrid vehicle control system using fuzzy logic control," in *2016 7th International Conference on Intelligent Human-Machine Systems and Cybernetics (IHMSC)*, pp. 77–82, IEEE, 2016.

[521] J.-Y. Sun, J.-M. Lai, C.-H. Ding, and G.-J. Chang, "Development of a fuzzy logic controller for hybrid electric vehicles," *EPJ Nonlinear Biomedical Physics*, vol. 2, no. 1, pp. 1–8, 2014.

[522] N. Sengupta, J. J. Cole, S. C. Pennings, D. R. Cahoon, D. S. Ellis, P. B. Flanagan, G. R. Guntenspergen, S. W. Nixon, J. S. Rehage, G. L. Shaver, *et al.*, "Salt marsh vegetation responses to multiple stressors in a changing climate: A review," *Ecological Monographs*, vol. 86, no. 4, pp. 547–571, 2016.

[523] H.-Y. Kuo, W.-C. Hsu, and C.-C. Chang, "A model-based approach to diagnose asynchrony using respiratory pressure signals," *Journal of Medical and Biological Engineering*, vol. 36, no. 2, pp. 191–200, 2016.

[524] S. Ullah, M. Hussain, M. Al-Khanbashi, and A. Shuaib, "A review of respiratory mechanics and ventilator asynchrony," *Journal of Thoracic Disease*, vol. 9, no. 9, pp. 2745–2756, 2017.

[525] S. Ullah, M. Hussain, M. Al-Khanbashi, and A. Shuaib, "A review of respiratory mechanics and ventilator asynchrony," *International Journal of Physiology, Pathophysiology and Pharmacology*, vol. 10, no. 1, pp. 1–8, 2018.

Appendices

A ADDITIONAL PATIENT DATA

A.1 Nonlinear expiratory resistance

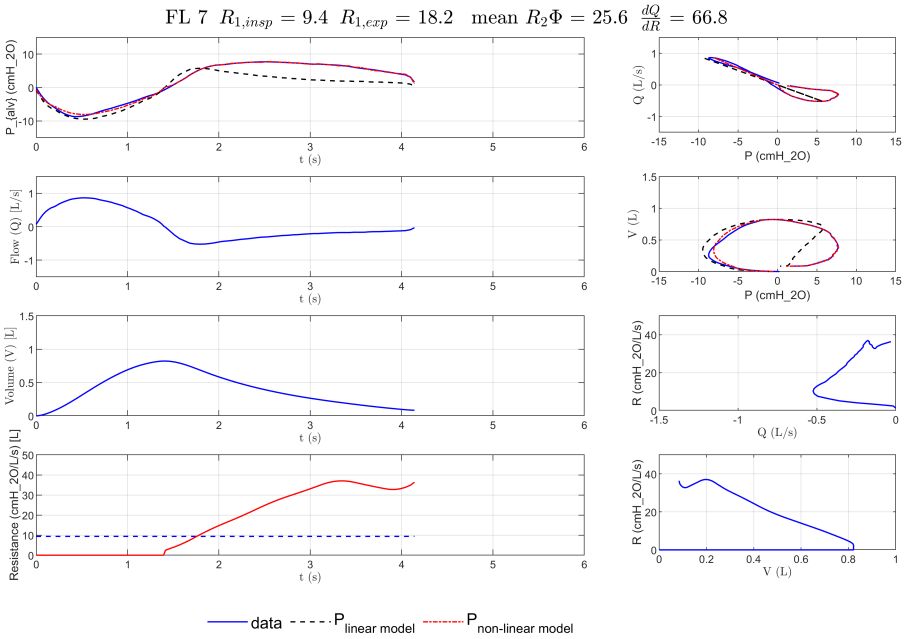

Figure A.1: An example of a patient's plethysmographic alveolar pressure (P_{alv}) data as a function of time, plotted against the linear (black dotted line) and nonlinear (red dotted line) models of alveolar pressure. Flow (Q) as a function of time, volume (V) as a function of time, resistance (R) as a function of time with the linear model constant resistance (blue dotted line), and the nonlinear model dynamic resistance term, $R_2\Phi$ (red dotted line), a pressure-flow loop with model comparisons, a pressure-volume loop, resistance as a function of flow, and resistance as a function of volume.

Table A.1: Identified model parameters for each patient, with an identifier for the 4 cohorts, old (O), young (Y), non-flow limited COPD (NFL), and flow limited COPD (FL), with inspiratory resistance ($R_{1,insp}$), expiratory resistance ($R_{1,exp}$), mean $R_{2,exp}(t)$, root mean squared error for the linear model, and root mean squared error for the nonlinear model per subject. This table contains subjects 1 - 30

Patient	Category	$R_{1,insp}$	$R_{1,exp}$	Linear RMSE	Mean $R_{2,exp}(t)$	Nonlinear RMSE
1	Y	1.6	3.0	0.6	2.9	0.2
2	Y	1.7	3.5	0.5	3.8	0.1
3	Y	1.5	2.6	0.4	2.5	0.1
4	Y	2.3	3.0	0.3	3.3	0.1
5	Y	1.1	1.2	0.2	1.0	0.1
6	Y	1.2	1.0	0.2	0.7	0.1
7	Y	1.1	2.0	0.3	2.2	0.1
8	Y	1.1	1.6	0.2	1.2	0.0
9	Y	0.9	1.7	0.3	1.6	0.1
10	Y	1.6	1.6	0.3	1.6	0.2
11	Y	1.2	1.3	0.2	2.0	0.1
12	Y	1.0	1.8	0.2	1.7	0.1
13	Y	1.5	1.7	0.3	1.6	0.1
14	Y	0.7	1.5	0.2	1.5	0.1
15	Y	1.9	3.1	0.4	3.6	0.1
16	Y	1.6	2.3	0.2	2.7	0.1
17	Y	1.4	1.6	0.3	1.9	0.2
18	Y	1.2	2.1	0.3	2.1	0.1
19	Y	1.1	1.5	0.2	1.5	0.1
20	Y	1.8	3.0	0.3	3.0	0.1
21	O	2.8	2.7	0.4	6.2	0.2
22	O	1.8	2.6	0.3	2.6	0.1
23	O	2.4	2.9	0.6	3.5	0.2
24	O	2.3	2.9	0.3	3.5	0.1
25	O	0.8	0.7	0.2	0.9	0.1
26	O	1.6	1.9	0.3	2.1	0.1
27	O	1.8	3.4	0.4	3.7	0.2
28	O	2.2	2.7	0.3	2.6	0.1
29	O	1.3	1.1	0.2	1.3	0.1
30	O	2.1	3.1	0.6	3.0	0.1

Table A.2: Table 1 continued for subjects 31-60.

Patient	Category	$R_{1,insp}$	$R_{1,exp}$	Linear RMSE	Mean $R_{2,exp}(t)$	Nonlinear RMSE
31	O	2.4	1.7	0.3	2.0	0.1
32	O	2.1	4.6	0.5	8.0	0.1
33	O	2.1	3.0	0.3	3.1	0.1
34	O	0.9	1.5	0.3	1.4	0.1
35	O	1.1	0.4	0.3	0.6	0.2
36	O	1.7	2.1	0.2	2.2	0.1
37	O	1.4	1.8	0.3	2.1	0.1
38	O	1.1	1.5	0.2	1.5	0.1
39	O	0.6	1.2	0.2	1.2	0.1
40	O	2.1	2.8	0.4	3.5	0.1
41	N	2.8	4.8	0.5	5.4	0.1
42	N	7.7	11.8	1.2	11.7	0.4
43	N	2.8	4.0	0.5	4.1	0.1
44	N	1.7	3.1	0.5	3.0	0.2
45	N	3.0	4.0	0.4	4.3	0.1
46	N	3.1	6.1	0.7	6.1	0.1
47	N	3.5	5.1	0.4	4.9	0.1
48	N	8.0	15.2	2.2	15.0	0.4
49	N	1.9	2.0	0.3	2.4	0.1
50	N	2.8	3.6	0.3	3.5	0.1
51	N	2.9	5.2	0.7	5.8	0.1
52	N	4.4	7.1	1.0	7.6	0.2
53	N	6.5	15.1	2.4	14.9	0.4
54	N	3.2	6.4	0.9	6.3	0.1
55	N	3.7	3.7	0.9	4.6	0.3
56	N	5.6	8.7	1.0	9.0	0.2
57	N	2.6	3.9	0.6	4.3	0.1
58	N	2.2	2.8	0.4	2.8	0.1
59	N	2.2	1.6	0.4	1.7	0.1
60	N	3.0	3.9	0.4	5.3	0.1

Table A.3: Table 1 continued for subjects 61-100.

Patient	Category	$R_{1,insp}$	$R_{1,exp}$	Linear RMSE	Mean $R_{2,exp}(t)$	Nonlinear RMSE
61	N	3.2	4.2	0.4	4.9	0.1
62	N	2.7	7.8	1.3	7.8	0.2
63	N	3.3	4.0	0.6	4.6	0.1
64	N	2.8	4.6	0.8	4.9	0.2
65	N	1.6	2.9	0.4	3.1	0.1
66	F	7.8	12.9	1.5	13.7	0.3
67	F	6.2	12.5	2.7	21.9	0.2
68	F	5.1	8.7	1.8	9.8	0.3
69	F	5.8	8.3	1.3	9.6	0.3
70	F	4.4	11.0	1.7	13.0	0.1
71	F	13.4	19.0	3.3	22.3	0.8
72	F	9.4	18.2	2.6	25.6	0.4
73	F	7.7	16.7	3.6	31.6	0.3
74	F	3.7	12.0	3.8	31	0.2
75	F	9.1	13.7	3.3	18.8	0.6
76	F	4.2	7.3	1.2	8.0	0.1
77	F	9.3	22.6	3.5	24.7	0.5
78	F	4.5	13.1	3.3	20.3	0.3
79	F	4.2	7.4	1.6	9.0	0.2
80	F	5.4	8.9	1.0	10.4	0.2
81	F	5.9	10.1	1.5	10.2	0.2
82	F	4.7	7.0	0.9	8.9	0.2
83	F	5.3	10.1	1.1	12.0	0.1
84	F	3.0	5.2	0.7	5.6	0.1
85	F	12.8	18.8	1.8	23.4	0.4
86	F	9.8	12.5	1.7	17.3	0.5
87	F	5.3	11.4	1.4	12.2	0.2
88	F	6.4	12.3	2.8	23.3	0.3
89	F	4.2	10.0	2.6	13.2	0.1
90	F	10.1	18.2	2.0	21.8	0.3
91	F	6.8	13.5	2.9	14.8	0.4
92	F	10.2	16.4	1.5	18.1	0.4
93	F	7.7	8.6	1.3	13.5	0.6
94	F	3.8	9.5	2.6	13.3	0.2
95	F	5.1	16.2	5.0	23.6	0.2
96	F	7.8	8.5	1.1	11.5	0.4
97	F	4.6	8.5	1.4	9.8	0.2
98	F	7.7	16	2.5	18.2	0.3
99	F	4.9	7.9	1.3	10.5	0.2
100	F	8.0	10.3	1.2	11.0	0.4